CONTROLLING ARCHITECTURE USING C2-SYMMETERIC CATALYSTS: FROM SMALL MOLECULES TO LARGE POLYMERS

A Dissertation

Presented to the Faculty of the Graduate School

of Cornell University

In Partial Fulfillment of the Requirements for the Degree of

Doctor of Philosophy

by

David Nicholas Vaccarello

August 2017

CONTROLLING ARCHITECTURE USING C2-SYMMETERIC CATALYSTS: FROM SMALL MOLECULES TO LARGE POLYMERS

David Nicholas Vaccarello, Ph. D.

Cornell University 2017

My doctoral studies have concentrated on the use of C2-symmetic catalysts to control the three-dimensional construction of molecules. The first half of my thesis focuses on asymmetric addition of phenols into Pd π-allyl complexes. This work was inspired by the natural product, sch202596, an antagonist for the galinin receptor that contains a highly stereogenic and compact carbasurgar structure appended onto a phenol by an allylic aryl-ether bond. A transformation was developed in which racemic allylic oxides underwent a Tsuji-Trost reaction to give diastereomeric π-allyl complexes. Addition of a nucleophile resulted in enantioenriched regioisomers in good yields. We termed this approach allylic oxide regio resolution (AORR). Using this approach, four different carbasurgar natural products were synthesized: streptol, MK7607, cyathiformine B and polyporapyranone G. Additionally, this method was extended to append carbasugar-like molecules onto complex natural products.

Furthermore, C2-symmetic catalysts were used to synthesize polymers with stereoregularity, which will be the focus of the second half of my thesis. Utilizing advances in chain walking polymerization, 1-butene was polymerized resulting in a novel isotactic semi-crystalline polymer. The ligand framework and reaction

conditions were probed in order to optimized the system, which gave an active catalyst that produced a polymer with few stereo and regioerros. Specifically, it was found that *ortho*-cumyl groups were necessary to maintain the stereochemical information through the chain walking steps. Additionally reaction conditions were explored and discovered that a reaction temperature of −40 °C and a concentration of approximately 8 M were the optimal conditions. Finally, the use of non-aromatic, high polarity, aprotic solvents proved beneficial.

BIOGRAPHICAL SKETCH

David Vaccarello was born on March 8th, 1990 to parents Anthony and Jean Vaccarello. He grew up in a suburb of Pittsburgh, Pennsylvania where he attended Pine-Richland school district. It was there that he discovered both his passion for science and running. While there, Dave took numerous elective science courses, specifically in chemistry, which he excelled at. Additionally, he completed eight seasons of cross-country and track as a Ram, setting several marks on the schools all-time performance list.

In 2008, Dave began his college career, as both a scientist and athlete, at Duquesne University in Pittsburgh, Pennsylvania. He competed as a Duke for the duration of his time as a distance runner on the cross country, indoor, and outdoor track teams. Beginning college, he enrolled as a chemistry major because it combined a subject he was passionate about with the strong scientific foundation he had already begun to build. As his coursework continued to deepen his understanding of chemistry, he was eager to begin research in an academic chemistry lab. He soon met Dr. Partha Basu and began research under his supervision, which changed the course of his life. In Basu's lab, Dave worked on synthetic routes for the *de novo* synthesis of the Molybdenum Cofactor. The combination of skill, art, and perseverance necessary for success in total synthesis was irresistible to Dave who wanted to make a career in it. Although graduate school was never an option in Dave's eyes, Dr. Basu saw early talent and a strong drive in his undergrad. With encouragement, Dave applied to graduate school in chemistry to enhance his training in organic synthesis.

In August 2012, Dave began his graduate studies at Cornell University in Ithaca, New York. There he joined the group of Dr. Chad Lewis where he worked on total synthesis and synthetic methodology. After spending three years in the group and completing the total synthesis of several carbasugar natural products, his time came to an abrupt end when Dr. Lewis left to join the research laboratories at Pfizer. Dave was quickly offered a position in the laboratories of Dr. Geoffrey Coates where he began his training in polymer chemistry. There, Dave was able to utilize the synthetic skills he had developed and apply them towards the development of new polymer catalysts.

While at Cornell, Dave received several awards including the Bayer Teaching Excellence Award in 2015 and the Simon Bauer Scholarship Award in 2016. He also participated in several outreach events hosted by the university such as Expanding Your Horizons and Kids Science Day. Dave continued to run, but at a recreational level, and completed his first half marathon in 1:15:09 in 2014. After graduating, Dave plans to move to Washington, DC and begin his postdoctoral appointment at the National Institute of Standards and Technology (NIST) in a collaborative project between Kathryn Beers and John Marino.

This dissertation is dedicated to my mother, Jean Biermeyer. Only with her constant love and support was this possible.

ACKNOWLEDGMENTS

It would have been impossible for me to make it through graduate school without the help and support of numerous people. Without them, I would not have made it. I would first like to thank both of my graduate advisors. Chad Lewis taught me more about synthetic chemistry and laboratory techniques than anyone else could have. He was always available for his students and was willing to stop what he was doing to help us whenever we needed it. He gave me the tools in synthetic chemistry that will allow me to be successful in any of my future endeavors. I would next like to thank Geoff Coates. He offered me a position and help without hesitation in a time that I needed it most. He was then exceptionally patient with me while I began learning a new subject late in my graduate career. Finally, he always kept my best interest in his mind. He sculpted projects that would suit my skills best and set me up for success. He also kept me on track to ensure that I would land on my feet and graduate on time. Without him, I would not have finished the program.

Next, I would like to acknowledge all my numerous coworkers. Meagan Hinze, Jess Daughtry, Anirudra Paul, Tony Tierno, and Matt Moschitto. Times were tough, but it helped to work with such a fun group of people who all shared the struggle together. Moreover, I would like to acknowledge Tony for always being available, regardless of which research group I may have been in. It was truly a pleasure having him around as a mentor and friend. I wish him the best of luck in his future. Additionally, I owe a lot to Matt. The projects we worked on together would not have gone as far without him. He gave me significant portions of his time in both

hands on training and helping to progress the projects. Without him, I certainly would not be where I am now. Both in and out of lab we made a good team. I'm sure he will continue to be successful.

I also need to acknowledge the Coates Group. I could not have asked for a better place to end up. They welcomed me with open arms and all did a part in helping me learn my way around the lab and steering me in the right direction. Specifically I would like to thank Kyle O'Connor, James Eagan, and Maria Sanford. I don't think an hour went by where I wasn't pestering one of them with a question. With their help and reassurance I was able to successfully navigate the field of polymer chemistry without going down to many dead ends or rabbit holes.

Furthermore, I would also like to thank those in the Department of Chemistry and Chemical Biology who have helped me including my committee members, Dave Collum and Kyle Lancaster. There was a lot going on behind the scenes that I will probably never know about, but they ensured I did not fall between any cracks and finished the program. I also need to thank my friends for giving me an outlet to vent and for fun times that gave me the energy to forge ahead. I had a solid support system that was always there for me when I needed it. Whether it was my friends from home, who made annual trips to visit me and tear up the town, or my coworkers who accompanied me to the Big Red Barn on Friday nights for $1 beers. I always had a group of people I could have fun with that served as an outlet for the frustrations of grad school.

Finally I would like to thank those closest to me. Jess is amazing. She is always at home waiting for me after the tough days of grad school. Although she may

claim that we are an equal team, she has helped me far more than I've helped her. I hope someday I can find a way to repay her. Additionally, she has allowed me to follow my dreams and adopt our crazy horse sized puppy, Toast. It requires approximately 100 people to keep him under control, but with Jess's help, the two of us seem to manage. To my parents, Lee has always been very supportive and kind. He made sure I always had a place to call home and always felt welcomed. I don't think I could ever thank my mother, Jean, enough. She has always been then for me. After my father died, she kept our family going. She miraculously found a way to pay for my undergraduate education, without which I would have never discovered my passion for chemistry. She also talked me down during countless late night phone calls during my undergraduate and graduate studies. I owe her everything.

TABLE OF CONTENTS

Chapter 1: Introduction to Carbasugars and Carbasugar Containing Natural Products, Tsuji-Trost Allylation, and Resolutions in Synthesis 1

1.1. Natural Products and Carbasugars 2

1.2. Tsuji-Trost Allylations 11

1.3. Resolutions in Synthesis 15

References and Notes 21

Chapter 2: Allylic Oxide Regio Resolution as a Tool for the Total Synthesis of Carbasugars 25

2.1. Introduction 26

2.2. Discovery and Optimization of AORR 28

2.3. AORR Application to Carbasugar Total Synthesis 36

2.4 Experimental 41

References and Notes 97

Chapter 3: A Brief Introduction to the History of Polyolefins and Chain walking Polymerizations 102

3.1. Introduction to Polymer Structures and Properties 103

3.2. Brief History of Polyolefins and Chain walking 109

References and Notes 122

Chapter 4: Synthesis of Semi-Crystalline Polyolefin Materials: Precision Methyl Branching Using Chiral Isoselective α-Diimine Nickel Catalysts 129

4.1. Introduction 130

4.2. Polymerization of 1-Butene 133

4.3. Experimental 143

References and Notes 170

Appendix 174

A.1. Spectra for Chapter 2 175

A.2. Spectra for Chapter 4 232

LIST OF SCHEMES, FIGURES, AND TABLES

Figure 1.1.	All FDA approved drugs from 1981–2010	2
Figure 1.2.	Examples of glycosylated phenolic natural products	4
Figure 1.3.	Different classes of glycomimetics	5
Figure 1.4.	Examples of natural carbasurgars and carbasugar containing compounds	7
Scheme 1.1	Proposed synthetic pathway for the synthesis of carbasugars by Nature	8
Scheme 1.2.	Strategies towards the synthesis of carbasugars	9
Scheme 1.3.	a) Boyd's synthesis of pericosine A. b) Koizumi's synthesis of carba-mannopyranose.	10
Scheme 1.4.	a) Generic Tsuji-Trost reaction. b) Catalytic cycle of Tsuji-Trost reaction.	11
Scheme 1.5	Mechanism for allyl-inversion and *anti*-addition to linear substrates.	13
Scheme 1.6	Mechanism of palladium-palladium allyl inversion in cyclic substrates	13
Figure 1.5.	a) Examples of TMLs. b) Lloyd-Jones model for selectivity. c) Trost wall-and-flap model.	14
Scheme 1.7.	Example of a classical resolution using stoichiometric reagent	16
Scheme 1.8.	Sharpless asymmetric epoxidation using chiral tartrates	16
Scheme 1.9.	a) Noyori dynamic kinetic resolution. b) Trost DKYAT of an allylic epoxide.	18
Scheme 1.10.	Fu’s parallel kinetic resolution of alkynes	19
Scheme 1.11.	Pfaltz and co-workers’ regio-divergent parallel kinetic resolution	20
Scheme 2.1.	Strategic allylic oxide regio-resolution (AORR) to access targeted carbasugar motifs	27
Table 2.1.	Regiochemical control of enantioinduction	28

Scheme 2.2	Proposed transition states for stereoinduction with observed product ratios	30
Table 2.2.	Predicted and observed er values for AORR in Scheme 2.2.	30
Table 2.3.	Phenolic scope of regiodivergence	33
Scheme 2.3.	Applying AORR to estradiol, tyrosine, and giseofulvin.	35
Scheme 2.4.	Kinetic and thermodynamic palladium allyl distribution and resulting diastereomers.	37
Scheme 2.5.	Applying AORR for the total synthesis of streptol, cyathiformine B, MK7607, and a new cyclitol. a) Results with a racemic oxide. b) Results with chiral pool	40
Table 2.4	Observed versus predicted enantiomeric ratios for AORR	69
Scheme 2.6.	Allylic oxide regio-resolution predictive model	70
Scheme 2.7.	Synthesis of dioxolane epoxide (**2.19**)	72
Scheme 2.8.	Thermodynamic AAOR pathway	81
Scheme 2.9.	Total synthesis of streptol and MK7607	84
Scheme 2.10.	Total synthesis of cyathiformine B type	89
Scheme 2.11.	Synthesis of new cyclitol **2.42**	92
Table 2.5.	Comparison of natural and synthetic samples	96
Figure 3.1.	a) Different types of tacticity of polymer side chains. b) Types of dyads and triads in polymer sequences	104
Figure 3.2.	Types of polymer architecture and branching	105
Figure 3.3.	Different structures for PE	106
Figure 3.4.	Stress-strain curves for different types of plastics	108
Scheme 3.1.	Monomer insertion into a propagating polymer chain	111
Scheme 3.2.	The Cossee-Arlman mechanism, or back-skip mechanism, for iso-selectivity	111

Scheme 3.3.	Ligand isomerization of phenoxy-imine catalyst during polymerization	113
Figure 3.5.	Original Brookhart α-diimine catalysts	114
Scheme 3.4.	Proposed chain walking mechanism	114
Scheme 3.5.	Associative displacement of propagating polymer chain through coordination of new olefin at axial site	116
Scheme 3.6.	Different modes of monomer insertion leading to different structures	117
Scheme 3.7.	a) Brookhart's stereoselective polymerization of cyclopentene. b) Taceuchi's stereoselective polymerization of non-conjugated dienes.	118
Scheme 3.8.	Coates's iso-selective polymerization of trans-2-butene	119
Scheme 3.9.	a) Coates's strategy for the production of elastomers by changing temperature. b) Iso-selective polymerization of PP at low temperatures to yield *i*PP	121
Scheme 4.1.	Nickel (II) catalyzed 4,2-enchainment polymerization of 1-butene	131
Figure 4.1.	α-Diimine nickel complexes used in this study	133
Table 4.1.	Catalyst screen for the polymerization of 1-butene	134
Scheme 4.2.	Proposed source of stereoselectivity in chain walking polymerization of 1-butene	135
Figure 4.2.	^{13}C NMR spectrum of 4,2-poly(1-butene) produced by complex **4.7**/MAO (Table 4.1, entry 7).	136
Table 4.2.	Effects of varying reaction conditions on the polymerization of 1-butene.	138
Table 4.3.	Solvent effects on the polymerization of 1-butene	140
Scheme 4.3.	Deuterated propylene study	141
Figure 4.3.	Representative tensile strength curve for 4,2-poly(1-butene)	142
Table 4.4.	^{13}C NMR signal assignments for 4,2-poly(1-butene) produced by nickel catalysts in this study	152
Figure 4.4.	Equations used to calculate enchainment pathways	153

Figure 4.5.	Representative ^{13}C NMR spectrum of 4,2-poly(1-butene)	154
Table 4.5.	Effect of reaction conditions on the polymerization of 1-butene using complex **4.5**	155
Table 4.6.	Effect of solvent on the polymerization of 1-butene using complex **4.5**	155
Figure 4.6.	4,2-poly(1-butene) produced by **4.1** (Table 4.1, entry 1)	156
Figure 4.7.	4,2-poly(1-butene) produced by **4.2** (Table 4.1, entry 2)	156
Table 4.7.	Crystal data and structure refinement for Rdv1	157
Table 4.8.	Atomic coordinates for **4.5**	159
Table 4.9.	Bond lengths [Å] and angles [°] for **4.5**	162
Figure 4.8.	X-ray crystal structure of **4.5**	169

LIST OF ABBREVIATIONS AND SYMBOLS

Ac: acetyl
AIBN: azobisisobutyronitrile
AORR: allylic oxide regio resolution
Ar: Aryl
BINAP: (2,2'-bis(diphenylphosphino)-1,1'-binaphthyl)
Bn: benzyl
Boc: *tert*-butoxycarbonyl
Bu: butyl
CAN: ceric ammonium nitrate
conc: concentration
COSY: correlated spectroscopy
Đ: (M_w/M_n) or dispersity of polymer sample
DART: direct analysis in real time
dba: dibenzylideneacetone
DBU: 1,8-diazabicyclo[5.4.0]undec-7-ene
DCM: dichloromethane
DEA: diethylamine
DFT: density function theory
DMAP: 4-dimethylaminopyridine
DMF: dimethylformamide
DMP: Dess-Martin periodinane
DMSO: dimethylsulfoxide
dr: diastereomeric ratio
DSC: differential scanning calorimetry
DYKAT: dynamic kinetic asymmetric transformation
ee: enantiomeric excess
EI: electron impact
er: enantiomeric ratio
ESI: electrospray ionization
Et: ethyl
FDA: Food and drug administration
GALR: galinin receptor
GPC: gel-permeation chromatography
DIBAl-H: diisoproylaluminium hydride
HDPE: high density polyethylene
HMBC: heteronuclear multiple bond correlation
HMDS: hexamethyldisilazide
HPLC: high-pressure liquid chromatography
HSQC: heteronuclear single quantum coherence
IC_{50}: half maximal inhibitory concentration
*i*PP: isotactic polypropylene

^{i}Pr: isopropyl
IR: infrared spectroscopy
K_i: inhibition constant, binding constant
LCMS: liquid chromatography mass spectrometer
LDA: lithium diisopropylamide
LDPE: low density polyethylene
LLDPE: linear low density polyethylene
m: meso dyad
MAO: methylaluminoxane
m-CPBA: *meta*-chloroperoxybenzoic acid
Me: methyl
M_n: number-average molecular weight
MOM: methoxymethyl
M.p.: melting point
M_w: weight-average molecular weight
NADH: nicotinamide adenosine dinucleotide
nap: naphthyl
NBS: N-bromosuccinimide
NMR: nuclear magnetic resonance
nOe: nuclear Overhauser effect
NOESY: nuclear Overhauser effect spectroscopy
NP: natural product
Nu: nucleophile
PE: polyethylene
Ph: phenyl
PIFA: bis(trifluoroacetoxy)iodobenzene
PMP: paramethoxyphenyl
PP: polypropylene
ppm: parts per million
PVC: polyvinyl chloride
py: pyridine
r: racemic dyad
rac: racemic
Rf: retention factor
ROSEY: rotating frame nuclear Overhauser effect spectroscopy
SGLT: sodium-glucose co-transporter
SM: starting material
*s*PP: syndiotactic polypropylene
TBAF: tetrabutylammonium fluoride
TBS: *tert*-butyldimethylsilyl
^{t}Bu: *tert*-butyl
TEMPO: (2,2,6,6-tetramethyl-piperidin-1-yl)oxyl
TES: triethylsilyl
Tf: trifluoromethylsulfonyl
TFA: trifluoroacetic acid

TFAA: trifluoroacetic anhydride
T_g: glass transition temperature
THF: tetrahydrofuran
TLC: thin layer chromatography
T_m: melting transition temperature
TML: Trost modular ligand
TOF: turnover frequency
T_{rxn}: temperature of reaction
t_{rxn} : length time of reaction
Ts: toluenesulfonyl
Tyr: tyrosine
UHMWPE: ultra-high molecular weight polyethylene
ω: terminal carbon of monomer that is not the olefin
Xantphos: 4,5-bis(diphenylphosphino)-9,9-dimethylxanthene

CHAPTER 1

Introduction to Carbasugars and Carbasugar Containing Natural Products, Tsuji-Trost Allylation, and Resolutions in Synthesis

1.1 Natural Products and Carbasugars

Total synthesis refers to the complete chemical synthesis of a complex molecule from simple, commercially available precursors. Since the beginnings of organic synthesis, total synthesis has always been the flagship of the science. The ability to recreate naturally occurring molecules in a laboratory setting has had a profound impact on human history and continues to play a critical role in modern society. Beginning in 1828 with Friedrich Wöhler's synthesis of urea and continuing to today, total synthesis has been transformed into an elegant combination of art and science whose development has been the result of painstaking efforts of countless scientists,[1] several of which were recognized with the Nobel prize.[2]

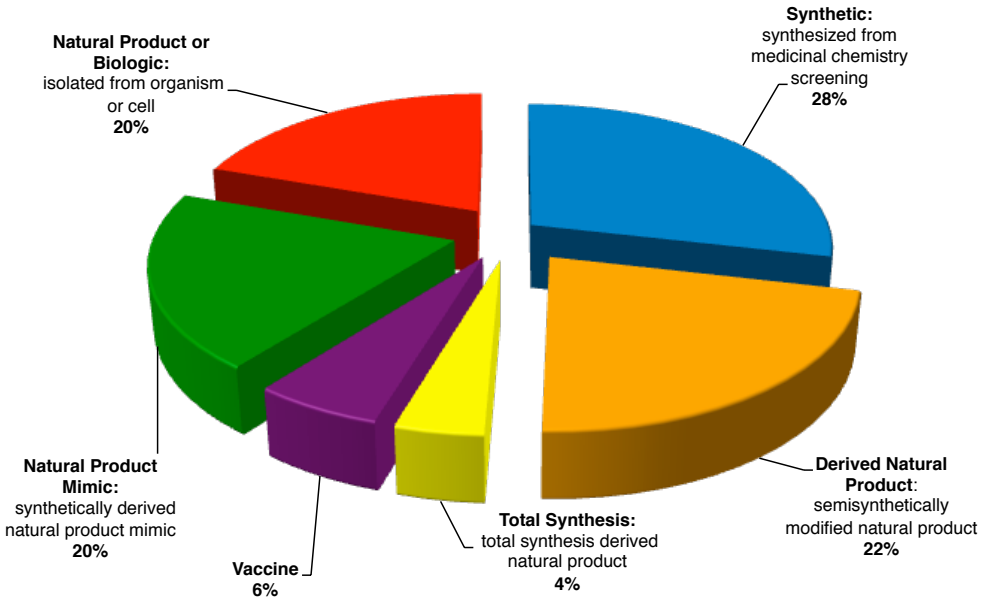

Figure 1.1. All FDA approved drugs from 1981–2010.[3]

Arguably, one of the largest impacts of chemical synthesis is on the pharmaceutical industry, as Figure 1.1 demonstrates. From 1980 to 2014,

approximately 46% of all FDA-approved pharmaceutical compounds were classified as, or coming from, natural products.[3] Semi-synthesis allows for the subsequent diversification of these complex scaffolds, yielding novel therapeutic agents. However, due to difficulties associated with isolating natural products, which typically requires tremendous amounts of biological starting material and tedious purifications resulting in low yields, we seek new routes to access these important compounds via total synthesis. Considering the percentage of drugs that rely on synthetic methods for their development is approximately 77%,[3] improving synthetic methods to render these materials remains a critical challenge at the forefront of organic synthesis.

One example that exemplifies these challenges and is of particular interest is sch202596. A spirocoumaranone, sch202596 was isolated from fungal culture of *Asperillus* sp. found in an abandoned uranium mine in Tuolemene, California. The novel compound was found to be an antagonist of the Galanin receptor,[4] which is considered an important target for the treatment of eating disorders. Synthetically, sch202596 has never been prepared, although attempts by Inoue[5] resulted in the total synthesis of (±) geodin, a related natural product that contains an identical core to sch202596 but lacks the carbasugar functionality. To complete the total synthesis of sch202596, we require a method for the synthesis of the carbasugar fragment as well as a process to append it onto its natural product core, geodin.

To understand carbasugars and their functionality, we must first review carbohydrates and glycoconjugates, which play an unprecedented role in biology and are ubiquitous throughout nature.[6] Due to their enormous structural diversity, glycoconjugates far exceed proteins or nucleic acids in their ability to encode for

cellular information. Their biological activities can range from simple energy sources to intercellular communication by activating complex signaling cascades through the binding of specific receptors.[7] When bound to natural products, carbohydrates enhance biological activity by increasing solubility, changing the mechanism of action, increasing potency, enhancing target-specific binding, or protecting against oxidative damage.[8] As a result, numerous natural products are found to contain this structural motif, as seen in Figure 1.2.

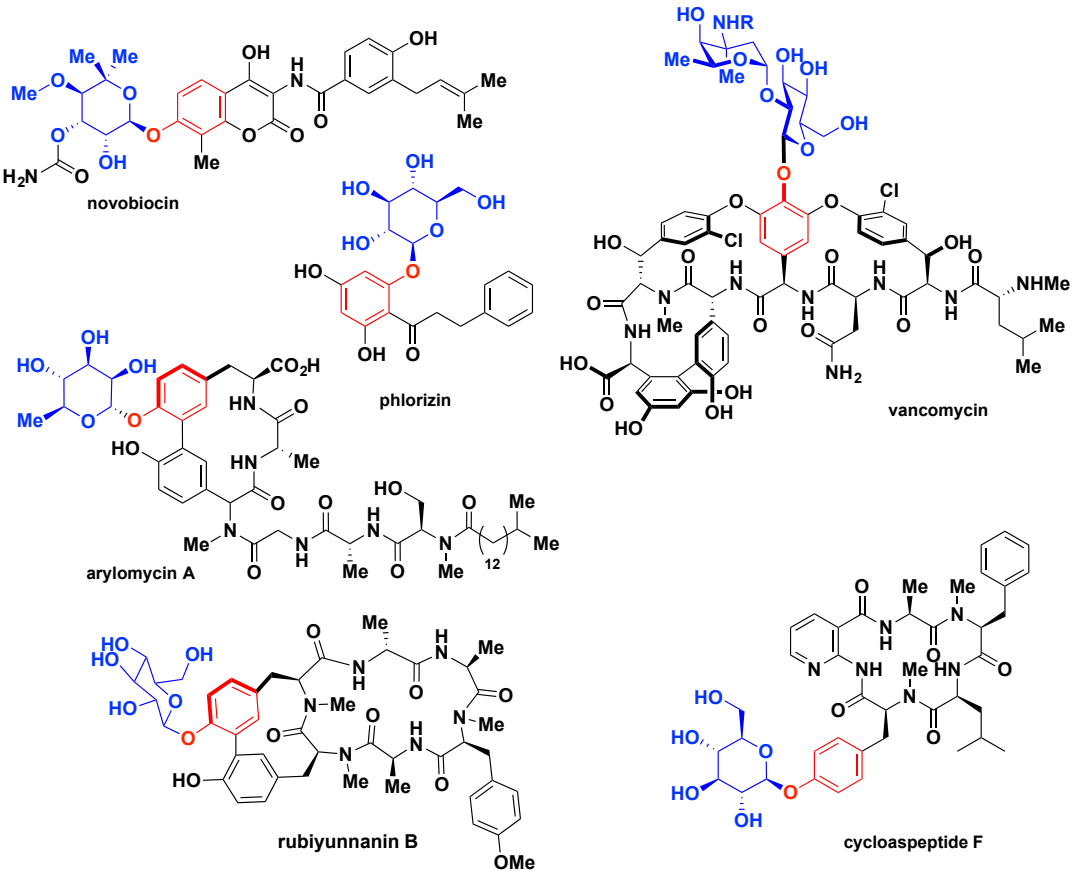

Figure 1.2. Examples of glycosylated phenolic natural products.

Although carbohydrates are biologically important, nature has developed mechanisms of deglycosylating them through scission of the glycosidic bond,

resulting in a free alcohol or phenol on the molecule. The phenol-containing molecules are particularly susceptible to this kind of deglycosylation because of the inherent stability and, therefore, lability of the phenoxide. Because of this inherent instability, half lives for phenolic charbohydrates are short, typically on the order of minutes to hours *in vivo*.[9] Natural products containing these types of phenol-bound carbohydrates are common and found in many forms, including quinones, flavonoids, tyrosine or phenylglycinol-bound polypeptides, and polyphenolic or highly substituted methoxy phenols. Once deglycosylation occurs, the agylcone species can suffer a variety of complications, ranging from a decrease in uptake or increase in excretion to decreased binding affinity or complete loss in specificity.[10] Preventing the degradation of these compounds and thus broaden their applicability has become an important field of study.

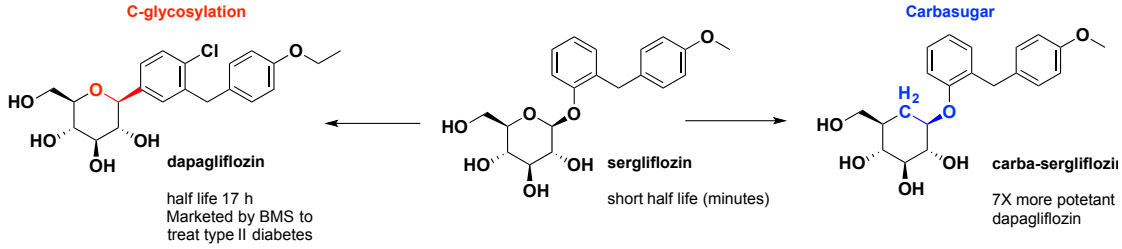

Figure 1.3. Different classes of glycomimetics.

One possible way to prevent deglycosylation is by using a non-degradable sugar or glycomimetic. While several strategies exist for increasing the stability of the glycoside, most approaches attempt to stabilize the glycosidic bond by removing the anomeric effect shown in Figure 1.3 by introducing a glycomimetic. This can be accomplished in two ways: C-glycosylation, where the oxygen leaving group moiety

is replaced with a carbon, or replacement of the endocylic oxygen in the tetrahydropyran with a methylene. Synthetic C-glycosylation has been particularly effective in the synthesis of dapagliflozin, a Bristol-Meyers Squibb marketed pharmaceutical that treats type II diabetes (Figure 1.3, left). The parent phenolic glycoside, sergliflozin, possesses a half life of only 15 minutes (presumably due to rapid deglycosylation), while the modified dapagliflozin has a half life of 17 hours.[10]

The second form of glycomimetic, where the endocyclic oxygen of carbohydrate has been replaced with a carbon linker, is commonly referred to as a carbasugar or carbocycle (Figure 1.4). Carbasugars possess a wide range of biological activity and are naturally occurring in several forms. Monomeric carba-pyranoses are rarest, with carba-galactopyranose being the only carba-pyranose found in Nature. Isolated from a *Streptomyces* broth, its bioactivity is still unknown.[11] Other, more prominent, forms of natural monomeric carbasugars are polyhydroxylcyclohexene derivatives, including MK7606, streptol, and the pericosine family members. More complex examples include polyporapyranone G and cyanthiformine B, which contain additional functionality appended to the polyhydroxylcyclohexene core. Like carbohydrates, natural carbasugars can also be found appended to the core of natural products (Figure 1.4, blue). Interesting examples include sch202596 and maximiscin, both of which possess attractive anti-cancer activity. Finally, a third class of natural carbasugars consists of polysaccharide polymers. Some examples include validamycin A (Figure 1.4, bottom), acarviosine, and acarbose, an important molecule used in the treatment of type II diabetes.[11]

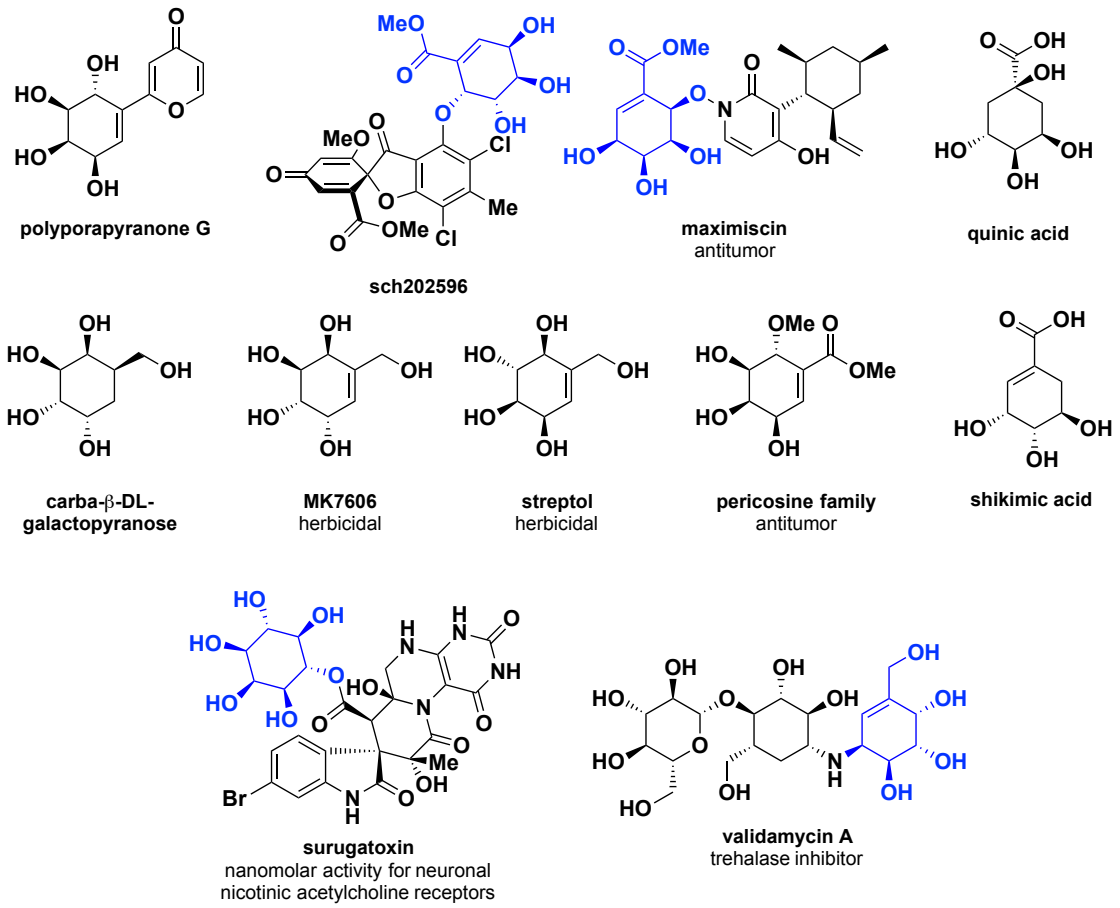

Figure 1.4. Examples of natural carbasugars and carbasugar containing compounds.

The biosynthesis of carbapyranoses occurs in several different ways, but the pentose phosphate pathway is the most predominate route.[11] This multi-step synthesis is believed to begin with sedo-heptalose-7-phosphate (**1.1**), which is then converted to a 6-membered carbocyclic intermediate (**1.7**), catalyzed by dehydroquinate synthase enzymes containing cobalt (Scheme 1.1).[12] From here, minor alterations such as epimerizations can occur to give the vast structural diversity seen in carbasugars. Alternatively, most shikimate-bound natural products, such as sch202596, are synthesized via the shikimic acid pathway.

Scheme 1.1. Proposed synthetic pathway for the synthesis of carbasugars by Nature.

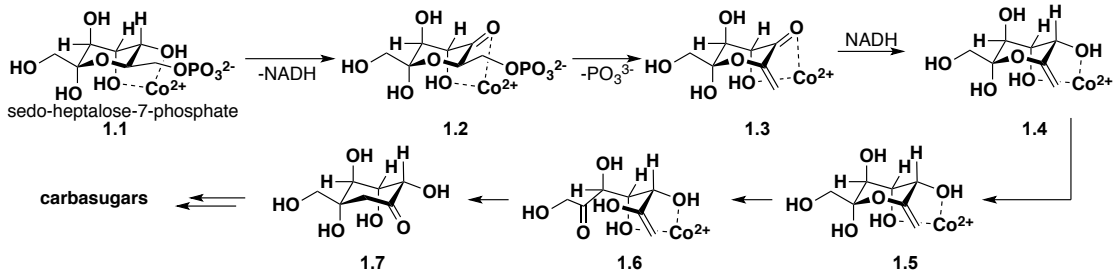

Besides their natural sources, carbasugars are also produced synthetically. The importance of synthetic carbasugars has been demonstrated by Shing and co-workers when testing compounds for use in treating type II diabetes, mentioned above (Figure 1.3, right).[10] The carbasugar variant showed a dramatic increase in selectivity and binding of the target of interest over the original carbohydrate-containing molecule (Figure 1.3, center). It is believed that the remarkable activity results from the metabolic stability imparted by the carbasugar, which maintains a structure nearly identical to the original molecule. Currently, over 140 carbasugars have been synthesized. When considering only carbasugars of the polyhydroxylcyclohexene form, there exist over 40 separate syntheses. To match the vast structural diversity of carbasugars, there are an equally diverse number of strategies and routes towards overcoming the synthetic obstacles to produce these compounds (Scheme 1.2).

The majority of carbasugar syntheses begin with compounds from the chiral pool, such as carbohydrates, tartrates, or natural cyclitols such as shikimic and quinic acid (Scheme 1.2, blue).[13] Syntheses starting from carbohydrates, similar to Nature, elongate an open chain hexose to a heptose, followed by a ring closure. Unlike Nature, though, which typically performs ring closure through an intramolecular aldol

reaction, these syntheses involve intramolecular Wittig olefinations or ring closing metathesis.[11] However, overall the chiral pool approach has several limitations. First, only a single enantiomer of the carbasugar is accessible from this route. This is problematic because the opposite enantiomer could have far superior biological activity. Second, each synthesis is unique to its target molecule; therefore, completely novel routes are required for new targets of interest.

Scheme 1.2. Strategies towards the synthesis of carbasugars.

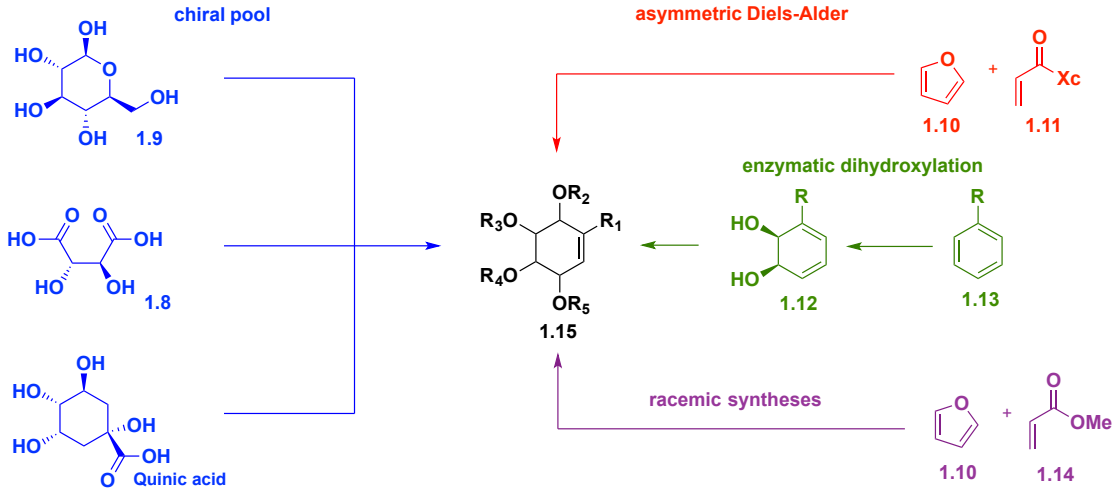

Another synthetic route towards carbasugars involves enzymatic dihydroxylation of arenes (Scheme 1.2, green).[14] This strategy has been employed by Boyd, Donahue, and Hüdlicky to synthesize a variety of carbasugars, including Pericosines A-C. Using Donahue's procedure, Boyd's efficient synthesis of pericosine A begins with the dihydroxylation of methyl benzoate to yield **1.17** using mutant strains of the soil bacterium *Pseudomonas putida* and *Escherichia coli* recombinant strains (Scheme 1.3a). This sets the stereochemistry for the remainder of the synthesis. Further oxidation OsO_4 to installs an additional set of diols (**1.18**). This is followed by

a few minor tailoring steps, including the introduction of a chloride and deprotection.[15] Overall, the approach suffers the same limitation as previous strategies in that it allows access to only a single enantiomer of the carbasugar.

Scheme 1.3. a) Boyd's synthsis of pericosine A. b) Koizumi's synthesis of carba-mannopyranose.

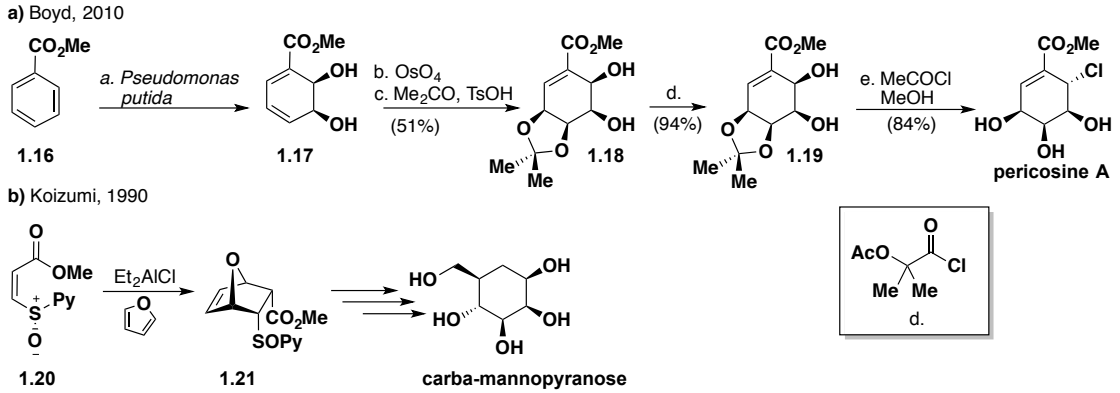

A third method for the synthesis of carbasugars is accomplished through Diels-Alder cycloadditions.[16] Many of these syntheses result in racemic products (Scheme 1.2, purple), but asymmetric routes that provide access to both enantiomers exist (Scheme 1.2, red). For example, Koizumi and coworkers synthesized a chiral sulfonate that undergoes a Diels-Alder cycloaddition to yield a bicyclic compound (scheme 1.3b). Subsequently, *endo* and *exo* isomers must be separated, followed by desulphenylation to give carba-mannopyranose in ten steps. It is important to note that in an enantiopure case, the enantiodetermining step occurs early in the synthesis, typically as the first step. The precious chiral material must then be carried through numerous steps to the final product. If the opposite enantiomer of final product is desired, the synthetic sequence must be restarted from the very beginning (**1.20**).

Furthermore, the initial source of chirality, typically a chiral auxiliary, must be removed, which adds additional steps to already lengthy sequences.

1.2 Tsuji-Trost allylations

Carbasugar skeletons commonly exhibit *syn*- or *anti*-1,2 and 1,4-cyclohexenediol structural motifs. Given the similarities of these structures, our goal was to develop a catalytic asymmetric reaction capable of generating both of these structural motifs from a single common precursor. Therefore, the reaction needs to be both stereoselective and regioselective when installing the desired hydroxyl moieties. There exist very few reactions that are capable of stereo as well as regiocontrol. One such reaction is the Tsuji-Trost allylation, which involves a palladium catalyzed substitution of allylic leaving groups (**1.22**) by a nucleophile (Scheme 1.4).[17] A wide variety of leaving groups are tolerated, including halides, carboxylates, and carbonates. This method can also be extended to allylic epoxides (**1.25**), where relief of epoxide ring strain (26-28 kcal/mol) is the driving force. An equally diverse number of nucleophiles are allowed, provided they are soft nucleophiles such as phthalimides, malonates, enolates, enamines, carboxylic acids, and phenols.

Scheme 1.4. a) Generic Tsuji-Trost reaction. b) Catalytic cycle of Tsuji-Trost reaction.

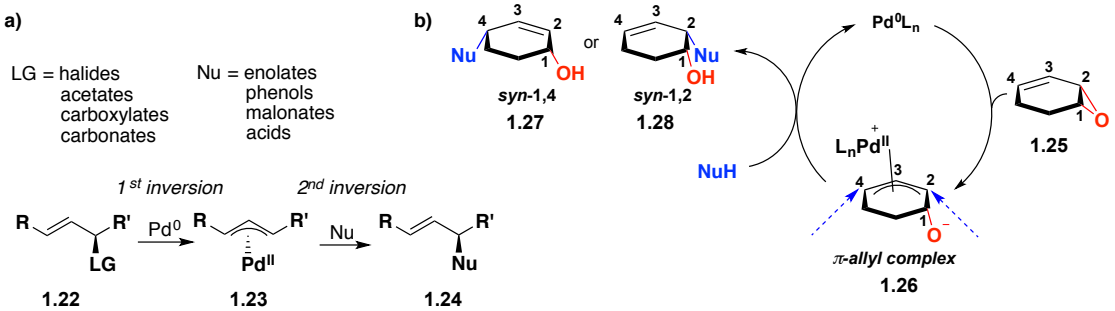

The Tsuji-Trost allylation proceeds by the addition of palladium(0) to an allylic leaving group (Scheme 1.4a, **1.22**). The displacement of the leaving group in an S_N2-type process results in a η^3 π-allyl complex (**1.23**). Subsequent nucleophile addition to the opposite face of the substrate forges the product (**1.24**) and displaces the palladium catalyst, which re-enters the catalytic cycle. Overall, this two-step mechanism proceeds through double inversion so that the product exhibits identical stereochemistry as the starting material (overall retention). When applied to linear substrates, η^3-η^1 isomerization (**1.30**–**1.33**) of the π-allyl complex can occur if it is significantly destabilized through factors such as $A^{1,3}$ or $A^{1,2}$ strain (Scheme 1.5, **1.30**). Bond rotation results in a new π-allyl complex (**1.33**), with subsequent nucleophilic addition giving products with inverted stereochemistry (**1.34**) compared to the starting material (**1.29**). In cyclic systems where bond rotation is impossible, the inversion of stereochemistry via this η^3-η^1-η^3 pathway is not observed. The regioselectivity of this reaction is controlled by electronic and steric factors with nucleophilic addition typically occurring at the less hindered terminus. When employing precursors such as allylic epoxides (Scheme 1.4b, **1.25**) or aziridines, the formation of the π-allyl generates an alkoxide (**1.26**) or amide. In most cases the incoming nucleophile protonates the anion, which results in a directed attack at the two position of the allyl complex (**1.28**).[18] Similar directed attacks are observed with nucleophiles capable of binding the anionic intermediate, such as $TMSN_3$[19] or $B(OPh)_3$.[20]

Scheme 1.5. Mechanism for allyl-inversion and *anti*-addition to linear substrates.

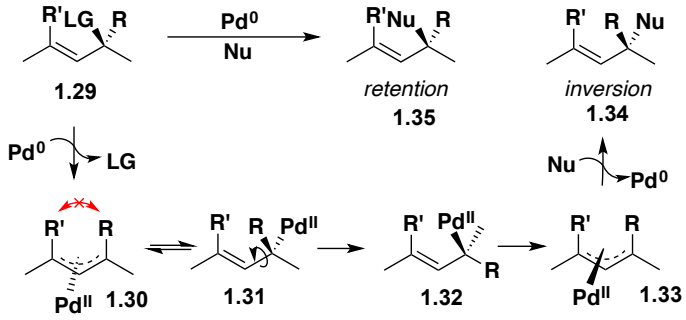

In addition to the routes described above, there exists another avenue for the formation of inverted, rather than retained, stereochemistry in the final product. As first described by Backväll using a system that employed an allylic acetate (Scheme 1.6, **1.36**), he observed inverted products (**1.39**). He speculated that this was the result of a destabilized π-allyl complex (**1.37**) being attacked by exogenous palladium(0) to yield a new, more stable π-allyl intermediate (**1.38**) with palladium(II) on the opposite face as before.[21] Using a high catalyst loading, he observed by ^{31}P NMR that two distinct π-allyl species were formed and were capable of interconverting. The ratio of retention/inversion products could be influenced by reaction conditions, and the inversion mechanism could be significantly reduced when using reactive allylic substrates, low palladium concentrations, and bidentate ligands.

Scheme 1.6. Mechanism of palladium-palladium allyl inversion in cyclic substrates.[21]

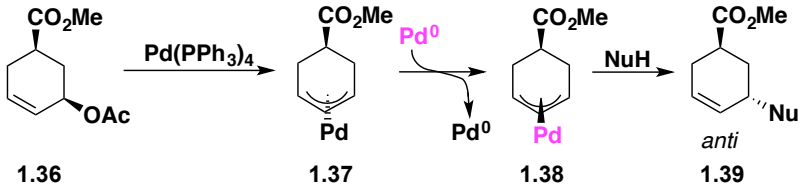

With the advent of asymmetric variants of the Tsuji-Trost allyation, a series of Trost Modular Ligands (TML) were concurrently developed.[22] TMLs are typically C2-symmetric and comprised of chiral diamine backbones that are amide bound to triarylphosphines. The most common TMLs are shown in Figure 1.5a and differ mainly in their bite angles. To help explain the outcome of reactions using these ligands, Trost originally developed a wall-and-flap model (Figure 1.5c) based on DFT studies.[23] In this model, the palladium-π-allyl sits in a pocket beneath the diammine backbone of the ligand. The phenyl groups of the ligand orient themselves to either serve as "walls" that block access to the substrate or "flaps" that allow access to the pocket.

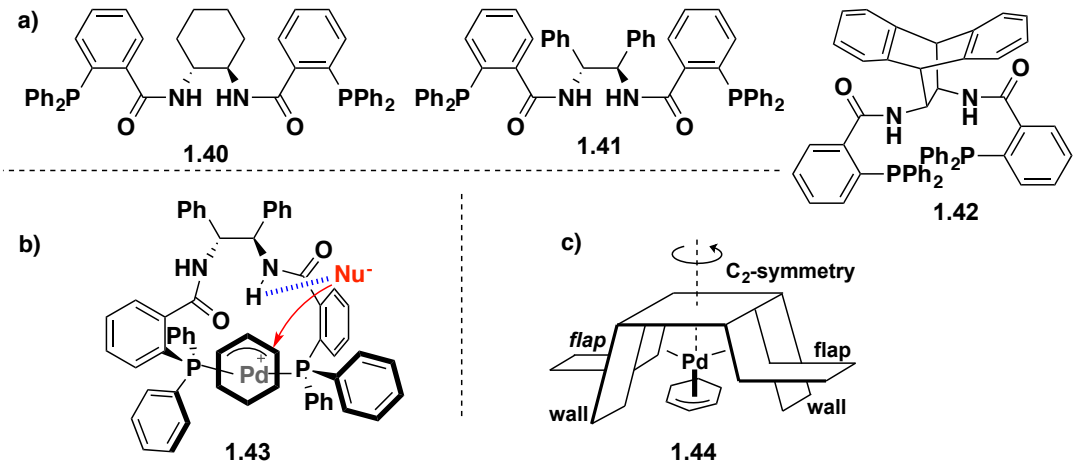

Figure 1.5. a) Examples of TMLs. b) Lloyd-Jones model for selectivity. c) Trost wall-and-flap model.

More recently, Guy Lloyd-Jones provided an alternative model to explain TML selectivity using a combination of fully deuterated TMLs and computational studies.[24] In this new model, the allyl moiety is positioned such that the amide can help ionize the leaving group and direct the incoming nucleophile into the π-allyl

(Scheme 1.5b, **1.43**). Lloyd-Jones coined the term "torqueselectivity" to describe the twisted conformation the ligand adopts in order to convey high levels of stereoinduction. This twisted profile results in one position of the allyl being slightly more exposed to the amide which is directing the attack of the incoming nucleophile. Although helpful, the model has not been used for allylic expoxides and Trost's "wall and flap" model still provides a useful explanation for almost all Tsuji-Trost asymmetric allylations.

1.3 Resolutions in Synthesis

Asymmetric catalysis is a useful method for producing stereocenters. Typically, a chiral catalyst imparts chirality onto a previously achiral material. Through this method, chiral TMLs allow many Tsuji-Trost reactions to proceed asymmetrically and install chiral centers with high levels of selectivity. An alternative approach for the generation of enantioenriched compounds is the resolution of racemic material, and chiral TMLs are also capable of this task. Resolutions can be broadly categorized into three major classes. The first are classical resolutions, which require stoichiometric amounts of chiral resolving agent (Scheme 1.7).[25] The chiral agent (**1.46**) associates to the substrate (**1.45**), either covalently or non-covalently, to generate diasteriomers (**1.47**) that are subsequently separated through other chemical means, such as crystallization. This technique is one of the oldest and most common, but its drawbacks include multistep procedures and the need for large sources of pre-existing chiral resolving agents. The second class is chiral chromatography, which relies on a chiral stationary phase to resolve pairs of enantiomers. Although effective,

the use of large volumes of solvent, long separation times, and cost of chiral chromatography supports make this method impractical for anything above analytical scale. The third class, catalysis, can be divided into multiple unique sub-classes, including kinetic, dynamic kinetic, and parrallel kinetic resolutions.

Scheme 1.7. Example of a classical resolution using stoichiometric reagent.[25]

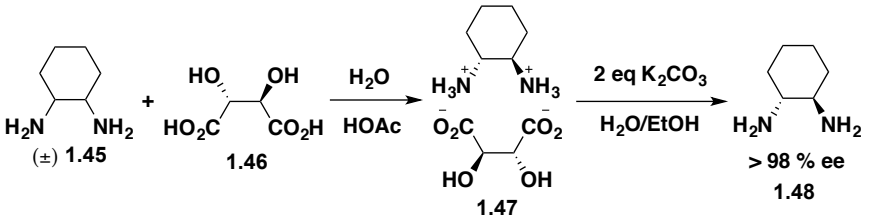

Kinetic resolutions were first pioneered by Jacobsen, Kagan, and Sharpless.[26,27] Notably, Sharpless's work focused on the use of chiral tartrates and $Ti(O^iPr)_4$ for the asymmetric epoxidation of allyl-alcohols, for which he was awarded the Nobel prize in 2001 (Scheme 1.8). In a kinetic resolution, a pair of enantiomers reacts with the chiral catalyst but at different rates, with one reacting much faster than the other. The result is a single enantioenriched product and enantioenriched starting material.[28] In order to obtain high levels of enantioinduction, a catalyst must have a high selectivity factor for one of the starting enantiomers. Another significant drawback to kinetic resolutions is their maximum theoretical yield of 50%.

Scheme 1.8. Sharpless asymmetric epoxidation using chiral tartrates.[27]

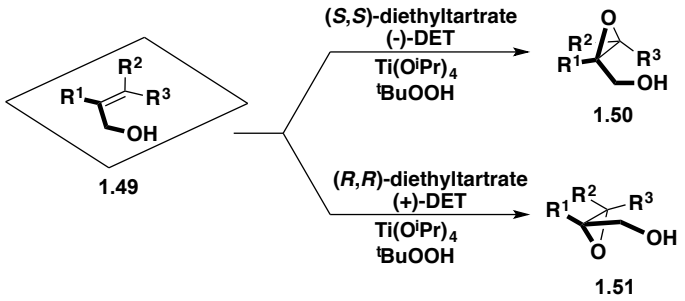

In contrast, dynamic and parallel kinetic resolutions achieve maximum theoretical yields of 100%. A dynamic kinetic resolution represents a unique case where enantiomers of starting material, or their respective intermediates before forming the final product, are interchangeable. In these situations, one enantiomer reacts readily with a chiral catalyst while the other does not. As the reactive material is consumed, the unreactive enantiomer is converted into the reactive form by some chemical means, such as base-mediated epimerization, in order to maintain equilibrium, and is then converted to product. An example of this was demonstrated by Noyori and co-workers[29] (Scheme 1.09a). Additionally, there exist numerous examples of Tsuji-Trost reactions that undergo this unique reactivity, which Trost coined the term dynamic kinetic asymmetric transformation (DYKAT) (Scheme 1.9b).[30] DYKAT's success relies on the ability of π-allyls to proceed through η^3-η^1-η^3 isomerization (**1.59**–**1.62**). This allows enantiomeric π-allyls, generated from a racemic starting material, to be converted into a single π-allyl that yields a sole enantioenriched product using a chiral ligand (**1.63**). Trost has exploited this strategy many times, such as in his total synthesis of furaquinocin E.[31] The critical stereocenter for the molecule is installed through a DKYAT, whose product is obtained in a 92:8 er before being further functionalized into the natural product.

Scheme 1.9. a) Noyori dynamic kinetic resolution.[29] b) Trost DKYAT of an allylic epoxide.[32]

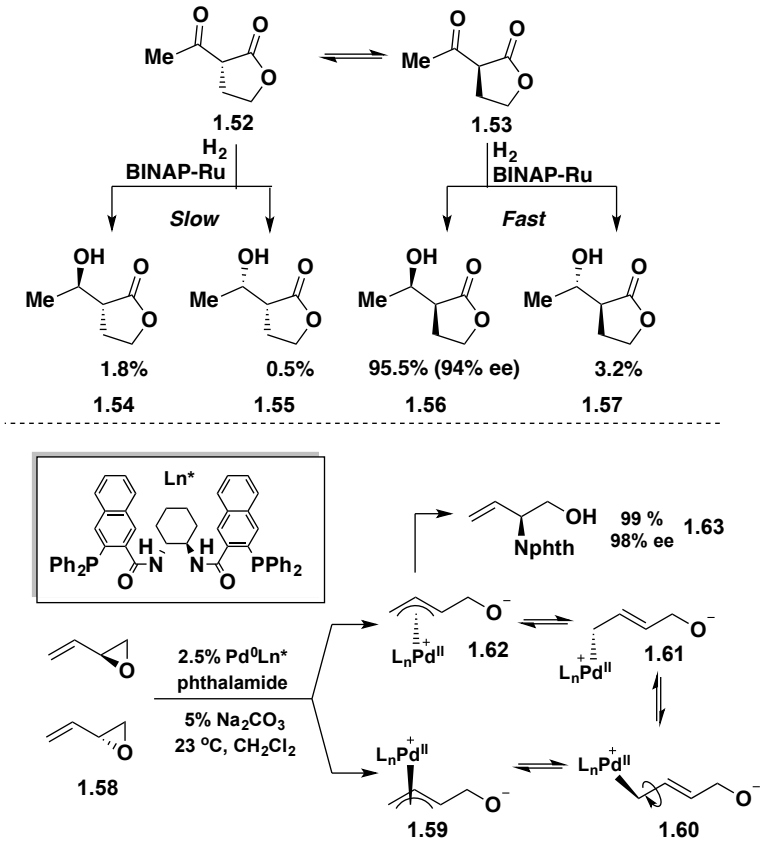

Although parallel kinetic resolutions are similar to dynamic kinetic resolutions in that both enantiomers of starting material are consumed to form product, parallel kinetic resolutions do not form a single product. Instead, each enantiomer of starting material reacts at a similar rate to produce two unique products where at least one of the products is enantioenriched.[33,11] As in kinetic resolutions, each product formed has a maximum potential of 50% yield, since each is derived from a single enantiomer of starting material. An excellent example of a parallel kinetic resolution of 4-alkynals is provided in Scheme 1.10, where Fu and co-workers use chiral rhodium-BINAP complexes to resolve racemic starting compound **1.64** into two different

enantioenriched products, **1.65** and **1.66,** in high ee at nearly the maximum theoretical yield of 50% for both.[34] The products result from two different insertions of the chiral catalyst across the alkyne. If enantiopure starting material **(+)-1.64** is subjected to the reaction conditions instead of a racemic mixture, a single product, **1.66**, is generated. Switching the enantiomer of the catalyst switches the product distribution to give compound **1.65** instead.

Scheme 1.10. Fu's parallel kinetic resolution of alkynes.[34]

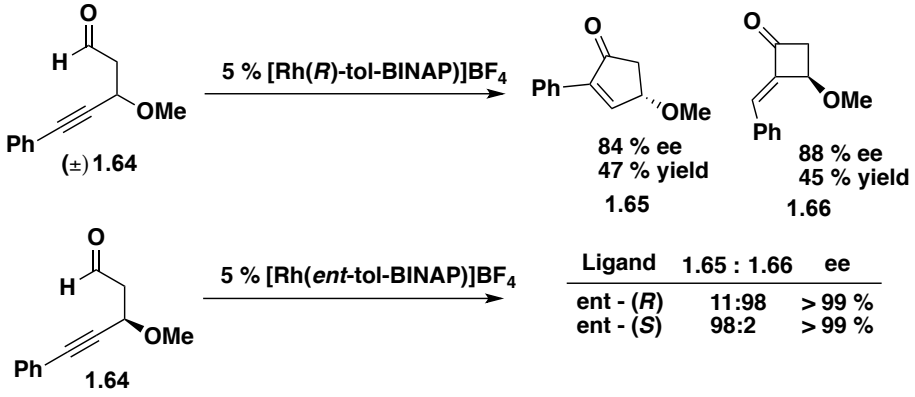

If the two products obtained from a parallel kinetic resolution install the same functional group but at different locations in the product, the procedure is called a regiodivergent parallel kinetic resolution. In the remainder of this thesis, we refer to this process as a *regio-resolution*. Regio-resolution is a subset of parallel kinetic resolution, where each enantiomer of a starting material reacts at a similar rate with a chiral catalyst to yield two regioisomeric enantioenriched compounds, which are separable. Few examples of regiodivergent parallel kinetic resolutions, or regio-resolutions, from Tsuji-Trost allylation reactions exist. Pfaltz and co-workers demonstrated that racemic allylic acetates can react with malonates, catalyzed by

chiral palladium(0), to give two enantioenriched products with addition at the 1 and 3 position of the allyl (Scheme 1.11).[35] When employing a single starting enantiomer of **1.67**, they observe mostly one product, **1.68,** in high yield. If the enantiomer of ligand is switched, so is the product distribution, giving **1.69** as the major compound.

Scheme 1.11. Pfaltz and co-workers' regio-divergent parallel kinetic resolution.[35]

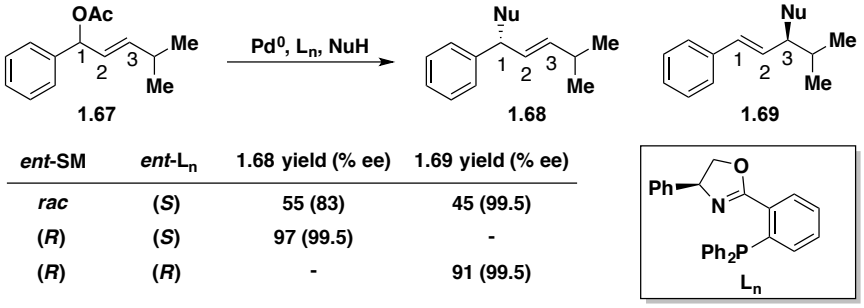

ent-SM	*ent*-L_n	1.68 yield (% ee)	1.69 yield (% ee)
rac	(*S*)	55 (83)	45 (99.5)
(*R*)	(*S*)	97 (99.5)	-
(*R*)	(*R*)	-	91 (99.5)

As we have seen, resolutions offer efficient and practical ways of generating enantiopure compounds. Particularly useful are parallel kinetic resolutions, which can diverge a single racemic synthon into multiple products. The ability to obtain multiple different products from a single intermediate is highly advantageous, especially if they are regio-isomers. Using this technique, a late stage common synthon could be efficiently transformed into multiple carbasugar products. Such an approach would offer significant improvement over current carbasugar syntheses, which mostly rely on linear routes from chiral starting materials to produce a single enantiomer and product. Further, the diverse array of stereogenic hydroxyls observed on carbasugars could be introduced through Tsuji-Trost allylation of an allylic epoxide. In the next chapter, we use these concepts to develop a new, more efficient method for synthesizing carbasugars.

References and Notes

(1) Nicolauo, K. C. Angew. Chem. Int. Ed., **2013**, 52, 131–146.

(2) Nicolauo, K. C. *Proc. R. Soc.* A 470 (470: 20130690/1-/17).

(3) Newman, D. J.; Cragg, G.M. *J. Nat. Prod.* **2012**, 75*,* 311–335.

(4) Min, C.; Mierzwa, R.; Truumees, I.; King, A.; Sapidou, E.; Barrabee, E.; Terracciano, J.; Patel, M.G.; Gullo, V.P.; Burrier, R.; Das, P.R.; Mittelman, S.; Puar, M.S. *Tetrahedron Lett.* **1997**, 38*,* 6111–6114.

(5) Katoh, T.; Ohmori, O.; Iwasaki, K.; Inoue, M.*Tetrahedron*, **2002**, 58, 1289–1299.

(6) Bertozzi, C. R.; Kiessling, L. L. *Science*, **2001**, 291, 2357–2364.

(7) (a) Cipolla, L.; Araujo, A. C.; Bini, D.; Gabrielli, L.; Russo, L.; Shaikh, N. *Expert Opin. Drug Discovery*, **2010**, 5, 721–737. (b) Kiessling, L. L.; Splain, R. A. *Annu. Rev. Biochem.*, **2010**, 79, 619–653. (c) Lepenies, B.; Yin, J.; Seeberger, P. H. *Curr. Opin. Chem. Biol.*, **2010**, 14, 404–411. (d) Agard, N. J.; Bertozzi, C. R. *Acc. Chem. Res.*, **2009**, 42, 788–797. (e) Boltje, T. J.; Buskas, T.; Boons, G. J. *Nat. Chem*., **2009**, 1, 611–622.

(8) Waymouth-Wilson, A. C. *Nat. Prod. Rep.* **1997**, 14, 99–110.

(9) (a) List, J. F.; Whaley, J. M. *Kidney Int.* **2011**, S20-27. (b) Ernst, B.; Magnani, J. L.; *Nat. Rev. Drug Discov.* **2009**, 8*,* 661–677.

(10) (a) Shing, T.K.; Ng, W.L.; Chan, J.Y.; Lau, C.B. *Angew. Chem. Int. Ed. Engl.* **2013**, 52*,* 8401–8405. (b) Hitotsuyanagi, Y.; Odagiri, M.; Kato, S.; Kusano, J.; Hasuda, T.; Fukaya, H.; Takeya, K. *Eur. J. Chem.* **2012**, 18*,* 2839–2846. (c) Fan, J.-T.; Chen, Y.-S.; Xu, W.-Y.; Du, L.; Zeng, G.-Z.; Zhang, Y.-M.; Su, J.; Li, Y.; Tan, N.-H. *Tetrahedron Lett.* **2010**, 51*,* 6810–6813.

(11) Arjona, O.; Gomez, A.M.; Lopez, J.C.; Plumet, J. *Chem. Rev.* **2007**, 107*,* 1919–2036.

(12) Mahmud, T.; Tornus, I.; Egelkrout, E.; Wolf, E.; Uy, C.; Floss, H.G.; Lee, S. *J. Am. Chem. Soc.* **1999**, *121,* 6973–6983.

(13) (a) Tripathi, S.; Shaikh, A.C.; Chen, C. *Org. Biomol. Chem.* **2011**, 9*,* 7306–7308. (b) Lygo, B.; Swiatyj, M.; Trabsa, H; Voyle, M. *Tetrahedron Lett.* **1994**, 35*,* 4197–4200. (c) Shing, T.K.; Cheng, H.M. *Org. Biomol. Chem.* **2009**, 7*,* 5098–5102. (d) Usami, Y.; Ueda, Y. *Synthesis* **2007**, *2007,* 3219-3225. (e) Usami, Y.; Takaoka, I.; Ichikawa, H.; Horibe, Y.; Tomiyama, S.; Ohtsuka, M.; Imanishi, Y.; Arimoto, M. *J. Org. Chem.* **2007**, 72*,* 6127–6134.

(14) Donohoe, T.J.; Blades, K.; Helliwell, M.; Waring, M.J.; Newcombe, N.J. *Tetrahedron Lett.* **1998**, 39*,* 8755–8758.

(15) Boyd, D.R.; Sharma, N.D.; Acaru, C.A.; Malone, J.F.; O'Dowd, C.R.; Allen, C.C.; Stevenson, P.J. *Org. Lett.* **2010**, 12*,* 2206–2209.

(16) Takahashi, T.; Kotsubo, H.; Namiki, T.; and Koizumi, T. *J. Chem. Soc., Perkin*

Trans. 1, **1990**, 3065–3072.

(17) (a) Tsuji, J.; Kataoka, H.; Kobayashi, Y. *Tetrahedron Lett.* **1981**, 22*,* 2575–2578. (b) Trost, B.M.; Crawley, M.L. *Chem Rev.* **2003**, 103*,* 2921–2944. (c) Kazmaier, U. **2011**. "Transition metal catalyzed enantioselective allylic substitution in organic synthesis." Springer Science & Business Media.

(18) (a) Trost, B.M.; Bunt, R.C.; Lemoine, R.C.; Calkins, T.L. *J. Am. Chem. Soc.* **2000**, 122*,* 5968–5976. (b) Trost, B.M.; Osipov, M.; Dong, G. *J. Am. Chem. Soc.* **2010**, 132*,* 15800–15807.

(19) Miyashita, M.; Mizutani, T.; Tadano, G.; Iwata, Y.; Miyazawa, M.; Tanino, K. *Angew. Chem. Int. Ed.* **2005**, 44*,* 5094–5097.

(20) Yu, X.Q.; Yoshimura, F.; Ito, F.; Sasaki, M.; Hirai, A.; Tanino, K.; Miyashita, M. *Angew. Chem. Int. Ed.* **2008**, 47*,* 750–754.

(21) (a) Bäckvall, J.E.; Granberg, K.L.;Heumann, A. *Isr. J. Chem.* **1991**, 31*,* 17–24. (b)Granberg, K.L.; Backvall, J.E. *J. Am. Chem. Soc.* **1992**, 114*,* 6858–6863.

(22) Trost, B.M.; Van Vranken, D.L; Bingel, C. *J. Am. Chem. Soc.* **1992**, 114*,* 9327–9343.

(23) Trost, B.M.; Toste, F.D. *J. Am. Chem. Soc.* **1999**, 121*,* 4545–4554.

(24) Butts, C.P.; Filali, E.; Lloyd-Jones, G.C.; Norrby, P.O.; Sale, D.A; Schramm, Y. *J. Am. Chem. Soc.* **2009**, 131*,* 9945–9957.

(25) (a) Jacques, J.; Collet, A.; Wilen, S. H. *Enantiomers, Racemates, and Resolutions*, Krieger, Malabar, FL, 1991. (b) Larrow, J. F.; Jacobsen E. N. *Org. Synth.* **1998**, 75, 1–11.

(26) (a) Schaus, S.E.; Brandes, B.D.; Larrow, J.F.; Tokunaga, M.; Hansen, K.B.; Gould, A.E.; Furrow, M.E.; Jacobsen, E.N. *J. Am. Chem. Soc.* **2002**, 124*,* 1307–1315. (b) See reference 26 and citations therein.

(27) Martin, V.S.; Woodard, S.S.; Katsuki, T.; Yamada, Y.; Ikeda, M.; Sharpless, K.B. *J. Am. Chem. Soc.* **1981**, 103*,* 6237–6240.

(28) Keith, J. M.; Larrow, J. F.; Jacobsen, E. N. *Adv. Synth. Catal.* **2001**, 343*,* 5–26.

(29) Kitamura, M.; Ohkuma, T.; Tokunaga, M.; Noyori, R. *Tetrahedron: Asymmetry* **1990**, 1, 1–4.

(30) For a review of DYKAT see: Ward, R.S. *Tetrahedron-Asym.* **1995**, 6*,* 1475–1490. For palladium examples see references 17 and 18.

(31) Trost, B.M.; Thiel, O.R; Tsui, H.-C *J. Am. Chem. Soc.* **2002**, 124*,* 11616–11617.

(32) Trost, B. M.; Toste, F. D. *J. Am. Chem. Soc*. **1999**, 121, 3543–3544.

(33) Vedejs, E.; Chen, X. *J. Am. Chem. Soc.* **1997**, 119*,* 2584–2585.

(34) Tanaka, K.; Fu, G.C. *J. Am. Chem. Soc.* **2003**, 125*,* 8078–8079.

(35) Loiseleur, O.; Elliott, M.C.; von Matt, P.; Pfaltz, A. *Helv. Chim. Acta.* **2000**, 83*,* 2287–2294.

CHAPTER 2

Allylic Oxide Regio Resolution as a Tool for the Total Synthesis of Carbasugars

Reproduced in part with permission from:

M. J. Moschitto, D. N. Vaccarello, C. A. Lewis, *Angewandte Chemie International Edition*, **2015**, 54, 2142–2145.

&

D. N. Vaccarello, M. J. Moschitto, C. A. Lewis, *Journal of Organic Chemistry*, **2015**, 80, 5252–5259.

2.1. Introduction

Carbasugars,[1] owing to their biomimicry of carbohydrates, possess a wide range of biological activity from antitumor to antibiotic to antifungal, and therefore are attractive targets for synthesis. Several classes of carbasugars, including MK7607, streptol, and cyathiformines, have been isolated as enantiopure products or racemates (Scheme 2.1). As described in Chapter 1, the contiguous array of stereogenic hydroxyls is typically derived from the chiral pool, enzymatic dihyroxylation of arenes, or asymmetric Diels-Alder reactions that have been used to synthesize the complex stereoarrays of natural and unnatural carbasugars. Each approach suffers its own limitation, but in all cases, the syntheses target a specific compound and single enantiomer with no intent to access the other enantiomer. Currently, there exists no single method for the synthesis of various carbasurgar stereoarrays, and their enantiomers, from a shared intermediate. A strategy that allows for enantio-, diastereo-, and regioselectivity from a common synthon could afford access to the gamut of biologically active carbasugars.

Scheme 2.1. Strategic allylic oxide regio-resolution (AORR) to access targeted carbasugar motifs.

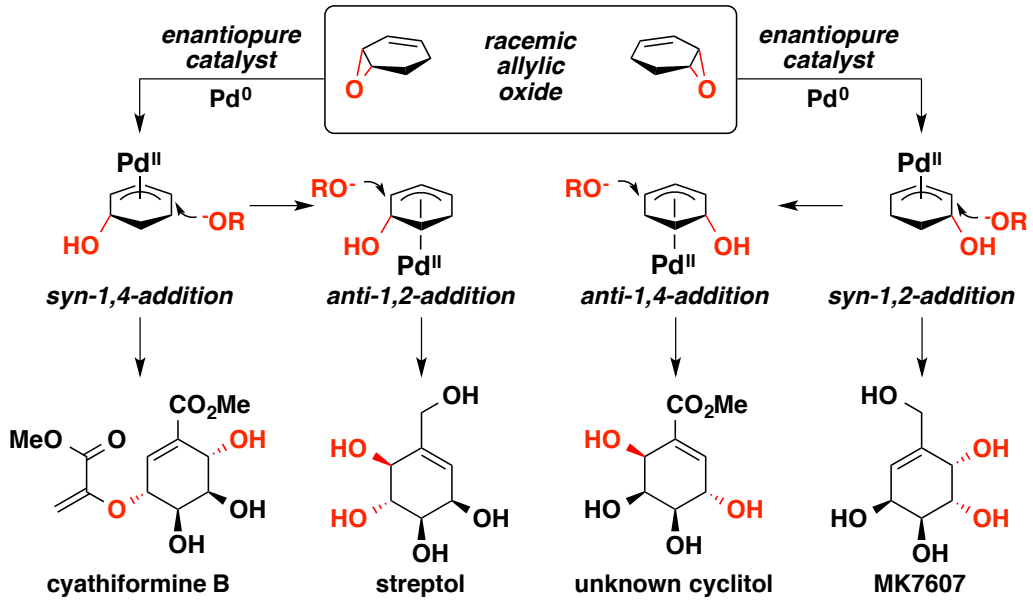

The majority of the carbasugars have *syn*- or *anti*-1,2- and 1,4-cyclohexendiol motifs. The four possible regioisomers (*syn*-1,2; *syn*-1,4; *anti*-1,2; *anti*-1,4) are notable for their relationship to a single precursor, an allylic oxide (Scheme 2.1). Ideally, a single synthon would provide all possible stereoisomers and streamline the preparation of several carbasugars. We propose the term allylic oxide regio-resolution (AORR) for this process of resolving a racemic allylic oxide to regioisomeric products using the Tsuji-Trost reaction.[2–3] Regioselective substitution[4] of enantioenriched allylic acetates with malonates has been investigated with chiral molybdenum[5] and palladium[6] complexes, resulting in regioisomeric products of 1,2- and 1,4-additions. Our efforts resulted in a catalyst-controlled AORR that delivers asymmetric 1,2- and 1,4-addition products that can be relayed to carbasugar natural products (see Scheme 2.1).

Table 2.1. Regiochemical control of enantioinduction.[a]

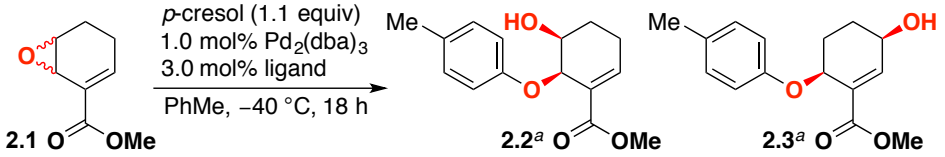

entry	oxide 2.1	ligand	2.1 er[b]	2.2 er[c]	2.3 er[c]	% yield[d] (2.1: 2.2: 2.3)
1	(±)	PPh_3	–	–	–	20:15:50
2	(±)	(*R*)-BINAP	–	–	–	n. d.[e]
3	(±)	(*R*,*R*)-**L1**	40:60	22:78	10:90	35:29:24
4	(±)	(*S*,*S*)-**L2**	57:43	96:4	93:7	2:39:34
5	(+)[f]	(*S*,*S*)-**L2**	92:8	**98:2**	32:68	31:**34**:**4**
6	(–)[g]	(*S*,*S*)-**L2**	10:90	24:76	**96:4**	28:**8**:**37**

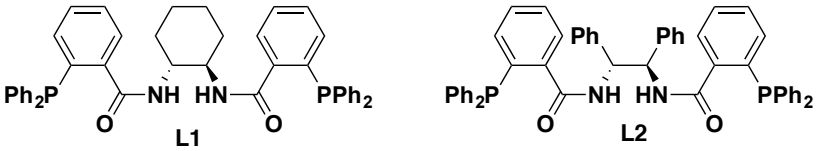

[a]Enantiomers shown are the major enantiomers derived from the *S*,*S*-ligand (entries 4–6). [b]Enantiomeric ratio of recovered epoxides was determined with GC analysis. [c]Enantiomeric ratios were determined with liquid chromatography analyses against prepared racemic standards. [d]Yield refers to isolated yields following silica gel chromatography. [e]Decomposition of epoxide. [f]Enantiomeric ratio of 92:8 favoring the (+)-**2.1** isomer. [g]Enantiomeric ratio of 10:90 favoring the (–)-**2.1** isomer. dba = dibenzylideneacetone, BINAP = 2,2'-bis(diphenylphosphino)-1,1'-binaphthyl.

2.2. Discovery and Optimization of AORR

We began our study using allylic oxide **2.1** as a model compound. It contains several critical moieties that could be subsequently transformed into carbasurgar framework, but has less complexity than a full carbasurgar making it an ideal candidate for probing reaction conditions. Oxide **2.1** was synthesized efficiently from benzoic acid according to literature procedures in four steps. Exposing a racemic mixture of oxide **2.1** to $Pd_2(dba)_3$, TML **L2**,[7] and *p*-cresol resulted in the isolation of

two products that were identified by ^{1}H NMR spectroscopy analysis of coupling constants and confirmed by COSY, to be the 1,2- and 1,4-nucleophilic addition products, **2.2** and **2.3**, respectively. **2.2**, the 1,2-product, was isolated in a 39% yield in 96:4 enantiomeric ratio (er), while **2.3**, the 1,4-product, was obtained in 34% yield with a 93:7 er (Table 2.1, entry 5). The relative stereochemistry of the two chiral centers were confirmed by X-ray crystal structure and ^{1}H NMR spectroscopy and found to be *syn* to one another, as expected. Small amounts of the starting oxide was recovered and found to be racemic providing the first signs that a regio-resolution was occurring. The cyclohexyl TML variant (**L1)** also yielded identical 1,2 and 1,4 products, albeit with reduced yields and observed enantioenrichment. Using $Pd(PPh_3)_4$ favored *syn*-1,4-addition (50% yield; Table 2.1, entry 1) over *syn*-1,2 addition (15%). The use of BINAP, a common chiral ligand, proved to be ineffectual. The high-conversion and enantioinduction of **2.2** and **2.3** and the absence of kinetic resolution of **2.1** (57:43 er after reaction) suggested that each epoxide enantiomer proceeds to a different regioisomer.

To test this hypothesis, we examined each enantioenriched epoxide of **2.1** under optimized conditions to gauge the "match"[8] to a single enantiomer of **L2** and confirm the anticipated selectivity toward either syn-1,2- or 1,4-addition (Table 2.1, entries 5 and 6). As predicted, the enantioenriched oxides smoothly converted to the *syn* products in an improved er. Notably, the (+)-oxide matched the *S*,*S* ligand to provide 1,2:1,4-addition products in an 8.5:1 ratio (entry 5), and the (−)-oxide switched the selectivity for a 1:4.6 ratio (entry 6). The recovered oxide showed no changes in enantiopurity for either entry (5 or 6).

Similar to Trost's stereoinduction of allylic acetates and carbonates,[2] the C_2-symmetric ligand blocks one of the two sites of the π-allyl, diverting each oxide to a different constitutional isomer of 1,2- or 1,4-addition. The proposed model fits the observed enantioenriched oxide data and provides a predictive basis for new studies of complex allylic oxides in total synthesis.[9]

Scheme 2.2. Proposed transition states for stereoinduction with observed product ratios.

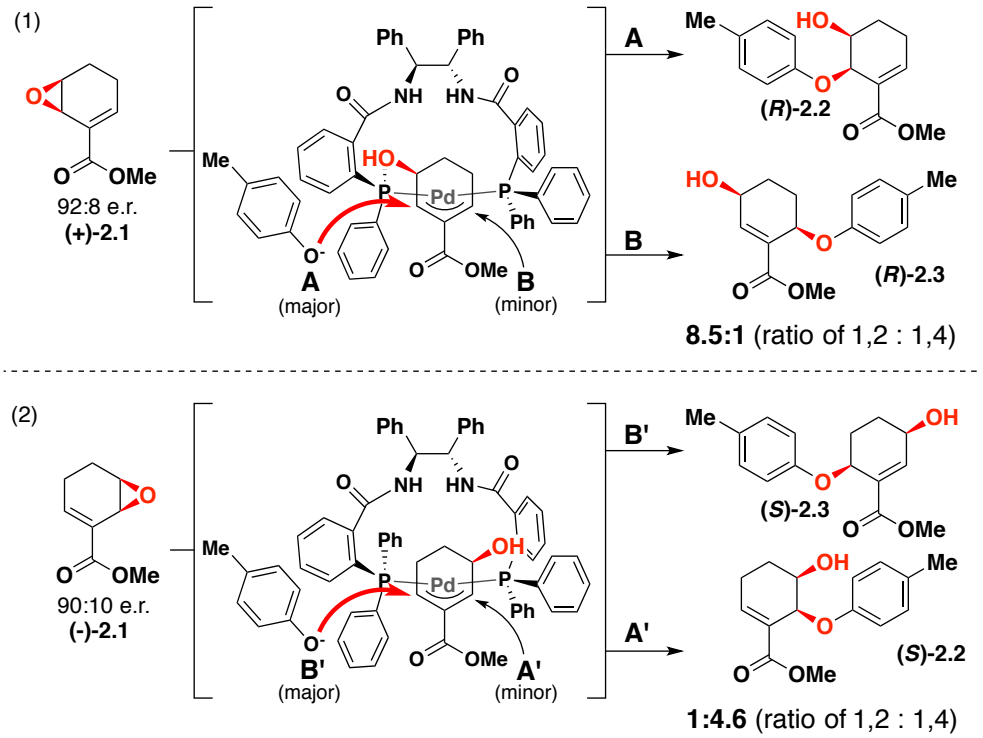

Table 2.2. Predicted and observed er values for AORR in Scheme 2.2.

	2.2 R:S		2.3 R:S	
	Predicted (er)	**Observed (er)**	**Predicted (er)**	**Observed (er)**
(+)-2.1 92:8 e.r.	99:1	98:2	67:33	68:32
(–)-2.1 90:10 e.r.	40:60	24:76	1:99	4:96

When oxide **(+)-2.1** is used, the π-allyl of the ester is generated within the complex, resulting in attack at the pro-(*R*) carbon for 1,2-addition (**2.2**; equation 1 in Scheme 2.2). The 1,4-addition is accessible using the **(–)-2.1** oxide (**2.3**; equation 2) via attack at the pro-(*S*) carbon. The selectivity of this addition is consistent with Lloyd-Jones and co-workers' studies[10] of the proposed transition states of the asymmetric allylic alkylation of cycloalkenyl esters.

The predicted enantiomeric ratios can be calculated using the observed ratio of 1,2:1,4- addition products and the enantiopurity of the oxide (Table 2.2). Beginning with the **(+)-2.1** (92:8 er), the *S*,*S* ligand predicts a 1,2-addition with an increase to 99:1 er and a decrease of the 1,4-addition product to 67:33. The observed 1,2-addition product matches a 98:2 er, with a 1,4-addition product er of 68:32. The **(−)-2.1** (90:10 er) with the *S*,*S* ligand predicts a 1:99 er of 1,4-addition products and a 40:60 er for the 1,2-addition. The observed 1,4-addition is within error at 4:96, and the 24:76 of the 1,2-addition is reasonable.

The utility of the AORR approach was then advanced with numerous phenols. Native phenol provided useful enantioinduction (Table 2.3, entry 1, 98:2 er for 1,2-addition, 91:9 for 1,4-addition) in a combined yield of 58%. Allylic oxide **2.1** was not recovered and the mass balance is suspected to be due to competitive beta-hydride elimination. Alkyl substitution (entries 2, 3) proved similar in stereoinduction and the recovered allylic oxide was weakly enantiomerically enriched. Other phenol donors such as electron releasing substituents were similarly well tolerated (entries 4 and 5) with the Boc-protected aniline providing lower conversion. 4-Hydroxy anisole[11] (entry 4) provided high levels of regiocontrol, enantioinduction, and conversion.

Furthermore, the absolute stereochemistry of addition could be determined using 4-hydroxy anisole under oxidative cleavage conditions to liberate a stereogenic hydroxyl and converge onto a known molecule. This strategy is critical to carbasurgar preparation via AORR. 4-Nitrophenol provided the highest enantioinduction (97:3 and 98:2 for 1,2- and 1,4-addition respectively, entry 6) albeit with low yield and degradation upon standing. Sterically larger arenes, including *ortho*- and *meta*-substitution (entry 7 and 8 respectively) behaved similarly, and both 1- and 2-naphthol offered less selectivity overall (entries 9 and 10). Interestingly, sesamol provided high enantioinduction for both addition modes (entry 11). In all cases, the absence of palladium resulted in no conversion.

With these data in hand, the application of the AORR method upon chiral phenolic scaffolds was examined. The substrates were chosen for their biological activity and for the emergence of diastereomers by competitive 1,2- or 1,4-addition to the palladium-allyl. Estradiol, tyrosine, and griseofulvin were selected and regiodiverged into four distinct diastereomers under catalyst control.

Silyl protected estradiol (**2.4**)[12] was first examined to gauge the suitability of larger phenol substrates with remote stereochemical elements for the regiodivergence (Scheme 2.3a). Interestingly, the regiodivergence provided high stereoselectivity for the 1,2- and 1,4-addition products with no detectable diastereomers. Using (*R,R*)-**L2**, the 1,2-adduct was obtained in 60% yield and the 1,4-adduct in 27%. The enhanced yield of the 1,2-product was surprising considering the achiral phenols were roughly equal in reactivity to produce 1,2- and 1,4-products. Switching to the (*S,S*)-**L2** ligand,

Table 2.3. Phenolic scope of regiodivergence.

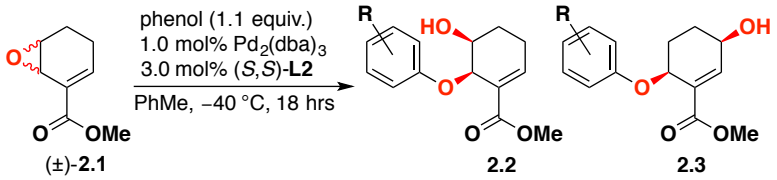

(±)-**2.1** **2.2** **2.3**

entry	phenol	**2.1** er[a]	Product	**2.2** er[b]	Product	**2.3** er[b]	% yield[c] (**2.1** : **2.2** : **2.3**)
1	**R** = H	-	**2.2a**	98:2	**2.3a**	91:9	0:31:27
2	**R** = 4-Me	57:43	**2.2b**	96:4	**2.3b**	93:7	2:39:34
3	**R** = 4-*t*Bu	52:48	**2.2c**	96:4	**2.3c**	91:9	24:28:34
4	**R** = 4-OMe	56:44	**2.2d**	85:15	**2.3d**	95:5	1:48:35
5	**R** = 4-NHBoc	51:49	**2.2e**	90:10	**2.3e**	84:16	29:21:23
6	**R** = 4-NO_2	50:50	**2.2f**	97:3	**2.3f**	98:2	64:4:4
7	**R** = 2,4-dimethyl	68:32	**2.2g**	94:6	**2.3g**	84:16	8:31:34
8	**R** = 3,5-dimethyl	52:48	**2.2h**	90:10	**2.3h**	91:9	23:31:34
9	**R** = 2-nap	-	**2.2i**	84:16	**2.3i**	84:16	0:33:33
10	**R** = 1-nap	-	**2.2j**	80:20	**2.3j**	88:12	0:35:38
11	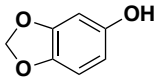	-	**2.2k**	90:10	**2.3k**	95:5	0:29:23

[a]Enantiomeric ratio of recovered epoxide was determined by GC analysis. [b]Enantiomeric ratios were determined by LC analysis against prepared racemic standards. [c]Yield refers to isolated yields following silica gel chromatography.

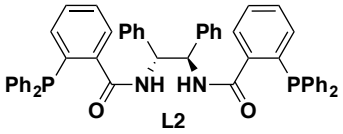

L2

the 1,2-adduct was obtained in 44% with an increase to 41% for the 1,4-addition product as compared to the (*R,R*)-**L2** ligand.

A more challenging regiodivergence was examined using tyrosine (**2.9**) (Scheme 2.3b). The protected amino-acid, as compared to estradiol, was predicted to be prone to mixtures of diastereomers from carbamate chelation to palladium[12] and/or populations of rotamers. Applying the AORR conditions resulted in the isolation of the 1,2- and 1,4-addition products in similar yield for each enantiomer of applied ligand. The additional constraints of the tyrosine moiety were reflected in the appearance of diastereomers for the 1,2-addition products: 4.37:1 for **2.10** and 4.20:1

for **2.12** in 45% and 51% yield respectively. The 1,4-adducts were isolated as single diastereomers in 40% yield for **2.11**, and 36% yield for **2.13**. The similarity in structure required the isolation of the 1,2- and 1,4-adducts as a co-mixture with ^{1}H NMR spectroscopy integration to determine yield of each isomer. The estradiol and tyrosine phenol substrates provided high-regiodivergence to the desired stereoisomers. Moving forward, the application of this method toward a multiply substituted hindered chiral phenol would demonstrate the robustness of the method with diverse phenolic substrates.

Polyketides continue to provide diverse functionality including spirocoumaranones such as griseofulvin,[14] geodin,[15] and Sch202596.[16] The interesting biological properties of these phenolic spirocycles make them ideal substrates for analog generation using AORR. The native structure of griseofulvin has recently been advanced as a cancer treatment[17] and is readily available in large quantities. Cleavage of the C-4 methyl[18] provided a chiral phenol donor (**2.14**) that was then studied for the AORR (Scheme 2.3c). In parallel with the estradiol and tyrosine studies, applying the (*R,R*)-**L2** ligand resulted in two products. The 1,2-adduct **2.15** (60%) was dominant as compared to the 1,4-adduct **2.16** (31%) with the remaining mass balance attributed to recovered griseofulvin (**2.14**). Similar to the tyrosine studies, the complexity of the 1,2- and 1,4-adducts required isolation as a co-mixture and determination of yield by ^{1}H NMR spectroscopy integration. Crude reaction mixture analysis showed no starting material remained, with griseofulvin being regenerated from degradation of the 1,2- and 1,4-adducts

Scheme 2.3. Applying AORR to estradiol, tyrosine, and giseofulvin.

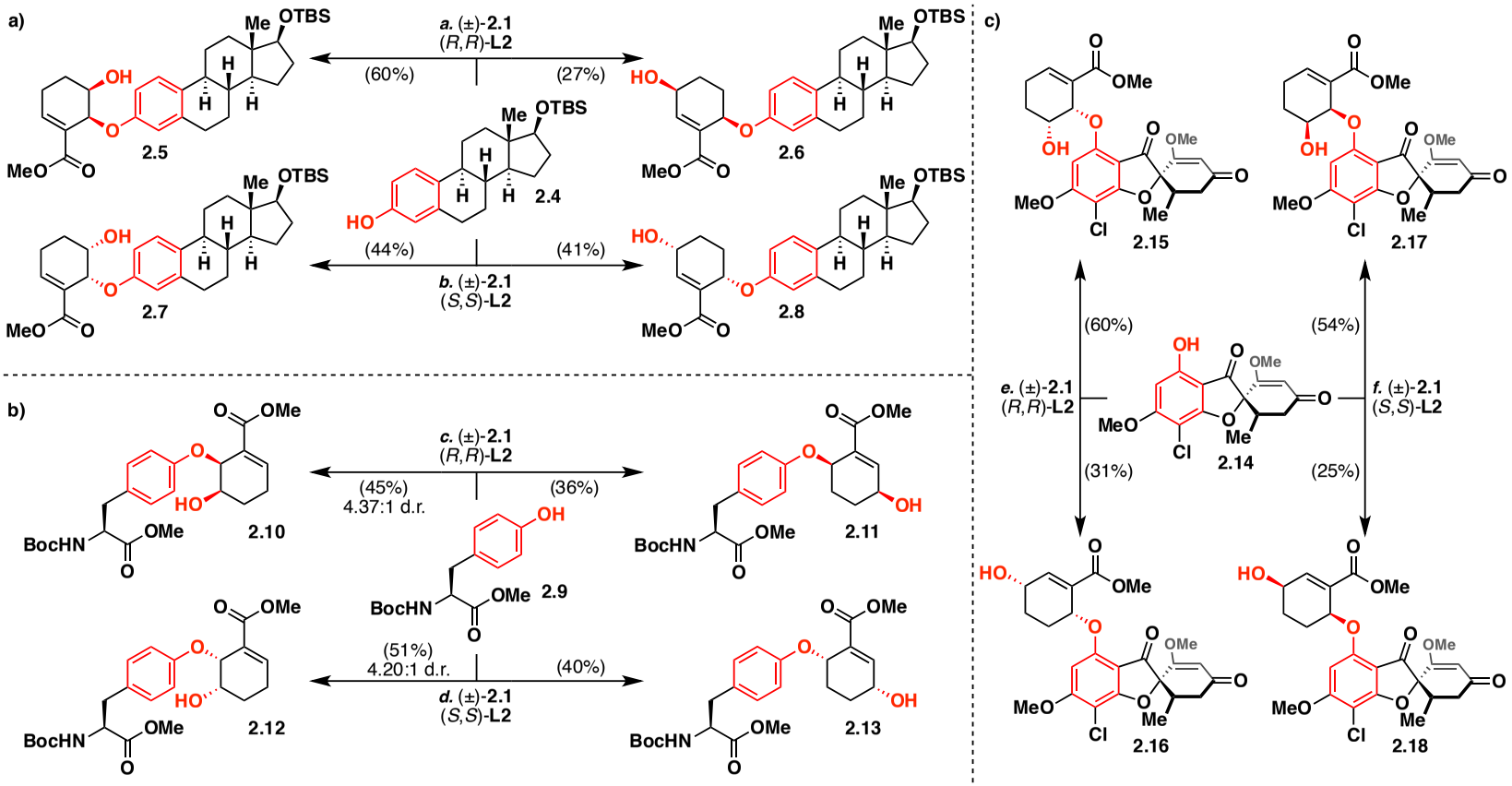

[a]Reagents and conditions: (a) 5.0 mol% $Pd_2(dba)_3$, 15.0 mol% (*R,R*)-**L2**, toluene, **2.1** (1.4 equiv.), –40 °C, 96 h; (b) 5.0 mol% $Pd_2(dba)_3$, 15.0 mol% (*S,S*)-**L2**, **2.1** (1.4 equiv.), toluene, –40 °C, 96 h; (c) 1.0 mol% $Pd_2(dba)_3$, 3.0 mol% (*R,R*)-**L2**, **2.1** (1.0 equiv.), toluene, –40 °C, 72 h; (d) 1.0 mol% $Pd_2(dba)_3$, 3.0 mol% (*S,S*)-**L2**, **2.1** (1.1 equiv.), toluene, –40 °C, 72 h; (e) 5.0 mol% $Pd_2(dba)_3$, 15.0 mol% (*R,R*)-**L2**, toluene, **2.1** (1.8 equiv.), –40 °C, 18 h; (f) 5.0 mol% $Pd_2(dba)_3$, 15.0 mol% (*S,S*)-**L2**, toluene, **2.1** (1.8 equiv.), –40 °C, 18 h.

during isolation.[19] The (*S,S*)-**L2** ligand proved similar in reactivity to provide 1,2-adduct **2.17** (54%) and 1,4-adduct **2.18** (25%) and recovered griseofulvin. The 1,2-addition products for both reactions was approximately double in yield as compared to the 1,4-products, a result we had observed previously with estradiol (Scheme 2.3a, **2.5**, (*R,R*)-**L2** ligand), and appears to substrate dependent. The presence of diastereomers associated with off-catalyst addition modes was less than 2% when examining the ^{1}H-NMR spectrum of the product mixture for both ligands.

2.3. AORR Application to Carbasugar Total Synthesis

The predictive model was then applied to carbasugar frameworks that incorporate additional functionality within the cyclohexenoate. Applying the AORR method to common synthon **2.19**[20] was anticipated to provide *syn*-1,2-addition (**2.22**) and *syn*-1,4-addition (**2.23**) products originating from the kinetic palladium π-allyl complex **2.21** (Scheme 2.4).

The steric demands of the substituted dioxolane may destabilize kinetic π-allyl complex **2.20**, resulting in conversion to the thermodynamic π-allyl complex **2.24** via an exogenous palladium(0) complex, as observed by Bäckvall.[21] Addition of the nucleophile to complex **2.25** results in two forms: *anti*-1,2 (**2.26**) and *anti*-1,4 (**2.27**). Previous efforts by Hudlicky and co-workers[22] have established that *anti*-1,2-addition of malonates to acetonide allylic oxides is possible but occurs in low yields or as mixtures of diastereomers. Common synthon **2.19** would be demonstrative of the kinetic to thermodynamic isomerization and would provide access to four classes of carbasugars.

Scheme 2.4. Kinetic and thermodynamic palladium allyl distribution and resulting diastereomers.

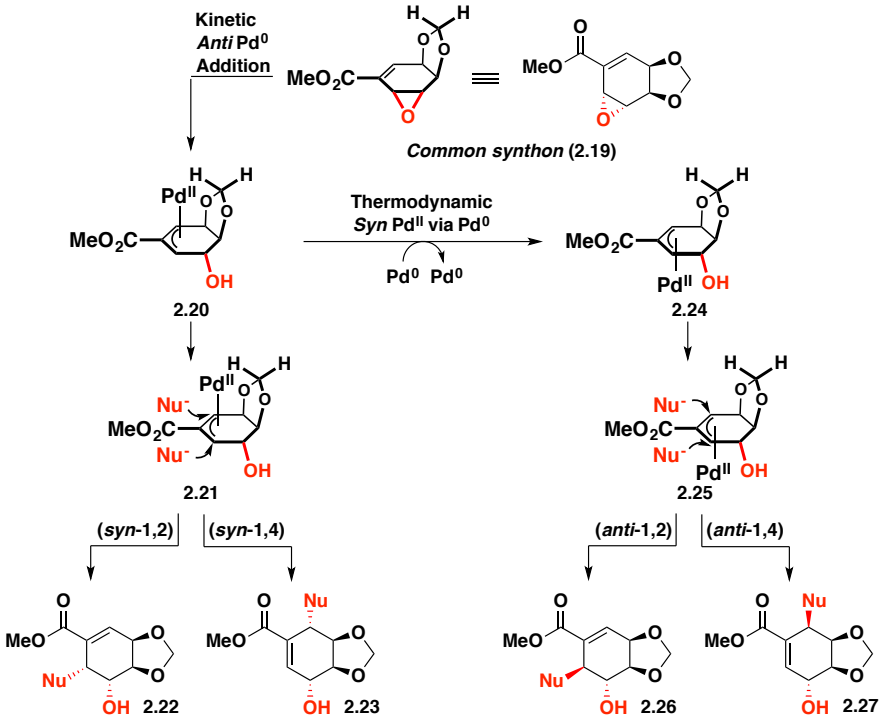

We discovered that all four possible regioisomers were formed from synthon **2.19** with the reaction proceeding to full conversion (Scheme 3a). *Anti*-1,2-addition product **2.30** was isolated in 14% yield[23] (90:10 er) and syn-1,4 product **2.31** in 16% yield (90:10 er). The high stereoselectivity, albeit with low yield, for each isomer reflects the additional constraints the dioxolane imposes on the palladium π-allyl system. The *syn*-1,2-addition product (**2.32**) was isolated in 25% yield (92:8 er) with the *anti*-1,4-addition product (**2.33**) detected in less than 1-2% by ^{1}H-NMR spectroscopy. The enhanced yield of the *syn*-1,2 product (**2.32**) was expected given the sterically encumbered *anti*-1,4-addition mode under these conditions. The three isolated regioisomeric products were then carried forward to three natural products.

The *anti*-1,2 product (**2.30**) comprises the stereoarray of streptol (**2.34**), a

potent plant growth inhibitor.[24] The conversion to streptol **2.34** was achieved by reducing the ester and protecting the transient acyl followed by cerium ammonium nitrate (CAN) oxidative cleavage of the anisole. The removal of the dioxolane using acetyl chloride and catalytic zinc chloride followed by global acyl cleavage proved uneventful. The *syn*-1,4 product (**2.31**) matches the unusual fungal metabolite cyathiformine B, a chorismic acid derivative.[25] The cyathiformine structure poses potential problems due to its sensitive enol pyruvate that could complicate the oxidative cleavage of the anisole and Lewis-acid mediated dioxolane removal. Proceeding forward, the installation of the diazophosphonate using rhodium acetate was followed by CAN oxidation with surprisingly little degradation. Horner–Wadsworth–Emmons olefination using gaseous formaldehyde provided cyathiformine B type **2.35**. The dioxolane proved difficult to remove with varying levels of success (not shown). The *syn*-1,2 product (**2.32**) mapped to MK7607[26] (**2.36**) and was targeted next. Following a similar approach to streptol, we prepared MK7607 in five steps.

The minor isomer, *anti*-1,4, **2.33**, was unisolable in the regio-resolution of oxide **2.19**. To carry out all possible additions to the allylic oxide, we determined that two criteria must be met to remove the other three regioisomers (*syn*-1,2; *syn*-1,4; *anti*-1,2): (1) the thermodynamic palladium complex must be formed to eliminate *syn*-1,2 and *syn*-1,4, and (2) the ligand must match the enantiopure oxide to eliminate *anti*-1,2 addition. The first criterion was satisfied via removal of the kinetic π-allyl isomer by increasing the steric crowding proximal to the palladium center. We hypothesized that a switch from a dioxolane to an acetonide would facilitate this population inversion, which was observed when applying racemic **2.38**[27] to the reaction conditions (see

experimental). The second criterion was fulfilled by evaluating the predicted model (Scheme 2.2) and observed modes of addition for streptol, cyathiformine B type, and MK7607, which revealed the (*S*,*S*)-**L2** to be optimal. Enantiopure acetonide oxide **2.38**[28] provided the previously unobtainable *anti*-1,4-product **2.41** in 44% yield via a predicted interconversion of **2.39** to **2.40** and ligand directed addition to the *anti*-1,4 site (Scheme 2.5b). Acylation, oxidative cleavage of the anisole and saponification of the acetate followed by acid-mediated hydrolysis of the acetonide gave the new cyclitol **2.42**.[29]

In conclusion, we developed a regiodivergent, catalyst-controlled, asymmetric addition of phenols to allylic oxides that leads to the synthesis of streptol, MK7607, cyathiformine B type, and a novel cyclitol. The AORR method tolerates complex, fully substituted cyclohexenoates to provide access to the enantiomers of carbasugar natural products. The mechanistic dichotomy of the *syn* versus *anti* chiral palladium complexes and the study of complex nucleophiles and allylic oxides will be reported in due course.

Scheme 2.5. Applying AORR for the total synthesis of streptol, cyathiformine B, MK 7607, and a new cyclitol. a) Results with a racemic oxide. b) Results with chiral pool.

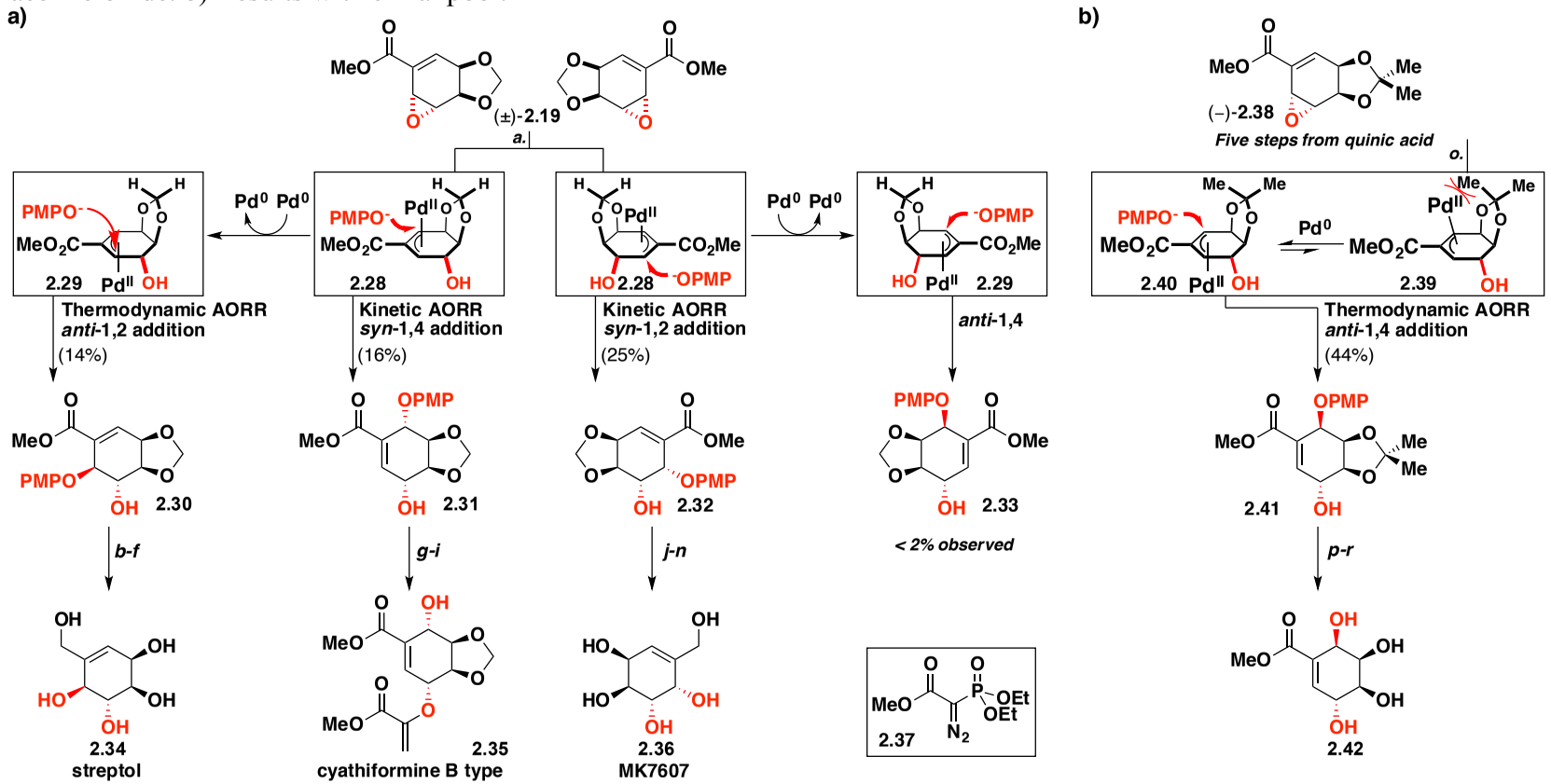

[a]Reagents and conditions: (a) 10 mol% $Pd_2(dba)_3$, 30 mol% (*R,R*)-**L2**, *p*-OMePhOH (1.2 equiv), PhMe, 23 °C, 48 h (14% **2.30** (90:10 er), 16% **2.31** (90:10 er), 25% **2.32** (92:8 er)); (b) DIBAlH (3.5 equiv), DCM, 0.3 h, 38%; (c) Ac_2O (3.0 equiv), DIPEA, DMAP, DCM. 0.3 h; (d) CAN (2.2 equiv), MeCN/H_2O 4:1, 0.20 h, 49% (two steps); (e) (1) AcCl, then $ZnCl_2$ (0.1 equiv) 0 to 23 °C; (2) H_2O, THF, 0.3 h; (f) NaOMe (1 equiv) MeOH, 16 h, 55% (two steps); (g) $Rh_2(OAc)_2$, **2.37**, DCM, 5 h, reflux, 64%; (h) CAN (2.2 equiv), MeCN/H_2O 4:1, 0.20 h, 81%; (i) LiHMDS, CH_2O, THF, 2 h, -78 °C, 71%; (j) DIBAlH (3.5 equiv), DCM, 0.3 h 28%; (k) Ac_2O (3 equiv), DIPEA, DMAP, DCM 0.3 h; (l) CAN (2.2 equiv), MeCN/H_2O 4:1, 0.20 h, 21% (two steps); (m) (1) AcCl, then $ZnCl_2$ (0.1 equiv) 0 to 23°C; (2) H_2O, THF, 0.3 h, (n) NaOMe (1 equiv) MeOH, 16 h, 57% (two steps), (o) 10 mol% $Pd_2(dba)_3$, 30 mol% (*S,S*)-**L2**, *p*-OMePhOH (1.2 equiv.), PhMe, 23 °C, 48 h, 44%; (p) (1) Ac_2O (3 equiv), DIPEA, DMAP, DCM, 0.3 h; (2) CAN (2. 2 equiv), MeCN/H_2O 4:1, 0.20 h, 63%; (q) (1) NaOMe, MeOH 0.1 h, 23 °C, 98%; (2) TFA, MeOH, 40 °C, 7 h, 51%. dba = dibenzylideneacetone, DIBAlH = diisobutylaluminum hydride, DIPEA = diisopropylethylamine, DMAP = 4-(dimethylamino)pyridine, CAN = ceric ammonium nitrate, LiHMDS = lithium hexamethyldisilylazide, TFA = trifluoroacetic acid.

2.4 Experimental

Methyl 1,3-cyclohexadiene-2-carboxylate was prepared according to literature procedures.[30] The diene carboxylate (2.01 g, 14.5 mmols, 1.0 equiv) was exposed to *m*-CPBA (3.38 g, 19.6 mmols, 1.3 equiv) in DCM (140.0 mL) at 0 °C for 6 h. The reaction was then poured into 100.0 mL of a cooled 1 M solution of NaOH, extracted with DCM (3 x 50.0 mL) and dried over Na_2SO_4. Flash column chromatography of the crude oil (9:1 hexanes/EtOAc, v/v) resulted in 1.36 g (61% yield) of a volatile colorless oil (**2.1**).

Enantioenriched epoxide **(+)-2.1** was prepared using the corresponding [*N*,*N*'-bis(3,5-di-tertbutylsalicylidene)-1,2cyclohexane-diaminato]manganese(III) chloride complex according to literature procedure.[31] To a buffered solution of 0.05 M Na_2HPO_4 and bleach (10.0 mL, 0.55 M in NaOCl) was added methyl 1,3-cyclohexadiene-2-carboxylate (400.0 mg, 2.89 mmol, 1.0 equiv) and *R,R* [*N*,*N*'-bis(3,5-di-tertbutylsalicylidene)-1,2cyclohexane-diaminato] manganese(III) chloride (185.0 mg, 0.289 mmol, 0.1 equiv) in DCM (4.0 mL). The reaction was stirred for 18 hours under air after which the layers were separated. The aqueous layer was extracted with DCM (10.0 mL), and the combined organic layers were washed with brine (10.0 mL), dried over Na_2SO_4 and concentrated *in vacuo*. Flash column chromatography (9.5:1 hexanes/EtOAc) yielded (80.3 mg, 0.519 mmol) enantioenriched **(+)-2.1** as a yellow oil. Analysis by chiral GC indicated **(+)-2.1** ($[\alpha]_D^{20.0}$ +31.9 (*c* 1.00, $CHCl_3$) was obtained in a 90:10 enantiomeric ratio.

Methyl 7-oxabicyclo[4.1.0]hept-2-ene-2-carboxylate (2.1)

^{1}H NMR (400 MHz, $CDCl_3$) δ 7.11 (m, 1H), 3.92 (m, 1H), 3.79 (s, 3H), 3.59 (m, 1H), 2.31 (m, 1H), 2.20 (m, 1H), 1.61 (m, 1H), 1.27 (m, 1H); **^{13}C NMR** (101 MHz, $CDCl_3$) δ 165.9, 143.0, 127.6, 54.2, 51.5, 45.8, 20.5, 19.7; **IR** (neat) ν = 2932, 2857, 1715, 1641, 1268 cm^{-1}; **TLC** R_f = 0.60 (9:1 hexanes/EtOAc v/v); **HRMS** (ES^+) calc'd for $C_8H_{10}O_3$ 154.0630; found 154.0625.

General Procedure A: Racemic epoxide **2.1** (43.0 mg, 0.279 mmol, 1.0 equiv.) was dissolved in 2.0 mL of toluene in a flame-dried vial outfitted with a septum followed by the addition of phenol (15.8 mg, 0.149 mmol, 0.6 equiv.). The resulting solution was degassed with argon and cooled to −40 °C. In a separate vial, $Pd_2(dba)_3$ (2.4 mg, 1.0 mol%) and (*S,S*)-**L2**[7] (6.6 mg, 3.0 mol%) were dissolved in 1.0 mL of toluene. The resulting purple solution was degassed and stirred at room temperature until it became yellow (approx. 10 min.). The solution was then cooled to −40 °C and added to the epoxide solution via syringe. The reaction was allowed to stir for 6 hours before additional phenol (16.4 mg (0.174 mmol, 0.6 equiv.) was added and the solution purged with argon. The reaction was stirred for an additional 12 hours at −40 °C before the reaction was quenched with an aqueous NH_4Cl solution, extracted with ether (2 x 1.5 mL), dried with $MgSO_4$, and concentrated under reduced pressure. The crude oil was purified by column chromatography (9:1 hexanes:EtOAc v/v) to give 1,2-product **2.2a** (21.5 mg, 31% yield, 98:2 e.r.) and 1,4-product **2.3a** (18.7 mg, 27% yield, 91:9 e.r.) as white solids.

Analytical standards used for the characterization of **2.2a** and **2.3a** were prepared from a separate trial giving enantiomeric ratios of 97:3 and 95:5 respectively.

Methyl (5S, 6R)-5-hydroxy-6-O-(phenoxy)-cyclohex-1-enecarboxylate (2.2a)

$[\alpha]_D^{20.0}$ −127.7 (*c* 1.00, $CHCl_3$); **M.p.** 63 – 66 °C; **^{1}H NMR** (400 MHz, $CDCl_3$) δ 7.32 – 7.25 (m, 2H), 7.20 – 7.15 (m, 2H), 7.15 – 7.12 (m, 1H), 7.02 – 6.91 (m, 1H), 5.28 (d, *J* = 3.7 Hz, 1H), 3.92 (dt, *J* = 11.5, 3.8 Hz, 1H), 3.61 (s, 3H), 2.54 (m, 1H), 2.39 – 2.26 (m, 1H), 2.10 – 1.93 (m, 1H), 1.93 – 1.82 (m, 1H); **^{13}C NMR** (75 MHz, $CDCl_3$) δ 166.5, 159.6, 144.0, 129.5, 122.0, 117.3, 115.9, 73.2, 69.5, 51.8, 25.3, 25.3; **IR** (film, cm^{-1}) 3435, 2950, 2360, 1710, 1595, 1490, 1250, 1227, 750; **TLC** R_f = 0.37 (7:3 hexanes:EtOAc v/v); **HPLC** 97:3 e.r., Chiral HPLC eluting at 1.0 mL/min with 95% hexanes:methanol. Retention times: R_T= 8.0 min, 10.7 min; **HRMS** (EI^+) *m/z* Calc'd for $C_{14}H_{16}O_4$ 248.1049, found 248.1047.

Methyl (3R, 6S)-3-hydroxy-6-O-(phenoxy)-cyclohex-1-enecarboxylate (2.3a)

$[\alpha]_D^{20.0}$ −20.8 (*c* 0.50, $CHCl_3$); **M.p.** 36 – 39 °C; **^{1}H NMR** (400 MHz, $CDCl_3$) δ 7.32 – 7.25 (m, 2H), 7.12 (t, *J* = 1.8, 1.8 Hz, 1H), 7.04 – 6.95 (m, 3H), 5.14 (br s, 1H), 4.34 (d, *J* = 8.5 Hz, 1H), 3.75 (s, 3H), 2.24 – 2.14 (m, 1H), 2.05 – 1.96 (m, 1H), 1.91 – 1.77 (m, 1H), 1.61 (tt, *J* = 14.2, 3.2 Hz, 1H); **^{13}C NMR** (75 MHz, $CDCl_3$) δ 166.3, 158.0, 145.8, 130.5, 129.6, 121.6, 116.9, 68.1, 67.8, 52.1, 26.5, 25.3; **IR** (film, cm^{-1}) 3403, 2950, 2358, 1718, 1490, 1250, 1226, 751; **TLC** R_f = 0.25 (7:3 hexanes:EtOAc v/v); **HPLC** 95:5 e.r., Chiral HPLC eluting at 1.0 mL/min with 90% hexanes:isopropanol. Retention times: R_T= 5.9 min, 6.6 min; **HRMS** (EI^+) *m/z* Calc'd for $C_{14}H_{16}O_4$ 248.1049, found 248.1055.

1,2-product **2.2b** (32% yield) and 25.0 mg (47% yield) of 1,4-product **2.3b** as white solids. The recovered epoxide **2.1** (2%) was recovered in 57:43 enantiomeric ratio.

Methyl (5*S*,6*R*)-5-hydroxy-6-(*p*-tolyloxy)cyclohex-1-ene-1-carboxylate (2.2b)

$[\alpha]_D^{20.0}$ −112.4 (*c* 1.00, $CHCl_3$); **M.p.** 88 – 90 °C **^{1}H NMR** ($CDCl_3$, 400 MHz) δ 7.14 (dd, *J* = 4.8, 3.0 Hz, 1H), 7.09 – 7.01 (m, 4H), 5.20 (d, *J* = 3.8 Hz, 1H), 3.88 (ddt, *J* = 11.4, 9.2, 3.7 Hz, 1H), 3.61 (s, 3H), 2.59 – 2.46 (m, 1H), 2.35 – 2.25 (m, 1H), 2.28 (s, 3H), 2.14 (d, *J* = 9.2 Hz, 1H), 2.02 – 1.92 (m, 1H), 1.90 – 1.80 (m, 1H); **^{13}C NMR** ($CDCl_3$, 100 MHz) δ 166.5, 157.5, 143.9, 131.3, 129.9, 129.4, 117.2, 73.4, 69.4, 51.8*, 51.8*, 25.2, 20.6; **IR** (film, cm^{-1}) 3450, 3312, 2219, 1698, 506, 1221, 983, 796, 734; **TLC** R_f = 0.32 (7:3 hexanes/EtOAc v/v); **HPLC** 96:4 e.r., Chiral HPLC eluting at 1.0 mL/min with 95% hexanes/isopropanol. Retention times: R_T= 7.6 min, 9.6 min; **HRMS** (EI^+) *m/z* Calc'd for $C_{15}H_{18}O_4$ 262.1205, found 262.1200. * denotes presumed rotamers in a 1:1 ratio.

Methyl (3*R*,6*S*)-3-hydroxy-6-(*p*-tolyloxy)cyclohex-1-ene-1-carboxylate (2.3b)

$[\alpha]_D^{20.0}$ −12.1 (*c* 1.00, $CHCl_3$); **M.p.** 94 – 98 °C; **^{1}H NMR** ($CDCl_3$, 400 MHz) δ 7.14 – 7.06 (m, 3H), 6.95 – 6.88 (m, 2H), 5.07 (br s, 1H), 4.36 – 4.28 (m, 1H), 3.76 (s, 3H), 2.29 (s, 3H), 2.21 – 2.14 (m, 1H), 2.04 – 1.96 (m, 1H), 1.92 – 1.77 (m, 1H), 1.57 (dt, *J* = 3.5 Hz, 14.2 Hz 1H); **^{13}C NMR** ($CDCl_3$, 75 MHz) δ 166.4, 155.9, 145.8, 131.0, 130.6, 130.1, 117.1, 68.6, 67.8, 52.1, 26.4, 25.3, 20.7; **IR** (film, cm^{-1}) 3175, 2954, 1713, 1508, 1251, 1226, 1025, 960, 812; **TLC** R_f = 0.21 (7:3 hexanes/EtOAc v/v); **HPLC** 93:7 e.r., Chiral HPLC eluting at 1.0 mL/min with 90% hexanes/isopropanol. Retention times: R_T= 5.7 min, 8.4 min; **HRMS** (EI^+) *m/z* Calc'd for $C_{15}H_{18}O_4$ 262.1205, found 262.1202.

1,2-product **2.2c** (21.9 mg, 28%, 96:4 e.r.) and 1,4-product **2.3c** (26.9 mg, 34%, 91:9 e.r.). Recovered epoxide **2.1** (9.5 mg, 24%, 52:48 e.r.).

Analytical standards used for the characterization of **2.2c** and **2.3c** were prepared from a separate trial giving enantiomeric ratios of 96:4 and 91:9 respectively.

Methyl (5S, 6R)-5-hydroxy-6-O-(4-*tert*-butylphenoxy)-cyclohex-1-enecarboxylate (2.2c)

$[\alpha]_D^{20.0}$ −92.4 (*c* 1.00, $CHCl_3$); **M.p.** 53 – 56 °C; **^{1}H NMR** ($CDCl_3$, 300 MHz) δ 7.35 – 7.24 (m, 2H), 7.15 (dd, *J* = 4.7, 3.0 Hz, 1H), 7.11 – 7.03 (m, 2H), 5.26 (d, *J* = 3.8 Hz, 1H), 3.90 (dt, *J* = 11.2, 3.7 Hz, 1H), 3.61 (s, 3H), 2.61 – 2.46 (m, 1H), 2.39 – 2.23 (m, 1H), 2.15 – 1.90 (m, 1H), 1.91 – 1.79 (m, 1H), 1.29 (s, 9H); **^{13}C NMR** ($CDCl_3$, 75 MHz) δ 166.6, 157.2, 144.6, 143.9, 134.7, 129.4, 126.3, 116.7, 73.1, 69.5, 51.8, 34.2, 31.6, 25.4, 25.2; **IR** (film, cm^{-1}) 3435, 2953, 2358, 1716, 1509, 1220, 1043; **TLC** R_f = 0.42 (7:3 hexanes:EtOAc v/v); **HPLC** 96:4 e.r, Chiral HPLC eluting at 1.0 mL/min with 95% hexanes:isopropanol. Retention times: R_T= 6.7 min, 7.2 min; **HRMS** (EI^+) *m/z* Calc'd for $C_{18}H_{24}O_4$ 304.1675, found 304.1661.

Methyl (3R, 6S)-3-hydroxy-6-O-(4-*tert*-butylphenoxy)-cyclohex-1-enecarboxylate (2.3c)

$[\alpha]_D^{20.0}$ −10.1 (*c* 0.75, $CHCl_3$); **^{1}H NMR** ($CDCl_3$, 400 MHz) δ 7.33 – 7.27 (m, 2H), 7.11 (br s, 1H), 6.96 – 6.91 (m, 2H), 5.11 (br s, 1H), 4.37 – 4.28 (m, 1H), 3.75 (s, 3H), 2.24 – 2.15 (m, 1H), 2.03 – 1.95 (m, 1H), 1.88 – 1.77 (m, 1H), 1.58 (tt, *J* = 14.2, 3.4 Hz, 1H), 1.29 (s, 9H); **^{13}C NMR** ($CDCl_3$, 100 MHz) δ 166.4, 155.6, 145.7, 144.2,

130.6, 126.4, 116.3, 68.0, 67.8, 52.1*, 52.1*, 34.2, 31.6, 26.5, 25.3; **IR** (film, cm^{-1}) 3399, 2952, 2867, 2359, 1718, 1508, 1250, 1225, 1030, 757; TLC R_f = 0.29 (7:3 hexanes:EtOAc v/v); **HPLC** 91:9 e.r., Chiral HPLC eluting at 1.0 mL/min with 90% hexanes:isopropanol. Retention times: R_T= 4.6 min, 6.0 min; **HRMS** (EI^+) *m/z* Calc'd for $C_{18}H_{24}O_4$ 304.1675, found 304.1673. * denotes presumed rotamers in a 1:1 ratio.

1,2-product **2.2d** (48% yield) as a pale yellow oil and 443.0 mg (35% yield) of 1,4-product **2.3d** as waxy white solid. The epoxide (**2.1**, >1%) was recovered in 56:44 enantiomeric ratio.

Methyl (5*S*,6*R*)-5-hydroxy-6-(4-methoxyphenoxy)cyclohex-1-ene-1-carboxylate (2.2d)

$[\alpha]_D^{20.0}$ −114.9 (*c* 1.00, $CHCl_3$); **^{1}H NMR** ($CDCl_3$, 300 MHz) δ 7.14 (dd, *J* = 4.6, 3.1 Hz, 1H), 7.12 – 7.04 (m, 2H), 6.84 – 6.78 (m, 2H), 5.11 (d, *J* = 3.7 Hz, 1H), 3.89 (dt, *J* = 11.3, 3.8 Hz, 1H), 3.77 (s, 3H), 3.61 (s, 3H), 2.61 – 2.46 (m, 1H), 2.39 – 2.22 (m, 1H), 2.06 – 1.95 (m, 1H), 1.91 – 1.81 (m, 1H); **^{13}C NMR** ($CDCl_3$, 75 MHz) δ 166.6, 154.8, 153.6, 143.9, 129.4, 118.9, 117.6, 114.5, 74.4, 69.4, 55.7, 51.8, 25.3; **IR** (film, cm^{-1}) 3481, 3004, 2950, 2834, 2359, 1709, 1500, 1211, 748; **TLC** R_f = 0.21 (7:3 hexanes/EtOAc v/v); **HPLC** 92:8 e.r., Chiral HPLC eluting at 1.25 mL/min with 99% hexanes/isopropanol for 20.00 minutes then a gradient from 1% to 30% isopropanol in hexanes from 20.01 to 40.00 minutes. Retention times: R_T= 29.2 min, 31.7 min; **HRMS** (EI^+) *m/z* Calc'd for $C_{15}H_{18}O_5$ 278.1154, found 278.1152.

Methyl (3*R*,6*S*)-3-hydroxy-6-(4-methoxyphenoxy)cyclohex-1-ene-1-carboxylate (2.3d)

$[\alpha]_D^{20.0}$ +15.5 (*c* 1.00, $CHCl_3$)†; **M.p.** 49 – 54 °C; **^{1}H NMR** ($CDCl_3$, 400 MHz) δ 7.09 (dd, *J* = 1.8 Hz, 1H), 7.01 – 6.96 (m, 2H), 6.86 – 6.81 (m, 2H), 4.97 (br s, 1H), 4.36 – 4.28 (m, 1H), 3.77 (s, 3H), 3.77 (s, 3H), 2.20 – 2.11 (m, 1H), 2.02 (d, *J* = 18.7 Hz, 1H), 1.90 – 1.80 (m, 1H), 1.55 (tt, *J* = 14.2, 3.2 Hz, 1H); **^{13}C NMR** ($CDCl_3$, 126 MHz) δ 166.4, 154.7, 152.1, 145.8, 130.6, 118.9, 114.7, 69.9, 67.8, 55.7, 52.1, 26.3, 25.2; **IR** (film, cm^{-1}) 3285, 2953, 2869, 1713, 1505, 1252, 1218, 1032, 826, 724; **TLC** R_f = 0.15 (7:3 hexanes/EtOAc v/v); **HPLC** 94:6 e.r., Chiral HPLC eluting at 1.00 mL/min with 90% hexanes/isopropanol. Retention times: R_T= 8.7 min, 14.4 min; **HRMS** (EI^+) *m/z* Calc'd for $C_{15}H_{18}O_5$ 278.1154, found 278.1167. †Analytical standard was obtained as the enantiomer of **2.3d** from the (*R,R)*-**L2** ligand.

1,2-product **2.2e** (20.7 mg, 21%, 90:10 e.r.) and 1,4-product **2.3e** (22.3 mg, 23%, 84:16 e.r.). Recovered epoxide **2.1** (12.1 mg, 29%, 51:49 e.r.).

Analytical standards used for the characterization of **2.2e** and **2.3e** were prepared from a separate trial giving enantiomeric ratios of 94:6 and 89:11 respectively.

Methyl (5S, 6R)-5-hydroxy-6-O-(4-N-Bocphenoxy)-cyclohex-1-enecarboxylate (2.2e)

$[\alpha]_D^{20.0}$ −92.4 (*c* 0.50, $CHCl_3$); **M.p.** 134 – 136 °C; **^{1}H NMR** ($CDCl_3$, 400 MHz) δ 7.27 – 7.23 (m, 2H), 7.15 (dd, *J* = 4.7, 3.0 Hz, 1H), 7.10 – 7.04 (m, 2H), 6.35 (s, 1H), 5.15 (d, *J* = 3.6 Hz, 1H), 3.88 (ddt, *J* = 12.2, 8.5, 3.8 Hz, 1H), 3.61 (s, 3H), 2.58 – 2.47 (m, 1H), 2.37 – 2.24 (m, 1H), 2.03 – 1.91 (m, 1H), 1.90 – 1.81 (m, 1H), 1.50 (s, 9H);

^{13}C NMR ($CDCl_3$, 75 MHz) δ 166.5, 155.5, 153.1, 144.0, 132.7, 129.3, 120.3, 118.0, 80.4, 73.9, 69.5, 51.9, 28.5, 25.3, 25.3; **IR** (film, cm^{-1}) 3481, 3358, 2974, 2921, 1720, 1695, 1511, 1210, 1150; **TLC** R_f = 0.13 (7:3 hexanes:EtOAc v/v); **HPLC** 94:6 e.r., Chiral HPLC eluting at 1.00 mL/min with 95% hexanes:isopropanol for 20.00 minutes then a gradient from 5% to 30% isopropanol in hexanes from 20.01 to 40.00 minutes. Retention times: R_T= 33.1 min, 35.5 min; **HRMS** (EI^+) *m/z* Calc'd for $C_{19}H_{25}O_6N$ 363.1682, found 363.1686.

Methyl (3R, 6S)-3-hydroxy-6-O-(4-N-Bocphenoxy)-cyclohex-1-enecarboxylate (2.3e)

$[\alpha]_D^{20.0}$ −19.8 (*c* 0.50, $CHCl_3$); **M.p.** 61 – 65 °C; **^{1}H NMR** ($CDCl_3$, 400 MHz) δ 7.28 – 7.23 (m, 2H), 7.10 (dd, *J* = 1.9, 1.6 Hz, 1H), 6.97 – 6.92 (m, 2H), 6.37 (s, 1H), 5.01 (t, *J* = 3.0 Hz, 1H), 4.36 – 4.29 (m, 1H), 3.74 (s, 3H), 2.18 – 2.09 (m, 1H), 2.02 – 1.94 (m, 1H), 1.81 (tdd, *J* = 13.0, 10.4, 2.9 Hz, 1H), 1.58 (tt, *J* = 14.5, 3.0 Hz, 1H), 1.49 (s, 9H); **^{13}C NMR** ($CDCl_3$, 100 MHz) δ 166.3, 154.0, 153.2, 145.8, 132.4, 130.6, 120.6, 117.9, 80.4, 69.1*, 69.1*, 67.8, 52.2*, 52.1*, 28.5, 26.4, 25.3; **IR** (film, cm^{-1}) 3342, 2950, 1702, 1509, 1254, 1220, 1160; **TLC** R_f = 0.12 (7:3 hexanes:EtOAc v/v); **HPLC** 89:11 e.r., Chiral HPLC eluting at 1.0 mL/min with 95% hexanes:isopropanol for 20.00 minutes then a gradient from 5% to 30% isopropanol in hexanes from 20.01 to 40.00 minutes. Retention times: R_T= 31.9 min, 34.0 min; **HRMS** (EI^+) *m/z* Calc'd for $C_{19}H_{25}O_6N$ 363.1682, found 363.1688. * denotes presumed rotamers in a 1:1 ratio.

1,2-product **2.2f** (3.2 mg, 4%, 97:3 e.r.) and 1,4-product **2.3f** (2.9 mg, 4%, 98:2 e.r.). Recovered epoxide **2.1** (27.6 mg, 64%, 50:50 e.r.).

Analytical standards used for the characterization of **2.2f** and **2.3f** were prepared from a separate trial giving enantiomeric ratios of 98:2 and 98:2 respectively.

Methyl (5S, 6R)-5-hydroxy-6-O-(4-nitrophenoxy)-cyclohex-1-enecarboxylate (2.2f)

$[\alpha]_D^{20.0}$ −108.2 (*c* 0.50, $CHCl_3$); **^{1}H NMR** ($CDCl_3$, 400 MHz) 8.22 – 8.17 (m, 2H), 7.26 – 7.21 (m, 3H), 5.44 (d, *J* = 3.7 Hz, 1H), 3.96 (ddt, *J* = 12.0, 8.0, 3.8 Hz, 1H), 3.66 (s, 3H), 2.58 (dtd, *J* = 20.3, 5.4, 2.3 Hz, 1H), 2.45 – 2.32 (m, 1H), 2.05 – 1.87 (m, 2H); **^{13}C NMR** ($CDCl_3$, 100 MHz) δ 166.1, 164.9, 145.1, 141.9, 128.2, 125.9, 116.6, 73.0, 69.8, 52.1*, 52.1*, 25.7, 25.2; **IR** (film, cm^{-1}) 3458, 2952, 1710, 1590, 1509, 1493, 1330, 1250; **TLC** R_f = 0.12 (7:3 hexanes:EtOAc v/v); **HPLC** 98:2 e.r., Chiral HPLC eluting at 1.0 mL/min with 95% hexanes:isopropanol for 20.00 minutes then a gradient from 5% to 30% isopropanol in hexanes from 20.01 to 40.00 minutes. Retention times: R_T= 35.9 min, 38.4 min; **HRMS** (EI^+) *m/z* Calc'd for $C_{14}H_{15}NO_6$ 239.0899, found 239.0898. * denotes presumed rotamers in a 1:1 ratio

Methyl (3R, 6S)-3-hydroxy-6-O-(4-nitrophenoxy)-cyclohex-1-enecarboxylate (2.3f)

$[\alpha]_D^{20.0}$ +37.5 (*c* 0.50, $CHCl_3$) †; **^{1}H NMR** ($CDCl_3$, 400 MHz) δ 8.24 – 8.17 (m, 2H), 7.18 (dd, *J* = 2.2, 1.4 Hz, 1H), 7.06 – 7.00 (m, 2H), 5.28 (s, 1H), 4.38 (s, 1H), 3.74 (s, 3H), 2.21 – 2.13 (m, 1H), 2.10 – 2.02 (m, 1H), 1.88 – 1.69 (m, 2H); **^{13}C NMR** ($CDCl_3$, 75 MHz) δ 165.9, 163.1, 146.6, 141.7, 129.4, 126.1, 115.8, 68.4, 67.5, 52.3, 26.4, 25.5; **IR** (film, cm^{-1}) 3391, 2950, 1708, 1438, 1255, 1041, 756; **TLC** R_f = 0.09

(7:3 hexanes:EtOAc v/v); **HPLC** 98:2 e.r., Chiral HPLC eluting at 1.0 mL/min with 95% hexanes:isopropanol for 20.00 minutes then a gradient from 5% to 30% isopropanol in hexanes from 20.01 to 40.00 minutes. Retention times: R_T= 31.9 min, 34.0 min; **HRMS** (EI^+) *m/z* Calc'd for $C_{14}H_{15}NO_6$ 239.0899, found 239.0895. †Analytical standard was obtained as the enantiomer of **2.3f** from the (*R,R*)-**L2**.

1,2-product **2.2g** (23.4 mg, 31%, 96:4 e.r.) and 1,4-product **2.3g** (25.8 mg, 34%, 84:16 e.r.). Recovered epoxide **2.1** (0.4 mg, 1%, 68:32 e.r.).

Analytical standards used for the characterization of **2.2g** and **2.3g** were prepared from a separate trial giving enantiomeric ratios of 85:15 and 90:10 respectively.

Methyl (5S, 6R)-5-hydroxy-6-O-(2,4-dimethylphenoxy)-cyclohex-1-enecarboxylate (2.2g)

$[\alpha]_D^{20.0}$ −106.6 (*c* 0.75, $CHCl_3$); **^{1}H NMR** ($CDCl_3$, 300 MHz) δ 7.19 – 7.11 (m, 2H), 7.00 – 6.89 (m, 2H), 5.20 (d, *J* = 3.7 Hz, 1H), 3.89 (ddt, *J* = 12.0, 8.0, 3.7 Hz, 1H), 3.57 (s, 3H), 2.62 – 2.47 (m, 1H), 2.41 – 2.31 (m, 1H), 2.25 (s, 3H), 2.14 (s, 3H), 2.07 – 1.96 (m, 1H), 1.93 – 1.83 (m, 1H); **^{13}C NMR** ($CDCl_3$, 75 MHz) δ 166.6, 155.5, 143.7, 131.5, 131.0, 129.8, 127.7, 127.3, 115.7, 73.5, 69.6, 51.8, 25.4, 25.4, 20.6, 16.5; **IR** (film, cm^{-1}) 3434, 2949, 1716, 1489, 1250, 1217, 1042; **TLC** R_f = 0.50 (7:3 hexanes:EtOAc v/v); **HPLC** 85:15 e.r., Chiral HPLC eluting at 1.0 mL/min with 90% hexanes:isopropanol. Retention times: R_T= 3.7 min, 4.2 min; **HRMS** (EI^+) *m/z* Calc'd for $C_{16}H_{20}O_4$ 276.1362, found 276.1357.

Methyl (3R, 6S)-3-hydroxy-6-O-(2,4-dimethylphenoxy)-cyclohex-1-enecarboxylate (2.3g)

$[\alpha]_D^{20.0}$ −19.4 (*c* 0.50, $CHCl_3$); **^{1}H NMR** ($CDCl_3$, 300 MHz) δ 7.10 (dd, *J* = 2.2, 1.3 Hz, 1H), 7.03 – 6.92 (m, 3H), 5.09 (br s, 1H), 4.39 – 4.27 (m, 1H), 3.74 (s, 3H), 2.26 (s, 3H), 2.15 (s, 3H), 2.13 – 2.06 (m, 1H), 2.05 – 1.96 (m, 1H), 1.93 – 1.78 (m, 1H), 1.65 – 1.58 (dt, *J* = 13.9, 3.3 Hz, 1H); **^{13}C NMR** ($CDCl_3$, 75 MHz) δ 166.4, 154.1, 145.3, 131.5, 130.8, 130.4, 128.0, 127.1, 114.3, 68.7, 67.7, 51.9, 26.6, 25.5, 20.5, 16.4; **IR** (film, cm^{-1}) 3415, 2949, 1719, 1499, 1250, 1219, 1032; **TLC** R_f = 0.40 (7:3 hexanes:EtOAc v/v); **HPLC** 90:10 e.r., Chiral HPLC eluting at 1.0 mL/min with 90% hexanes:methanol. Retention times: R_T= 4.2 min, 5.0 min; **HRMS** (EI^+) *m/z* Calc'd for $C_{16}H_{20}O_4$ 276.1362, found 276.1367.

1,2-product **2.2h** (21.5 mg, 31%, 90:10 e.r.) and 1,4-product **2.3h** (24.5 mg, 34%, 91:9 e.r.). Recovered epoxide **2.1** (9.2 mg, 23%, 52:48 e.r.).

Analytical standards used for the characterization of **2.2h** and **2.3h** were prepared from a separate trial giving enantiomeric ratios of 90:10 and 92:8 respectively.

Methyl (5S, 6R)-5-hydroxy-6-O-(3,5-dimethylphenoxy)-cyclohex-1-enecarboxylate (2.2h)

$[\alpha]_D^{20.0}$ −93.3 (*c* 1.00, $CHCl_3$); **^{1}H NMR** ($CDCl_3$, 400 MHz) δ 7.15 (dd, *J* = 4.7, 3.0 Hz, 1H), 6.77 (s, 2H), 6.63 (s, 1H), 5.26 (d, *J* = 3.7 Hz, 1H), 3.90 (ddt, *J* = 12.3, 8.2, 3.7 Hz, 1H), 3.64 (s, 3H), 2.53 (dtd, *J* = 20.0, 5.2, 3.0 Hz, 1H), 2.33 (dddd, *J* = 9.7, 6.4, 3.1, 1.1 Hz, 1H), 2.28 (s, 6H), 2.02 – 1.92 (m, 1H), 1.90 – 1.82 (m, 1H); **^{13}C NMR** ($CDCl_3$, 100 MHz) δ 166.5, 159.5, 143.9, 139.2, 129.4, 123.8, 114.8, 72.7, 69.5, 51.8*, 51.8*, 25.4, 25.2, 21.5; **IR** (film, cm^{-1}) 3434, 2949, 1714, 1590, 1293, 1246, 1150, 1039, 755; TLC R_f = 0.53 (7:3 hexanes:EtOAc v/v); **HPLC** 90:10 e.r., Chiral

HPLC eluting at 1.25 mL/min with 97% hexanes:methanol. Retention times: R_T= 6.0 min, 6.4 min; **HRMS** (EI^+) *m/z* Calc'd for $C_{16}H_{20}O_4$ 276.1362, found 276.1352. * denotes presumed rotamers in a 1:1 ratio.

Methyl (3R, 6S)-3-hydroxy-6-O-(3,5-dimethylphenoxy)-cyclohex-1-enecarboxylate (2.3h)

$[\alpha]_D^{20.0}$ −14.0 (*c* 0.75, $CHCl_3$); **M.p.** 93 – 95 °C; **^{1}H NMR** ($CDCl_3$, 400 MHz) δ 7.10 (dd, *J* = 2.2, 1.4 Hz, 1H), 6.63 (s, 3H), 5.11 (br s, 1H), 4.37 – 4.28 (m, 1H), 3.76 (s, 3H), 2.28 (s, 6H), 2.18 (ddt, *J* = 14.5, 4.0, 2.6 Hz, 1H), 2.04 – 1.95 (m, 1H), 1.86 – 1.78 (m, 1H), 1.58 (dt, *J* = 14.0, 3.3 Hz, 1H); **^{13}C NMR** ($CDCl_3$, 75 MHz) δ 166.4, 157.9, 145.7, 139.3, 130.7, 123.4, 114.5, 67.9, 67.7, 52.1, 26.5, 25.3, 21.5; **IR** (film, cm^{-1}) 3408, 2949, 1717, 1590, 1292, 1252, 1150, 1031; **TLC** R_f = 0.29 (7:3 hexanes:EtOAc v/v); **HPLC** 92:8 e.r., Chiral HPLC eluting at 1.25 mL/min with 90% hexanes:isopropanol. Retention times: R_T= 3.6 min, 4.2 min; **HRMS** (EI^+) *m/z* Calc'd for $C_{16}H_{20}O_4$ 276.1362, found 276.1370.

1,2-product **2.2i** (25.8, 33%, 84:16 e.r.) and 1,4-product **2.3i** (25.7 mg, 33%, 84:16 e.r.). No recovered epoxide **2.1.**

Analytical standards used for the characterization of **2i** and **3i** were prepared from a separate trial giving enantiomeric ratios of 89:11 and 97:3 respectively.

Methyl (5S, 6R)-5-hydroxy-6-O-(2-naphthoxy)-cyclohex-1-enecarboxylate (2.2i)

$[\alpha]_D^{20.0}$ −124.3 (*c* 2.00, $CHCl_3$); **M.p.** 82 – 86 °C; **^{1}H NMR** ($CDCl_3$, 400 MHz) δ 7.78 – 7.74 (m, *J* = 8.4, 6.9 Hz, 3H), 7.57 (d, *J* = 2.5 Hz, 1H), 7.43 (ddd, *J* = 8.1, 6.8, 1.3, 1H), 7.34 (ddd, *J* = 8.2, 6.8, 1.2, 1H), 7.30 (dd, *J* = 8.9, 2.5 Hz, 1H), 7.19 (dd, *J* = 4.8,

3.0 Hz, 1H), 5.44 (d, *J* = 3.6 Hz, 1H), 4.02 – 3.92 (m, 1H), 3.58 (s, 3H), 2.62 – 2.50 (m, 1H), 2.40 – 2.27 (m, 1H), 2.07 – 1.97 (m, 1H), 1.94 – 1.85 (m, 1H); **^{13}C NMR** ($CDCl_3$, 100 MHz) δ 166.5, 157.4, 144.2, 134.5, 129.6, 129.4, 129.2, 127.6, 127.1, 126.3, 124.0, 119.6, 111.3, 73.2, 69.6, 51.8, 25.3, 25.3; **IR** (film, cm^{-1}) 3431, 3055, 2949, 1709, 1250, 1212, 1041, 747; **TLC** R_f = 0.29 (7:3 hexanes:EtOAc v/v); **HPLC** 89:11 e.r., Chiral HPLC eluting at 1.25 mL/min with 99% hexanes:isopropanol then a gradient of 1% to 30% isopropanol in hexanes from 20.01 to 40.00 minutes. Retention times: R_T= 26.2 min, 29.9 min; **HRMS** (EI^+) *m/z* Calc'd for $C_{18}H_{18}O_4$ 298.1205, found 298.1215.

Methyl (3R, 6S)-3-hydroxy-6-O-(2-naphthoxy)-cyclohex-1-enecarboxylate (2.3i)

$[\alpha]_D^{20.0}$ −5.7 (*c* 0.50, $CHCl_3$); **M.p.** 63 – 66 °C; **^{1}H NMR** ($CDCl_3$, 400 MHz) δ 7.79 – 7.71 (m, 3H), 7.44 (ddd, *J* = 8.2, 6.8, 1.3 Hz, 1H), 7.34 (ddd, *J* = 8.1, 6.9, 1.2 Hz, 1H), 7.31 (d, *J* = 2.5 Hz, 1H), 7.20 (dd, *J* = 8.9, 2.5 Hz, 1H), 7.16 (dd, *J* = 2.2, 1.4 Hz, 1H), 5.30 (t, *J* = 2.9 Hz, 1H), 4.36 (dddd, *J* = 10.5, 6.1, 2.2, 1.1 Hz, 1H), 3.75 (s, 3H), 2.32 – 2.25 (m, 1H), 2.07 – 1.98 (m, 1H), 1.94 – 1.81 (m, 1H), 1.67 (tt, *J* = 14.2, 3.2 Hz, 1H); **^{13}C NMR** ($CDCl_3$, 100 MHz) δ 166.4, 155.8, 146.0, 134.6, 130.4, 129.6, 129.4, 127.7, 126.9, 126.4, 123.9, 120.0, 109.9, 68.0*, 68.0*, 67.8, 52.2*, 52.2*, 26.6, 25.2; **IR** (film, cm^{-1}) 3420, 2949, 2359, 1717, 1250, 1214, 1031, 748; **TLC** R_f = 0.18 (7:3 hexanes:EtOAc v/v); **HPLC** 97:3 e.r., Chiral HPLC eluting at 1.25 mL/min with 99% hexanes:isopropanol then a gradient from 1% to 30% isopropanol in hexanes from 20.01 to 40.00 minutes. Retention times: R_T= 31.0 min, 31.5 min; **HRMS** (EI^+) *m/z* Calc'd for $C_{18}H_{18}O_4$ 298.1205, found 298.1194. * denotes presumed rotamers in a 1:1 ratio.

1,2-product **2.2j** (27.3 mg, 35%, 80:20 e.r.) and 1,4-product **2.3j** (29.8 mg, 38%, 88:12 e.r.). No recovered epoxide **2.1**.

Analytical standards used for the characterization of **2.2j** and **2.3j** were prepared from a separate trial giving enantiomeric ratios of 80:20 and 90:10 respectively.

Methyl (5S, 6R)-5-hydroxy-6-O-(1-naphthoxy)-cyclohex-1-enecarboxylate (2.2j)

$[\alpha]_D^{20.0}$ −123.2 (*c* 0.50, $CHCl_3$); **^{1}H NMR** ($CDCl_3$, 400 MHz) δ 8.19 – 8.13 (m, 1H), 7.83 – 7.77 (m, 1H), 7.49 – 7.39 (m, 5H), 7.24 (dd, *J* = 4.9, 2.9 Hz, 1H), 5.52 (d, *J* = 3.7 Hz, 1H), 3.99 (ddt, *J* = 11.7, 9.8, 3.7 Hz, 1H), 3.44 (s, 3H), 2.69 – 2.58 (m, 1H), 2.47 – 2.33 (m, 1H), 2.21 – 2.09 (m, 1H), 2.01 – 1.93 (m, 1H); **^{13}C NMR** ($CDCl_3$, 100 MHz) δ 166.5, 155.5, 144.2*, 144.2*, 134.7, 129.4, 127.8*, 127.7*, 126.6, 126.3*, 126.2*, 126.1*, 126.1*, 126.1*, 126.1*, 125.5*, 125.4*, 121.9*, 121.9*, 121.5*, 121.5*, 109.4, 73.9, 73.8, 69.7, 51.8*, 51.7*, 25.6, 25.5; **IR** (film, cm^{-1}) 3390, 2951, 1709, 1395, 1246, 1235, 1091, 1042, 770; **TLC** R_f = 0.28 (7:3 hexanes:EtOAc v/v); **HPLC** 80:20 e.r., Chiral HPLC eluting at 1.0 mL/min with 95% hexanes:methanol. Retention times: R_T= 10.7 min, 15.4 min; **HRMS** (EI^+) *m/z* Calc'd for $C_{18}H_{18}O_4$ 298.1205, found 298.1201. * denotes presumed rotamers in a 1:1 ratio.

Methyl (3R, 6S)-3-hydroxy-6-O-(1-naphthoxy)-cyclohex-1-enecarboxylate (2.3j)

$[\alpha]_D^{20.0}$ +67.0 (*c* 1.00, $CHCl_3$); **M.p.** 132 – 135 °C; **^{1}H NMR** ($CDCl_3$, 400 MHz) δ 8.25 – 8.18 (m, 1H), 7.82 – 7.77 (m, 1H), 7.50 – 7.35 (m, 4H), 7.20 (dd, *J* = 2.2, 1.3 Hz, 1H), 7.08 (d, *J* = 7.4, 1H), 5.41 (t, *J* = 3.0 Hz, 1H), 4.42 – 4.35 (m, 1H), 3.70 (s, 3H), 2.30 – 2.22 (m, 1H), 2.07 – 1.87 (m, 2H), 1.68 (dt, *J* = 14.0, 3.4 Hz, 1H); **^{13}C NMR** ($CDCl_3$, 100 MHz) δ 166.4, 153.8, 145.9, 134.7, 130.6, 127.5, 126.7, 126.4,

126.0, 125.3, 122.3, 120.9, 107.2, 68.2, 67.8, 52.2*, 52.2*, 26.9, 25.4; **IR** (film, cm^{-1}) 3244, 3052, 2950, 2359, 1717, 1256, 1234, 771; **TLC** R_f = 0.19 (7:3 hexanes:EtOAc v/v); **HPLC** 90:10 e.r., Chiral HPLC eluting at 1.0 mL/min with 98% hexanes:methanol. Retention times: R_T= 7.9 min, 11.6 min; **HRMS** (EI^+) *m/z* Calc'd for $C_{18}H_{18}O_4$ 298.1205, found 298.1207. * denotes presumed rotamers in a 1:1 ratio.

1,2-product **2.2k** (23.1 mg, 29%, 90:10 e.r.) and 1,4-product **2.3k** (18.5 mg, 23%, 95:5 e.r.). No recovered epoxide **2.1**.

Analytical standards used for the characterization of **2.2k** and **2.3k** were prepared from a separate trial giving enantiomeric ratios of 92:8 and 95:5 respectively.

Methyl (5S, 6R)-5-hydroxy-6-O-(1,3-benzodioxol-5-yl)-cyclohex-1-enecarboxylate (2.2k)

$[\alpha]_D^{20.0}$ +104.4 (*c* 1.00, $CHCl_3$); **^{1}H NMR** ($CDCl_3$, 400 MHz) δ 7.14 (dd, *J* = 4.7, 3.0 Hz, 1H), 6.74 (d, *J* = 2.5 Hz, 1H), 6.68 (d, *J* = 8.4 Hz, 1H), 6.60 (dd, *J* = 8.5, 2.5 Hz, 1H), 5.91 (s, 2H), 5.08 (d, *J* = 3.7 Hz, 1H), 3.87 (ddt, *J* = 11.5, 9.2, 3.8 Hz, 1H), 3.65 (s, 3H), 2.52 (dtd, *J* = 20.1, 5.3, 2.8 Hz, 1H), 2.37 – 2.25 (m, 1H), 2.02 – 1.91 (m, 1H), 1.90 – 1.81 (m, 1H); **^{13}C NMR** ($CDCl_3$, 100 MHz) δ 166.5, 155.0, 148.1, 144.0, 142.6, 129.2, 109.8, 108.0, 101.3, 100.8, 74.8, 69.5, 51.9*, 51.9*, 25.3, 25.3; **IR** (film, cm^{-1}) 3446, 2950, 2360, 1710, 1480, 1242, 1175, 1035, 746; **TLC** R_f = 0.20 (7:3 hexanes:EtOAc v/v); **HPLC** 92:8 e.r., Chiral HPLC eluting at 1.0 mL/min with 95% hexanes:isopropanol. Retention times: R_T= 20.4 min, 23.4 min; **HRMS** (EI^+) *m/z* Calc'd for $C_{15}H_{16}O_6$ 292.0947, found 292.0952.

Methyl (3R, 6S)-3-hydroxy-6-O-(1,3-benzodioxol-5-yl)-cyclohex-1-enecarboxylate (2.3k)

$[\alpha]_D^{20.0}$ −16.7 (*c* 0.75, $CHCl_3$); **M.p.** 70 – 73 °C; **^{1}H NMR** ($CDCl_3$, 400 MHz) δ 7.09 (s, 1H), 6.70 (d, *J* = 8.4 Hz, 1H), 6.63 (d, *J* = 2.4 Hz, 1H), 6.48 (dd, *J* = 8.5, 2.5 Hz, 1H), 5.92 (q, *J* = 1.43, 1.41 Hz, 2H), 4.93 (t, *J* = 2.8 Hz, 1H), 4.35 – 4.29 (m, 1H), 3.78 (s, 3H), 2.21 – 2.10 (m, 1H), 2.04 – 1.97 (m, 1H), 1.91 – 1.76 (m, 1H), 1.54 (tt, *J* = 14.4, 3.2 Hz, 1H); **^{13}C NMR** ($CDCl_3$, 100 MHz) δ 166.3, 153.3, 148.3, 145.7, 142.6, 130.5, 109.8, 108.1, 101.3, 100.9, 70.2, 67.8, 52.2*, 52.2*, 26.4, 25.2; **IR** (film, cm^{-1}) 3408, 2950, 1715, 1482, 1254, 1177, 1033; **TLC** R_f = 0.14 (7:3 hexanes:EtOAc v/v); **HPLC** 95:5 e.r., Chiral HPLC eluting at 1.0 mL/min with 90% hexanes:isopropanol. Retention times: R_T= 8.9 min, 12.4 min; **HRMS** (EI^+) *m/z* Calc'd for $C_{15}H_{16}O_6$ 292.0947, found 292.0935. * denotes presumed rotamers in a 1:1 ratio.

Allylic-oxide Regio Resolution of Estradiol

17-O-*tert*butyldimethylsilylestradiol (**2.4**) was prepared according to literature procedures using a bis-TBS protection followed by selective removal of the phenolic silane.[12] In addition to the discussed use of the (*S,S*)-**L2**, (*R,R*)-**L2** was also used and the results are included below. Products are a single diastereomer unless otherwise noted.

In a flame-dried flask outfitted with a septum, racemic epoxide **2.1** (68.0 mg, 0.44 mmol, 1.4 equiv) was dissolved in 6.5 mL of toluene followed by 17-O-*tert*butyldimethylsilylestradiol **2.4** (120.0 mg, 0.31 mmol, 1.0 equiv.). The resulting solution was degassed with argon and cooled to −40 °C. In a separate flask, $Pd_2(dba)_3$

(14.7 mg, 5.0 mol%) and (*R,R*)-**L2** (36.7 mg, 15.0 mol%) were dissolved in 4.0 mL of toluene. The resulting purple solution was degassed and stirred at room temperature until it became yellow (approx. 10 min.). The solution was then cooled to −40 °C and added to the epoxide solution via syringe. After 96 hours at −40 °C, the reaction was concentrated to a volume of 2.0 mL and then purified by flash chromatography (9:1, hexanes:EtOAc v/v) to yield **2.5** (101.5 mg, 60%) and **2.6** (46.9 mg, 27%), both as white solids and single diastereomers. The epoxide (**2.1**, 22%) was recovered in 93:7 enantiomeric ratio.

Methyl (5R, 6S)-5-hydroxy-6-O-(17-O-*tert*butyldimethylsilylestradiol)-cyclohex-1-enecarboxylate (2.5)

$[\alpha]_D^{20.0}$ −97.3 (*c* 1.00, $CHCl_3$); M.p. 38 – 42 °C; **^{1}H NMR** (400 MHz, $CDCl_3$) δ 7.19 (d, *J* = 8.8 Hz, 1H), 7.14 (dd, *J* = 4.6, 3.1 Hz, 1H), 6.92 (dd, *J* = 8.6, 2.8 Hz, 1H), 6.87 (d, *J* = 2.8 Hz, 1H), 5.25 (d, *J* = 3.7 Hz, 1H), 3.91 (dt, *J* = 11.3, 3.7 Hz, 1H), 3.66 (s, 3H), 3.64 (t, *J* = 7.7 Hz, 1H), 2.88 – 2.77 (m, 1H), 2.57 – 2.48 (m, 1H), 2.37 – 2.22 (m, 2H), 2.21 – 2.11 (m, 1H), 2.11 – 1.79 (m, 6H), 1.66 – 1.63 (m, 1H), 1.55 – 1.03 (m, 7H), 0.89 (s, 9H), 0.73 (s, 3H), 0.03 (s, 3H), 0.02 (s, 3H); **^{13}C NMR** (75 MHz, $CDCl_3$) δ 166.5, 157.3, 143.8, 138.1, 134.1, 129.4, 126.4, 117.1, 114.1, 81.8, 72.7, 69.4, 51.8, 49.8, 44.2, 43.6, 38.9, 37.2, 31.0, 29.9, 27.4, 26.4, 25.9, 25.3, 25.1, 23.3, 18.2, 11.4, −4.3, −4.6; **IR** (film, cm^{-1}) 3433, 2926, 2854, 1717, 1495, 1246, 1094, 834, 773; **TLC** R_f = 0.57 (7:3 hexanes:EtOAc v/v). **HRMS** (EI^+) *m/z* Calc'd for $C_{32}H_{48}SiO_5$ 540.3271, found 540.3263.

Methyl (3S, 6R)-3-hydroxy-6-O-(17-O-*tert*butyldimethylsilylestradiol)-cyclohex-1-enecarboxylate (2.6)

$[\alpha]_D^{20.0}$ −25.6 (*c* 1.00, $CHCl_3$); **M.p.** 43 – 47 °C; **^{1}H NMR** (400 MHz, $CDCl_3$) δ 7.20 (d, *J* = 8.1 Hz, 1H), 7.10 (dd, *J* = 2.2, 1.3 Hz, 1H), 6.79 (dd, *J* = 8.6, 2.8 Hz, 1H), 6.73 (d, *J* = 2.7 Hz, 1H), 5.09 (br s, 1H), 4.32 (dddd, *J* = 10.6, 6.1, 2.1, 1.0 Hz, 1H), 3.76 (s, 3H), 3.64 (t, *J* = 7.9 Hz, 1H), 2.89 – 2.78 (m, 1H), 2.34 – 2.10 (m, 3H), 2.04 – 1.76 (m, 5H), 1.71 – 1.03 (m, 10H), 0.89 (s, 9H), 0.74 (s, 3H), 0.04 (s, 3H), 0.02 (s, 3H); **^{13}C NMR** (100 MHz, $CDCl_3$) δ 166.4, 155.7, 145.8, 138.2, 133.8, 130.6, 126.5, 117.0, 114.0, 81.8, 67.9*, 67.9*, 67.8, 52.1*, 52.1*, 49.8, 44.2, 43.7, 38.9, 37.2, 31.1, 29.9, 27.4, 26.5, 26.4, 26.0, 25.3, 23.4, 18.2, 11.4, −4.3, −4.6; **IR** (film, cm^{-1}) 3389, 2926, 2853, 1719, 1496, 1247, 1094, 834, 773; **TLC** R_f = 0.43 (7:3 hexanes:EtOAc v/v). **HRMS** (EI^+) *m/z* Calc'd for $C_{32}H_{48}SiO_5$ 540.3271, found 540.3263. * denotes presumed rotamers in a 1:1 ratio.

In a flame-dried flask outfitted with a septum, racemic epoxide **2.1** (121.6 mg, 0.788 mmol, 1.4 equiv) was dissolved in 7.0 mL of toluene followed by 17-O-*tert*butyldimethylsilylestradiol **2.4** (208.1 mg, 0.539 mmol, 1.0 equiv.). The resulting solution was degassed with argon and cooled to −40 °C. In a separate flask, $Pd_2(dba)_3$ (26.2 mg, 5.0 mol%) and (*S,S*)-**L2** (67.0 mg, 15.0 mol%) were dissolved in 4.0 mL of toluene. The resulting purple solution was degassed and stirred at room temperature until it became yellow (approx. 10 min.). The solution was then cooled to −40 °C and added to the epoxide solution via syringe. After 96 hours at −40 °C, the reaction was concentrated to a volume of 2.0 mL and then purified by flash chromatography (9:1, hexanes:EtOAc, (v/v) to yield **2.7** (127.9 mg, 44%) and **2.8** (119.2 mg, 41%) both as

white solids and single diastereomers. The epoxide (**2.1**, 18%) was recovered in 66:34 enantiomeric ratio.

Methyl (5S, 6R)-5-hydroxy-6-O-(17-O-*tert*butyldimethylsilylestradiol)-cyclohex-1-enecarboxylate (2.7)

$[\alpha]_D^{20.0}$ −28.0 (*c* 1.00, $CHCl_3$); **M.p.** 56 – 60 °C; **^{1}H NMR** (400 MHz, $CDCl_3$) δ 7.19 (d, *J* = 8.7 Hz, 1H), 7.14 (dd, *J* = 4.6, 3.1 Hz, 1H), 6.94 (dd, *J* = 8.6, 2.8 Hz, 1H), 6.85 (d, *J* = 2.6 Hz, 1H), 5.25 (d, *J* = 3.7 Hz, 1H), 3.91 (ddt, *J* = 11.3, 9.1, 3.7 Hz, 1H), 3.65 (s, 3H), 3.64 (t, *J* = 8.5 Hz, 1H), 2.86-2.79 (m, 1H), 2.58 – 2.47 (m, 1H), 2.37 – 2.23 (m, 2H), 2.20 – 2.11 (m, 1H), 2.06-1.80 (m, 6H), 1.71 – 1.59 (m, 1H), 1.54-1.07 (m, 7H), 0.89 (s, 9H), 0.74 (s, 3H), 0.04 (s, 3H), 0.02 (s, 3H); **^{13}C NMR** (100 MHz, $CDCl_3$) δ 166.4, 157.3, 143.7, 138.0, 133.9, 129.3, 126.3, 116.9, 114.3, 81.8, 72.7, 69.4, 51.7*, 51.7*, 49.7, 44.2, 43.6, 38.8, 37.2, 31.0, 29.8, 27.3, 26.4, 25.9, 25.2*, 25.1*, 23.3, 18.1, 11.4, −4.3, −4.7; **IR** (film, cm^{-1}) 3435, 2928, 2855, 1719, 1496, 1246, 1095, 834, 774; **TLC** R_f = 0.57 (7:3 hexanes:EtOAc v/v). **HRMS** (EI^+) *m/z* Calc'd for $C_{32}H_{48}SiO_5$ 540.3271, found 540.3264. * denotes presumed rotamers in a 1:1 ratio.

Methyl (3R, 6S)-3-hydroxy-6-O-(17-O-*tert*butyldimethylsilylestradiol)-cyclohex-1-enecarboxylate (2.8)

$[\alpha]_D^{20.0}$ +27.5 (*c* 0.50, $CHCl_3$); **M.p.** 64 – 69 °C; **^{1}H NMR** (400 MHz, $CDCl_3$) δ 7.20 (d, *J* = 8.6 Hz, 1H), 7.10 (dd, *J* = 2.4, 1.3 Hz, 1H), 6.80 (dd, *J* = 8.3, 2.5 Hz, 1H), 6.71 (d, *J* = 2.6 Hz, 1H), 5.09 (br s, 1H), 4.34 – 4.30 (m, 1H), 3.75 (s, 3H), 3.64 (t, *J* = 8.0 Hz, 1H), 2.88 – 2.77 (m, 1 H), 2.32 – 2.11 (m, 3H), 2.04 – 1.76 (m, 5H), 1.74 – 1.03 (m, 10H), 0.89 (s, 9H), 0.74 (s, 3H), 0.03 (s, 3H), 0.02 (s, 3H); **^{13}C NMR** (100 MHz,

$CDCl_3$) δ 166.4, 155.6, 146.0, 138.2, 133.8, 130.4, 126.4, 116.8, 114.3, 81.8, 67.9, 67.7, 52.1, 49.7, 44.2, 43.6, 38.9, 37.2, 31.0, 29.9, 27.3, 26.4, 26.3, 25.9, 25.2, 23.3, 18.2, 11.4, −4.3, −4.6; **IR** (film, cm^{-1}) 3410, 2928, 2855, 1720, 1496, 1247, 1095, 834, 773; **TLC** R_f = 0.43 (7:3 hexanes:EtOAc v/v). **HRMS** (EI^+) *m/z* Calc'd for $C_{32}H_{48}SiO_5$ 540.3271, found 540.3268.

Allylic-oxide Regio Resolution of Tyrosine

In addition to the discussed use of (*S,S*)-**L2**, (*R,R*)-**L2** was also tested and the results are shown below. Products are shown to be a single diastereomer unless otherwise noted.

In a flame dried flask outfitted with a septum, racemic epoxide **2.1** (264.7 mg, 1.71 mmol, 1.05 equiv.) was dissolved in 12.0 mL of toluene followed by the addition of Boc-L-Tyr-OMe **2.9** (482.5 mg, 1.63 mmol, 1.0 equiv.). The resulting solution was degassed with argon and cooled to −40 °C. In a separate flask, $Pd_2(dba)_3$ (12.4 mg, 1.0 mol%) and (*R,R*)-**L2** (34.2 mg, 3.0 mol%) of was dissolved in 1.0 mL of toluene. The resulting purple solution was degassed and stirred at room temperature until it became yellow (approx. 10 min.). The solution was then cooled to −40 °C and added to the epoxide solution via syringe. The reaction was allowed to stir for 72 hours before being worked up as in general procedure A. The reaction was purified by flash chromatography (7:3 hexanes:EtOAc v/v) to yield 664.3 mg of an inseparable mixture of **2.10** (45% yield, 4.37:1 diastereomeric ratio), **2.11** (36% yield as a single diastereomer) and 0.8 mg of recovered oxide (59:41 e.r.). Analytical standards of **2.10** and **2.11** were purified by preparatory HPLC (90:10 to 1:99 water:acetonitrile v/v) and

yields of **2.10** and **2.11** were determined by ^{1}H NMR analysis of the homogenous mixture.

Methyl (5S, 6R)-5-hydroxy-6-O-(Boc-L-Tyr-OMe)-cyclohex-1-enecarboxylate (2.10)

Note: The following data are for the major diastereomer isolated (4.37:1).

^{1}H NMR (400 MHz, $CDCl_3$) δ 7.16 (dd, *J* = 4.7, 3.0 Hz, 1H), 7.08 – 7.00 (m, 4H), 5.23 (d, *J* = 3.7 Hz, 1H), 4.95 (br d, *J* = 8.1 Hz, 1H), 4.56 – 4.50 (m, 1H), 3.90 (dt, *J* = 11.2, 3.8 Hz, 1H), 3.71 (s, 3H), 3.61 (s, 3H), 3.07 – 2.95 (m, 2H), 2.58 – 2.48 (m, 1H), 2.38 – 2.25 (m, 1H), 2.04 – 1.84 (m, 2H), 1.42 (s, 9H); **^{13}C NMR** (100 MHz, $CDCl_3$) δ 172.5, 166.5, 158.8, 155.2, 144.1, 130.6, 130.4 129.3, 117.5, 80.1, 73.3, 69.5, 54.6, 52.3, 51.8, 37.6, 28.4, 25.4, 23.5. Optical rotation, IR, and HRMS were not obtained due to mixture of diastereomers.

Methyl (3R, 6S)-3-hydroxy-6-O-(Boc-L-Tyr-OMe)-cyclohex-1-enecarboxylate (2.11)

$[\alpha]_D^{20.0}$ +36.4 (*c* 1.00, $CHCl_3$); **M.p.** 38 – 42 °C; **^{1}H NMR** (400 MHz, $CDCl_3$) δ 7.11 (t, *J* = 1.6 Hz, 1H), 7.01 (d, *J* = 8.1 Hz, 2H), 6.94 – 6.88 (m, 2H), 5.07 (t, *J* = 2.8 Hz, 1H), 5.01 (d, *J* = 8.3 Hz, 1H), 4.53 (dt, *J* = 8.7, 6.0 Hz, 1H), 4.36 – 4.26 (m, 1H), 3.72 (s, 3H), 3.70 (s, 3H), 3.01 (tt, *J* = 14.1, 6.8 Hz, 2H), 2.17 – 2.09 (m, 1H), 2.00 – 1.92 (m, 1H), 1.80 (tdd, *J* = 12.9, 10.3, 2.7 Hz, 1H), 1.57 (tt, *J* = 14.3, 3.2 Hz, 1H), 1.41 (s, 9H); **^{13}C NMR** (100 MHz, $CDCl_3$) δ 172.5, 166.3, 157.1, 155.2, 145.8, 130.5, 128.9, 128.7, 117.0, 80.0, 68.2, 67.8, 54.6, 52.3*, 52.3*, 52.1*, 52.1*, 37.6, 28.4, 26.5, 25.3; **IR** (film, cm^{-1}) 3370, 2951, 1718, 1508, 1255, 1167, 1031; **TLC** R_f = 0.17 (7:3

hexanes:EtOAc v/v). **HRMS** (EI^+) *m/z* Calc'd for $C_{23}H_{31}O_8N$ 449.2049, found 449.2056. * denotes presumed rotamers in a 1:1 ratio.

In a flame-dried flask outfitted with a septum, racemic epoxide **2.1** (301.0 mg, 1.02 mmol, 1.0 equiv.) was dissolved in 12.0 mL of toluene followed by the addition of Boc-L-Tyr-OMe **2.9** (562.1 mg, 1.0 mmol, 0.98 equiv.). The resulting solution was degassed with argon and cooled to −40 °C. In a separate flask, $Pd_2(dba)_3$ (14.5 mg, 1.0 mol%) and (*S,S*)-**L2** (39.3 mg, 3.0 mol%) was dissolved in 6.0 mL of toluene. The resulting purple solution was degassed and stirred at room temperature until it became yellow (approx. 10 min.). The solution was then cooled to −40 °C and added to the epoxide solution via syringe. The reaction was allowed to stir for 72 hours before being worked up as in general procedure A. The reaction was purified by flash chromatography (7:3 hexanes:EtOAc v/v) to yield 712.0 mg of an inseparable mixture of **2.12** and **2.13** and 43.4 mg of recovered oxide (53:47 e.r.). Analytical standards of **2.12** and **2.13** were purified by preparatory HPLC (90:10 to 1:99 water:acetonitrile v/v) and yields of **2.12** (51% yield, 4.20 d.r. as determined by ^{1}H NMR) and **2.13** (40% yield as a single diastereomer) were determined by ^{1}H NMR analysis of the homogenous mixture.

Methyl (5R, 6S)-5-hydroxy-6-O-(Boc-L-Tyr-OMe)-cyclohex-1-enecarboxylate (2.12)

Note: The following data are for the major diastereomer isolated (4.20:1).

^{1}H NMR (400 MHz, $CDCl_3$) δ 7.15 (dd, *J* = 4.7, 3.0 Hz, 1H), 7.08 – 6.99 (m, 4H), 5.22 (d, *J* = 3.6 Hz, 1H), 5.00 – 4.96 (m, 1H), 4.55 – 4.50 (m, 1H), 3.89 (dt, *J* = 11.4,

3.7 Hz, 1H), 3.70 (s, 3H), 3.60 (s, 3H), 3.06 – 2.96 (m, 2H), 2.57 – 2.48 (m, 1H), 2.36 – 2.27 (m, 1H), 2.02 – 1.93 (m, 1H), 1.89 – 1.80 (m, 1H), 1.41 (s, 9H); **^{13}C NMR** (100 MHz, $CDCl_3$) δ 172.5, 166.5, 158.8, 155.2, 144.1, 130.6, 130.4, 129.2, 117.5, 80.0, 73.3, 69.5, 54.6, 52.3, 51.8, 37.5, 28.4, 25.3, 25.3. Optical rotation, IR, and HRMS were not obtained due to mixture of diastereomers.

Methyl (3S, 6R)-3-hydroxy-6-O-(Boc-L-Tyr-OMe)-cyclohex-1-enecarboxylate (2.13)

$[\alpha]_D^{20.0}$ +10.2 (*c* 0.50, $CHCl_3$); **^{1}H NMR** (400 MHz, $CDCl_3$) δ 7.11 (t, *J* = 1.7 Hz, 1H), 7.03 – 6.99 (m, 2H), 6.95 – 6.90 (m, 2H), 5.10 (t, *J* = 2.9 Hz, 1H), 4.96 (d, *J* = 8.3 Hz, 1H), 4.54 (q, *J* = 6.7 Hz, 1H), 4.40 – 4.27 (m, 1H), 3.75 (s, 3H), 3.72 (s, 3H), 3.02 (qd, *J* = 14.0, 5.9 Hz, 2H), 2.19 – 2.13 (m, 1H), 2.04 – 1.96 (m, 1H), 1.87 – 1.73 (m, 1H), 1.59 (tt, *J* = 14.2, 3.2 Hz, 1H), 1.42 (s, 9H); **^{13}C NMR** (100 MHz, $CDCl_3$) δ 172.5, 166.3, 157.1, 155.2, 146.1, 130.4, 130.2, 128.9, 117.0, 80.0, 68.2, 67.8, 54.6, 52.3*, 52.3*, 52.2*, 52.1*, 37.4, 28.4, 26.2, 25.2; **IR** (film, cm^{-1}) 3369, 2951, 1718, 1508, 1256, 1167, 1031; **TLC** R_f = 0.17 (7:3 hexanes:EtOAc v/v). **HRMS** (EI^+) *m/z* Calc'd for $C_{23}H_{31}O_8N$ 449.2049, found 449.2042. * denotes presumed rotamers in a 1:1 ratio.

Allylic-oxide Regio Resolution of Griseofulvin

4-des-methyl-griseofulvin **2.14** was prepared by the demethylation of griseofulvin following a literature procedure.[14] In addition to the discussed use of (*S,S*)-DPEN-ligand **L2**, (*R,R*)-DPEN-ligand **L2** was also tested and the results are shown below. Products are shown to be a single diastereomer unless otherwise noted.

In flame-dried flask outfitted with a septum, racemic epoxide **2.1** (81.2 mg, 0.527 mmol, 1.8 equiv.) was dissolved in 1.3 mL of toluene followed by the addition of 4-des-methyl-griseofulvin **2.14** (99.5 mg, 0.294 mmol, 1.0 equiv.). The resulting solution was thoroughly degassed with argon and cooled to −40 °C. In a separate flask, $Pd_2(dba)_3$ (17.1 mg, 5.0 mol%) and (*R,R*)-**L2** (39.9 mg, 15.0 mol%) was dissolved in 0.6 mL of toluene. The resulting purple solution was degassed and stirred at room temperature until it became yellow (approx. 10 min.). The solution was then cooled to −40 °C and added to the epoxide solution via syringe. The reaction was continued at −40 °C and monitored by ^{1}H NMR spectroscopy until total consumption of the starting phenol was observed (approx. 18 hours). The reaction was then concentrated to dryness and was purified by flash chromatography (100% DCM, then 95:5 DCM:MeOH v/v) using Florisil as the stationary phase to yield 132.4 mg of a mixture containing **2.15** (60% yield), **2.16** (31% yield), and 9.0 mg of recovered phenol **2.14** (9%). Degradation of the products on Florisil is suspected to regenerate griseofulvin **2.14**. Similar degradation, but to a much greater extent, was observed when using silica as the stationary phase. Analytical standards of **2.15** and **2.16** could be separated from one another and purified by a silica column (5:1 toluene/acetone v/v) then preparatory HPLC (80:20 to 35:65 water:acetonitrile v/v over 35 minutes) to remove **2.14**. Both products were isolated as white solids.

Methyl (5R, 6S)-5-hydroxy-6-O-(4-des-methyl-griseofulvin)-cyclohex-1-enecarboxylate (2.15)

$[\alpha]_D^{20.0}$ +366.6 (*c* 1.00, $CHCl_3$); **M.p.** 90 – 92 °C; **^{1}H NMR** ($CDCl_3$, 400 MHz) δ 7.30 (dd, *J* = 4.9, 2.7 Hz, 1H), 7.18 (s, 1H), 5.55 (s, 1H), 5.24 (d, *J* = 3.4 Hz, 1H), 4.05 (s,

3H), 3.79 (dt, *J* = 12.0, 3.8 Hz, 1H), 3.75 (s, 3H), 3.63 (s, 3H), 2.93 (dd, *J* = 16.2, 13.3 Hz, 1H), 2.82 (ddd, *J* = 13.4, 6.7, 4.3 Hz, 1H), 2.59 (dt, *J* = 20.4, 5.3 Hz, 1H), 2.48 – 2.30 (m, 2H), 2.24 – 2.09 (m, 1H), 2.00 – 1.89 (m, 1H), 0.95 (d, *J* = 6.6 Hz, 3H); **^{13}C NMR** ($CDCl_3$, 100 MHz) δ 196.8, 194.1, 170.8, 169.0, 166.7, 165.2, 158.6, 146.8, 127.9, 106.8, 105.1, 98.4, 97.1, 91.1, 77.3, 69.3, 57.4, 56.8, 52.2, 40.2, 36.6, 25.8, 24.6, 14.4; **IR** (film, cm^{-1}) 3457, 2949, 1709, 1611, 1584, 1224, 1210, 753; **TLC** R_f = 0.28 (1:4 acetone:toluene v/v); **HRMS** (DART) *m/z* Calc'd for $C_{24}H_{26}ClO_9$ $(M+H)^+$: 493.1260, found 493.1269.

Methyl (3S, 6R)-3-hydroxy-6-O-(4-des-methyl-griseofulvin)-cyclohex-1-enecarboxylate (2.16)

$[\alpha]_D^{20.0}$ +298.9 (*c* 1.00, $CHCl_3$); M.p. 126 – 128 °C; **^{1}H NMR** ($CDCl_3$, 400 MHz) δ 7.18 (d, *J* = 1.3 Hz, 1H), 6.55 (s, 1H), 5.52 (s, 1H), 5.35 (br s, 1H), 4.33 (ddd, *J* = 9.2, 6.2, 2.0 Hz, 1H), 4.02 (s, 3H), 3.71 (s, 3H), 3.63 (s, 3H), 2.95 (dd, *J* = 16.5, 13.4 Hz, 1H), 2.88 – 2.73 (m, 1H), 2.60 (br s, 1H), 2.39 (dd, *J* = 16.6, 4.6 Hz, 1H), 2.18 – 1.92 (m, 3H), 1.71 (tt, *J* = 13.7, 3.5 Hz, 1H), 0.91 (d, *J* = 6.6 Hz, 3H); **^{13}C NMR** ($CDCl_3$, 100 MHz) δ 197.0, 192.2, 171.0, 169.3, 166.2, 164.6, 156.7, 147.6, 128.9, 106.5, 104.9, 97.8, 93.9, 90.7, 70.8, 67.4, 57.2, 56.8, 52.1, 40.0, 36.7, 27.0, 26.4, 14.3; **IR** (film, cm^{-1}) 3399, 2950, 1711, 1611, 1585, 1357, 1224, 751; **TLC** R_f = 0.17 (1:4 acetone:toluene v/v); **HRMS** (DART) *m/z* Calc'd for $C_{24}H_{26}ClO_9$ $(M+H)^+$: 493.1260, found 493.1268.

In a flame dried flask outfitted with a septum, racemic epoxide **2.1** (81.2 mg, 0.527 mmol, 1.8 equiv.) was dissolved in 1.3 mL of toluene followed by the addition

of 4-des-methyl-griseofulvin **2.14** (99.5 mg, 0.294 mmol, 1.0 equiv.). The resulting solution was thoroughly degassed with argon and cooled to −40 °C. In a separate flask, $Pd_2(dba)_3$ (16.7 mg, 5.0 mol%) of and (*S*,*S*)-**L2** (38.9 mg, 15.0 mol%) was dissolved in 0.6 mL of toluene. The resulting purple solution was degassed and stirred at room temperature until it became yellow (approx. 10 min.). The solution was then cooled to −40 °C and added to the epoxide solution via syringe. The reaction was continued at −40 °C and monitored by ^{1}H NMR spectroscopy until total consumption of the starting phenol was observed (approx. 18 hours). The reaction was then concentrated to dryness and purified by flash chromatography (100% DCM, then 95:5 DCM:MeOH v/v) using Florisil as the stationary phase to yield 132.4 mg of a mixture containing **2.17 (**54% yield), **2.18** (25% yield), and 6.2 mg of recovered phenol **2.14** (6%). Degradation of the products on Florisil is suspected to regenerate griseofulvin **2.14**. Similar degradation, but to a much greater extent, was observed when using silica as the stationary phase. Analytical standards of **2.17** and **2.18** could be separated from one another and purified by a silica column (5:1 toluene/acetone v/v) then preparatory HPLC (80:20 to 35:65 water:acetonitrile v/v over 35 minutes) to remove **17**. Both products were isolated as white solids.

Methyl (5S, 6R)-5-hydroxy-6-O-(4-des-methyl-griseofulvin)-cyclohex-1-enecarboxylate (2.17)

$[\alpha]_D^{20.0}$ +61.0 (*c* 1.00, $CHCl_3$); **M.p.** 196 – 198 °C; **^{1}H NMR** ($CDCl_3$, 300 MHz) δ 7.32 – 7.27 (m, 1H), 7.20 (s, 1H), 5.53 (s, 1H), 5.23 (d, *J* = 3.8 Hz, 1H), 4.05 (s, 3H), 3.81 (dt, *J* = 11.7, 3.9 Hz, 1H), 3.74 (s, 3H), 3.60 (s, 3H), 3.05 (dd, *J* = 16.5, 13.5 Hz, 1H), 2.91 – 2.81 (m, 1H), 2.64 – 2.52 (m, 1H), 2.50 – 2.28 (m, 2H), 2.23 – 2.09 (m,

1H), 2.04 – 1.91 (m, 1H), 0.94 (d, J = 6.5 Hz, 3H); **^{13}C NMR** ($CDCl_3$, 100 MHz) δ 196.9, 194.7, 170.6, 169.1, 166.7, 165.3, 158.7, 146.8, 127.9, 107.2, 104.9, 98.6, 97.8, 90.8, 77.7, 69.2, 57.4, 56.8, 52.2, 40.2, 36.5, 25.8, 24.6, 14.3; **IR** (film, cm^{-1}) 3468, 2949, 1709, 1611, 1224, 1046, 753; **TLC** R_f = 0.26 (1:4 acetone:toluene v/v); **HRMS** (DART) *m/z* Calc'd for $C_{24}H_{26}ClO_9$ $(M+H)^+$: 493.1260, found 493.1268.

Methyl (3R, 6S)-3-hydroxy-6-O-(4-des-methyl-griseofulvin)-cyclohex-1-enecarboxylate (2.18)

$[\alpha]_D^{20.0}$ +96.9 (*c* 1.00, $CHCl_3$); **M.p.** 102 – 104 °C; **^{1}H NMR** ($CDCl_3$, 400 MHz) δ 7.15 (dd, J = 2.4, 1.2 Hz, 1H), 6.53 (s, 1H), 5.51 (s, 1H), 5.34 (d, J = 3.2 Hz, 1H), 4.33 (ddd, J = 10.3, 6.2, 2.6 Hz, 1H), 4.01 (s, 3H), 3.70 (s, 3H), 3.60 (s, 3H), 3.04 – 2.93 (m, 1H), 2.87 – 2.78 (m, 1H), 2.47 – 2.35 (m, 2H), 2.20 – 1.94 (m, 2H), 1.73 (tt, J = 13.9, 3.6 Hz, 1H), 0.94 (d, J = 6.7 Hz, 3H); **^{13}C NMR** ($CDCl_3$, 100 MHz) δ 197.0, 192.2, 171.0, 169.3, 166.2, 164.5, 156.6, 147.5, 129.0, 106.7, 104.8, 97.8, 94.1, 90.6, 70.9, 67.5, 57.2, 56.7, 52.2, 40.1, 36.5, 27.0, 26.4, 14.4; **IR** (film, cm^{-1}) 3400, 2940, 1712, 1612, 1357, 1177, 750; **TLC** R_f = 0.17 (1:4 acetone:toluene v/v); **HRMS** (DART) *m/z* Calc'd for $C_{24}H_{26}ClO_9$ $(M+H)^+$: 493.1260, found 493.1272.

Predicted and Observed Enantiomeric Ratios

From the results shown (Scheme 2.6a), a model was developed. The absolute stereochemistry of the 1,2-addition product derived from the conditions in Table 2.1 was determined by comparison. Acylation and deprotection yielded (*5R-6S*)-Methyl-5,6-dihydroxycyclohex-1-ene carboxylate (**2.43**), a known compound (Scheme 2.6b). Combined with the data in Table 2.1 (entry 5), the 1,2-product must be derived from the (+) enantiomer of (±)-**2.1**. This allows for a table of selectivity to be created (Scheme 2.6c). Thus given a stock of (+)-**2.1** with a known enantiomeric ratio, both the resulting enantiomeric ratios of **2.2b** and **2.3b**, as well as the ratio of **2.2b**:**2.3b** can be estimated. A solution of (+)-**2.1** in 92:8 e.r. can react in two ways with the palladium complex. The 92% portion (+)-**2.1** will react, according to the model, when (*S,S*)-**L2** is utilized, to favor 1,2-addition in a 96:4 enantiomeric ratio. Thus, the 92% portion (+)-**2.1** will react to form 88.32% (*R*)-**2.2b**, and 3.68% of (*S*)-**2.3b**. The 8% of the stock of (–)-**2.1** will react, favoring the 1,4-addition, to form 0.56% and 7.44% of (*S*)-**2.2b** and (*R*)-**2.3b** (derived from the enantiomeric ratio of **2.3b** with (±)-**2.1**). Combining these numbers for both **2.2b** and **2.3b** provides the predicted enantiomeric ratio. Additionally, the ratio of **2.2b**:**2.3b** can be predicted. The result shows excellent agreement between predicted and observed data (Table 2.1, entry 5). The calculations can be repeated employing a stock of 90:10 (−)-**2.1**. Excellent agreement is observed in the predicted verses observed e.r. of **2.3b** and in the ratio of **2.2b** and **2.3b** . The increased enantiomeric ratio of observed **2.2b** does between not agree with the predicted to the same extent as seen before; we are unable to at this time explain this increase in enantiomeric ratio.

Table 2.4. Observed versus Predicted Enantiomeric Ratios for AORR.

	92:8 e.r. (+)-**2.1** Epoxide			10:90 e.r. (−)-**2.1** Epoxide		
	2.2b e.r.	**2.3b** e.r.	Ratio **2.2b**:**2.3b**	**2.2b** e.r.	**2.3b** e.r.	Ratio **2.2b**:**2.3b**
Predicted	99:1	33:67	8.0:1.0	60:40	1:99	1.0:5.40
Observed	98:2	32:68	8.5:1.0	76:24	4:96	1.0:4.6

Two aspects of note are: First, (±)-**2.1** reacts under normal conditions to yield a 1:1.14 ratio of **2.2b**:**2.3b**; these calculations do not take this into account and assume the ratio to be that of 1:1. Second, the model does not take into account the epoxide degradation. Results from each enantiomeric run (Table 2.1, entry 5 and 6), show substantial recovery of isolated **2.1**. Thus from this only the predicted ratio of **2.2b**:**2.3b** can be determined. Work is ongoing to understand the increased degradation when employing enantiopure epoxides.

Scheme 2.6. Allylic oxide regio-resolution predictive model.

a. Racemic Studies

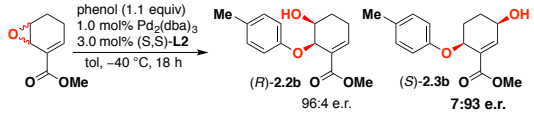

b. Assignment of oxide **2.1** stereochemistry

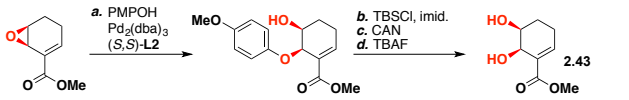

Found: $[\alpha]_{23}^{D}$ -48.0 (c 1, $CHCl_3$)

Lit: $[\alpha]_{23}^{D}$ -53.3 (c 1.6, $CHCl_3$)

c. Predictive table of selectivity

Epoxide	Designation	$[\alpha]_{23}^{D}$	Synthesized from:	(*S*,*S*)-DPEN favors:	(*R*,*R*)-DPEN favors:
	*S*,*R*	+30.5	(*R*,*R*) Mn(salen)	1,2-addition product	1,4-addition product
	*R*,*S*	–31.9	(*S*,*S*) Mn(salen)	1,4-addition product	1,2-addition product

d. Predicted Enantiomeric Ratios for (+)-2.1

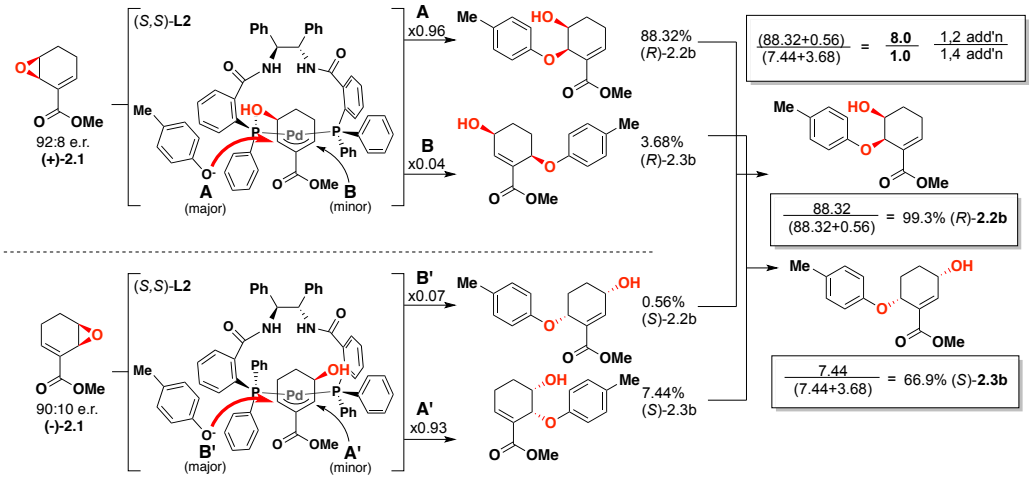

e. Predicted Enantiomeric Ratios for (–)-2.1

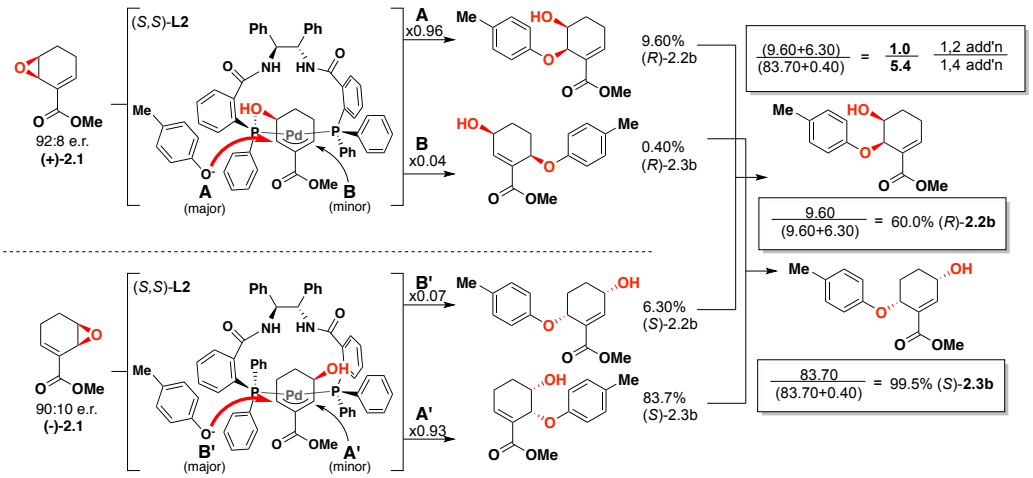

(*5R-6S*)-Methyl-5,6-dihydroxycyclohex-1-ene carboxylate (2.43)

To a solution of **2.2b** (129.0 mg, 0.464 mmol, 1.0 equiv, 78:22 e.r.) in dichloromethane (4.5 mL) was added DMAP (5.0 mg, 0.041 mmol, 0.09 equiv), imidazole (63.1 mg, 0.464 mmol, 1.0 equiv), and TBSCl (140.0 mg, 0.183 mmol, 1.0 equiv). Upon completion, the reaction was concentrated *in vacuo* and purified via flash chromatography (2:1 hexanes/EtOAc, v/v) to yield 167.6 mg (43% yield). **^{1}H NMR** (300 MHz, $CDCl_3$) δ 7.14 (m, 1H), 7.10 (m, 2H), 6.60 (m, 2H), 5.03 (d, J = 2.9 Hz, 1H), 3.81 (dt, J = 11.9, 3.5 Hz, 1H), 3.75 (m, 1H), 3.75 (s, 3H), 3.73 (s, 3H), 2.51 (m, 1H), 2.3 (m, 1H), 2.18 (m, 1H), 1.68 (m, 1H), 0.71 (s, 9H), −0.01 (s, 3H), −0.14 (s, 3H).

The protected alcohol above (167.6 mg, 0.427 mmol, 1.0 equiv) was suspended in 1.0 mL MeCN and 1.0 mL H_2O. The reaction was cooled to 0 °C and ceric ammonium nitrate (538.4 mg, 0.982 mmol, 2.3 equiv) was added in one portion. The reaction was stirred at 0 °C for 5 minutes and then passed through a plug of silica (eluting with EtOAc) and concentrated. The residue was purified by flash chromatography (1:1 hexanes/EtOAc, v/v) to yield 40.0 mg of product (33 % yield). **^{1}H NMR** (400 MHz, $CDCl_3$) δ 7.11 (dd, J = 4.8, 2.9 Hz, 1H), 4.45 (d, J = 4.1 Hz, 1H), 3.78 (s, 3H), 7.76 (m, 1H) 2.81 (d, J = 1.6 Hz, 1H), 2.41 (dtd, J = 20.1, 5.4, 2.2 Hz, 1H), 2.30 – 2.11 (m, 1H), 1.97 – 1.77 (m, 1H), 1.62 (m, 1H), 0.92 (s, 9H), 0.11 (s, 6H).

To the alcohol above (40.0 mg, 0.140 mmol, 1.0 equiv) in THF (1.0 mL), was added TBAF (14.0 μL, 0.14 mmol, 1.0 equiv, 1M in THF) at 0 °C. The reaction was

warmed to 23 °C and stirred. Upon completion, the reaction was concentrated and purified by flash chromatography (1:1 hexanes/EtOAc, v/v) to yield 11.0 mg (45% yield) of **2.43** as a colorless oil and compared to authentic spectra of the known compound.[32]

Methyl (*5S*, *6R*)-5,6-dihydroxycyclohex-1-ene carboxylate (2.43)

$[\alpha]_D^{20.0}$ −48.0 (*c* 1.00, $CHCl_3$, 78:22 e.r.); **^{1}H NMR** (400 MHz, $CDCl_3$) δ 7.09 (t, *J* = 3.9 Hz, 1H), 4.53 (bs, 1H), 3.84 (m, 1H), 3.53 (d, *J* = 3.0 Hz, 1H), 2.43 (m, 1H), 2.21 (m, 1H), 1.85 (m, 1H), 1.70 (m, 1H); **^{13}C NMR** (75 MHz, $CDCl_3$) δ 167.34, 143.34, 129.90, 67.72, 65.37, 51.81, 24.79, 23.95; **TLC** R_f = 0.10 (1:1 hexanes/EtOAc v/v).

Literature (*Org. Biomol. Chem.* **2009**, 7, 2619 – 2627)[32]: **$[\alpha]_D^{20.0}$** −52.9 (c 2.9, >99:1 e.r.); **^{1}H NMR** (300 MHz, $CDCl_3$) δ 7.02 (dd, *J* = 4.4, 3.3 Hz, 1H), 4.46 (d, *J* = 3.1 Hz, 1H), 4.05 (s, 1H), 3.70 (m, 4H), 3.52 (s, OH), 2.42-2.30 (m, 1H), 2.21 – 2.09 (m, 1H), 1.18 – 1.61 (m, 1H); **^{13}C NMR** (75 MHz, $CDCl_3$) δ 167.2, 143.3, 130.4, 68.5, 64.8, 51.8, 24.7, 24.2; **TLC:** R_f = 0.29 (1:1 hexanes/EtOAc v/v).

Scheme 2.7. Synthesis of dioxolane epoxide (**2.19**).

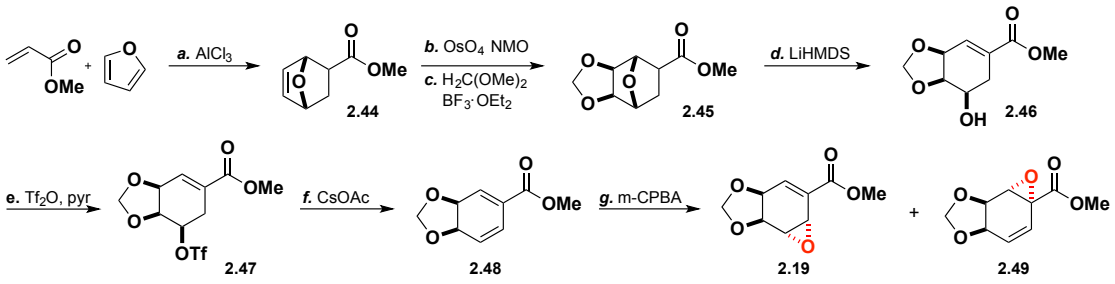

2.44 was prepared according to modified literature procedures.[33]

A flame dried round bottom flask was charged with methyl acrylate (70.0 mL) and cooled to −20 °C. $AlCl_3$ (3.5 g) was then added portionwise followed by the dropwise addition of furan (60 mL). Once the addition was complete (0.5 h), the reaction was warmed to 23 °C and stirred for 5 h. Water (20 mL) was added and the layers separated and the organic layer was concentrated. The red oil was diluted with DCM, dried over Na_2SO_4 and concentrated to yield a red oil, which was used without further purification.

The red oil (57.0 g) from above was dissolved in 1.5 L of acetone and 140.0 mL of water. NMO (112.6 g total weight of solution, 50% in water) was added followed by the addition of OsO_4 (12.0 mL, 185 mmol, 0.5mol%, 0.15 M in DCM). The reaction was stirred for 48 hours or until starting material disappeared. Sodium sulfite (20.0 g) was then added to the reaction and stirred for 0.5 h before the solvent was removed under reduced pressure. The resulting oil was dissolved in a minimal amount (ca. 15 mL) of EtOAc and cooled to 0 °C. The precipitate was collected and washed with Et_2O. This procedure was repeated to yield 40.0 g of diol whose spectra agreed with known data.[33]

Methyl (3a*S*,4*S*,7*R*,7a*R*)-hexahydro-4,7-epoxybenzo[*d*][1,3]dioxole-5-carboxylate (2.45)

The diol above (7.0 g, 37.5 mmol) was dissolved in a solution of $CH_2(OMe)_2$ (60.0 mL) and DCM (65.0 mL) and was cooled to 0 °C. $BF_3{\cdot}OEt_2$ (18.0 mL, 0.106 mol, 3 equiv) in DCM (65.0 mL) was added dropwise via an addition funnel over 0.5 h. The reaction was then stirred for 0.5 h at 0 °C and then diluted with water (20.0 mL). The organic layer was dried with Na_2SO_4 and concentrated under reduced pressure to yield

a black oil which was purified by flash chromatography (1:1 EtOAc/hexanes, v/v) to yield 6.67 g (33.1 mmol, 88% yield) as a mixture of endo and exo isomers of **2.43** (the isomers can be separated using flash chromatography [2:1 hexanes/EtOAc, v/v]).

Endo (major) Isomer: **^{1}H NMR** (300 MHz, $CDCl_3$) δ 5.06 (d, *J* = 1.0 Hz, 1H), 4.77 (d, *J* = 1.0 Hz, 1H), 4.64 (d, *J* = 6.0 Hz, 1H), 4.55 (d, *J* = 6.0 Hz, 1H), 4.22 (s, 2H), 3.69 (s, 3H), 2.95 (dt, *J* = 11.3, 5.5 Hz, 1H), 1.90 (dddd, *J* = 12.6, 11.4, 6.0, 1.1 Hz, 1H), 1.72 (ddd, *J* = 13.1, 5.2, 1.1 Hz, 1H); **^{13}C NMR** (75 MHz, $CDCl_3$) δ 171.9, 97.0, 81.9, 81.0, 80.2, 79.4, 52.3, 43.3, 27.6; **IR** (film, cm^{-1}) 2955, 1729, 1200, 1048; **TLC** R_f = 0.80 (2:1 EtOAc/hexanes, v/v); **HRMS** (DART) *m/z* calc for $C_9H_{12}O_5$ $(M+H)^+$: 201.0757, found 201.0752.

Methyl (3a*S*,7*R*,7a*R*)-7-hydroxy-3a,6,7,7a-tetrahydrobenzo[*d*][1,3]dioxole-5-carboxylate (2.46)

A solution of HMDS (8.5 mL, 39.0 mmol, 1.2 equiv) in dry THF (150.0 mL) was cooled to −78 °C and *n*-BuLi (23.3 mL, 37.3 mmol, 1.1eq, 1.6M in hexanes) was added slowly. The reaction was stirred for 20 minutes at −78 °C before **2.45** (6.70 g, 33.9 mmol) in THF (50.0 mL) was added via cannula in one portion. After stirring for 20 minutes the flask was allowed to warm to 0 °C, quenched with water (10.0 mL), and extracted with EtOAc (2 x 20.0 mL). Drying over Na_2SO_4, concentration *in vacuo* and flash chromatography (1:1 hexanes/EtOAc, v/v) yielded an amber oil (6.2 g, 31 mmol, 91%).

^{1}H NMR (500 MHz, $CDCl_3$) δ 6.71 (s, 1H), 4.96 (s, 1H), 4.95 (s, 1H), 4.72 (bs, 1H), 4.22 (dd, *J* = 6.2, 2.7 Hz, 1H), 3.93 (m, 1H), 3.73 (s, 3H), 2.72 (d, *J* = 6.2 Hz, 1H), 2.61 (dd, *J* = 16.9, 5.0 Hz, 1H), 2.41 (dd, *J* = 16.9, 9.2 Hz, 1H); **^{13}C NMR** (126 MHz, $CDCl_3$) δ 166.5, 132.9, 131.3, 95.0, 75.6, 72.7, 67.1, 52.2, 27.9; **IR** (film, cm^{-1}) 3452, 2952, 1713, 1436, 1241, 1049, 728; **TLC** R_f = 0.45 (1:1 hexanes/EtOAc, v/v); **HRMS** (DART) *m/z* calc for $C_9H_{12}O_5$ $(M+H)^+$: 201.0757, found 201.0753.

Methyl (3a*S*,7*R*,7a*S*)-7-(((trifluoromethyl)sulfonyl)oxy)-3a,6,7,7a-tetrahydrobenzo[*d*][1,3]dioxole-5-carboxylate (2.47)

2.46 (9.553g, 47.7 mmol) was dissolved in DCM (230.0 mL) and cooled to 0 °C. Pyridine (7.60 mL, 95.5 mmol, 2 equiv) was added followed by the dropwise addition of Tf_2O (9.60 mL, 57.3 mmol, 1.1 equiv) in DCM (25.0 mL). The reaction was stirred at 0 °C for 20 minutes and then rapidly washed with 1M HCl (2 x 10 mL), dried over Na_2SO_4 and concentrated. Purification via flash chromatography (1:1 hexanes/EtOAc, v/v) yields unstable triflate (12.4 g, 38.5 mmol, 80% yield) as a pale oil.

^{1}H NMR (500 MHz, $CDCl_3$) δ 6.84 (m, 1H), 5.16 (ddd, *J* = 8.2, 5.0, 2.6 Hz, 1H), 5.06 (s, 1H), 5.05 (s, 1H), 4.84 (m, 1H), 4.39 (dd, *J* = 5.7, 2.3 Hz, 1H), 3.80 (s, 3H), 2.91 (ddt, *J* = 17.0, 8.7, 2.2 Hz, 1H), 2.82 (dd, *J* = 17.1, 5.1 Hz, 1H). **^{13}C NMR** (126 MHz, $CDCl_3$) δ 165.5, 133.0, 129.6, 122.4, 119.8, 117.3, 114.8, 95.9, 82.8, 73.1, 72.9, 52.7, 25.9; **IR** (film, cm^{-1}) 2957, 1719, 1657, 1409, 1268, 1141, 913; **TLC** R_f = 0.75 (1:1 hexanes/EtOAc, v/v); **HRMS** (DART) *m/z* calc for $C_{10}H_{11}F_3O_7S$: 333.0150 $(M+H)^+$, found 333.0241.

Methyl (3a*S*,7a*R*)-3a,7a-dihydrobenzo[*d*][1,3]dioxole-5-carboxylate (2.48)

Triflate, **2.47** (2.80 g, 8.6 mmol) was dissolved in DMF (40.0 mL) and anhydrous CsOAc (1.73 g, 10.1 mmol, 1.05 equiv) was added in one portion. The reaction was stirred for 1.75 h. Saturated $NaHCO_3$ (50.0 mL) was added carefully and the organic layer was extracted with Et_2O (2 x 50.0 mL) and washed (2 x 100.0 mL) with brine. Drying over Na_2SO_4 and concentration under reduced pressure yields unstable diene **2.48** as white needles, which were sufficiently pure for the next step. Analytical samples were purified by flash chromatography (5:1 Et_2O/pentane, v/v) to yield a white powder.

M.p. 55 – 57 °C; **^{1}H NMR** (300 MHz, $CDCl_3$) δ 6.85 (d, *J* = 3.8 Hz, 1H), 6.55 (d, *J* = 10.0 Hz, 1H), 6.03 (dd, *J* = 10.0, 3.9 Hz, 1H), 4.78 (s, 1H), 4.77 (s, 1H), 4.72 (dd, *J* = 9.3, 3.8 Hz, 1H), 4.55 (dd, *J* = 9.3, 4.4 Hz, 1H), 3.87 (s, 3H); **^{13}C NMR** (126 MHz, $CDCl_3$) δ 165.6, 132.0, 127.7, 124.6, 122.9, 91.0, 69.9, 69.6, 52.2; **IR** (film, cm^{-1}) 2851, 1717, 1441, 1250, 1089; **HRMS** (DART) *m/z* calc for $C_9H_{10}O_4$: 183.0652 $(M+H)^+$, found 183.0649.

Methyl (3a*S*,5a*S*,6a*S*,6b*S*)-3a,5a,6a,6b-tetrahydrooxireno[2',3':3,4]benzo[1,2-*d*][1,3]dioxole-5-carboxylate (2.19) & Methyl (3a*R*,5a*R*,6a*S*,6b*R*)-6a,6b-dihydrooxireno[2',3':3,4]benzo[1,2-*d*][1,3]dioxole-5a(3a*H*)-carboxylate (2.49)

To a flame dried round bottom flask was added crude diene **2.48** (2.5 g, 13.7 mmol) in DCM (60.0 mL). *m*-CPBA (3.50 g, 15.1 mmol, 1.1 equiv, 75%) in DCM (40.0 mL) was then added dropwise and the reaction heated to 40 °C for 18 h. The reaction was cooled and washed with saturated sodium thiosulfate (30.0 mL) and saturated sodium

bicarbonate (2 x 30.0 mL), dried over Na_2SO_4 and concentrated. The oil obtained was purified by flash chromatography (9:1 hexanes/EtOAc, v/v) to yield 1.30 g (6.54 mmol, 24% yield) of a 2:1 ratio of inseparable epoxides.

Based on analysis of the ^{1}H NMR spectrum and literature precedence, the ^{1}H NMR for both **2.49** and **2.19** can be determined, the ^{13}C NMR however is a mixture of the two compounds and is consistent with literature[2,3]: **^{1}H NMR (2.49)** (500 MHz, $CDCl_3$) δ 6. 76 (bs, 1H), 4.96 (s, 1H), 4.90z (m, 1H), 4.60 (m, 2H), 3.94 (dd, *J* = 3.9, 1.7 Hz, 1H), 3.80 (s, 3H), 3.67 (dd, *J* = 3.7, 1.5 Hz, 1H); **^{1}H NMR (2.19)** (500 MHz, $CDCl_3$) δ 6.51 (dd, *J* = 10.6, 1.6 Hz, 1H), 5.80 (dd, *J* = 10.5, 2.6 Hz, 1H), 4.96 (s, 1H), 4.86 (s, 1H), 4.60 (m, 1H), 4.52 (m, 1H), 3.89 (d, *J* = 1.8 Hz, 1H), 3.78 (s, 3H); **^{13}C NMR (2.49 & 2.19)** (75 MHz, $CDCl_3$) δ 168.7, 165.2, 137.7, 129.7, 129.4, 124.4, 95.3, 94.7, 70.4, 70.4, 70.1, 69.9, 55.0, 53.1, 52.4, 51.6, 49.3, 45.9; **TLC** R_f = 0.40 (4:1 hexanes/EtOAc, v/v).

Allylic Oxide Regio Resolution of (±)-2.19

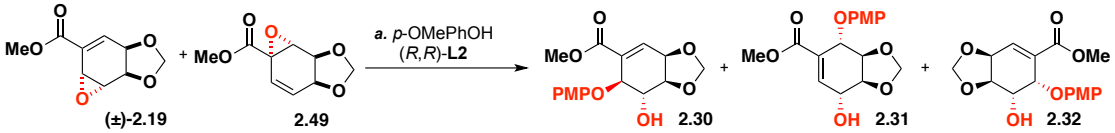

328.7 mg (1.65 mmol, 1.0 equiv) of a mixture containing racemic epoxide **2.19** and **2.49** (2:1 by 1H NMR respectively) was dissolved in 5.5 mL of toluene in a flame-dried round bottom flask outfitted with a septum followed by the addition of 253.7 mg (2.04 mmol, 1.2 equiv) of *p*-methoxyphenol. The resulting solution was thoroughly degassed with argon. In a separate round bottom flask, 77.0 mg (5 mol%) of $Pd_2(dba)_3$ and 198.3 mg (15 mol%) of DPEN-ligand **L2** was dissolved in toluene (2.8 mL). The

purple solution was degassed and stirred at room temperature until it became yellow (approx. 10 min.) and then added to the epoxide solution via syringe. The reaction was allowed to stir for 18 hours before an additional 61.1 mg (4 mol%) $Pd_2(dba)_3$ and 158.0 mg (12 mol%) of DPEN-ligand **L2** in 4.0 mL of toluene was added. The reaction was stirred for an additional 12 hours at room temperature before being concentrated. The crude oil was then purified by column chromatography (4:4:1 DCM/hexanes/EtOAc) to give 56.2 mg of 1,4-product **2.31** (16% yield, 90:10 er) and 139.5 mg (39% yield) of a mixture of 1,2-products **2.30** and **2.32** as a pale yellow oil. ^{1}H NMR spectroscopy analysis determined the ratio of products to be 14% **2.30** (90:10 er) and 25% **2.32** (92:8 er). The 1,2-products were separated by column chromatography (95:5 DCM/ether) to give pure *anti*-1,2 product **2.30** and *syn*-1,2 product **2.32** as pale yellow oils. *Anti*-1,4 product **2.33** was observed by ^{1}H NMR spectrum in 1-2%, but could not be isolated.

Additional regio resolutions were attempted and provided the following data: 1) **2.30** was obtained in 16% yield (94:6 er), **2.31** in 8% yield (89:11 er), and **2.32** in 24% yield (90:10 er); 2) **2.30** was obtained in 10% yield (96:4 er), **2.31** in 12% yield (84:16 er), and **2.32** in 23% yield (90:10 er).

Methyl (3a*R*,6*S*,7*R*,7a*S*)-7-hydroxy-6-(4-methoxyphenoxy)-3a,6,7,7a-tetrahydrobenzo[*d*][1,3]dioxole-5-carboxylate (2.30)

$[\alpha]_D^{20.0}$ +11.8 (*c* 0.50, $CHCl_3$); **^{1}H NMR** (300 MHz, $CDCl_3$) δ 7.10 – 7.03 (m, 2H), 6.91 (d, *J* = 3.8 Hz, 1H), 6.88 – 6.80 (m, 2H), 5.13 (s, 1H), 5.07 (s, 1H), 4.97 (d, *J* = 4.3 Hz, 1H), 4.80 (dd, *J* = 6.4, 3.8 Hz, 1H), 4.34 (dd, *J* = 4.8, 4.7 Hz, 1H), 4.27 (dd, *J* = 6.3, 5.2 Hz, 1H), 3.78 (s, 3H), 3.76 (s, 3H); **^{13}C NMR** (100 MHz, $CDCl_3$) δ 166.0,

155.0, 152.6, 134.2, 132.5, 119.1, 114.7, 94.8, 75.1, 75.0, 70.8, 68.0, 55.8, 52.3; **IR** (film, cm^{-1}) 3465, 2954, 1719, 1505, 1246, 1214, 104, 1033; **TLC** R_f = 0.28 (9:1 DCM/Ether v/v); **HPLC** 94:6 e.r., Chiral HPLC eluting at 1.00 mL/min with 90% hexanes/isopropanol. Retention times: R_T= 15.6 min, 21.9 min; **HRMS** (ESI) *m/z* Calc'd for $C_{16}H_{18}O_7Na$ $(M+Na)^+$ 345.09447, found 345.0933.

Methyl (3a*R*,4*S*,7*R*,7a*S*)-7-hydroxy-4-(4-methoxyphenoxy)-3a,4,7,7a-tetrahydrobenzo[*d*][1,3]dioxole-5-carboxylate (2.31)

$[\alpha]_D^{20.0}$ +44.5 (*c* 0.50, $CHCl_3$); **^{1}H NMR** (400 MHz, $CDCl_3$) δ 7.51 (d, *J* = 6.4 Hz, 1H), 7.05 – 6.97 (m, 2H), 6.88 – 6.80 (m, 2H), 5.38 (d, *J* = 1.9 Hz, 1H), 4.96 (s, 1H), 4.67 (s, 1H), 4.65 (dd, *J* = 6.9, 2.2 Hz, 1H), 4.55 (d, *J* = 7.0 Hz, 1H), 4.51 – 4.44 (m, 1H), 3.80 (s, 3H), 3.78 (s, 3H); **^{13}C NMR** (100 MHz, $CDCl_3$) δ 165.7, 155.5, 150.5, 143.7, 132.7, 118.5, 114.9, 94.2, 77.2, 74.7, 64.8, 55.7, 52.4; **IR** (film, cm^{-1}) 3490, 2948, 1719, 1505, 1246, 1211, 1089, 1032; **TLC** R_f = 0.27 (7:3 hexanes/EtOAc v/v); **HPLC** 89:11 e.r., Chiral HPLC eluting at 1.00 mL/min with 90% hexanes/isopropanol. Retention times: R_T= 21.4 min, 26.5 min; **HRMS** (ESI) *m/z* Calc'd for $C_{16}H_{18}O_7Na$ $(M+Na)^+$: 345.09447, found 345.09420.

Methyl (3a*S*,6*S*,7*S*,7a*R*)-7-hydroxy-6-(4-methoxyphenoxy)-3a,6,7,7a-tetrahydrobenzo[*d*][1,3]dioxole-5-carboxylate (2.32)

$[\alpha]_D^{20.0}$ +96.6 (*c* 1.00, $CHCl_3$); **^{1}H NMR** (300 MHz, $CDCl_3$ δ 7.05 – 6.99 (m, 3H), 6.84 – 6.78 (m, 2H), 5.23 (d, *J* = 3.2 Hz, 1H), 5.12 (s, 1H), 5.01 (s, 1H), 4.85 (dd, *J* = 7.0, 3.1 Hz, 1H), 4.53 (dd, *J* = 7.7, 7.2 Hz, 1H), 3.92 (dd, *J* = 7.8, 3.3 Hz, 1H), 3.76 (s, 3H), 3.70 (s, 3H); **^{13}C NMR** (100 MHz, $CDCl_3$) δ 165.4, 155.0, 152.3, 137.6, 132.1, 118.9, 114.5, 94.8, 75.9, 74.6, 73.1, 70.7, 55.6, 52.3; **IR** (film, cm^{-1}) 3445, 2951, 1721,

1504, 1253, 1211, 1078, 1033; **TLC** R_f = 0.17 (9:1 DCM/Ether v/v); **HPLC** 90:10 e.r., Chiral HPLC eluting at 1.25 mL/min with 95% hexanes/methanol. Retention times: R_T= 58.6 min, 62.9 min; **HRMS** (ESI) *m/z* Calc'd for $C_{16}H_{18}O_7Na$ $(M+Na)^+$ 345.09447, found 345.09426.

Thermodynamic pathway: isolation of *anti*-addition products

To test whether the thermodynamic pathway (*anti* addition modes) was operable, racemic acetonide-protected *trans*-epoxide **2.38** was synthesized in 7 steps from furan and methyl acrylate according to literature procedures and was obtained as an inseparable mixture of oxide isomers **2.38** and **2.50** (68:32 ratio).[20] Exposure to standard conditions resulted in both 1,2 and 1,4 *anti* addition modes. The *syn*-1,2 addition product was isolated in 20% yield (97:3 er); the *anti*-1,4 addition product was isolated in a 3% yield (80:20 er). Due to the low yield of the 1,4-*anti* addition product, we examined our model (*vide supra*) and determined that we could use enantiopure epoxide (−)-**2.38** (obtained from quinic acid)[20], employ ligand (*S,S*)-**L2** and augment our 1,4-*anti* product.

Scheme 2.8. Thermodynamic AAOR pathway.

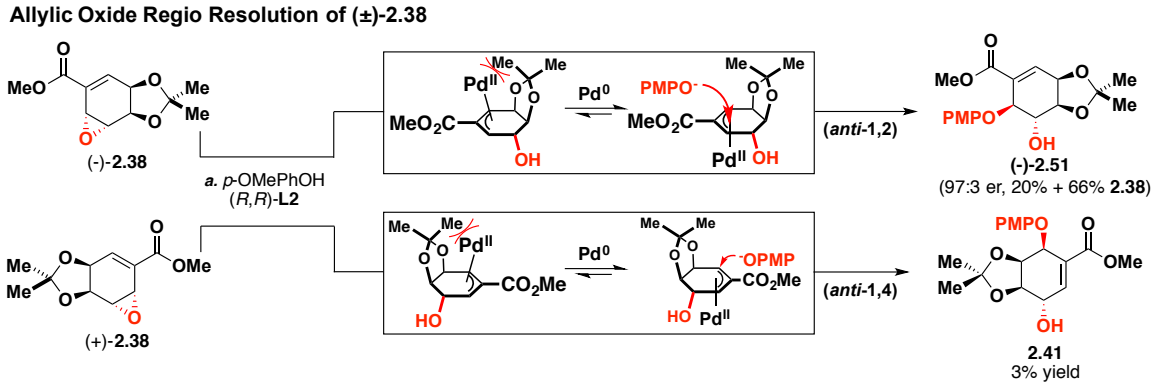

Preparation of (−)-2.41 – from racemic oxide: 876.0 mg (3.87 mmol) of a racemic mixture of **2.38** and **2.50** (68:32 respectively) was dissolved in 30 mL of toluene with 368.8 mg (2.97 mmol, 1.2 equiv with respect to epoxide **2.38**) of *p*-methoxyphenol and degassed with argon, then cooled to 0 °C. In a separate flask, 122.6 mg (5 mol%) $Pd_2(dba)_3$ was added to a solution of 312.1 mg (15 mol%) **L2** in 15 mL of toluene and degassed with argon until the purple solution became yellow. The solution was then cooled to 0 °C. The palladium solution was then added to the epoxide solution and the resulting yellow solution was warmed to room temperature. After 72 h, an additional 5.0 mL toluene solution containing 63.0 mg (2.5 mol%) $Pd_2(dba)_3$ and 157.6 mg (7.5 mol%) ligand, was added. After an additional 24 h, the reaction was purified by column chromatography (4:1 hexanes/EtOAc v/v) using silica that was previously deactivated with triethylamine to give 183.1 mg of 1,2-addition product **(−)-2.51** (20% yield) and 22.8 mg (3%) of 1,4-addition product **2.41**. Both products were isolated as pale yellow oils. The recovered oxides (**2.38** and **2.50**, 63%) was obtained in 64:36 and 51:49 enantiomeric ratios respectively.

Methyl (3a*R*,6*S*,7*R*,7a*S*)-7-hydroxy-6-(4-methoxyphenoxy)-2,2-dimethyl-3a,6,7,7a-tetrahydrobenzo[*d*][1,3]dioxole-5-carboxylate (2.51)

$[\alpha]_D^{20.0}$ −20.2 (*c* 1.00, $CHCl_3$); **^{1}H NMR** (400 MHz, $CDCl_3$) δ 7.03 (d, *J* = 9.0 Hz, 2H), 6.85 (dd, *J* = 3.8, 1.1 Hz, 1H), 6.81 (d, *J* = 9.1 Hz, 2H), 4.94 (dd, *J* = 5.3, 1.0 Hz, 1H), 4.75 (ddd, *J* = 6.2, 3.8, 1.1 Hz, 1H), 4.29 (td, *J* = 6.2, 0.7 Hz, 1H), 4.22 (dd, *J* = 6.3, 5.2 Hz, 1H), 3.76 (s, 3H), 3.70 (s, 3H), 1.52 – 1.49 (s, 3H), 1.40 (s, 3H). **^{13}C NMR** (101 MHz, $CDCl_3$) δ 168.4*, 165.8*, 154.4*, 152.8*, 134.3*, 134.2*, 131.9, 118.2, 114.3, 110.8, 75.8*, 75.7*, 70.8*, 70.7*, 70.0, 55.5*, 55.4*, 51.9*, 51.8*, 27.7, 25.8; **IR** (film, cm^{-1}) 3451, 2967, 2933, 1720, 1504, 1250, 1030; **TLC** R_f = 0.53 (1:1 hexanes/EtOAc v/v); **HPLC** 97:3 e.r., Chiral HPLC eluting at 1.0 mL/min with 90% hexanes/isopropanol. Retention times: R_T= 9.6 min, 22.6 min; **HRMS** (DART) *m/z* Calc'd for $C_{14}H_{16}O_4$ $(M+H)^+$ 350.1366, found 350.1369. * denotes presumed rotamers in a 1:1 ratio.

Methyl (3a*S*,4*S*,7*S*,7a*R*)-7-hydroxy-4-(4-methoxyphenoxy)-2,2-dimethyl-3a,4,7,7a-tetrahydrobenzo[*d*][1,3]dioxole-5-carboxylate (2.41)

$[\alpha]_D^{20.0}$ −141.1 (*c* 1.00, $CHCl_3$); **M.p.** 55 – 58 °C; **^{1}H NMR** ($CDCl_3$, 400 MHz) δ 7.03 – 6.99 (m, 3H), 6.83 – 6.77 (m, 2H), 5.20 (d, *J* = 3.2 Hz, 1H), 4.97 (dd, *J* = 6.8, 3.1 Hz, 1H), 4.56 (dd, *J* = 7.7, 6.8 Hz, 1H), 3.92 (ddd, *J* = 7.6, 6.1, 3.2 Hz, 1H), 3.76 (s, 3H), 3.69 (s, 3H), 1.48 (s, 3H), 1.43 (s, 3H); **^{13}C NMR** ($CDCl_3$, 126 MHz) δ 165.68, 155.10, 152.43, 138.34, 131.39, 119.02, 114.57, 110.28, 76.18, 74.73, 72.73, 72.01, 55.71, 52.35, 27.66, 25.29; **IR** (film, cm^{-1}) 3340, 2934, 1720, 1505, 1211, 1054; **TLC**

R_f = 0.23 (7:3 hexanes/EtOAc v/v); **HRMS** (DART) *m/z* Calc'd for $C_{18}H_{23}O_7$: 351.1444 $(M+H)^+$, found 351.1441.

A mixture of enantiopure epoxide (−)-**2.38** and **2.50** were synthesized in 5 steps from quinic acid according to literature procedure.[6] Exposure of (−)-**2.38** to the general conditions, increased the yield of **2.41** to 44% with no loss of enantiopurity. It is worth nothing that a switch in the catalyst to (*R,R*)-**L2** did result in a population shift to favor the 1,2 *anti* addition product.

Preparations of 2.41 from (−)-2.38 – enantiopure augmentation: 244.9 mg (0.99 mmol, 1 equiv) of a mixture containing enantiopure epoxide **2.38** and **2.50** (68:32 respectively) was dissolved in 6.0 mL of toluene. 161.5 mg (1.30 mmol, 1.3 equiv) of *p*-methoxyphenol was added and the resulting pale yellow solution was degassed thoroughly with argon. In a separate flask, 50.2 mg (5 mol%) of $Pd_2(dba)_3$ and 129.4 mg (15 mol%) **L2** were added to 4.0 mL of toluene and degassed with argon until the purple solution became yellow. The solution was added via syringe at room temperature to the reaction containing the epoxide. The reaction stirred under inert atmosphere for 24 h before an additional 50.1 mg (5 mol%) $Pd_2(dba)_3$ and 130.3 mg (15% mol) **L2** dissolved in 4.0 mL of toluene was added. The reaction stirred for an additional 12 hours before being concentrated to give a yellow oil. The reaction was then purified by column chromatography (4:1 hexanes/EtOAc) to give 112.3 mg (44% yield) of *anti*-1,4 product **2.41** and 38.0 mg (15% yield) of *anti*-1,2 product **2.51** with no recovered starting material.

Total synthesis of streptol and MK7607

Scheme 2.9. Total synthesis of streptol and MK7606.

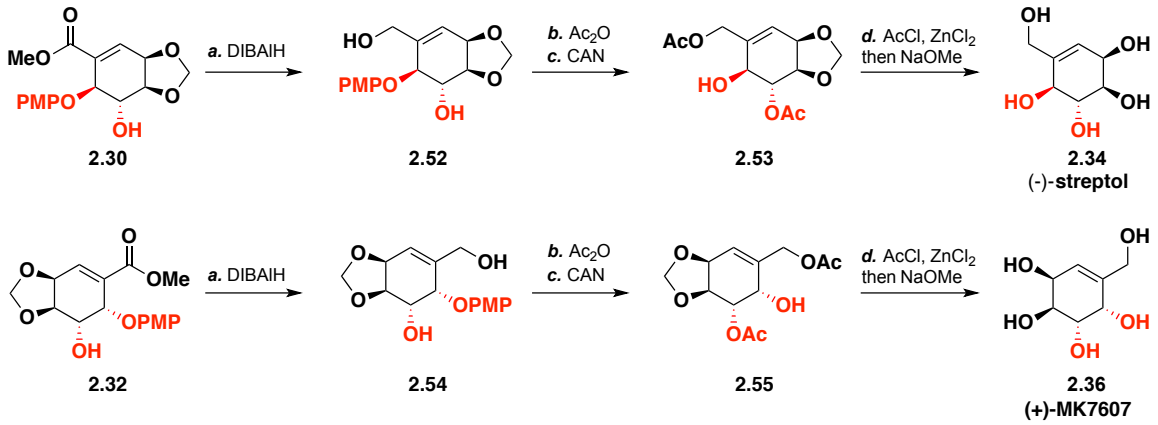

Reduction of 2.30 and 2.32:

2.32 (70.0 mg, 0.217 mmol) was dissolved in dichloromethane (1.0 mL) and cooled to −78 °C under argon. DIBAl-H (700 µL, 0.694 mmol, 3.2 equiv, 1M in DCM) was added dropwise over 5 minutes. The reaction was stirred for 0.5 h at −78 °C and quenched with methanol. The reaction was warmed to room temperature and 2.0 mL of a 1:1 solution of 30% sodium potassium tartrate and a 30% aqueous ethanolamine were added and stirred for 1 h. The now clear solution was extracted with hot EtOAc (5 x 2.0 mL), washed with cold 1M HCl (1.0 mL), dried over Na_2SO_4 and concentrated. Flash chromatography (1:1 hexanes/EtOAc, v/v) yielded 20.0 mg (0.068 mmol, 28% yield) **2.54**.

(3a*R*,4*S*,5*S*,7a*S*)-6-(hydroxymethyl)-5-(4-methoxyphenoxy)-3a,4,5,7a-tetrahydrobenzo[*d*][1,3]dioxol-4-ol (2.54)

$[\alpha]_D^{20.0}$ +45.5 (*c* 1.00, $CHCl_3$); **M.p.** 109 – 112 °C; **^{1}H NMR** (400 MHz, $CDCl_3$) δ 6.99 (d, *J* = 9.0 Hz, 1H), 6.83 (d, *J* = 9.0 Hz, 1H), 5.92 (d, *J* = 3.5 Hz, 1H), 5.04 (s, 1H), 4.96 (s, 1H), 4.85 (d, *J* = 3.4 Hz, 1H), 4.72 (t, *J* = 5.0 Hz, 1H), 4.37 (t, *J* = 6.2 Hz, 1H), 4.23 (dd, *J* = 6.2, 3.4 Hz, 1H), 4.18 (d, *J* = 6.4 Hz, 1H), 3.77 (s, 2H); **^{13}C NMR** (126 MHz, $CDCl_3$) δ 155.3, 152.1, 140.0, 122.1, 118.6, 115.0, 94.6, 76.0, 75.5, 72.4, 69.5, 63.9, 55.8; **IR** (film, cm^{-1}) 3330, 1608, 1214, 1184, 811; **TLC** R_f = 0.20 (1:1 hexanes/EtOAc, v/v); **HRMS** (DART) *m/z* calc for $C_{15}H_{22}NO_6$ $(M+NH_4)^+$ 312.1447, found 312.1432.

2.30 (55.0 mg, 0.171 mmol) was converted to **2.52** (19.0 mg, 0.065mmol, 38 % yield) in the same manner as above.

(3a*S*,4*R*,5*S*,7a*R*)-6-(hydroxymethyl)-5-(4-methoxyphenoxy)-3a,4,5,7a-tetrahydrobenzo[*d*][1,3]dioxol-4-ol (2.52)

$[\alpha]_D^{20.0}$ −42.0 (*c* 1.00, $CHCl_3$); **M.p.** 109–112 °C; **^{1}H NMR** (600 MHz, $CDCl_3$) δ 7.03 (m, 2H), 6.83 (m, 2H), 5.98 (dq, *J* = 3.3, 1.5 Hz, 1H), 5.22 (s, 1H), 5.03 (s, 1H), 4.75 (ddd, *J* = 8.4, 2.3, 1.2 Hz, 1H), 4.51 (ddd, *J* = 6.9, 3.6, 1.5 Hz, 1H), 4.27 (m, 2H), 4.24 (dd, *J* = 8.6, 6.8 Hz, 1H), 3.96 (td, *J* = 8.5, 2.6 Hz, 1H), 3.77 (s, 3H), 3.48 (s, 1H), 2.56 (d, *J* = 2.8 Hz, 1H); **^{13}C NMR** (101 MHz, $CDCl_3$) δ 154.9, 153.5, 143.1, 119.7, 117.6, 115.0, 95.4, 79.7, 76.8, 72.9, 72.5, 62.8, 55.8; **IR** (film, cm^{-1}) 3310, 33239, 2926, 1506, 1210; **TLC** R_f = 0.30 (2:1 EtOAc/hexanes, v/v); **HRMS:** (DART) *m/z* calc for $C_{15}H_{22}NO_6$ $(M+NH_4^+)$ 312.1447, found 312.1437.

Acylation and oxidative deprotection

2.54 10.0 mg, 0.034 mmol) was dissolved in 0.30 mL DCM. $^{i}Pr_2NEt$ (17.0 μL, 0.102 mmol, 3 equiv), DMAP (2.0 mg) and Ac_2O (10 μg, 0.102 mmol, 3equiv) was added and stirred for 0.5 h. The reaction was diluted with saturated sodium bicarbonate solution (1.0 mL) and extracted with EtOAc (2 x 2.0 mL). The organic layers were combined and dried over Na_2SO_4 and concentrated to yield diacetate that was used without further purification.

The diacetate from above (11.5 mg, 0.030 mmol) was dissolved in 4:1 MeCN/H_2O (0.15 mL) and cooled to 0 °C. To this was added ceric ammonium nitrate (36.6 mg, 0.067 mmol, 2.2 equiv) and the reaction stirred for 15 minutes. The solution was washed with saturated sodium bicarbonate (1.0 mL) and extracted with EtOAc (2 x 2.0 mL). The organic layers were combined, dried over Na_2SO_4 and concentrated under reduced pressure. Flash chromatography (2:1 hexanes/EtOAc to 1:1 hexanes/EtOAc, v/v) yielded 2.0 mg (0.007 mmol, 21% yield over two steps) of **2.55**.

((3a*S*,6*S*,7*S*,7a*S*)-7-acetoxy-6-hydroxy-3a,6,7,7a-tetrahydrobenzo[*d*][1,3]dioxol-5-yl)methyl acetate (2.55)

$[\alpha]_D^{20.0}$ +52.5 (*c* 0.20, $CHCl_3$); **^{1}H NMR** (400 MHz, $CDCl_3$) δ 6.00 (m, 1H), 5.10 (m, 1H), 5.09 (s, 1H), 4.96 (s, 1H), 4.68 (q, *J* = 13.6 Hz, 2H), 4.60 (m, 1H), 4.48 (dd, *J* = 8.1, 6.5 Hz, 1H), 4.38 (t, *J* = 3.8 Hz, 1H), 2.17 (s, 3H), 2.11 (s, 3H); **^{13}C NMR** (101 MHz, $CDCl_3$) δ ^{13}170.9, 170.7, 137.6, 124.4, 94.8, 77.4, 72.9, 72.6, 66.0, 64.7, 21.3, 21.0; **IR** (film, cm^{-1}) 3229, 1615, 1505, 1230; **TLC** R_f = 0.33 (1:1 hexanes/EtOAc, v/v); **HRMS** (DART) *m/z* calc for $C_{12}H_{27}O_7$ $(M+H)^+$: 273.0974, found 273.0964.

2.52 (20.0 mg, 0.068 mmol) was converted to **2.53** (9.0 mg, 0.033 mmol, 48.5 % yield) in the same manner as above.

((3a*R*,6*S*,7*R*,7a*R*)-7-acetoxy-6-hydroxy-3a,6,7,7a-tetrahydrobenzo[*d*][1,3]dioxol-5-yl)methyl acetate (2.53)

$[\alpha]_D^{20.0}$ −2.5 (*c* 0.90, $CHCl_3$); **^{1}H NMR** (500 MHz, $CDCl_3$) δ 5.87 (m, 1H), 5.17 (m, 1H), 5.15 (s, 1H), 5.01 (s, 1H), 4.83 (d, *J* = 13.7 Hz, 1H), 4.65 (d, *J* = 13.7 Hz, 1H), 4.54 (m, 1H), 4.25 (t, *J* = 6.8 Hz, 1H), 4.15 (d, *J* = 6.9 Hz, 1H), 2.14 (s, 3H), 2.10 (s, 3H); **^{13}C NMR** (126 MHz, $CDCl_3$) δ 171.3, 170.9, 139.2, 121.1, 95.2, 74.1, 72.9, 72.4, 68.3, 63.8, 21.2, 21.0; **IR** (film, cm^{-1}) 3466, 2922, 1738, 1227, 1040; **TLC** R_f = 0.39 (1:1 hexanes/EtOAc, v/v); **HRMS** (DART) *m/z* calc for $C_{12}H_{27}O_7$ $(M+H)^+$: 273.0974, found 273.0964.

Deprotection of dioxolane

A round bottom flask was charged with **2.55** (5.8 mg, 0.021 mmol) under argon and cooled to 0 °C. Freshly distilled AcCl (0.25 mL) was then added and the solution stirred for 10 minutes at 0 °C. Anhydrous $ZnCl_2$ (ca 1 mg,) was added and the reaction stirred at 0 °C for 0.3 h before being warmed to room temperature and stirred for an additional 0.3 h. Disappearance of nonpolar (high R_f) compound by TLC indicated completion of reaction. The solution was diluted with 1.0 mL THF and concentrated to a third of its volume. Water (0.5 mL) was then added and stirred for 10 minutes. The reaction is then extracted with EtOAc (2 x 3.0 mL), dried over Na_2SO_4 and concentrated. The material is passed through a plug of silica gel (1:1 hexanes/EtOAc,

v/v) to yield MK7607-tetracetate (5.5 mg, 0.015 mmol, 70% yield). **^{1}H-NMR (**400 MHz, $CDCl_3$) δ 6.04 (d, *J* = 4.8 Hz, 1H), 5.74 (d, *J* = 4.2 Hz, 1H), 5.50 (dd, *J* = 10.4, 4.2 Hz, 1H), 5.34 (dd, *J* = 10.5, 4.3 Hz, 1H), 4.58 (d, *J* = 13.8 Hz, 1H), 4.56 (m, 1H) 4.50 (d, *J* = 13.8 Hz, 1H), 2.14 (s, 3H), 2.09 (s, 3H), 2.08 (s, 3H), 2.02 (s, 3H).

The above tetraacetate (5.5 mg, 0.15 mmol) was dissolved in anhydrous methanol (0.10 mL) and cooled to 0 °C. NaOMe in MeOH (15 µL, 0.15 mmol, 1 equiv, 1M solution, freshly prepared from Na and MeOH is then added. The reaction was warmed and stirred at room temperature for 12 h. Water (0.1 mL) was added followed by DOWEX 50X2-200 (washed with methanol) until the pH of the solution was 2. After filtration, the solution was concentrated to yield 1.50 mg (0.0085 mmol, 57% yield) of MK7607 (**2.36**).

$[\alpha]_D^{20.0}$ +41.3 (*c* 0.15, H_2O); **^{1}H NMR** (500 MHz D_2O) δ 5.85 (dt, *J* = 5.0, 1.6 Hz, 1H), 4.31 (ddd, *J* = 5.1, 3.2, 2.0 Hz, 1H), 4.24 (d, *J* = 3.6 Hz, 1H), 4.14 (s, 2H), 3.88 (dd, *J* = 10.4, 3.9 Hz, 1H), 3.85 (dd, *J* = 10.4, 3.7 Hz, 1H); **^{13}C NMR** (126 MHz, D_2O) δ 142.2, 126.0, 70.6, 70.3, 68.6, 68.0, 64.0; **IR** (film, cm^{-1}) 3316, 2946, 2833, 1651, 1447, 1258, 1010; **HRMS** (DART) *m/z* calc for $C_7H_{12}O_5$: 177.0763 $(M+H)^+$, found 177.0758.

2.53 (9.0 mg, 0.033 mmol) was converted to streptol (**2.34**) (3.1 mg, 0.018 mmol, 55% yield) in the same manner as above.

$[\alpha]_D^{20.0}$ -24.0 (c 0.1, H_2O); **^{1}H NMR** (500 MHz D_2O) δ 5.84 (dd, *J* = 5.5, 1.7 Hz, 1H), 4.27 (t, *J* = 4.8 Hz, 1H), 4.23 (d, *J* = 14.2 Hz, 1H), 4.14 (d, *J* = 14.1 Hz, 1H), 4.07 (d, *J* = 7.6 Hz, 1H), 3.69 (dd, *J* = 10.7, 7.8 Hz, 1H), 3.57 (dd, *J* = 10.7, 4.2 Hz, 1H); **^{13}C NMR** (126 MHz, D_2O) δ 142.1, 122.1, 72.5, 72.2, 70.6, 66.1, 61.2; **IR** (film, cm^{-1}) 3298, 2906, 1671, 1374, 1008, 878, 824; **HRMS** (ESI^+) *m/z* calc for $C_7H_{12}O_5Na$ $(M+Na)^+$, 199.0582, found 199.0581.

Scheme 2.10. Total synthesis of cyathiformine B type.

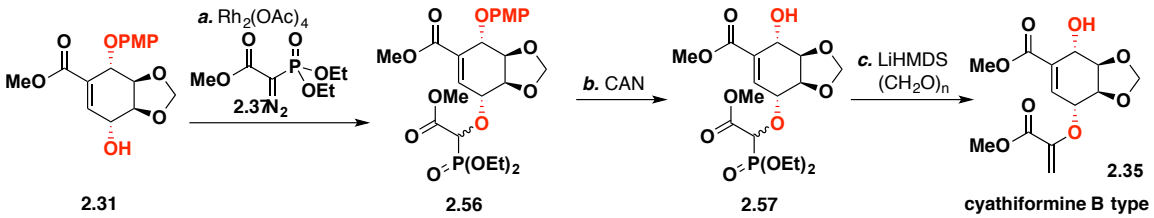

Total synthesis of cyathiformine B type

26.3 mg (0.082 mmol, 1 equiv) of **2.31** was dissolved in 1.0 mL of DCM. To the clear colorless solution was added a catalytic amount (0.8 mg) of $Rh_2(OAc)_4$ turning the solution a pale green. The solution was heated to 85 °C and a separate solution containing 35.2 mg (0.149 mmol, 1.8 equiv) of diazophosphate, **2.37** in 1.5 mL of DCM was added dropwise over 10 minutes. The reaction continued at reflux for 3 h before cooling to room temperature. The reaction was then concentrated and purified by column (2:1 then 1:1 hexanes/EtOAc, v/v) to give 27.9 mg (64%) of **2.56** as a clear colorless oil (mixture of diastereomers) and 3.8 mg (14%) of recovered starting material **2.31**.

Methyl (3a*R*,4*S*,7*R*,7a*S*)-7-(1-(diethoxyphosphoryl)-2-methoxy-2-oxoethoxy)-4-(4-methoxyphenoxy)-3a,4,7,7a-tetrahydrobenzo[*d*][1,3]dioxole-5-carboxylate (2.56)

$[\alpha]_D^{20.0}$ −12.3 (*c* 1.00, $CHCl_3$); **^{1}H NMR** ($CDCl_3$, 300 MHz) δ 7.08 (d, *J* = 3.7 Hz, 1H), 7.04 – 6.97 (m, 5H), 6.86 – 6.80 (m, 4H), 5.23 – 5.20 (m, 2H), 5.04 (s, 2H), 4.89 (d, *J* = 19.7 Hz, 1H), 4.82 (d, *J* = 6.3 Hz, 2H), 4.71 (d, *J* = 18.6 Hz, 1H), 4.51 (dd, *J* = 6.2, 4.0 Hz, 1H), 4.47 – 4.41 (dd, *J* = 6.2, 4.2 Hz, 1H), 4.35 (td, *J* = 4.0, 1.1 Hz, 1H), 4.32 – 4.28 (m, 2H), 4.28 – 4.18 (m, 9H), 3.83 (d, *J* = 2.6 Hz, 5H), 3.78 – 3.74 (m, 18H), 1.37 – 1.31 (m, 12H); **^{13}C NMR** ($CDCl_3$, 75 MHz) δ 168.7, 167.9, 165.5, 165.4, 155.0, 151.8, 151.7, 137.6, 137.0, 131.5, 130.8, 118.0, 117.9, 114.8, 94.3, 76.2, 75.9, 75.0, 74.7, 71.3, 71.2, 64.1, 55.8, 53.0, 52.3, 16.6; **IR** (film, cm^{-1}) 2953, 1725, 1506, 1260, 1214, 1024; **TLC** R_f = 0.11, 0.19 (1:2 hexanes/EtOAc, v/v); **HPLC** 86:14 e.r.; **HRMS** (DART) *m/z* Calc'd for $C_{23}H_{32}O_{12}P$ $(M+H)^+$: 531.1626, found 531.1603. Characterization was performed on a 1:1 mixture of inseparable diastereomers.

39.0 mg (0.074 mmol, 1 equiv) of **2.56** was dissolved in 4.0 mL of 4:1 MeCN/H_2O v/v solution. The solution was cooled to 0 °C and ceric ammonium nitrate (88.9 mg, 0.162 mmol, 2.2 equiv) was added in a single portion. After 5 minutes the solutions had become orange the starting material had been consumed by this time. The reaction was diluted with water and the organics extracted with EtOAc (3 x 7.0 mL). The extracts were dried with Na_2SO_4, filtered, and concentrated. Purification by column (2:1 EtOAc/hexanes, v/v) gave 23.6 mg (76%) of **2.57** as a red oil.

Methyl (3a*R*,4*S*,7*R*,7a*S*)-7-(1-(diethoxyphosphoryl)-2-methoxy-2-oxoethoxy)-4-hydroxy-3a,4,7,7a-tetrahydrobenzo[*d*][1,3]dioxole-5-carboxylate (2.57)

$[\alpha]_D^{20.0}$ −17.8 (*c* 1.00, $CHCl_3$); **^{1}H NMR** ($CDCl_3$, 400 MHz) δ 7.09 (t, *J* = 4.2 Hz, 3H), 5.01 (s, 1H), 4.98 (s, 1H), 4.76 (s, 1H), 4.72 (s, 1H), 4.70 – 4.63 (m, 2H), 4.57 (d, *J* = 19.0 Hz, 1H), 4.45 (dd, *J* = 7.1, 3.8 Hz, 1H), 4.42 – 4.36 (m, 3H), 4.36 – 4.28 (m, 3H), 4.26 – 4.15 (m, 8H), 3.86 – 3.80 (m, 12H), 1.37 – 1.29 (m, 12H); **^{13}C NMR** ($CDCl_3$, 75 MHz) δ 168.8, 167.8, 167.3, 165.9, 137.7, 137.3, 136.4, 134.9, 94.4, 94.3, 79.0, 78.9, 76.0, 75.8, 75.7, 75.6, 75.1, 75.0, 66.0, 65.6, 64.1, 64.0, 53.2, 53.1, 52.6, 16.6, 16.5; **IR** (film, cm^{-1}) 3481, 2912, 1723, 1253, 1092, 1021, 980; **TLC** R_f = 0.29 (EtOAc); **HPLC** 87:13 e.r.; **HRMS** (DART) *m/z* Calc'd for $C_{16}H_{19}O_{11}P$ $(M+H)^+$: 425.1207, found 425.1188. Characterization performed on a 1:1 mixture of inseparable diastereomers

71.2 mg (0.168 mmol, 1.0 equiv) of **2.57** was dissolved in 4.0 mL of anhydrous THF and cooled to −78 °C under argon to give a pale yellow solution. Fresh LiHMDS, prepared from the addition of 225.0 µL *n*-BuLi to 75.0 µL of HMDS in 4.0 mL of THF at −78 °C, was added slowly turning the solution brown. The reaction stirred for 0.5 h at −78 °C before the dropwise addition of a 9.0 mL solution of THF containing freshly cracked formaldehyde (711.1 mg, 100 equiv). After stirring at bath temp for 0.3 h, the reaction was transferred to a bath at 0 °C and allowed to stir for 0.5 h, upon which it was quenched with 8.0 mL of a saturated NH_4Cl. The product was extracted in EtOAc (3 x 10.0 mL) and dried with Na_2SO_4. The crude product was filtered though

a pad of celite then purified by column (1:1 EtOAc/hexanes, v/v) to give 36.1 mg (71%) of product **2.35** as a yellow oil.

Methyl (3a*R*,4*S*,7*R*,7a*S*)-4-hydroxy-7-((3-methoxy-3-oxoprop-1-en-2-yl)oxy)-3a,4,7,7a-tetrahydrobenzo[*d*][1,3]dioxole-5-carboxylate (2.35)

$[\alpha]_D^{20.0}$ −39.9 (*c* 1.00, $CHCl_3$); **^{1}H NMR** ($CDCl_3$, 400 MHz) 7.14 (d, *J* = 4.6 Hz, 1H), 5.60 (d, *J* = 3.2 Hz, 1H), 5.04 (s, 1H), 4.93 (d, *J* = 3.3 Hz, 1H), 4.82 (dd, *J* = 4.6, 3.1 Hz, 1H), 4.79 – 4.73 (m, 2H), 4.53 – 4.44 (m, 2H), 3.82 (s, *3*H), 3.80 (s, 3H); **^{13}C NMR** ($CDCl_3$, 125 MHz) δ 165.8, 163.1, 148.6, 136.8, 136.3, 98.2, 94.4, 78.4, 74.8, 71.4, 65.2, 52.9, 52.6; **IR** (film, cm^{-1}) 3477, 2923, 1721, 1438, 1255, 1168, 1091, 1032; **TLC** R_f = 0.77 (EtOAc); **HPLC** 87:13 e.r.; **HRMS** (DART) *m/z* Calc'd for $C_{13}H_{17}O_8$ $(M+H)^+$: 301.0918, found 301.0903.

Scheme 2.11. Synthesis of new cyclitol **2.42**.

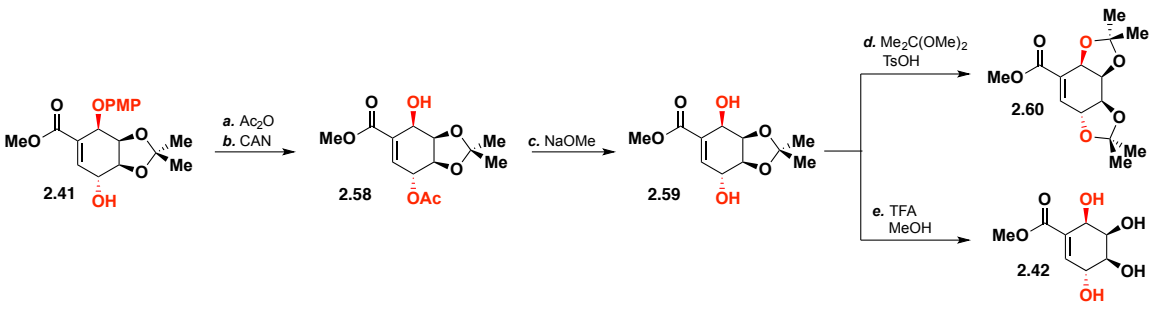

Total Synthesis of Cyclitol 2.42

214.6 mg (0.613 mmol, 1 equiv) of **2.41** was dissolved in 10 mL of anhydrous DCM. 200 µL (2.12 mol, 3.5 equiv) of acetic anhydride was added followed by 330 µL (1.89 mmol, 3.0 equiv) of diisopropylethylamine and 1 mg (cat.) of DMAP. The reaction

stirred for 1 h at room temperature before TLC showed consumption of starting material. The reaction was then quenched with 2.0 mL of 1M HCl and organic layer separated then dried with $MgSO_4$. Filtration and concentration yielded the crude acetate which was used without further purification. **^{1}H NMR** ($CHCl_3$, 300 MHz) δ 7.15 (d, *J* = 3.3 Hz, 1H), 7.04 – 7.98 (m, 2H), 6.83 – 6.76 (m, 2H), 5.42 (d, *J* = 2.9 Hz, 1H), 5.02 (dd, *J* = 6.7, 3.4 Hz, 1H), 4.91 – 4.77 (m, 2H), 3.78 (d, *J* = 0.6 Hz, 3H), 3.76 (s, 3H), 1.79 (s, 3H), 1.47 (s, 3H), 1.44 (s, 3H).

The crude acetate was dissolved in a 10.5 mL of 4:1 MeCN/H_2O (v/v) solution. The solution was cooled to 0 °C and 760.0 mg (1.39 mmol, 2.1 equiv) of ceric ammonium nitrate was added in a single portion. After 5 minutes, TLC showed consumption of the starting material. The resulting yellow solution was diluted with 10.0 mL of water and the organic layer was extracted with EtOAc (3 x 10.0 mL). The extracts were combined and dried with Na_2SO_4. Filtration and concentration gave the crude product that was purified by column (7:3 hexanes/EtOAc v/v) yielding 78.3 mg of **2.58** (45% over 2 steps) of a yellow oil.

Methyl (3aR,4R,7R,7aS)-7-acetoxy-4-hydroxy-2,2-dimethyl-3a,4,7,7a-tetrahydrobenzo[d][1,3]dioxole-5-carboxylate (2.58)

$[\alpha]_D^{20.0}$ −96.3 (*c* 1.00, $CHCl_3$); **^{1}H NMR** ($CDCl_3$, 300 MHz) δ 7.01 (d, *J* = 3.5 Hz, 1H), 5.02 (dd, *J* = 8.6, 3.4 Hz, 1H), 4.85 (dd, *J* = 6.5, 3.6 Hz, 1H), 4.81 (d, *J* = 3.4 Hz, 1H), 4.56 (dd, *J* = 8.6, 6.5 Hz, 1H), 3.80 (s, 3H), 2.16 (s, 3H), 1.44 (s, 3H), 1.39 (s, 3H); **^{13}C NMR** ($CDCl_3$, 75 MHz) δ 170.5, 165.8, 136.6, 132.7, 110.5, 73.4, 72.7, 72.3, 64.3, 52.5, 27.6, 25.6, 21.2; **IR** (film, cm^{-1}) 3371, 3072, 2987, 1722, 1237, 1062, 853;

TLC R_f = 0.29 (7:3 hexanes/EtOAc v/v); **HRMS** (DART) *m/z* Calc'd for $C_{13}H_{19}O_7$ $(M+H)^+$: 287.1125, found 287.1119.

29.0 mg (0.101 mmol, 1 equiv) of starting material **2.58** was dissolved in 1.0 mL of anhydrous MeOH under argon and cooled to 0 °C to give a yellow solution. In a separate flask, 7.1 mg (0.309 mmol, 3 equiv) of sodium metal was added to 1 mL of anhydrous MeOH under argon. This solution was then added dropwise to the solution containing the starting material causing it to brown. After 5 minutes, all the starting material had been consumed and the reaction was acidified to pH = 3 using 1M HCl causing the solution to lighten in color. The product was the extracted with EtOAc (3 x 3 mL) and dried with Na_2SO_4. Filtration and concentration gave 19.7 mg (80%) of the diol (**2.59**) as a yellow oil. **^{1}H NMR** (CDCl3, 400 MHz) δ 6.91 (d, *J* = 3.5 Hz, 1H), 4.79 (ddd, *J* = 6.0, 3.4, 0.8 Hz, 1H), 4.66 (d, *J* = 3.6 Hz, 1H), 4.43 (t, *J* = 6.2 Hz, 1H), 4.05 (dd, *J* = 6.4, 3.6 Hz, 1H), 3.81 (s, 3H), 1.39 (s, 3H), 1.38 (s, 3H).

The crude diol **2.59** was dissolved in 2.5 mL of anhydrous acetone and 2.5 mL 2,2-dimethoxypropane to give a yellow solution. 900.0 mg (6.34 mmol, excess) of Na_2SO_4 was added and a catalytic amount of *p*-TsOH. The reaction was heated to reflux under N_2 for 1 hour. Once the starting material was consumed by TLC, the reaction was cooled and washed with a saturated $NaHCO_3$ solution. The product was extracted with DCM (3 x 3.0 mL) and dried with Na_2SO_4. Filtration and concentration gave 17.8 mg (78%) of the product as a yellow oil. No further purification was necessary.

Methyl (3a*R*,5a*R*,8a*S*,8b*R*)-2,2,7,7-tetramethyl-3a,5a,8a,8b-tetrahydrobenzo[1,2-*d*:3,4-*d'*]bis([1,3]dioxole)-4-carboxylate (2.60)

$[\alpha]_D^{20.0}$ +26.8 (*c* 1.00, $CHCl_3$); **^{1}H NMR** ($CDCl_3$, 300 MHz) δ 6.72 – 6.70 (m, 1H), 4.96 (d, *J* = 5.6Hz, 1H), 4.69 – 4.64 (m, 2H), 4.58 (ddd, *J* = 4.9, 2.9, 1.3 Hz, 1H), 3.82 (s, 3H), 1.39 (s, 3H), 1.37 (s, 3H), 1.32 (s, 3H), 1.30 (s, 3H); **^{13}C NMR** ($CDCl_3$, 75 MHz) δ 166.5, 136.8, 129.1, 109.8, 109.3, 73.6, 72.4, 70.7, 69.2, 52.4, 28.0, 27.7, 26.4, 26.0; **IR** (film, cm^{-1}) 2986, 2934, 1726, 1247, 1059, 851; **TLC** R_f = 0.80 (1:1 hexanes/EtOAc v/v); **HRMS** $[M+H]^+$ *m/z* Calc'd for $C_{15}H_{18}O_5$ 285.1333, found 285.1326.

5.4 mg (0.022 mmol, 1 equiv) of the crude diol **2.59** was dissolved in 0.5 mL of methanol and 100 μL of water. Trifluoroacetic acid (15 μL, 10 equiv) was then added. The resulting solution was heated to 40 °C. Once the starting material was consumed by TLC (approx. 7 h), the reaction was diluted with toluene and concentrated to dryness. The resulting film was washed with ether (3 x 1.0 mL) and then dried under vacuum to yield 2.3 mg (51%) as an off-white foam as streptol (**2.42**).

$[\alpha]_D^{20.0}$ −193.0 (*c* 0.10, CH_3OH); **^{1}H NMR** (D_2O, 400 MHz) δ 7.00 (d, *J* = 4.9 Hz, 1H), 4.71 (d, *J* = 4.0 Hz, 1H), 4.51 (t, *J* = 4.6 Hz, 1H), 3.98 (dd, *J* = 10.4, 4.3 Hz, 1H), 3.92 (dd, *J* = 10.4, 4.0 Hz, 1H), 3.84 (s, 3H); **^{13}C NMR** (CD_3OD, 125 MHz) δ 167.9, 139.5, 132.0, 68.2, 67.7, 65.5, 65.5, 52.6; **IR** (film, cm^{-1}) 3285, 2948, 2837, 1651, 1405, 1010; **TLC** (reverse phase) R_f = 0.89 (9:1 H_2O/MeCN v/v); **HRMS** (DART) *m/z* Calc'd for $C_8H_{13}O_6$ $(M+H)^+$: 205.0707, found 205.0709.

Table 2.5. Comparison of natural and synthetic samples.

Natural **Streptol**	Current synthesis of **Streptol**
^{1}H NMR (D_2O, 400MHz) [24]	
3.61 (dd J = 11, 4 Hz)	3.57 (dd, J = 10.7, 4.2 Hz)
3.73 (dd J =11, 8 Hz)	3.69 (dd, J = 10.7, 7.8 Hz)
4.11 (dq J = 8, 1 Hz)	4.07 (d, J = 7.6 Hz)
4.17 (d J = 14 Hz)	4.14 (d, J = 14.1 Hz)
4.26 (dq J = 14, 1 Hz)	4.23 (d, J = 14.2 Hz)
4.33 (dd J = 5, 4 Hz)	4.27 (t, J = 4.8 Hz)
5.88 (dq J = 5, 1 Hz)	5.84 (dd, J = 5.5, 1.7 Hz)
^{13}C NMR (D_2O, 100MHz) [34]	
62.0	62.0
66.0	66.0
71.2	71.2
72.7	72.7
73.0	73.0
122.8	122.8
142.8	142.8
Optical Rotation[8], $[\alpha]_D^{20.0}$	
+88.1 (c 0.3, H_2O)	−70.6 (c 0.17, H_2O)

Natural **MK7607**	Current synthesis of **MK7607**
^{1}H NMR (D_2O, 400MHz) [25]	
3.86(dd, J = 3.6, 10.2, 1H)	3.85 (dd, J = 10.4, 3.7 Hz, 1H)
3.89(dd, J = 3.6, 10.2, 1H)	3.88 (dd, J = 10.4, 3.9 Hz, 1H)
4.16 (s, 2H)	4.14 (bs, 2H)
4.25(d, J = 3.6, 1H)	4.24 (d, J = 3.6 Hz, 1H)
4.32(dd, J = 4.2, 4.2, 1H)	4.31 (ddd, J = 5.1, 3.2, 2.0 Hz, 1H)
5. 85(d, J = 4.9. 1H).	5.85 (dt, J = 5.0, 1.6 Hz, 1H)
^{13}C NMR (D_2O, 100MHz) [34]	
63.0	64.0
67.0	68.0
67.6	68.6
69.3	70.3
69.6	70.6
125.1	126.0
142.2	142.2
Optical Rotation[8], $[\alpha]_D^{20.0}$	
+210 (c 1.0, H_2O)	+41.3 (c 0.15, H_2O)

References and Notes

(1) The number of existing carbasugars is reportedly more than 140, see: (a) O. Arjona, A. M. Gomez, J. C. Lopez, J. Plumet, *Chem. Rev.* **2007**, 107, 1919–2036. (b) Y. Kobayashi, *Glycoscience;* B. Fraser-Reid, K. Tatsuta, J. Thiem, Eds.; Springer:Berlin, 2008, 1913–1997. Carbasugars amenable to the reported chemistry include: rancinamycin I–IV, gabosine A–O, COTC, nigrospoxydon C, epoxydine A-B, cyanoformate A–C, pericosine A–E, piperonol A and B, uvacalol A–K, phomoxin A–C, and lincitol A and B.

(2) (a) J. Tsuji, H. Kataoka, Y. Kobayashi, *Tetrahedron Lett*. **1981**, 22, 2575–2578; (b) B. M. Trost, G. A. Molander, *J. Am. Chem. Soc.* **1981**, 103, 5969–5972. For in-depth reviews of asymmetric allylic alkylations, see: (c) B. M. Trost, D. L. Van Vranken, *Chem. Rev*. **1996**, 96, 395–422. (d) B. M. Trost, M. L. Crawley, *Chem. Rev*. **2003**, 103, 2921–2943.

(3) For additional examples of vinyl oxides by Trost and coworkers, see: (a) B. M. Trost, R. C. Bunt, R. C. Lemoine, T. L. Calkins, *J. Am. Chem. Soc.* **2000**, 122, 5968–5976; (b) B. M. Trost, C. Jiang, *J. Am. Chem. Soc.* **2001**, 123, 12907–12908.

(4) For recent reviews of divergent and regioselective reactions with chiral substrates, see: (a) L. C. Miller, R. Sarpong, *Chem. Soc. Rev*. **2011**, 40, 4550–4562; (b) R. R. Kumar, H. Kagan, B. *Adv. Synth. Catal*. **2010**, 352, 231–242.

(5) D. L. Hughes, M. Palucki, N. Yasuda, R. A. Reamer, P. J. Reider. *J. Org. Chem.* **2002**, 67, 2762–2768.

(6) (a) T. Hayashi, A. Yamamoto, Y. Ito, *J. Chem. Soc. Chem. Commun*. **1986**, 14, 1090–1092. (b) O. Loiseleur, M. C. Elliott, P.von Matt, A. Pfaltz, *Helv. Chim. Acta* **2000**, 83, 2287–2294. (c) H. Daimon, R. Ogawa, S. Itagaki, I. Shimizu, *Chem. Lett*. **2004**, 33, 1222–1223. (d) G. R. Cook, S. Sankaranarayanan, *Org. Lett*. **2001**, 3, 3531–3533. (e) O. Jacquet, J. Y. Legros, M. Coliboeuf, J. -C. Fiaud, *Tetrahedron* **2008**, 64, 6530–6536.

(7) For the initial discovery and application of the DPEN ligand, see: B. M. Trost, D. L. Van Vranken, C. Bingel, *J. Am. Chem. Soc.* **1992**, 114, 9327–9343.

(8) S. Masamune, W. Choy, J. S. Petersen, L. R. Sita, *Angew. Chem., Int. Ed. Engl*. **1985**, *24*, 1–30; *Angew. Chem. Int. Ed*. **1985**, 97, 1–31.

(9) See experimental for details.

(10) (a) C. P. Butts, E. Fiali, G. C. Lloyd-Jones, P. Norrby, D. A. Sale, Y. Schramm, *J. Am. Chem. Soc*. **2009**, 131, 9945–9957; (b) G. C. Lloyd-Jones, S. C. Stephen, I. J. S. Fairlamb, A. Martorell, B. Dominguez, P. M. Tomlin, M. Murray, J. C. Fernandez, T. Riis-Johannessen, T. Guerziz, *Pure Appl. Chem.* **2004**, 76, 589–601.

(11) B. M. Trost, J. L. Guzner, O. Dirat, Y. H. Rhee, *J. Am. Chem. Soc.* **2002**, 124, 10396–10415.

(12) Jadhav, V. H.; Lee, S. B.; Jeong, H.-J.; Lim, S. T.; Sohn, M.-H.; Kim, D. W. *Tetrahedron Lett.* **2012**, 53, 2051–2053.

(13) The directing capability of carbamates for palladium mediated Heck reactions was observed by Rawal and coworkers, see: (a) Rawal, V. H.; Michoud, C. *J. Org. Chem*. **1993**, 58, 5583–5584. A Boc-directed C-H activation has been

established: (b) Wang, D. -H; Hao, X. -S.; Wu, D. -F.; Yu, J. -Q. *Org. Lett*. **2006**, 8, 3387–3390. The use of carbamates to direct palladium catalyzed arene-arene couplings has recently been reported: (c) Zhao, X.; Yeung, C. S., Dong, V. M. *J. Am. Chem. Soc*. **2010**, 132, 5837–5844.

(14) Griseofulvin isolation: (a) Oxford, A. E.; Raistrick, H.; Simonart, P. *Biochem. J.* **1939**, *33*, 240–248. Structure determination: (b) Grove, J. F.; MacMillan, J.; Mulholland, T. P. C.; Rogers, M. A. T. *J. Chem. Soc.* **1952**, 3977–3987. For a review of the chemistry of griseofulvin, see: (c) Petersen, A. B.; Rønnest, M. H.; Larsen, T. O.; Clausen, M. H. *Chem. Rev*. **2014**, 114, 12088–12107.

(15) Geodin isolation: (a) Raistrick, H.; Smith, G. *Biochem. J.* **1936**, 30, 1315–1322. Structure determination: (b) Barton, D. H. R.; Scott, A. I. *J. Chem. Soc.* **1958**, 1767–1772. Crystal structure: (c) Rønnest, M. H.; Nielsen, M. T.; Leber, B.; Mortensen, U. H.; Krämer, A.; Clausen, M. H.; Larsen, T. O.; Harris, P. *Acta Cryst*. **2011**, C67, o125–o128.

(16) Sch202596 isolation: Chu, M.; Mierzwa, R.; Truumes, I.; King, A.; Sapidou, E.; Barrabee, E.; Terracciano, J.; Patel, M. G.; Gullo, V. P.; Burrier, R.; Das, P. R.; Mittelman, S.; Puar, M. S. *Tetrahedron Lett*. **1997**, 38, 6111–6114.

(17) (a) Ho, Y. S.; Duh, J. S.; Jeng, J. H.; Wang, Y. J.; Liang, Y. C.; Lin, C. H.; Tseng, C. J.; Yu, C. F.; Chen, R. J.; Lin, J. K. *Int. J. Cancer* **2001**, 91, 393–401; (b) Rathinanamy, K.; Jindal, B.; Asthana, J.; Singh, P.; Balaji, P. V.; Panda, D. *BMC Cancer* **2010**, 10, 213 – 216; (c) Panda, D.; Rathinasamy, K.; Santra, M. K.; Wilson, L. *Proc. Nat. Acad. Sci. USA* **2005**, *102*, 9878–9883;

(18) Rønnest, M. H.; Harris, P.; Gotfredsen, C. H.; Larsen, T. O.; Clausen, M. H.

Tetrahedron Lett. **2010**, 51, 5881 – 5882.

(19) The use of Florisil greatly diminished the degradation as compared to silica gel.

(20) Oxide **2.19** can be prepared in seven steps and is based on: (a) S. A. Bowles, M. M. Campbell, M. Sainsbury, G. M. Davies, *Tetrahedron.* **1990**, 46*,* 3981–3992; (b) Y. Usami, K. Suzuki, K. Mizuki, H. Ichikawa, M. Arimoto, *Org. Biomol. Chem.* **2009**, 7*,* 315–318; (c) M. M. Campbell, A. D. Kaye, M. Sainsbury, R. Yavarzadeh, *Tetrahedron.* **1984**, 40*,* 2461–2470.

(21) The isomerization of π-allyl complexes via palladium(0) attack as reported by Bäckvall and Murahashi is instructive, see: (a) K. L. Granberg, J. E. Bäckvall, *J. Am. Chem. Soc.* **1992**, 114, 6858–6863; (b) J. E. Bäckvall, K. L. Granberg, A. Heumann, *Isr. J. Chem*. **1991**, 31, 17–24; (c) S. Murahashi, Y. Taniguchi, Y. Imada, Y. Tanigawa, Y. *J. Org. Chem.* **1989**, *54*, 3292–3303.

(22) M. B. Banwell, N. Haddad, T. Hudlicky, T. C. Nugent, M. F. Mackay, S. L. Richards, *J. Chem. Soc. Perkin Trans*. **1997**, 1, 1779–1792.

(23) Initial isolation of the regiodivergence provided **2.31** in 16% yield with products **2.30** and **2.32** as a co-mixture in 39% yield. An extended ^{1}H-NMR analysis determined the ratio of products to be 14% **2.30** and 25% **2.32**. Yields and er data for additional runs may be found in the Supporting Information.

(24) A. Isogai, S. Sakuda, J. Nakayama, S. Watanabe, A. Suzuki, *Agric. Biol. Chem.* **1987**, 51, 2277–2279.

(25) Y. Nobuji, C. Noriko, M. Takashi, U. Shigeru, H. Kenzou, I. Michiaki, *Jpn. Koka Tokkyo Koho*, JP, 06306000, **1994**.

(26) A. Arnone, R. Cardillo, G. Nasini, O. V. de Pava, *Tetrahedron* **1993**, 49, 7251–

7258.

(27) Racemic oxide **2.38** can be prepared in seven steps; see reference 20.

(28) Enantiopure oxide **2.38** can be prepared in five steps diverging from the preparation of oxide **2.19**. Y. Usami, M. Ohsugi, K. Mizuki, H. Ichikawa, M. Arimoto, *Org. Lett.* **2009**, 11, 2699–2701.

(29) Structure **2.42** may be a member of the rancinamycin family or the pericosines (desmethyl).

(30) D. L. Boger, M. Patel, F. Takusagawa, *J. Org. Chem*. **1985**, 50, 1911–1916

(31) W. Zhang, E. N. Jacobsen, *J. Org. Chem.* **1991**, 56, 2296–2298.

(32) F. Fabris, J. Collins, B. Sullivan, H. Leisch, T. Hudlicky, *Org. Biomol. Chem.* **2009**, 7, 2619–2627.

(33) Patent US4555581 A1, 1985; S. A. Bowles, M. M. Campbell, M. Sainsbury, G. M. Davies.

(34) Adams, H.; Anderson, J. C.; Bell, R.; Neville, D. J.; Peel, M. R.; Tomkinson, N. C. O. *J. Chem. Soc., Perkin Trans. 1* **1998**, 3967–3974.

CHAPTER 3

A Brief Introduction to the History of Polyolefins and Chain Walking Polymerizations

3.1 Introduction to Polymer Structures and Properties

Polymer properties and their applications are inescapably linked to their molecular weight, architecture, and topology.[1,2] Changes in any of these characteristics can produce profound effects on the behavior of the final material. As a result, a primary focus in polymer chemistry is the development of new methods for controlling these variables. One topological property of particular interest is tacticity, which refers to the relative arrangement of adjacent chiral centers along a polymer backbone (Figure 3.1a). Atactic polyolefins (Figure 3.1a, left) are amorphous (noncrystalline), soft waxy materials with low physical strength. Conversely, iso- (Figure 1.3a, right) and syndiotactic (Figure 1.3a, center) polyolefins are usually highly crystalline with high physical strength. This strength comes from the ability of the regular structures to pack into a crystal lattice, whereas unordered structures cannot, and the crystallinity leads to higher physical strength and increased resistance to chemical degradation. Some of the most profound effects of tacticity are observed in polypropylene (PP). Isotactic polypropylene (*i*PP) is a strong, semi-crystalline polymer used as plastic and fiber with a melting point of ~165 °C.[3,4] Its annual production is around 55 million tons worldwide. Atactic polypropylene, on the other hand, is amorphous and ranges from oily to waxy in appearance. Its major use is in asphalt blends or formulations for lubricants, adhesives, or sealants, but the volumes produced are trivial compared to its isotactic counterpart. Although syndiotactic polypropylene (*s*PP) is also crystalline and shows good physical properties, its production volumes are also lower than that of *i*PP because historically *i*PP has been easier to produce and more popular.[5]

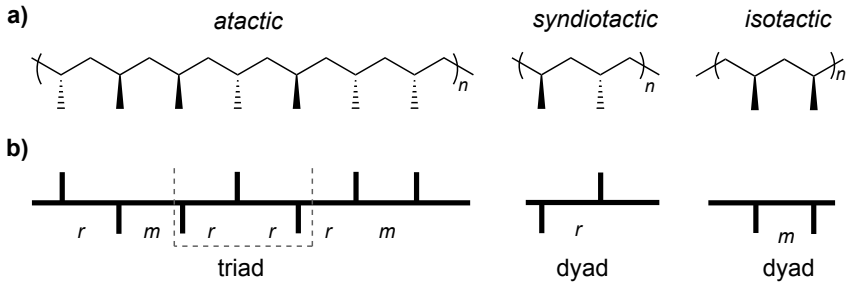

Figure 3.1. a) Different tacticities of polymer side chains. b) Types of dyads and triads in polymer sequences.

Polymer tacticity is easily measured using high-resolution ^{1}H and ^{13}C NMR spectroscopy and is most commonly accomplished by measuring the dyad and triad ratios.[6] Dyad tacticity refers to the fraction of pairs of adjacent repeating units that are iso- or syndiotactic to one another. The dyads are usually referred to as *meso* (*m*) (Figure 1.3b, right) or *racemic* (*r*) (Figure 1.3b, center) depending on the relative orientation of two adjacent stereocenters, as shown in Figure 3.1b, which depicts a segment of polymer as a horizontal line and configuration of the stereocenter in the repeating unit as a vertical line. The direction of the branch denotes the relative stereochemistry. When branches are on the same side of the polymer, it is a *meso* dyad (*m*) with an isotactic structure, while opposite sides gives a *racemic* dyad (*r*) with syndiotactic structure. Triad tacticity measures three adjacent stereocenters, or two adjacent dyads, and is designated as (*mm*), (*rr*), or (*mr*) (Figure 1.3b, left).

If (*r*) = (*m*) = 0.5, or (*mm*) = (*rr*) = 0.25 and (*mr*) = 0.5, and the dyads and triads are randomly distributed throughout the polymer, then the material is atactic. If the polymer is completely isotactic, then (*m*) = (*mm*) = 1, and if the polymer is completely syndiotactic, then (*r*) = (*rr*) = 1. In reality, most polymers lie somewhere in-between. If isotacticity predominates, then (*m*) > 0.5 and (*mm*) > 0.25, and if

syndiotacticity predominates, then (r) > 0.5 and (rr) > 0.25. By measuring the dyads and triads by NMR spectroscopy, the overall tacticity of the polymer can be resolved. Using high-resolution ^{13}C NMR spectroscopy, tetrad, pentad, and higher sequences can be observed to further elucidate the polymer microstructure.[6,7]

The crystalline melting temperature (T_m) in crystalline and semi-crystalline polymers can be understood by looking at physical changes that occur upon cooling a liquid polymer. When cooled, a polymer's rotational, translational, and vibrational energies decrease. When the rotational and translational energies have fallen to effectively zero, and if certain symmetry requirements are met (ex: stereoregularity), crystallization occurs. During crystallization, polymer chains pack in an ordered lattice structure;[8] the temperature at which this occurs is the T_m of the polymer. Above this temperature, the polymer is a liquid. Below this temperature, crystallites can exist, and they are responsible for the high mechanical properties observed in PE and PP. T_m is measured by differential scanning calorimetry (DSC).[9]

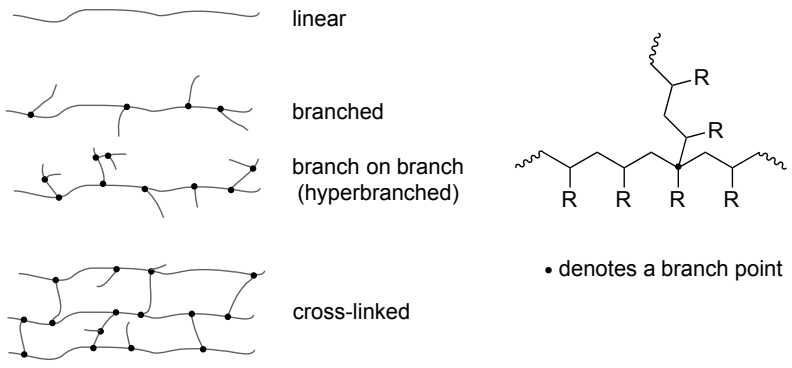

Figure 3.2. Types of polymer architecture and branching.

A second important property of polymers is the architecture of their backbones, which is classified as linear, branched, or cross-linked (Figure 3.2). In a

linear polymer, monomer molecules are linked in one continuous path such that there are only two end groups per polymer chain. A branched polymer contains side chains that protrude from the main chain at various branch points, resulting in more than two end groups per polymer chain. These branches can be of various lengths, distances from one another, and densities to yield a variety of structures. Typically, as branching increases, polymer crystallinity decreases because branched polymers do not pack as well as linear molecules into crystal lattices.[10] This is also true for polymers that contain branches of varying length. It is crucial to note that branched polymers differ from linear polymers with side groups, such as PP, where the side group (methyl) is part of the monomer structure. Finally, cross-linked polymers (Figure 3.2, bottom) are structures in which the polymer molecules are linked to one another at points other than their end groups.[11] The cross-links can be installed during or after the polymerization and can be of varying lengths. Further, the number of links can be varied to change properties of the material.

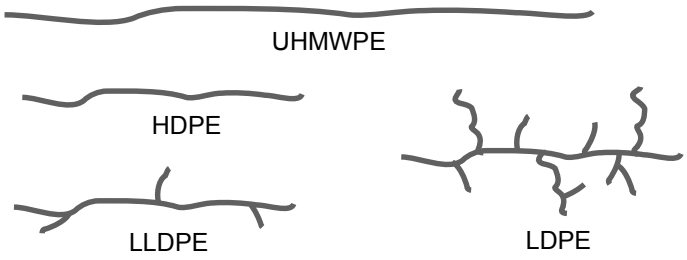

Figure 3.3. Different structures for PE.

The importance of polymer architecture, namely its effects on polymer properties, is clearly demonstrated by PE (Figure 3.3). Linear production results in high-density polyethylene (HDPE), which has few branches (0.5-3 per 500 monomer

units) and high crystallinity (133–138 °C). This material is typically derived from traditional Ziegler-Natta catalysts and shows good mechanical properties such as stiffness, high tensile strength, chemical resistance, and a high melting temperature.[3,12] It has a variety of uses, including blow-molded products such as bottles, toys, and pails, injection-molded objects, and extruded products like piling, tubing, and truck bed liners. Similarly, ultra-high molecular weight polyethylene (UHMWPE) is produced in highly crystalline forms with molecular weights exceeding 2.5 million g/mol, compared to HDPE's molecule weights of 50-250 kg/mol. UHMWPE is often spun into fibers for bulletproof vests and other high-impact-resistant materials.[13] Alternatively, the branching of linear low-density polyethylene (LLDPE) is controlled by copolymerizing it with α-olefins such as propene, butene, and hexene, but maintains a mostly linear structure.[14] This material is also generated from Ziegler-Natta catalysts or metallocene catalysts. The branching reduces crystallinity, making this material more flexible for applications like plastic bags, stretch wrap, lids, and flexible tubing. Low density polyethylene (LDPE) has uncontrolled amounts (15-30 methyl groups per 500 monomers) and types of branching because it is generated using radical polymerization.[15] It is even more flexible than LLDPE due to the higher branch content. Its applications include very soft and pliable snap on lids, six-pack rings, and foam-type packaging. All of these polymers and their applications stem from the same monomer that has been polymerized with simple changes in molecular weight and architecture, hence the importance of these crucial features.

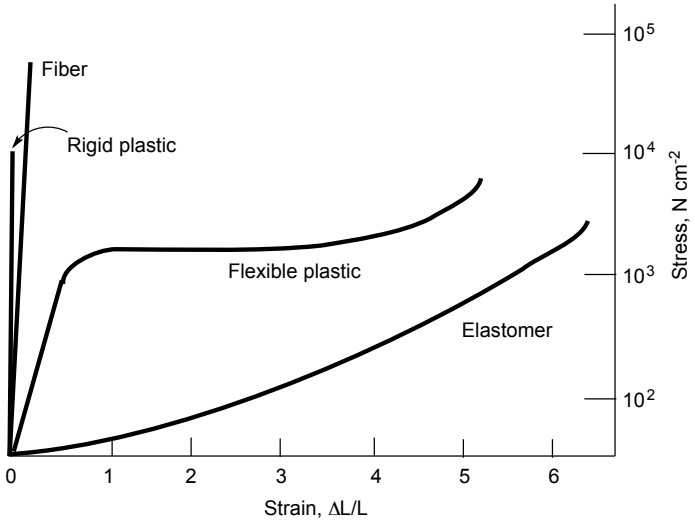

Figure 3.4. Stress-strain curves for different types of plastics.

As discussed above, a polymer's molecular weight, tacticity, and architecture affect its mechanical properties. Other important polymer properties include deformation and flow characteristics under stress, which are often determined from stress-strain properties, i.e. by measuring elongation (strain) while applying tension (stress) until the polymer pulls apart (Figure 3.4).[16] Four important quantities can be characterized from stress-strain studies: 1) modulus, or resistance to deformation, 2) tensile strength, or the stress required to pull apart the sample, 3) ultimate elongation, or the amount of elongation before the sample pulls apart, and 4) elastic elongation, or the extent of reversible elongation (return back to original shape). These properties are often dictated by the degree of crystallinity and crosslinking as well as the glass transition temperature (T_g) and T_m. Typically, high degrees of cross-linking or crystallinity result in a material that has high strength with low extensibility.

Given the global importance of polymers, it is clear why novel polymers and structures are of significant interest. More specifically, because of the critical role that

structure plays in a polymer's properties and, therefore, possible applications, we seek greater control over polymer topology. Achieving this goal requires developing new structures and catalysts as well as methods that allow total control over the synthesis. In the next section, we review on one particular class of polymer, polyolefins, whose properties we are particularly interested in controlling.

3.2 Brief History of Polyolefins and Chain walking

Polyolefins constitute the largest class of polymers in terms of production. They are formed from the polymerization of olefin precursors, such as ethylene or propylene, to make plastics and have revolutionized society. Annually, 80 million tons of polyethylene (PE),[17] 55 million tons of polypropylene (PP),[18] and 39 million tons of polyvinylchloride (PVC)[19] are produced globally, making them the three largest manufactured polymers, all of which are polyolefins. There are several reasons why polyolefins dominate the global market, including their significantly lower cost of production, but it is their highly desirable mechanical properties and ease of tunability that have allowed polyolefins to flourish and become indispensable in our daily lives.

Karl Ziegler[20] first discovered that ethylene could be polymerized at atmospheric pressure to produce high molecular weight PE. This method was later expanded to include higher olefins, such as propylene, by Giulio Natta,[21] who also discovered that stereoregular polymers are possible. For their contributions, both scientists shared the 1963 Nobel Prize in chemistry. What eventually became known as Ziegler-Natta catalysis started with a heterogeneous mixture of $TiCl_3$ and alkyl aluminums such as Et_3Al or Et_2AlCl. Early industrial processes were very inefficient,

with isoselectivity of PP ranging from 20–40% and only 1% of the Ti species being active. Over two decades, this process was improved to produce PP with isotacticity above 90% and with significantly improved activity.[22] Today, the combination of catalyst and co-catalyst has become more complex, but the general principle remains the same, with the majority of commercial polyolefins being produced through Ziegler-Natta catalysis.

Due to its heterogeneous nature, the mechanism of polymerization remains poorly understood,[23] although it is believed to involve π-complexation of monomer to transition metal (Scheme 3.1, **3.1**). This step is followed by an insertion process with both cationic and anionic features that involves a concerted nucleophilic attack from the carbanion on the end of the polymer chain with the α-carbon of a momoner's double bond (**3.2**). This is coupled with an electrophilic attack by the cationic metal on the alkene π-electrons.[24] Using an isoselective Ziegler-Natta catalyst, the insertion of the monomer occurs exclusively via primary insertion, i.e. 1,2-addition. The observed isoselectivity[25] is believed to arise from a back-skip mechanism, also known as the *Cossee-Arlman mechanism* (Scheme 3.2*)*.[26] Here, a monomer coordinates to a vacant site around the titanium center (**3.5**). A migratory insertion of the polymer chain occurs, according to the mechanism described above, to generate a new vacant site (**3.7**) and lengthen the growing polymer. If this new vacant site were to coordinate a monomer and proceed through a migratory insertion, then the resulting polymer would be syndiotactic (**3.8**). Therefore, the polymer chain migrates back to its original position to regenerate the vacant site and proceed isoselectively (**3.9**). Propagation occurs via a site control mechanism. [26d, 27]

Scheme 3.1 Monomer insertion into a propagating polymer chain.[24]

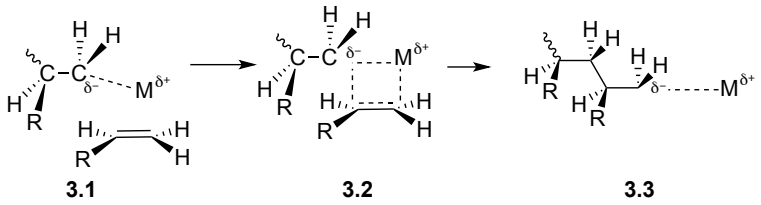

Scheme 3.2 The Cossee-Arlman mechanism, or back-skip mechanism, for iso-selectivity.[26]

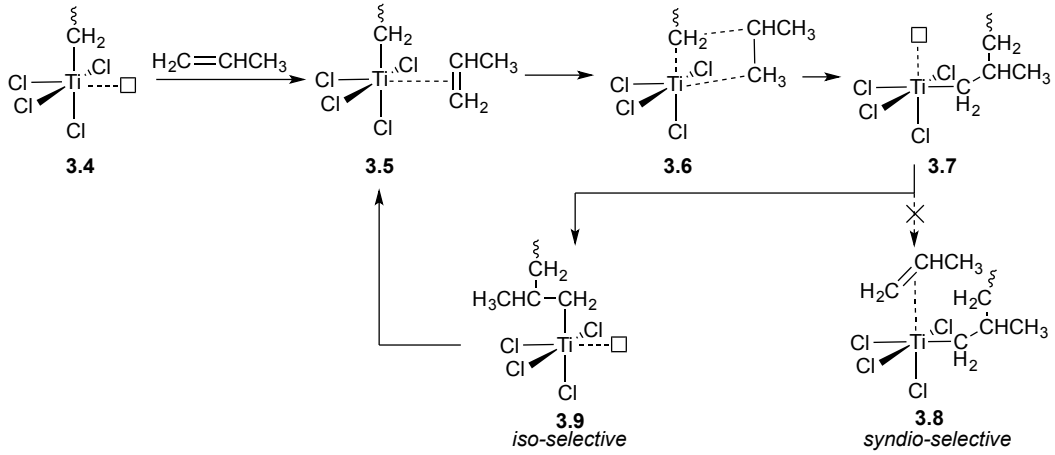

In an attempt to better understand heterogeneous Ziegler-Natta catalysts and their isoselective nature, chemists turned their focus to metallocenes as soluble initiator model systems. It quickly became clear that homogeneous catalysts offered alternative means of olefin polymerization, while solving many of the issues seen in heterogeneous systems. For example, metallocenes are nearly 100-fold more active than heterogeneous systems because of their enhanced solubility and the fact that every transition metal site is active.[23a] Furthermore, each metal center resides in an identical coordination environment, which results in polymers with narrower molecular weight distributions and regular regio- and stereochemistry. This class of

catalyst can also be purified, isolated, and fully characterized by techniques such as NMR spectroscopy, allowing for easy reproducibility and mechanism determination, since the molecular structure can be well-established. The first metallocenes studied where titanocene and zirconocence dichlorides,[28] but the catalysts were later expanded to include numerous transition metals and structures. Metallocene research spanned several decades and produced many notable advancements (see Ref. 29).

Although metallocenes are highly active and valuable, the search for new and interesting initiators/catalysts extended beyond the metallocenes, since new catalysts offer new ways to control molecular architecture, molecular weight, and regio- or stereoregularity. Commercial interests also required new catalysts that had not yet been patented. One such class of catalyst was the bisphenoxy-imines (Scheme 3.3). Pioneered by Fujita and Coates, these catalysts showed good ethylene polymerization activity with both zirconium and titanium, giving high molecular weights.[30] They also exhibited unique stereoselectivity in propylene polymerizations, generating *s*PP even though a C_2-symmetric catalyst was expected to produce *i*PP. This phenomenon results from an interesting ligand isomerization procedure caused by a steric clash between the propagating species and inserting monomer (**3.11**). The isomerization event relieves the steric decompression (**3.13**) and produces the observed stereoselectivity. Additionally, fluorination of the aniline dramatically increases activity, and the catalyst is "living" if fluorination occurs at the *ortho*-positions.[31] Living polymerizations are of interest because of their ability to produce block copolymers and functionalized polymers, but they do not occur with standard Ziegler-Natta catalysts, and there exist few examples with metallocenes.

Scheme 3.3 Ligand isomerization of phenoxy-imine catalyst during polymerization.

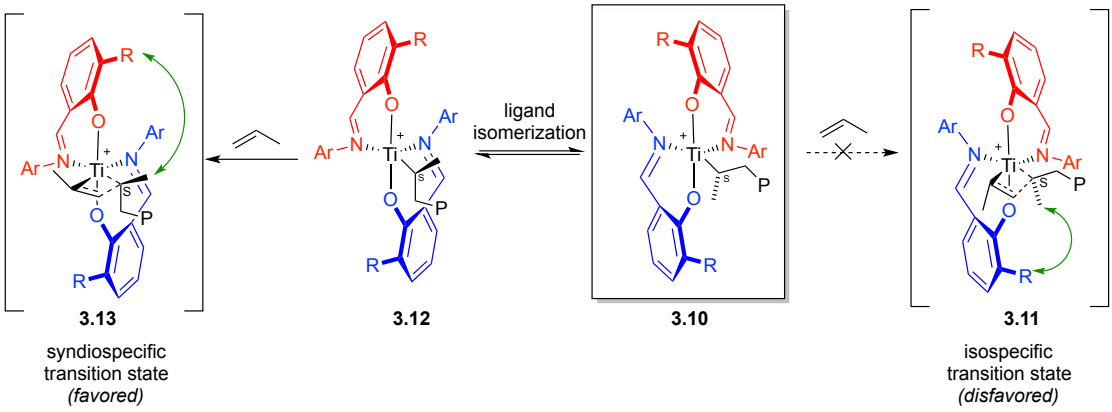

Another class of catalyst includes α-diimine chelates of late transition metals, shown in Figure 3.5. This particular class became the focus of intense study because of certain unique properties, including their reduced oxophilicity, which allows for the incorporation of polar monomers. This feat was previously impossible with early transition metallocenes (zirconium, titanium, chromium). Unlike early transition metals, late transition metals such as palladium or nickel had been previously unexplored because of their tendency to dimerize or oligomerize olefins along a competing β-hydride elimination pathway.[32] However, chemists later discovered that, with the appropriate choice of ligand, these metals could be harnessed as useful polymerization catalysts. Bulky α-diimine ligands in Figure 3.5 favored monomer insertion over β-hydride pathways and allowed access to weight-average molecular weights of 10^4–10^6 PE in the presence of MAO and ethylene.[22a, 33] Simultaneously with these studies, it was discovered that late transition metal catalysts can undergo chain walking during polymerization.

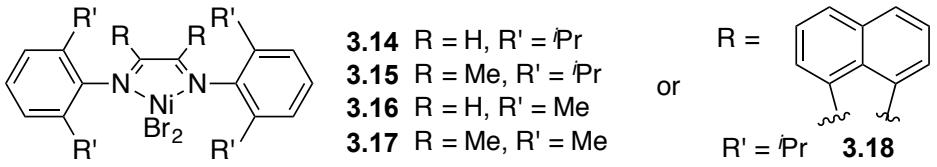

Figure 3.5. Original Brookhart α-diimine catalysts.

Chain walking is a unique phenomenon during which the catalyst of an actively propagating polymer chain (Scheme 3.4, **3.19**) can undergo consecutive β-hydrogen elimination reactions (**3.21**) followed by reinsertion reactions with the opposite regiochemistry (**3.22**). This process positions the active species at various locations along the polymer backbone from which further propagation can occur. Chain walking was first observed by Mörhing and Fink when investigating the polymerization of α-olefins using a nickel aminobis(imino)phosphorane catalyst.[34] They described their observation as a "migration" of the catalyst along the propagating polymer chain.

Scheme 3.4 Proposed chain walking mechanism.

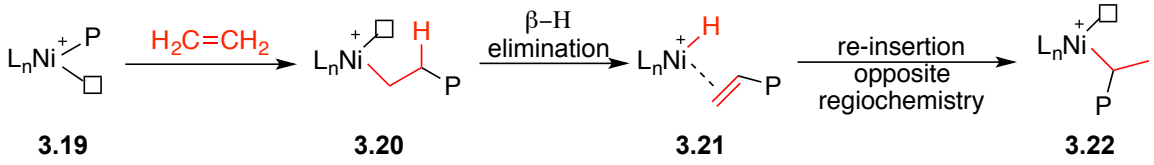

Brookhart and coworkers performed the first detailed studies on this mechanism. They first investigated the polymerization of ethylene, propylene, and 1-hexene using nickel or palladium α-diimine.[35] In all cases, the polymerization yielded high molecular weight materials that were amorphous due to high branch content. Further, they determined that the branching content could be modulated by simple

changes in reaction conditions such as pressure and temperature. For example, running the reaction at cooler temperatures suppressed branching and produced semi-crystalline PE with T_m = 132 °C. Since Brookhart's seminal work over 20 years ago, important advancements have been made in the field of chain walking polymerization, making it an even more valuable process. Although a variety of different catalysts have been used for chain walking,[36] here we focus on α-diimine catalysts, particularly those containing nickel.

α-Diimines constitute a versatile class of bidentate ligands. They are easily synthesized, typically from an acid catalyzed condensation of amines with dicarbonyls or from a nucleophilic attack on a bis-imidoyl chloride precursor. Because the scaffold is modular and easily manipulated, a wide breadth of ligands can be rapidly synthesized. In most cases, bulky axial substituents on the ligands were necessary in order to substantially reduce the rate of chain transfer (Scheme 3.5).[33a,34] Moreover, axial bulk destabilized the catalytic ground state and led to faster monomer insertion. Both of these features are credited for the high molecular weights observed with these catalysts.[37] Activation of these complexes, among other methods,[38] is typically accomplished through the use of alkylaluminium reagents such as methylaluminoxane (MAO).[39] Generally, palladium is nearly 1000x less active than nickel[35] but produces more branches and can tolerate as well as incorporate polar monomers.[40] The degree of branching can be altered by a variety of experimental variables, including pressure, temperature, and concentration. As mentioned previously, a simple change in metal center from nickel to palladium can cause an increase in the number of branches, often producing hyperbranched (branch on branch) materials.

Scheme 3.5 Associative displacement of propagating polymer chain through coordination of new olefin at axial site.

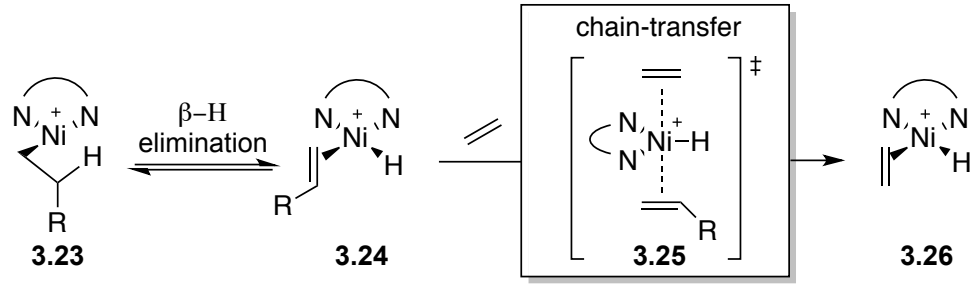

Another interesting result of chain walking polymerization stems from how the monomer inserts into the propagating polymer chain (Scheme 3.6). For any given monomer, there are two main modes of insertion: 1,2 or 2,1. For a 1,2 pathway, the polymer chain is added to the 2-position of the α-olefin monomer while the active metal center migrates to 1-position. If the metal center then chain walks to the ω-position (last carbon of the monomer) before inserting a new monomer, the process is known as ω,2-enchainment and results in regular methyl branching along an otherwise linear PE backbone.[41] Conversely, if a 2,1 insertion occurs, the growing polymer chain is added to the 1-position of the monomer while the active metal species is added to the 2-position. If the metal catalyst chain walks to the ω-position before reinsertion, this is termed ω,1-enchainment and produces linear PE regardless of the simple α-olefin monomer used. This latter process is also referred to as chain-straightening.[42] Regardless of the insertion (1,2 vs 2,1), if complete chain walking to the ω-position does not occur before insertion of a new monomer, branches of various lengths along the polymer backbone result. This interesting outcome means that, for any given monomer feedstock, there exists a variety of different microstructures that can be produced through chain walking. Therefore, controlling the insertion pathway

as well as degree of chain walking remains a critical challenge for chemists and often requires significant optimization for every new system.

Scheme 3.6 Different modes of monomer insertion leading to different structures.

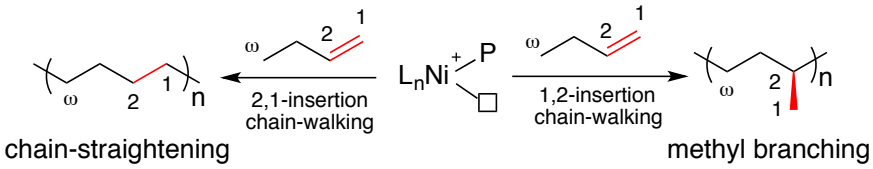

As previously discussed, tacticity plays a crucial role in a polymer's crystallinity and mechanical properties. *i*PP is typically produced using early metal catalysts such as titanium or zirconium. However, although highly active, early metal catalysts are easily poisoned by heteroatoms, therefore they require rigorous air-free conditions, which make it impossible to incorporate polar monomers. To resolve these issues, chemists have turned to late transition metal catalyst such as nickel and palladium; however, uncontrolled chain walking has limited the development of these catalysts for commercial use. Although chain walking polymerizations have made great progress over the last two decades in controlling molecular weights, dispersities, degree of branching, and insertion mode, stereoselective chain walking polymerizations remain an elusive challenge.[43]

Notable achievements have been made using α-diimine catalysts in stereoselective polymerizations. Specifically, Brookhart with DuPont reported that polymerization of cyclopentene using α-diimine nickel(II) and palladium(II) complexes (**3.27**) forms modestly isotactic ([*mm*] = 0.44) cis-1,3-polycyclopentene (Scheme 3.7a).[44] Although only modestly isotactic, the polymer still had an impressive

T_m = 330 and molecular weights up to 251 kg/mol for samples soluble enough for GPC analysis. However, in addition to low stereoselectivity, the polymers also suffered from broad dispersities (M_w/M_n = 2.5) and long reaction times (6 days). Furthermore, the catalyst never chain-walks through the stereocenter generated from monomer insertion. Therefore, this reaction is an example of a stereoselective insertion followed by chain walking and not stereoselective chain walking. Similarly, the Osakada-Takeuchi group has also accessed a variety of stereoregular structures through the polymerization of non-conjugated dienes and cyclo-olefins (Scheme 3.7b, **3.31**).[45] As in Brookhart's reaction, the stereoselectivity is derived from the insertion of the monomer and not chain walking.

Scheme 3.7 a) Brookhart's stereoselective polymerization of cyclopentene.[44] b) Taceuchi's stereoselective polymerization of non-conjugated dienes.[45]

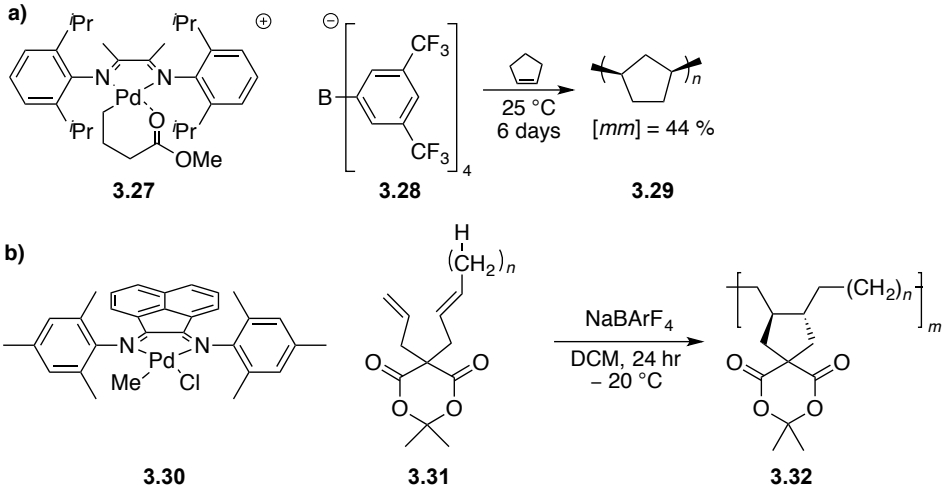

There are very few reports of chain walking polymerization of simple linear olefins into stereoregular polymers. The Coates group has made progress in this field. For instance, they previously reported the polymerization of trans-2-butene into iso-

1,3-poly(2-butene)[46] (**3.37**) but with a catalyst system that was only modestly isoselective (Scheme 3.8). The resulting polymers exhibited low melting temperatures (T_m < 67 °C), and the reaction suffered from low yields, long reaction times, and reliance upon using symmetrical monomors due to regio-irregular insertion by the catalyst. Similar to the previously described systems, the stereoselectivity of the reaction is derived from the insertion event and not stereoselective chain walking.

Scheme 3.8 Coates's iso-selective polymerization of trans-2-butene.

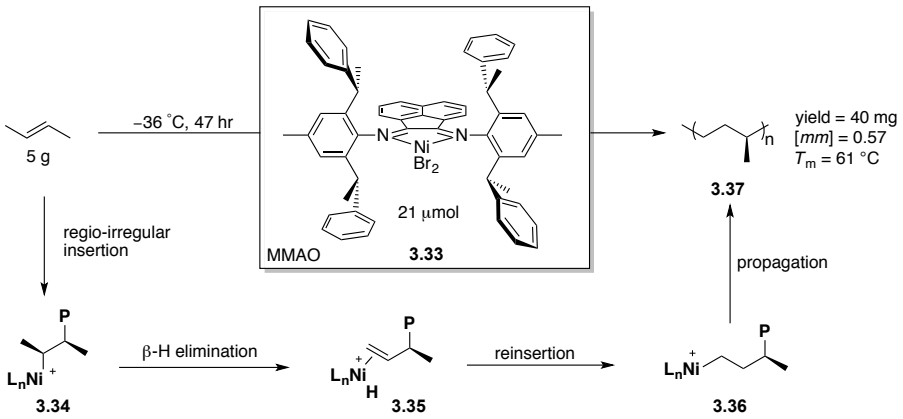

Subsequently, the Coates group developed highly isoselective nickel catalysts for the polymerization of propylene (Scheme 3.9a, **3.40**).[47] However, application to higher α-olefins resulted in decreased ω,2-enchainment and tacticity, and stereoselectivity was only observed at low temperatures (−60 °C). At ambient temperatures, a variety of regio- and stereo-errors were formed, yielding an amorphous material. Exploiting this behavior, the authors were able to synthesize block copolymers by simply warming and cooling the reaction to produce a thermoplastic elastomer. Bazan *et. al.* also demonstrated the ability to polymerize propylene in a stereoselective manner, achieving low crystallinity (T_m = 59 °C)

(Scheme 3.9b).[48] Similar to Coates's reaction, this system could only achieve selectivity at low temperatures.

In summary, chain walking polymerizations offer an attractive way to generate new polymer architectures from previously explored monomers. Given the strong structure-property relationship observed in polymers, it remains crucial that polymerizations are carried out in a controlled manner; however, exercising control over these systems is complicated by the nature of the chain walking mechanism. Although significant progress has been made, stereocontrol in chain walking remains a challenge. Specifically, there exists no polymerization system where the stereocenter is eliminated through chain walking and subsequently re-installed in a stereospecific manner. Catalysts capable of better controlling this process would allow access to new architectures with improved mechanical properties. With these goals in mind, the next chapter focuses on the development of a new isotatic polyolefin material and catalysts for its generation.

Scheme 3.9 a) Coates's strategy for the production of elastomers by changing temperature.[47] b) Iso-selective polymerization of PP at low temperatures to yield *i*PP.[48]

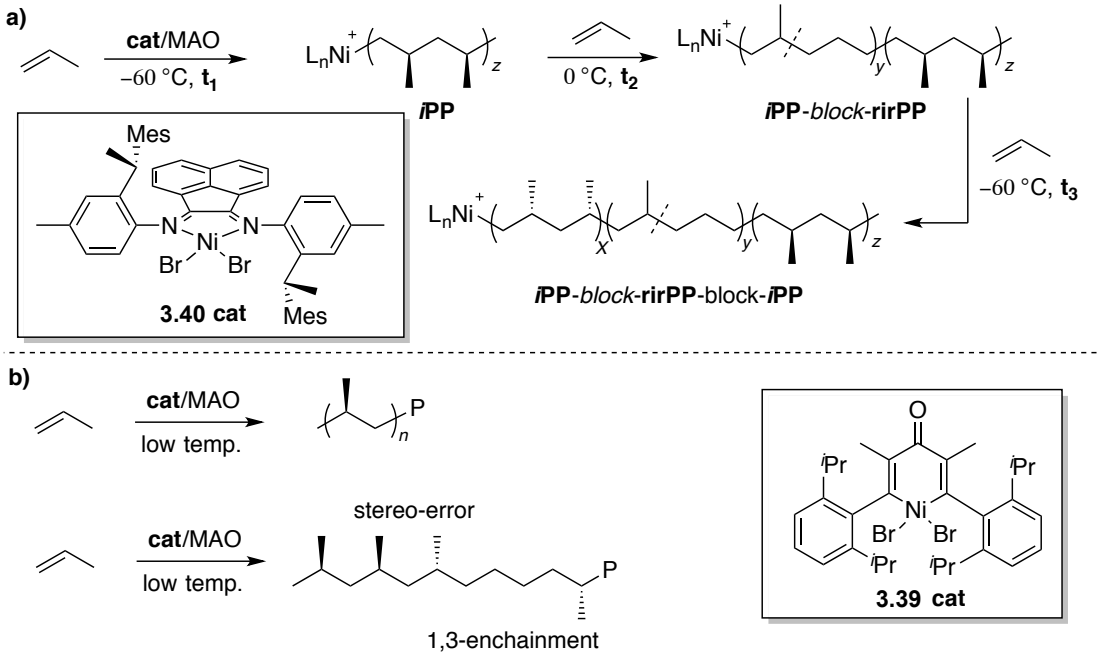

References and Notes

(1) Edgecombe, B. D.; Stein, J. A.; Frećhet, J. M. J.; Xu, Z.;Kramer, E. J. *Macromolecules* **1998**, 31, 1292−1304.

(2) Harth, E. M.; Hecht, S.; Helms, B.; Malmstrom, E. E.; Frećhet, J. M. J.; Hawker, C. J. *J. Am. Chem. Soc*. **2002**, 124, 3926−3938.

(3) Juran, R., ed., *Modern Plastic Encyclopedia*, Breskin & Charlton, New York, **1989**.

(4) Barbé, P. C.; Cecchin, G.; Noristi, L. *Adv. Polym. Sci.* **1987**, 81, 1–81.

(5) Youngman, E. A.; Boor, J. Jr., "*Syndotactic Poypropylene*," pp. 33–69 in *Macromolecular Reviews*, Vol. Peterlin, A.; Goodman, M.; Okamura, S.; Zimm, B. H.; Mark, H. F., eds., Wiley-Interescience, New York, **1967**.

(6) (a) Bovey, F. A. *High Resolution NMR of Macromolecules,* Academic Press, New York, **1972**. (b) Bovey, F. A. *Chain Structure and Conformation of Macromolecules*, Academic Press, New York, **1982**. (c) Bovey, F. A.; Mirau, P. *NMR of Polymers*, Academic Press, New York, **1996**. (d) Tonelli, A. E. *NMR Spectroscopy and Polymer Microstructue*, VCH, New York, **1989**. (e) Zambelli, A.; Gatti, G. *Macromolecules* **1978**, 11, 485–489.

(7) Farina, M. "The Stereochemistry of Linear Macromolecules,''pp. 1–112 in *Topics in Stereochemistry*, Vol. 17, Eliel, E. L.; Wien, S. H., eds., Wiley, New York, **1987**.

(8) Van Krevelen, D. W.; Nijenhuis, K. T. *Properties of polymers: their correlation with chemical structure; their numerical estimation and prediction from additive group contributions*. Elsevier, **2009**, and references therein.

(9) Gray, A. P. *Thermochimica Acta.* **1970**, 1, 563–579.

(10) (a) Reding, F. P.; Lovell, C. M. *J. Poly. Sci., Part A* **1956**, 157–159. (b) Willbourn, A. H. *J. Poly. Sci., Part A* **1959**, 569–597.

(11) (a) Flory, P. J.; Rehner Jr, J. *The Journal of Chemical Physics* **1943** 11, 512–520. (b) Kim, J. H.; Kim, J. Y.; Lee, Y. M.; Kim, K. Y. *Journal of applied polymer science*, **1992**, *45*, 1711–1717. (c) Deng, G.; Tang, C.; Li, F.; Jiang, H.; Chen, Y. *Macromolecules* **2010**, 43, 1191–1194.

(12) Beach, D. L.; Kissin, Y. V., "High Density Polyethylene," pp. 454–490 in *Encylopedia of Polymer Science and Engineering*, 2nd ed. Vol. 6, Mark, H. F.; Bikales, N. M.; Overberger, C. G.; Menges, G. eds., Wiley-Interscience, New York, **1986**.

(13) Kelly, J. M. *J. Macromol. Sci. Part C* **2002**, 42, 355–371.

(14) James, D. E., "Linear Low Density Polyetheylene," pp. 429–454 in Encyclopedia of Polymer Science and Engineering, 2nd ed., Vol. 6, Mark, H. F.; Bikales, N. M.; Overberger, C. G.; Menges, G. eds., Wiley-Interscience, New York, **1986**.

(15) Koak, K. W., "Low Density Polytheylene (High Pressure)," pp. 386 – 429 in *Encyclopedia of Polymer Science and Engineering*, Vol. 6, Mark, H. F.; Bikales, N. M.; Overberger, C. G.; Menges, G., eds., Wiley-Interscience, New York, **1986**.

(16) (a) Billmeyer, F. W. Jr., *Texbook of Polymer Science*, Chaps. 11, 12, Wiley-interscience, New York, **1984**. (b) Nielsen, L. E.; Landel, R. F. Mechanical Properties of Polymers and Composites, 2nd ed., Marcel Dekker, New York, **1994**.

(17) Piringer, OPo G.; Baner, Albert Lawrence (2008). *Plastic Packaging: Interactions with Food and Pharmaceuticals (2nd ed.)*

(18) http://www.ceresana.com/en/market-studies/plas4cs/polypropylene/

(19) http://www.plas4cstoday.com/study-global-pvc-demand-grow-32-annually-through-2021/196257501821043

(20) Zielger, K.; Holzkamp, E.; Briel, H.; Martin, H. *Angew. Chem.* **1955**, 67, 426.

(21) Natta, G.; Pino, P.; Corradini, P.; Danusso, F.; Mantica, E.; Mazzanti, G.; Moraglio, G. *J. Am. Chem. Soc.* **1955**, 77, 1708–1710.

(22) (a) Bohm, L. L. *Macromol. Symp.* **2001**, 173, 53. (b) Busico, V.; Cipullo, R.; Segre, A. L.; Talarico, G., Vacatello, M.; Castelli, V. V. A. *Macromolecules* **2001**, 34, 8412–8415. (c) Cecchin, G.; Mornini, G.; Pellicini, A. *Macromol. Symp.* **2001**, 173, 195–209. (d) Chadwick, J. C. *Macromol. Symp.* **2001**, 173, 21–35. (e) Chadwick, J. C.; Morini, G.; Balbontin, G.; Camurati, I.; Heere, J. J. R.; Mingozzi, I.; Testoni, F. *Macromol. Chem. Phys.* **2001**, 202, 1995–2002. (f) Chien, J. C. W.; Wu, J.-C.; Kuo, C.-I *J. Polym. Sci. Polym. Chem. Ed.* **1982**, 20, 2019–2032. (g) Hu, Y.; Chien, J. C. W. *J. Polym. Sci. Polym. Chem. Ed.* **1988**, 26, 2003.

(23) (a) Sinn, H.; Kaminsky, W. *Advances in Organometallic Chemistry* **1980**, *18*, 99–149. (b) Corradini, P.; Guerra, G.; Cavallo, L. *Accounts of chemical research*, **2004**, 37, 231–241.

(24) Burfield, D. R. *Polymer* **1984**, 25, 1647–1654.

(25) (a) Kuran, W., P*riniciples of Coordination Polymerization*, Wiley, New York, **2001**. (b) Tait, P. J. T.; Watkins, N. D. "Monoalkene Polymerization: Mechanisms," Chap. 2 in *Comprehensive Polymer Science*, Vol. 4, Eastmond, G. C.; Ledwith, A.; Russo, S.; and Sigwalt, P. eds., Pergamon Press, Oxford, **1989**.

(26) (a) Arlman, E. J.; Cossee, P. *J. Catalysis* **1964**, 3, 99–104. (b) Ewen, J. *J. Mol. Catal. A* **1999**, 140, 225–233. (c) Rappe, A. K.; Skiff, W. M.; Casewit, C. J. *Chem. Rev.* **2000**, 100, 1435–1456. (d) Resconi, L.; Cavallo, L.; Fait, A.; Piemontesi, F. *Chem. Rev.* **2000**, 100, 1253–1346.

(27) (a) Heatley, F.; Salovy, R.; Bovey, F. A. *Macromolecules* **1969**, 2, 619–623. (b) Wolfsgruber, C.; Zannoni, G.; Rigamonti, E.; Zambelli, A. *Makromol. Chem.* **1975**, 176, 2765–2769.

(28) (a) Breslow, D. S.; Newburg, N. R. *J. Am. Chem. Soc.* **1957**, 79, 5072–5073. (b) Natta, G.; Pino, P.; Mazzanti, G.; Giannini, U.; Mantica, E.; Peraldo, E. *J. Polym. Sci.* **1957**, 26, 120–123.

(29) (a) Hlatky, G. G. *Coordination Chemistry Reviews*, **1999**,181, 243–296. (b) Kaminsky, W. *Journal of the Chemical Society, Dalton Transactions* **1998**, 9, 1413–1418.

(30) (a) Tian J.; Coates, G. W.; *Angew. Chem. Int. Ed. Engl.* **2000**, 39, 3626–3629. (b) Tian, J.; Hustad, P. D.; Coates, G. W.; *J. Am. Chem. Soc.* **2001**, 123, 5134–

5135. (c) Makio, H.; Kashiwa, N.; Fujita, T. *Adv. Synth. Catal.* **2002**, 344, 477–493.

(31) Edson, J. B.; Wang, Z.; Kramer, E. J.; Coates, G. W. *J. Am. Chem. Soc.* **2008**, *130*, 4968–4977.

(32) Rix, F.; Brookhart, M. *J. Am. Chem. Soc.* **1995**, 117**,** 1137–1138.

(33) (a) Gates, D. P.; Svejda, S. A.; Onate, E.; Killian C. M.; Johnson, L. K.; White, P. S.; Brookhart, M. *Macromolecules* **2000**, 33, 2320–2334. (b) Gibson, V. C.; Spitzmesser, S. K. *Chem. Rev.* **2003**, 103, 283–316.

(34) Möhring, V. M.; Fink, G. *Angew. Chem., Int. Ed. Engl.* **1985**, 24, 1001−1003.

(35) Johnson, L. K.; Killian, C. M.; Brookhart, M. *J. Am. Chem. Soc.* **1995**, 117, 6414−6415.

(36) (a) Younkin, T. R.; Connor, E. F.; Henderson, J. I.; Friedrich, S. K.; Bansleben, D. A.; Grubbs, R. H. *Science* **2000**, 287, 460−462. (b) Weberski, M. P.; Chen, C.; Delferro, M.; Zuccaccia, C.; Macchioni, A.; Marks, T. J. *Organometallics* **2012**, 31, 3773−3789. (c) hen, Z.; Mesgar, M.; White, P. S.; Daugulis, O.; Brookhart, M. *ACS Catal.* **2015**, 5, 631−636. (d) Song, D. P.; Ye, W. P.; Wang, Y. X.; Liu, J. Y.; Li, Y. S. *Organometallics* **2009**, 28, 5697−5704. (e) Bianchini, C.; Giambastiani, G.; Luconi, L.; Meli, A. *Coord. Chem. Rev.* **2010**, 254, 431−455.

(37) (a) Deng, L.; Woo T. K.; Cavallo, L.; Margl, P.M.; Ziegler, T *J. Am. Chem. Soc.* **1997**, 119, 6177–6186. (b) Musaev, D. G.; Svensson, M.; Morokuma, K.; Stromberg, S.; Zetterberg, K.; Siegbahn, P. E. M. *Organometallics* **1997**, 16,

1933–1945.

(38) (a) Moody, L. S.; Mackenzie, P. B.; Killian, C. M.; Lavoie, G. G.; Ponasik, J. A. Jr.; Barrett, A. G.; Smith, T. W. Pearson, J. C, **2002** World patent WO. (b) Brookhart, M.; Grant, B.; Volpe, A. F. (1992) *Organometallics* **1992**, 11, 3920–3922. (c) Yakelis, N. A.; Bergman, R. G. *Organometallics* **2005**, 24, 3579–3581.

(39) Kaminsky, W.; Miri, M.; Sinn, H.; Woldt, R. *Macromol. Rapid. Commun.* **1983**, 4, 417–421.

(40) Johnson, L.K.; Mecking, S.; Brookhart, M. *J. Am. Chem. Soc.* **1996**, 118, 267–268.

(41) Rose, J. M.; Cherian, A. E.; Coates, G. W. *J. Am. Chem. Soc.* **2006**, 128, 4186–4187.

(42) O'Connor, K. S.; Watts, A.; Vaidya, T.; LaPointe, A. M.; Hillmyer, M. A.; Coates, G. W. *Macromolecules* **2016**, 49, 6743–6751.

(43) (a) Guan, Z.; Popeney, C. S. *Top. Organomet. Chem.* **2009**, 26, 179–220. (b) Guo, L.; Dai, S.; Sui, X.; Chen C. *ACS Catal.* **2016**, 6, 428−441.

(44) McLain, S. J.; Feldman, J.; McCord, E. F.; Gardner, K. H.; Teasley, M. F.; Coughlin, E. B.; Sweetman, K. J.; Johnson, L. K.; Brookhart, M. *Macromolecules* **1998**, 31, 6705–6707.

(45) (a) Okada, T.; Park, S.; Takeuchi, D.; Osakada, K. *Angew. Chem., Int. Ed.* **2007**,

46, 6141–6143. (b) Okada, T.; Takeuchi, D.; Shishido, A.; Ikeda, T.; Osakada, K. *J. Am. Chem. Soc*. **2009**, 131, 10852–10853. (c) Okada, T.; Takeuchi, D.; Osakada, K. *Macromolecules* **2010**, 43, 7998–8006. (d) Park, S.; Okada, T.; Takeuchi, D.; Osakada, K., *Chem. Eur. J.* **2010**, 16, 8662–8678. (e) Takeuchi, D.; Osakada, K., *Polymer* **2016**, 82, 392–405.

(46) Cherian, A. E.; Lobkovsky, E. B.; Coates, G. W. *Chem. Commun*. **2003**, 2566–2567.

(47) Rose, J. M.; Deplace, F.; A. Lynd, N.; Wang, Z.; Hotta, A.; Lobkovsky, E. B.; Kramer, E. J.; Coates, G. W. *Macromolecules* **2008**, 41, 9548–9555.

(48) (a) Azoulay, J. D.; Schneider, Y.; Galland, G. B.; Bazan, G. C. *Chem. Commun.* **2009**, 6177−6179. (b) Azoulay, J. D.; Gao, H.; Koretz, Z. A.; Kehr, G.; Erker, G.; Shimizu, F.; Galland, G. B.; Bazan, G. C. *Macromolecules* **2012**, 45, 4487−4493.

CHAPTER 4

Synthesis of Semi-Crystalline Polyolefin Materials: Precision Methyl Branching Using Chiral Isoselective α-Diimine Nickel Catalysts

4.1. Introduction

Given the massive global production of PE and *i*PP and the importance of these materials to modern society, new semicrystalline polyolefins produced from readily available, inexpensive feedstocks would be of significant interest. 1-Butene meets these criteria, and can easily be accessed from both petroleum and biorenewable sources. It can be produced by the dehydration of 1-butanol,[1] a biomass-derived fuel,[2] or by the dimerization of sugar-derived ethylene.[3] Polymerization of 1-butene using Ziegler-Natta catalysis results in isotactic 1,2-poly(1-butene) which exhibits superior mechanical properties relative to *i*PP and PE.[4] However, its complex crystallization hinders its use in many applications.[5] Crystallization from the melt gives a kinetically favored polymorph (form II), which slowly transforms over several days at room temperature to yield a more thermodynamically stable structure (form I), resulting in dimensional changes of the material. Recent advances have attempted to address this issue, potentially allowing 1,2-poly(1-butene) to be more widely utilized.[5]

Scheme 4.1. Nickel (II) catalyzed 4,2-enchainment polymerization of 1-butene.

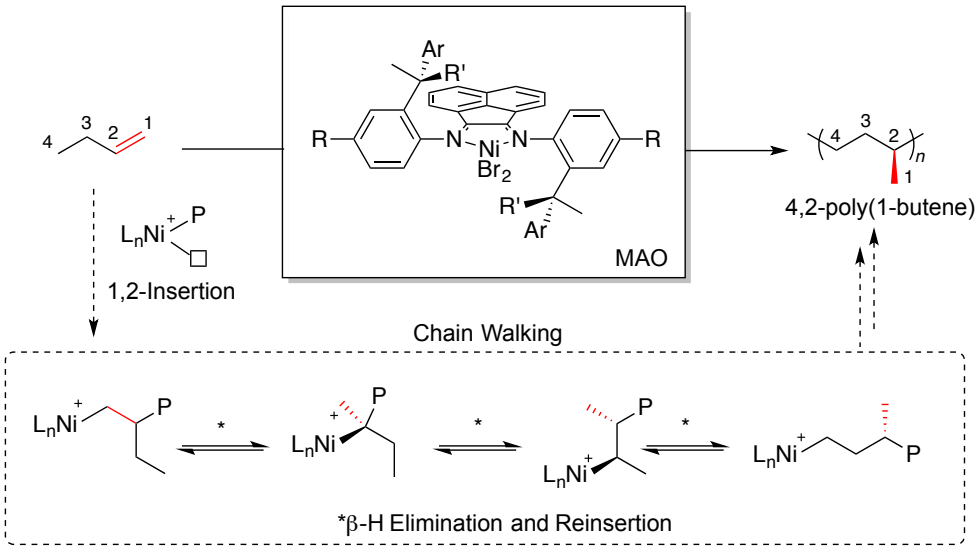

Since their discovery for olefin polymerization, α-diimine nickel(II) and palladium(II) catalysts have received considerable attention.[6] The major hallmark of these catalysts is their ability to undergo an isomerization event known as chain walking, where consecutive β-hydrogen elimination followed by reinsertion into metal hydride bond relocates the metal center along the polymer chain. These reactions place the active species at various positions along the polymer backbone, allowing for the preparation of numerous polymer topologies from simple olefin feedstocks.[7] The relative rates of chain walking versus insertion can be tuned by catalyst choice and reaction conditions which directly impacts the resulting polymer microstructure.[8]

Exhibiting control over polymer tacticity using late metal catalysts is a challenge. By nature of the chain walking mechanism, previously installed stereocenters can easily be scrambled during polymerization. Notable advancements have been achieved, with Brookhart and DuPont reporting the polymerization of

cyclopentene using α-diimine Ni(II) and Pd(II) complexes to form modestly isotactic cis-1,3-polycyclopentene.[9] The Osakada-Takeuchi group has also accessed a variety of stereoregular structures through the polymerization of non-conjugated dienes and cycloolefins.[10] Sigman and coworkers identified a rare example of enantioselective chain walking in a redox-relay oxidative Heck-arylation using chiral palladium catalysts. After arylation, the catalyst walks through a branch point and maintains a high enantiomeric ratio of the original stereocenter.[11]

Despite this progress, there are very few reports for the chain walking polymerization of simple linear olefins into stereoregular structures. We previously reported the polymerization of *trans*-2-butene into *iso*-1,3-poly(2-butene);[12] however, the catalyst system was only modestly isoselective ([*mm*] = 0.41–0.64) with the resulting polymers exhibiting low melting temperatures (T_m < 67 °C). Additionally, we developed nickel catalysts that produced *i*PP presumably through the isoselective enchainment of propylene.[13] However, application to higher α-olefins resulted in materials with poor thermal properties due to increased long chain branching and decreased tacticity.[14] Based on our previous results yielding semicrystalline iso-1,3-poly(2-butene), we believed an isoselective catalyst capable of preserving the stereochemistry from the insertion event could produce a similar polymer with a high melt transition temperature from 1-butene (Scheme 4.1). To the best of our knowledge, there have been no reports of late metal polymerization catalysts that can perform *both* isoselective monomer insertion *and* stereocontrolled chain walking in tandem.

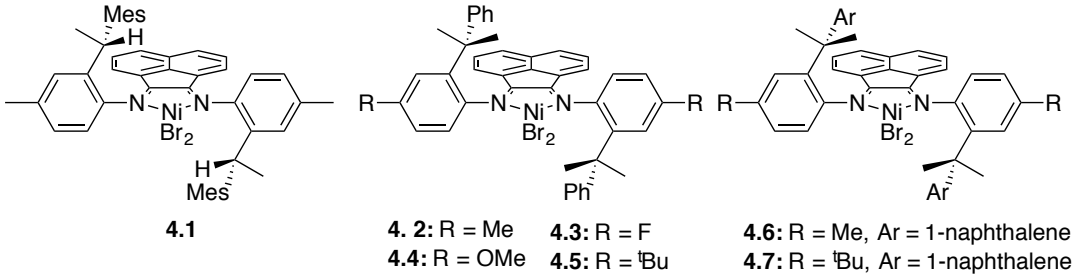

Figure 4.1. α-Diimine nickel complexes used in this study.

4.2. Polymerization of 1-Butene

Herein, we report on the synthesis and utilization of a family of nickel α-diimine complexes for the polymerization of 1-butene (Figure 4.1). Complex **4.1** activated with methylaluminoxane (**4.1**/MAO) has previously been shown to produce *i*PP with melting temperatures up to 137 °C.[15] However, the polymerization of 1-butene generates an amorphous material.[14] Analysis of the material by ^{13}C NMR spectroscopy revealed that 1,2-insertion followed by isomerization to the chain end before subsequent insertion (4,2-enchainment) is the primary insertion mode. However, limited stereocontrol as evidenced by a low [*mm*] triad value limits polymer crystallinity (Table 4.1, entry 1). We hypothesized that increasing the steric bulk around the metal center using a cumyl-derived complex (Figure 4.1, complex **4.2**) may be more effective for the regio- and stereoselective polymerization of 1-butene, with the additional steric bulk potentially preserving the stereochemical information imparted by the initial insertion event.

Table 4.1. Catalyst screen for the polymerization of 1-butene.[a]

entry	complex	yield (mg)	TOF[b] (h^{-1})	$M_{n(theo)}$ (kDa)	M_n[c] (kDa)	$Đ$[c] (M_w/M_n)	enchainment type (mole fraction)			[*mm*][d]	α[e]	T_m[f] (°C)
							4, 1[d]	4, 2[d]	1, 2[d]			
1	**4.1**	598	44	59.8	70.0	1.26	0.06	0.88	0.02[h]	0.43	0.74	–[g]
2	**4.2**	122	9	12.2	12.8	1.60	0.04	0.94	0.02	0.75	0.91	77
3	**4.3**	233	17	23.3	23.5	1.48	0.03	0.93	0.04	0.79	0.92	80
4	**4.4**	220	16	22.0	21.0	1.51	0.04	0.91	0.05	0.73	0.90	73
5	**4.5**	234	17	23.4	14.7	1.57	0.03	0.93	0.03[h]	0.80	0.93	85
6	**4.6**	200	15	20.0	18.5	1.60	0.03	0.91	0.06	0.80	0.93	86
7	**4.7**	298	22	29.8	20.5	1.69	0.03	0.93	0.04	0.84	0.94	85

[a]Polymerization conditions: 3.0 ± 0.2 g 1-butene (53.5 mmol), 10 μmol Ni complex in 2 mL CH_2Cl_2, 1.0 mmol MAO; t_{rxn} = 24 h, T_{rxn} = −40 °C. [b]Turnover frequency, TOF = (mol monomer consumed)(mol catalyst)$^{-1}$(time)$^{-1}$. [c]Determined by gel permeation chromatography at 150 °C in 1,2,4-trichlorobenzene versus polyethylene standards. [d]Determined using ^{13}C NMR spectroscopy; equations can be found in the supporting information. [e]Probability factor of three consecutive 4,2-units having the same relative stereochemistry, determined using the equation $[mm] = \alpha^3+(1-\alpha)^3$. [f]Determined by differential scanning calorimetry, endotherm from 2nd heating cycle. [h]Additional signals are present that correspond to long chain branching. [g]No detectable T_m.

Activation of complex **4.2** with MAO in the presence of 1-butene resulted in the production of a white, powdery material. GPC and DSC analysis revealed a polymer with modest molecular weight (12.8 kDa), controlled unimodal molecular weight distribution (1.60), and a melting temperature (T_m) of 77 °C (Table 4.1, entry 2). Analysis by ^{13}C NMR spectroscopy revealed a microstructure composed primarily of 4,2-poly(1-butene) units from 4,2-enchainment (4, 2 = 0.94) and high amounts of isotacticity ([*mm*] = 0.75). The observed tacticity is considerably higher than that reported previously for the polymerization of trans-2-butene ([*mm*] = 0.41–0.64).[12]

Scheme 4. 2. Proposed source of stereoselectivity in chain walking polymerization of 1-butene.

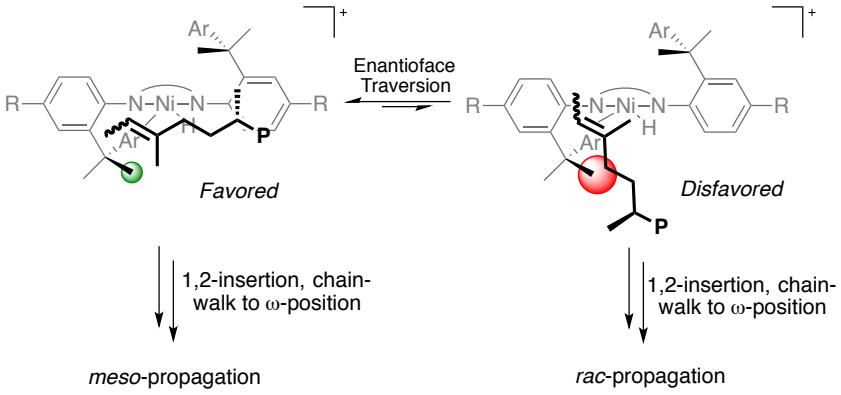

The addition of *ortho*-cumyl groups had a dramatic effect on the isoselectivity of the resulting 4,2-poly(1-butene). We believe that the steric environment created from this specific substitution pattern facilitates both the necessary enantioface coordination event *and* stereoselective chain isomerization. Enantioface traversion during the chain isomerization event is limited by the methyl substituent in the cumyl group, resulting in the observed isoselectivity (Scheme 4.2). Additionally, a π-stacking interaction with the *ortho*-aryl substituents and the acenaphthene backbone can be observed in the

solid state for complex **4.2**.[13] We believe this π-stacking interaction persists in solution at the low reaction temperature, causing the catalyst to maintain a very specific steric environment, which contributes to the observed selectivity.

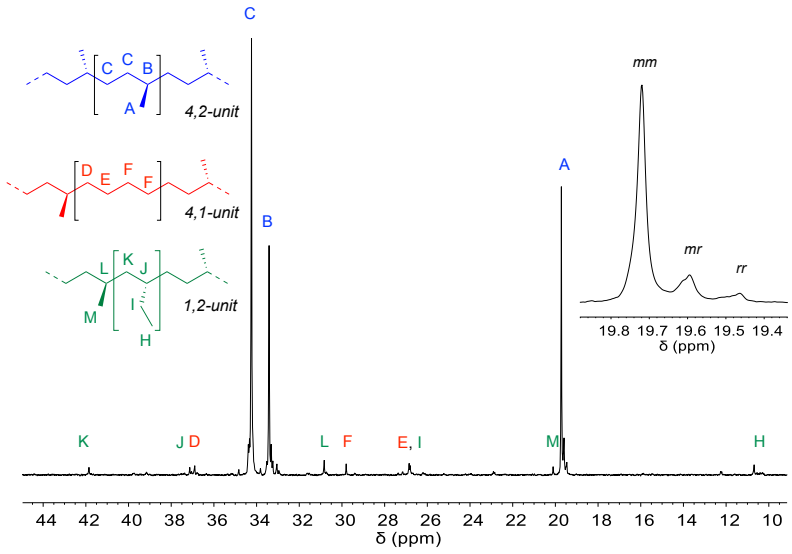

Figure 4.2. ^{13}C NMR spectrum of 4,2-poly(1-butene) produced by complex **4.7**/MAO (Table 4.1, entry 7**).**

To probe our assumptions regarding the source of selectivity for 1-butene polymerization, perturbations to the ligand framework were made. Electronic variants of the *ortho*-cumyl nickel complexes were first studied. It was found that MAO-activated **4.3** bearing electron withdrawing fluoro-substituents produced materials with higher molecular weight (23.3 kDa), slightly elevated T_m (80 °C), and improved isotacticity ([*mm*]= 0.79) compared to 4.**2**/MAO. MAO-activated **4.4**, bearing electron donating methoxy-substituents, however, produced materials with a decreased T_m (73 °C) and lower isotacticity ([*mm*]= 0.73). Selectivity for 4,2-enchainment also decreased slightly for **4.4**/MAO (0.91). We also studied a *tert*-butyl substituted

complex **4.5**, which is slightly more electron donating than complex **4.2** with the methyl substituent. To our surprise, **4.5**/MAO produced 4,2-poly(1-butene) with the highest levels of isotactity in the whole electronic series ([*mm*] = 0.80) and a T_m of 85 °C. From analysis of the crystal structure, we believe distal steric effects may rigidify the active catalyst structure and inhibit rotation of the aryl side chains away from the acenaphthene backbone, allowing for the π-stacking interaction to be better maintained. Another viable possibility is that the *tert*-butyl substituents in **4.5** affect the ion pairing interaction of the cationic nickel complex and the MAO activator, such that an improvement in selectivity is observed.[16]

We continued probing this system by modifying the aryl substituent of the cumyl group from phenyl (**4.2**) to 1-napthyl (**4.6**). Complex **4.6**/MAO exhibited similar tacticity to that of complex **4.5**/MAO ([*mm*] = 0.80) and a similar T_m of 86 °C. We believe the π-stacking interaction between the 1-napthyl group and the acenapthene backbone is enhanced due to the additional π-cloud overlap, resulting in a more rigidified structure that contributes to the desired regio- and stereoselectivity. After observing the enhanced selectivities for materials produced by MAO-activated **4.5** and **4.6**, we attempted to further rigidify the system by synthesizing complex **4.7**, bearing both *tert*-butyl and 1-napthyl substituents (Figure 4.1). The polymer produced by **4.7**/MAO exhibited improved isotacticity ([*mm*] = 0.84) compared to the polymers produced by **4.5**/MAO and **4.6**/MAO (Figure 4.2). Interestingly, despite the increase in tacticity, there was no improvement in the observed thermal properties of the resulting material (Table 4.1, entry 7).

Table 4.2. Effects of Varying REaction Conditions on the Polymerization of 1-Butene.[a]

entry	T_{rxn} (°C)	conc (M)	yield (mg)	M_n[b] (kDa)	$Đ$[b] (M_w/M_n)	T_m[c] (°C)
1	−10	7.8	262	10.8	1.95	–[d]
2	−30	7.8	420	23.7	1.80	66
3	−40	7.8	234	14.7	1.57	85
4	−50	7.8	173	10.6	1.81	85
5	−40	6.0[e]	163	12.4	1.46	80
6	−40	9.1[f]	464	16.3	2.17	73

[a]Polymerization conditions: 3.0 ± 0.2 g 1-butene (53.5 mmol), 10 μmol of complex **4.5** in 2 mL CH_2Cl_2, 100 equiv. MAO; t_{rxn} = 24 h, T_{rxn} = −40 °C. [b]Determined by gel permeation chromatography at 150 °C in 1,2,4-trichlorobenzene versus polyethylene standards. [c]Determined by differential scanning calorimetry, endotherm from 2nd heating cycle. [d]No detectable T_m. [e]1.5 ± 0.2 g 1-butene (26.8 mmol). [f]6.0 ± 0.2 g 1-butene (107.0 mmol).

The thermal properties of 4,2-poly(1-butene) are influenced not only by tacticity, but also by branch composition. A small percent of ethyl branches were detected in these systems, which can be installed through 1,2-insertion of 1-butene without chain walking. Ethyl branches can considerably reduce T_m and crystallinity.[17] When 1,2-enchainment pathways are minimized in these systems, increased melting temperatures are generally observed (Table 4.1, entry 5). Another defect observed in this system arises from 4,1-enchainment, where 2,1-insertion followed by complete chain walking produces a linear polyethylene segment. Due to the small amount of these units (< 5%), it is difficult to quantify its effect on the properties of the resulting 4,2-poly(1-butene).[18] Recent studies have shown that *i*PP with < 5% 3,1-insertions, made with related cumyl-substituted catalysts retained most of its crystallinity, suggesting that the effect in this system may also be small.[19]

We further studied the effects of reaction conditions on the thermal properties of the resulting polymers produced by **4.5**/MAO. Reaction temperature had a dramatic effect on polymer thermal properties. By increasing the temperature from −40 °C to −30 °C, the melting temperature of the resulting material dropped considerably from 85 °C to 66 °C. Increasing the reaction temperature further to −10 °C resulted in a complete loss of crystallinity. Cooling the reaction to −50 °C decreased the reaction rate and polymer yield, and resulted in materials with similar thermal properties to those produced at −40 °C. The effect of 1-butene concentration was also studied. Increasing the concentration from the standard 7.8 M to 9.1 M resulted in a higher yield but a decrease in tacticity ([*mm*] = 0.61) and melting temperature (Table 4.2, entry 6). Decreasing the concentration of 1-butene to 6.0 M resulted in a material with a slightly depressed melting temperature compared to the standard conditions (Table 4.2, entry 5) caused by a decrease in polymer tacticity ([*mm*] = 0.70).

Reaction solvent also played an important role in material properties. Dichloromethane was found to be the most suitable solvent for this system (Table 4.3, entry 1). Using aromatic solvents generally resulted in a decrease in the T_m of the polymer. We suspect that aromatic solvents may have competitive interactions with at the acenaphthene backbone, disrupting of the π-stacking interaction with the cumyl side-chain. Unexpectedly, 1,2-difluorobenzene produced a high T_m material, contrary to the other aromatic solvents screened. This may be a result of its significantly higher polarity potentially affecting the ion pairing interaction.

Table 4.3. Solvent Effects on the Polymeriztion of 1-Butene.[a]

entry	solvent	TOF[b] (h^{-1})	yield (mg)	M_n[c] (kDa)	$Đ$[c] (M_w/M_n)	T_m[d] (°C)
1	CH_2Cl_2	17	234	14.7	1.57	85
2	PhMe	15	198	12.2	1.96	79
3	PhCl	25	338	21.1	1.85	76
4	$C_6H_4F_2$[e]	17	223	10.9	2.05	82

[a]Polymerization conditions: 3.0 ± 0.2 g 1-butene (53.5 mmol), 10 μmol of complex **4.5** in 2 mL solvent, 1.0 mmol MAO; t_{rxn} = 24 h, T_{rxn} = −40 °C. [b]Turnover frequency, TOF = (mol monomer consumed)(mol catalyst)$^{-1}$(time)$^{-1}$. [c]Determined by gel permeation chromatography at 150 °C in 1,2,4-trichlorobenzene versus polyethylene standards. [d]Determined by differential scanning calorimetry, endotherm from 2nd heating cycle. [e]1,2-difluorobenzene.

Returning to our assertion of stereoselective insertion versus chain walking, it is not immediately clear why complex **1**/MAO produces *i*PP from propylene but atactic polymer from higher α-olefins. Conceivably, propylene polymerization can proceed through two different mechanisms that lead to the same *i*PP product: (1) consecutive isoselective insertions *without* chain walking, or (2) consecutive isoselective insertions *with* stereocontrolled chain walking. To confirm which mechanism is operative for propylene, we performed a deuterium study using [3-d_3]propylene at −78 °C and **4.1**/MAO. If chain walking is occurring, the deuterium atoms should scramble throughout the polymer backbone. Under these conditions, however, the deuterium atoms remained on the methyl branches of the polymer, demonstrating that chain walking during the polymerization of propylene does not occur (Scheme 4.3). This strongly suggests that tacticity is lost in the chain walking step of the polymerization of higher α-olefins using **4.1**/MAO. Since the formation of 4,2-poly(1-butene) requires chain isomerization, we believe the isotactic enchainment

of 1-butene presented in this work is the first example of stereoselective chain walking.

Scheme 4.3. Deuterated Propylene Study.

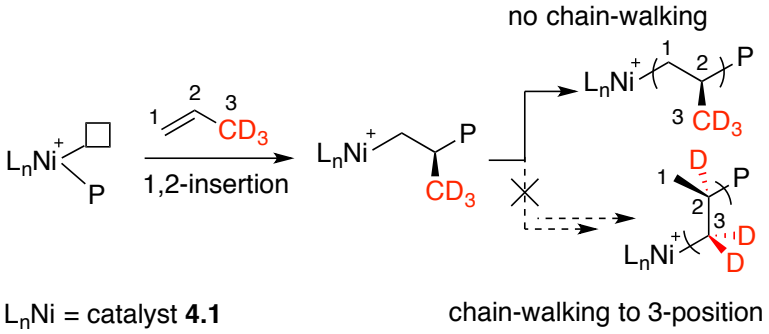

Finally, we examined the mechanical properties of 4,2-poly(1-butene). Polymer films were melt-pressed, directly into a tensile bar mold, at 95 °C under a pressure of 5.2 MPa for 15 min and cooled at a rate of ~6 °C/min to 22 °C. The tensile bars were subsequently used for analysis of mechanical properties. Tensile strength was measured for a sample produced by **4.5** and Figure 4.3 shows a representative tensile strength curve. Interestingly, the resulting material experiences yielding at relatively low stress values (~5 MPa) in comparison to other thermoplastics such as *i*PP.[1] After yielding, the material experiences high elongations up to 600% strain before breaking with a gradual increase in stress during elongation.

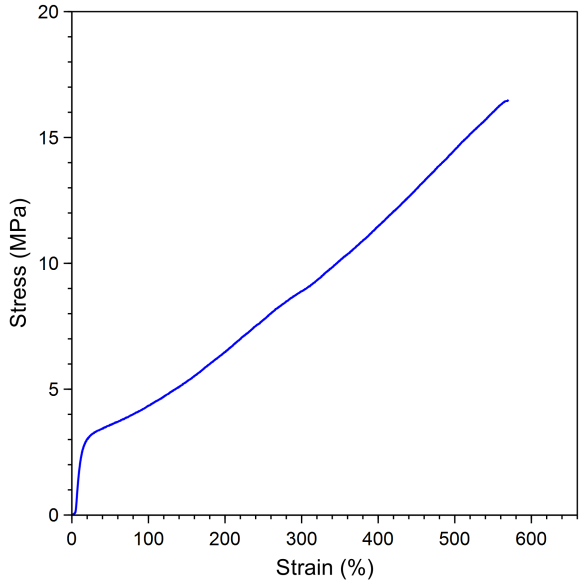

Figure 4.3. Representative tensile strength curve for 4,2-poly(1-butene). 3.0 ± 0.2 g 1-butene, 10 μmol of Ni complex **4.5** in 2 mL CH_2Cl_2, 100 equiv. MAO; t_{rxn} = 168 h, T_{rxn} = −40 °C. yield = 3.52 g, M_n = 29.5 kDa, $Đ$ = 1.60, T_m = 80 °C.

In summary, we performed the iso- and regioselective polymerization of 1-butene using cationic α-diimine nickel(II) complexes to produce semi-crystalline 4,2-poly(1-butene). The methyl substituents on the cumyl-groups of the ligand are crucial for preventing enantioface traversion and retaining stereochemical information. Furthermore, rigidifying the structure of the active catalyst through π-stacking interactions with the catalyst backbone was also beneficial for improving tacticity. This system represents the first example of re-establishing stereochemistry of a branch unit after it has been eliminated through the chain walking mechanism. This method allows access to isotactic polymers from simple, inexpensive feedstocks. Additional catalyst development is currently in progress to further increase the selectivity of this unique process.

4.3. Experimental

General Considerations

All manipulations of air- and/or water-sensitive compounds were carried out under dry nitrogen using a Braun UniLab drybox or standard Schlenk techniques. NMR spectra were acquired using either a Varian Mercury (300 MHz) or a Varian Inova (400 MHz) and were referenced versus residual nondeuterated solvent solvent shifts (^{1}H, ^{13}C). Polymer NMR spectra were acquired using a Bruker AV III HD with broadband Prodigy cryoprobe and were referenced versus residual nondeuterated solvent solvent shifts (^{1}H, ^{13}C). The mass spectrum was recorded using a Exactive Plus Orbitrap Mass Spectrometer with a DART SVP ion source from Ion Sense or a Waters MALDI Micro MX system. The sample was prepared by using the dried droplet method with no matrix present. Ionization was by a 257 nm UV nitrogen laser and the accelerating potential was 17.2 keV. The spectrum was recorded using the reflectron in positive ion mode. Molecular weights (M_n and M_w) and polydispersities (M_w/M_n) were determined by high temperature gel permeation chromatography (GPC) using a Waters Alliance GPCV 2000 GPC equipped with a Waters DRI detector and viscometer. The column set (four Waters HT 6E and one Waters HT2) was eluted with 1,2,4-trichlorobenzene containing 0.01 wt. % di-*tert*-butylhydroxytoluene (BHT) at 1.0 mL/min at 150 °C. Data were calibrated using monomodal polyethylene standards. Polymer melting points (T_m) and glass transition temperatures (T_g) were measured by differential scanning calorimetry (DSC) using a TA Instruments Q1000 calorimeter equipped with an automated sampler. Analyses were performed in crimped aluminum pans under nitrogen and data were collected from the second

heating run at a heating rate of 10 °C/min from -70 to 200 °C, and processed with TA Q series software.

Materials

Toluene and hexanes were purified over columns of alumina and copper (Q5). Methylene chloride was purified over an alumina column and degassed by three freeze-pump-thaw cycles before use. 1,2-difluorobenzene, chloroform, dibromomethane, and chlorobenzene were dried over crushed CaH_2 for 24 hours and degassed by three freeze-pump-thaw cycles before use. Acenaphthenequinone (Aldrich), α-methylstyrene (Aldrich), 4-fluoroaniline (Aldrich), formic acid (Aldrich), trifluoromethanesulfonic acid (CF_3SO_3H, Aldrich), 1-Butene (Aldrich), and (dimethoxyethane)$NiBr_2$ ((DME)$NiBr_2$, Strem) were used without further purification. Methylaluminoxane (MAO) was generously donated from Albemarle Corporation as a 30% wt solution in toluene which was dried by evaporation of volatiles giving a white powder. Complexes **4.1**, **4.2**, and **4.6** were synthesized as previously reported.[13,15]

4-Fluoro-2-(2-phenylpropan-2-yl)aniline (4.8). CF_3SO_3H (0.54 mL, 6.0 mmol) was added to a mixture of 4-fluoroaniline (2.85 mL, 30.0 mmol) and α-methylstyrene (3.90 mL, 30.0 mmol). The mixture was heated to 160 °C and allowed to react for 20 h. The reaction was quenched with a solution of saturated $NaHCO_3$, followed by an extraction with dichloromethane. Organics were combined, dried over $MgSO_4$, filtered, and concentrated. The crude product was chromatographed on silica (95:5 hexanes:ethyl acetate) and dried to give a light purple solid (2.98 g, 43 %). **^{1}H NMR**

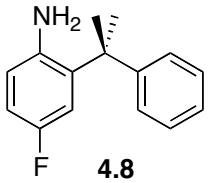

4.8

(500 MHz, $CDCl_3$): δ 7.34–7.28 (m, 4H, ArH), 7.25–7.18 (m, 2H, ArH) 6.79 (m, 1H, ArH), 6.47 (dd, J = 5.23 Hz, J = 8.62 Hz, 1H, ArH), 3.02 (broad s, 2H, NH_2), 1.68 (s, 6H, $C(CH_3)_2$). **^{13}C NMR** (125 MHz, $CDCl_3$): δ 156.5 (d, J_{CF} = 235.0 Hz), 148.6, 140.6 (d, J_{CF} = 2.1 Hz), 135.3 (d, J_{CF} = 5.7 Hz), 129.0, 126.5, 125.9, 118.0 (d, J_{CF} = 7.7 Hz), 113.7 (d, J_{CF} = 2.9 Hz), 113.5, (d, J_{CF} = 1.4 Hz) , 42.5 (d, J_{CF} = 1.1 Hz), 28.9. **HRMS** (DART) *m/z* calc for $C_{15}H_{17}NF$ $(M+H)^+$: 230.1345, found 230.1345.

***rac*-ArN=C(An)C=NAr (Ar = 4-flouro-2-(2-phenylpropan-2-yl)phenyl; An = acenaphthene) (4.9).** In a sealed vial a mixture of **4.8** (0.504 g, 2.20 mmol), acenaphthenequinone (0.182 g, 1.00 mmol), and anhydrous $ZnCl_2$ (0.157 g, 1.15 mmol) in glacial acetic acid (2.2 mL) was heated to 130 °C with stirring for 1 h. Upon stirring, bright yellow solids precipitated. The solution was cooled briefly (5 minutes) and then filtered over a Buchner funnel. The yellow solids were washed with AcOH (3x2 mL) and then washed with Et_2O (8x3 mL). Drying in vacuo afforded a yellow solid (58 %). A small portion was set aside, wit the rest immediately used in the next step. The intermediate (0.317 g) was dissolved in DCM (100 mL) in an Erlenmeyer flask. A solution of excess potassium oxalate hydrate in water (4 mL) was added. The biphasic reaction was stirred vigorously for 1 h. The organic layer was separated and dried over Na_2SO_4, filtered, and concentrated to give a bright yellow solid (0.206 g, 80 %, 69% over two steps). **^{1}H NMR** (500 MHz, d_2-TCE, 100 °C) δ 7.77 (d, J = 7.9 Hz, 2H, ArH), 7.39 (d, J = 10.6 Hz, 2H, ArH), 7.28 (br s, 2H, ArH), 7.11 (d, J = 7.5 Hz, 4H, ArH), 7.02 (m, 2H, ArH), 6.88–6.58 (m, 8H, ArH), 6.36 (br s, 2H, ArH), 1.85 (br s, 12H, $C(CH_3)_2$). **^{13}C NMR** (125 MHz, d_2-TCE, 100 °C): δ 159.9 (d, J_{CF} = 241.8 Hz), 148.8, 141.2, 130.1, 127.7, 126.9, 126.6 (br s), 126.2, 124.2, 122.7 (br s),

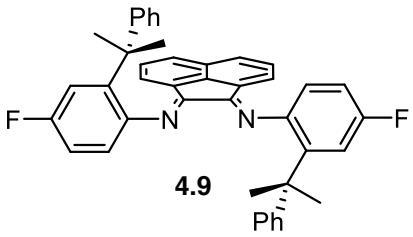

4.9

119.3 (br s), 114.2 (d, J_{CF} = 21.8 Hz), 112.9 (d, J_{CF} = 21.8 Hz), 42.8, 28.4 (br s). **HRMS** (DART) *m/z* calc for $C_{42}H_{35}N_2F_2$ $(M+H)^+$: 605.2762, found 605.2762.

***rac*-(ArN=C(An)C=NAr)NiBr$_2$ (Ar = 4-flouro-2-(2-phenylpropan-2-yl)phenyl; An = acenaphthene) (4.3). 4.9** (0.388 g, 0.642 mmol) and (DME)$NiBr_2$ (0.198 g, 0.0.642 mmol) were combined under N_2. CH_2Cl_2 (ca. 15mL) was added to afford a dark red solution, which was allowed to stir for 18 h. The reaction mixture was filtered through Celite under N_2 and volatiles were then removed *in vacuo*. The crude red solid was redissolved in CH_2Cl_2 and layered with hexanes to afford a dark red microcrystalline solid (0.092 g, 17 %). **MALDI** (m/z): 822.8.

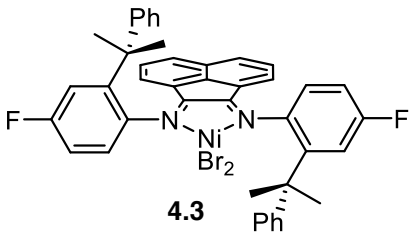

4.3

4-OMe-2-(2-phenylpropan-2-yl)aniline (4.10). CF_3SO_3H (0.30 mL, 3.38 mmol) was added to a mixture of *p*-Anisidine (3.13 g, 25.4 mmol) and α-methylstyrene (2.20 mL, 16.9 mmol). The mixture was heated to 160 °C and allowed to react for 20 h. The crude product was chromatographed on silica (90:10 hexanes:ethyl acetate) and dried in vacuo to afford a light beige solid (2.77 g, 68 %). **^{1}H NMR** ($CDCl_3$, 500 MHz): δ 7.32–7.27 (m, 4H, ArH), 7.24–7.18 (m, 2H, ArH), 7.10 (d, *J* = 2.8 Hz, 1H, ArH), 6.67 (dd, *J* = 2.9 Hz, *J* = 8.5 Hz, 1H, ArH), 6.50 (d, *J* = 8.5 Hz, 1H, ArH) 3.81 (s, 3H, OCH_3), 2.90 (s, 2H, NH_2), 1.69 (s, 6H, $C(CH_3)_2$). **^{13}C NMR** (125 MHz, $CDCl_3$): δ 152.6, 149.2, 138.3, 135.5, 128.9, 126.3, 126.0, 118.3, 114.0, 111.5, 55.8, 42.6, 29.1. **HRMS** (DART) *m/z* calc for $C_{16}H_{20}NO$ $(M+H)^+$: 242.1545, found 242.2544.

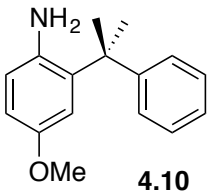

4.10

***rac*-ArN=C(An)C=NAr (Ar = 4-OMe-2-(2-phenylpropan-2-yl)phenyl; An = acenaphthene) (4.11).** In a sealed vial a mixture of **4.10** (0.600 g, 2.49 mmol), acenaphthenequinone (0.216 g, 1.18 mmol), and glacial acetic acid (0.43 mL, 7.58 mmol) in toluene (3.1 mL) was heated and stirred at 100 °C for 16 h. The solution was removed from heat for 5 minutes, followed by filtration over Celite® and washing with DCM. Volatiles were removed in vacuo until a sticky, orange solid was obtained. The crude mixture was triturated in cold hexanes (~20 mL), filtered, and then washed with copious cold hexanes (~100 mL). Drying in vacuo afforded a bright orange powder (0.191 g, 26 %). **^{1}H NMR** (500 MHz, d_2-TCE, 100 °C) δ 7.74 (d, J = 7.1 Hz, 2H, ArH), 7.23 (br s, 4H, ArH), 7.15 (d, J = 6.7 Hz, ArH), (broad s, 12H, $C(CH_3)_2$). **^{13}C NMR** (125 MHz, d_2-TCE, 100 °C) δ 158.9, 156.6, 149.4, 144.0, 140.6, 130.1, 128.9, 127.3, 126.8, 126.5, 126.3, 124.0, 122.6, 119.1, 114.4, 111.1, 55.5, 42.9, 28.6. **HRMS** (DART) *m/z* calc for $C_{44}H_{41}N_2O_2$ $(M+H)^+$: 629.3162, found 629.3177.

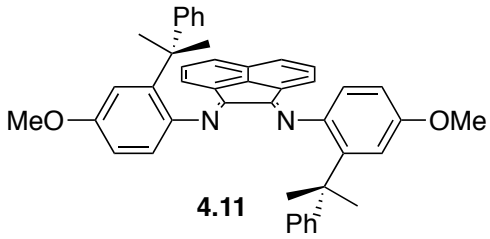

4.11

***rac*-(ArN=C(An)C=NAr)NiBr$_2$ (Ar = 4-OMe-2-(2-phenylpropan-2-yl)phenyl; An = acenaphthene) (4.4). 4.11** (0.191g, 0.304 mmol) and (DME)$NiBr_2$ (0.092 g, 0.298 mmol) were combined under N_2 in a Schlenk flask. CH_2Cl_2 (7 mL) was added to afford a dark red solution, which was allowed to stir at 22 °C for 18 hours. The reaction mixture was filtered through Celite under N_2 and volatiles were removed *in vacuo*. The crude red solid was redissolved in CH_2Cl_2 and layered with hexanes to afford dark red blocky crystals (0.155 g, 62 %).

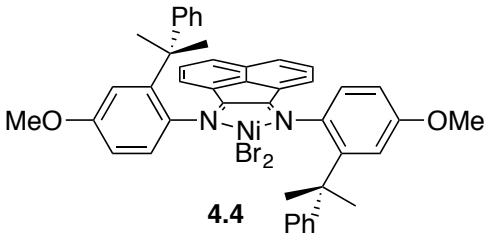

4.4

4-^{t}Bu-2-(2-phenylpropan-2-yl)aniline (4.12). CF_3SO_3H (0.10 mL, 1.1 mmol) was added to a mixture of 4-^{t}butylaniline (2.52 g, 16.9 mmol) and α-methylstyrene (0.40 g, 3.4 mmol). The mixture was heated to 160 °C and allowed to react for 20 hours before it was diluted with EtOAc and washed with a saturated solution of $NaHCO_3$. The organic solution was dried over Na_2SO_4, filtered, and concentrated to give a crude brown oil. The crude product was chromatographed on silica (95:5 hexanes/ethyl acetate) to give a pale yellow oil (0.399 g, 44 %). **^{1}H NMR** (400 MHz, $CDCl_3$) δ 7.45 (d, *J* = 2.3 Hz, 1H), 7.30 – 7.21 (m, 4H), 7.19 – 7.11 (m, 1H), 7.06 (dd, *J* = 8.2, 2.3 Hz, 1H), 6.44 (d, *J* = 8.2 Hz, 1H), 2.98 (br s, 2H), 1.65 (s, 6H), 1.30 (s, 9H). **^{13}C NMR** (126 MHz, $CDCl_3$) δ 149.6, 141.9, 140.9, 133.0, 128.8, 126.1, 125.9, 124.0, 123.3, 117.1, 42.6, 34.2, 31.8, 29.2. **HRMS** (DART) *m/z* calc for $C_{19}H_{26}N$ $(M+H)^+$: 268.2065, found 268.2061.

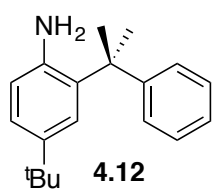

4.12

***rac*-ArN=C(An)C=NAr (Ar = 4-^{t}Bu-2-(2-phenylpropan-2-yl)phenyl; An = acenaphthene) (4.13).** In a sealed vial a mixture of **4.12** (0.399 g, 1.5 mmol), acenaphthenequinone (0.108 g, 0.60 mmol), and $ZnCl_2$ (0.092 g, 0.67 mmol) in glacial acetic acid (3 mL) was heated to 130 °C with stirring for 2 h. Upon cooling to room temperature, a brown solid crashed out. The solid was filtered and washed with Et_2O. The solid was then dissolved in DCM (5 mL) and added to a solution of water (5 mL) and excess potassium oxalate hydrate. The biphasic reaction was stirred vigorously for 12 h. The organic layer was separated and dried over Na_2SO_4, filtered, and concentrated to give a red orange solid (0.260 g, 64 %). **^{1}H NMR** (400 MHz, $CDCl_3$) δ 7.71 – 7.60 (m, 4H), 7.28 (s, 2H), 7.14 (t, *J* = 7.7 Hz, 2H), 7.06 (d, *J* = 7.9

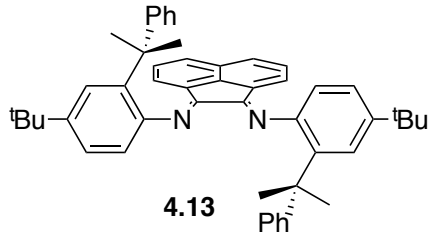

4.13

Hz, 4H), 6.71 (d, J = 8.1 Hz, 2H), 6.48 (d, J = 8.3 Hz, 4H), 6.14 (s, 2H), 1.82 (s, 12H), 1.44 (s, 18H). **^{13}C NMR** (126 MHz, $CDCl_3$) δ 158.8, 150.0, 148.1, 146.93, 141.1, 138.1, 130.1, 129.1, 127.5, 126.9, 126.7, 126.6, 124.0, 123.8, 123.6, 123.1, 117.9, 43.0, 34.8, 31.9. **HRMS** (DART) *m/z* calc for $C_{50}H_{53}N_2$ $(M+H)^+$: 681.4209, found 681.4208.

***rac*-(ArN=C(An)C=NAr)NiBr$_2$ (Ar = 4-^{t}Bu-2-(2-phenylpropan-2-yl)phenyl; An = acenaphthene) (4.5). 4.13** (0.260 g, 0.38 mmol) and (DME)$NiBr_2$ (0.117 g, 0.38 mmol) were combined under N_2. CH_2Cl_2 (ca. 5mL) was added to afford a dark red solution, which was allowed to stir for 18 h. The reaction mixture was filtered through Celite under N_2 and volatiles were then removed *in vacuo*. The crude red solid was redissolved in a minimum amount of CH_2Cl_2 and layered with hexanes (4 x the volume of DCM) to afford a dark red crystalline solid (0.226 g, 66 %).

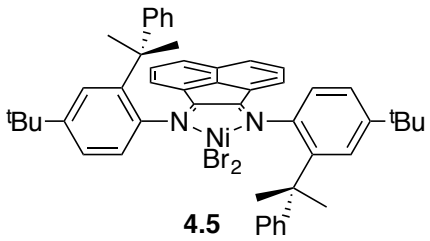

4.5

4-^{t}Bu-2-(2-(naphthalen-1-yl)propan-2-yl)aniline (4.14). CF_3SO_3H (0.40 mL, 4.5 mmol) was added to a mixture of 4-^{t}Bu-aniline (12.0 g, 80.4 mmol) and 1-(prop-1-en-2-yl)naphthalene (2.54 g, 15.1 mmol) and 2 mL xylenes. The mixture was heated to 160 °C and allowed to react for 20 h. The material was then cooled to room temperature and washed with a saturated solution of $NaHCO_3$ and dried over Na_2SO_4. The crude product was chromatographed on silica (95:5 hexanes:ethyl acetate) to give an off-white solid (596 mg, 12 %). **^{1}H NMR** (500 MHz, $CDCl_3$) δ 7.90 (d, J = 8.8 Hz, 1H), 7.84 – 7.81 (m, 2H), 7.80 (d, J = 8.2 Hz, 1H), 7.73 (d, J = 2.3 Hz, 1H), 7.52 (t, J = 7.8 Hz, 1H), 7.36 (ddd, J = 8.0, 6.7, 1.1 Hz, 1H), 7.13 (ddd, J = 8.5, 6.8, 1.4 Hz, 1H), 7.08 (dd, J = 8.2, 2.3 Hz, 1H), 6.35 (d, J = 8.1 Hz, 1H), 3.03 (s, 2H), 1.94 (s,

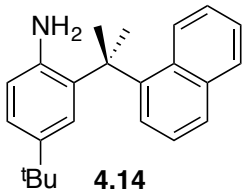

4.14

6H), 1.44 (s, 9H). **^{13}C NMR** (125 MHz, $CDCl_3$) δ 145.3, 142.0, 141.7, 134.9, 133.3, 131.4, 129.0, 128.2, 125.9, 125.5, 125.4, 125.0, 123.8, 123.1, 122.6, 117.1, 43.2, 34.4, 31.9. **HRMS** (DART) *m/z* calc for $C_{23}H_{28}N$ $(M+H)^+$: 318.2222, found 318.2215.

***rac*-ArN=C(An)C=NAr (Ar = 4-^{t}Bu-2-(2-(naphthalen-1-yl)propan-2-yl)aniline; An = acenaphthene) (4.15).** In a sealed vial a mixture of **4.14** (0.597 g, 1.9 mmol), acenaphthenequinone (0.114 g, 0.62 mmol), glacial acetic acid (0.244 g, 4.1 mmol) were dissolved in anhydrous PhMe (3 mL). 4Å mol sieves were added and the solution was heated to 130 °C with stirring for 12 h. After cooling to room temperature, a crude solution was purified by column chromatography (95:5 hexanes/ethyl acetate) with no additional workup. Analytical samples were prepared by dissolving the purified material in a minimum amount of DCM and layering with MeOH, producing orange needles upon crystallization (180 mg, 37%). **^{1}H NMR** (500 MHz, d_2-TCE, 100 °C) δ 8.01 (d, J = 8.6 Hz, 2H), 7.85 (br s, 2H), 7.58 (d, J = 7.4 Hz, 2H), 7.45 (br s, 2H), 7.32 (d, J = 8.1 Hz, 2H), 7.12 – 6.96 (m, 8H), 6.92 – 6.70 (m, 6H), 6.25 (br s, 2H), 2.10 (br s, 12H), 1.50 (br s, 18H). **^{13}C NMR** (125 MHz, d_2-TCE, 100 °C) δ 157.7, 147.1, 146.9, 145.5, 140.1, 138.3, 134.2, 131.0, 129.5, 128.3, 126.8, 126.4, 125.9, 124.3, 124.3, 123.8, 123.4, 123.4, 122.7, 121.8, 117.7, 43.8, 34.3, 31.4, 29.2. **HRMS** (DART) *m/z* calc for $C_{58}H_{57}N_2$ $(M+H)^+$: 781.4522, found 781.4532.

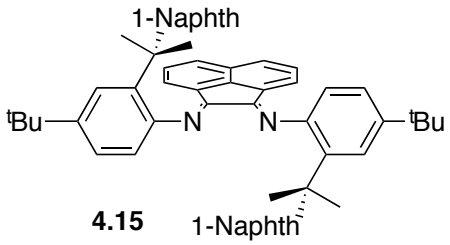

4.15

***rac*-(ArN=C(An)C=NAr)NiBr$_2$ (Ar = 4-^{t}Bu-2-(2-(naphthalen-1-yl)propan-2-yl)aniline; An = acenaphthene) (4.7). 4.15** (0.180 g, 0.231 mmol) and (DME)$NiBr_2$ (0.071 g, 0.231 mmol) were combined under N_2. CH_2Cl_2 (ca. 15 mL) was added to

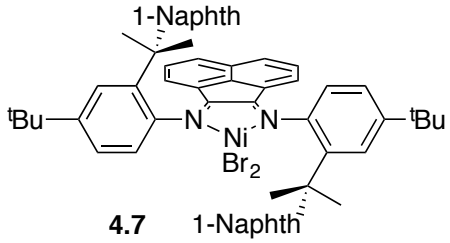

4.7

afford a dark red solution, which was allowed to stir at 23°C for 18 h. The reaction mixture was filtered through Celite under N_2 and volatiles were then removed *in vacuo*. The crude red solid was then dissolved in a minimum amount of DCM and layered with 4x volume of hexanes to afford red needles (0.116 g, 50 %).

General Procedure for the Polymerization of 1-Butene

A 60 mL Fisher Porter tube was charged with a stir bar and dMAO (0.060 g, 1.0 mmol) under N_2. 1-Butene (3.0 g ± 0.2 g, 0.05 mol) was condensed into the vessel at -78 °C. The reaction vessel was then transferred to a cooling bath at −40 °C and the solution was allowed to equilibrate at this temperature for 15 min. The appropriate pre-catalyst (10 μmol) was dissolved in 2 mL of DCM, drawn into a gas-tight syringe and then injected to initiate the polymerization. The reaction was stirred at −40 °C for 24 h before quenching with ~2 mL MeOH. The polymer was precipitated with copious amounts of acidic methanol (5% HCl/MeOH), followed by stirring of the suspension until the color faded, giving a white suspension. The polymer was filtered, washed with methanol, and dried to constant weight *in vacuo.*

^{13}C NMR Signal Assignments

Signals were assigned based on DEPT-135 and previous assignments performed in the literature.[20] Chemical shifts were normalized to the residual nondeuterated tetrachloroethane signal at 73.78 ppm. The naming convention developed by Usami and Takayami is listed in the table below.[21] Common structural motifs found in these polymers are also drawn below with their respective peak assignments for clarity.

Table 4.4. ^{13}C NMR signal assignments for 4,2-poly(1-butene) produced by nickel catalysts in this study.

Signal Label	Chemical Shift (ppm)	Assignment (xBn)	Reference
A	19.26–19.76	$1B_1$	21a
B	32.71–33.49	brB_1	21a
C	33.78–34.36	$\alpha\beta B_1$	21a
D	36.48–37.54	αB_1	21b
E	26.25–27.30	βB_1	21c
F	25.65	γB_1	21c
G	29.25	$\delta B_{1\text{-}n}$	21b, 21c
H	10.22–10.68	$1B_2$	21b
I	26.05	$2B_2$	21b
J	36.97	brB_2	This Work
K	41.70	$\alpha\alpha B_1B_2$	21c
L	30.68	brB_1	21d
M	19.96	$1B_1$	21d
N	39.01	brB_2	21c

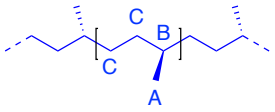

4,2-unit
(1,2-insertion, full walk)

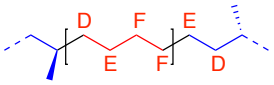

4,1-unit
(2,1-insertion, full walk)

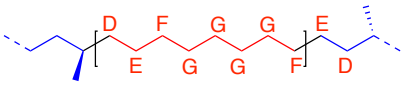

consecutive 4,1-units
(2,1-insertion, full walk)

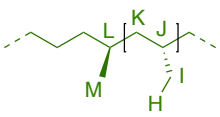

1,2-unit
(1,2-insertion, no walk, then 1,2-insertion)

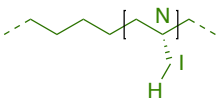

1,2-unit
(1,2-insertion, no walk, then 2,1-insertion)

Derivation of Values for Enchainment Pathways

Signals A, B, and C all arise from the main 4,2-poly(1-butene) structure which comes from ω,2-enchainment. Signals L and M are included as part of ω,2-enchainment because they are part of a 4,2-unit. If ω,1-enchainment occurs after ω,2-enchainment, signals D, E, and F are installed. However, this enchainment causes signals C from the 4,2-unit to change into D and E. When ω,2-enchainment occurs after ω,1-enchainment, additional D and E signals are observed which are associated with the 4,1-unit. This means that half of the signals from D and E are associated with a 4,2-unit and the other half with a 4,1-unit. Thus. we split the integrations for these signals between ω,2 and ω,1-enchainment. Successive ω,1-enchainments lead to signal G in the 4,1-unit. Signals H, I, J, K and N all arise solely from 1,2-enchainment. There is evidence of a small portion of isolated ethyl branches in these materials which give signals H, I, N, and D. We chose not to correct for D in this situation since the effect of the correction is very small. In some cases, there are signs of longer chain branches that arise from multiple insertion pathways. These are small and not included in the main calculations.

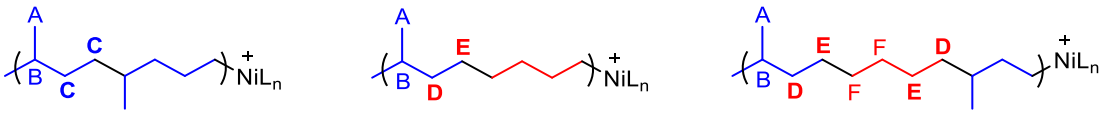

$$(4,2) = \frac{[A+B+C+0.5(D+E)+L+M]}{\Sigma(A\text{-}N)}$$

$$(4,1) = \frac{[0.5(D+E)+F+G]}{\Sigma(A\text{-}N)} \qquad (1,2) = \frac{[H+I+J+K+N]}{\Sigma(A\text{-}N)}$$

Figure 4.4. Equations used to calculate enchainment pathways.

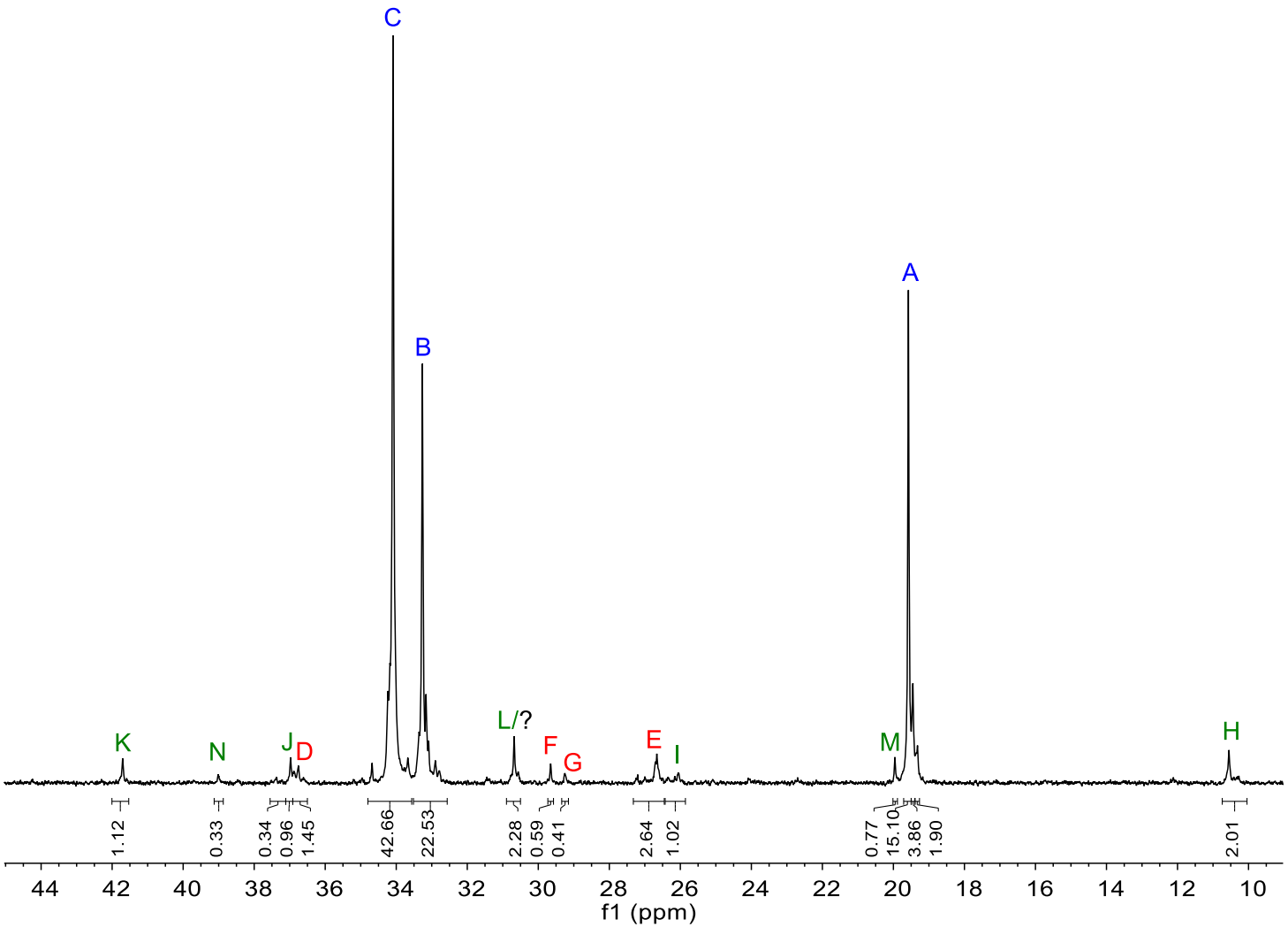

Figure 4.5. Representative ^{13}C NMR spectrum of 4,2-poly(1-butene) produced by complex **4.4** (Table 4.1, entry 4).

Expanded Tables for Effect of Reaction Conditions on the Polymerization of 1-Butene using 4.5.

Table 4.5. Effect of Reaction Conditions on the Polymerization of 1-Butene using complex **4.5**.[a]

entry	temp (°C)	conc (M)	yield (mg)	M_n[b] (kDa)	$Đ$[b] (M_w/M_n)	T_m[c] (°C)	4,1[d]	4,2[d]	1,2[d]	[*mm*][d]
1	−10	7.8	262	10.8	1.95	–	n.d.[g]	n.d.[g]	n.d.[g]	n.d.[g]
2	−30	7.8	420	23.7	1.80	66	0.17	0.79	0.04	0.53
3	−40	7.8	234	14.7	1.57	85	0.03	0.93	0.03	0.80
4	−50	7.8	173	10.6	1.81	85	0.02	0.96	0.02	0.80
5	−40	6.0[e]	163	12.4	1.46	80	0.05	0.91	0.04	0.70
6	−40	9.1[f]	464	16.3	2.17	73	0.14	0.83	0.03	0.59

[a]Polymerization conditions: 3.0 ± 0.2 g 1-butene (53.5 mmol), 10 μmol of complex **4.5** in 2 mL CH_2Cl_2, 100 equiv. MAO; t_{rxn} = 24 h, T_{rxn} = −40 °C. [b]Determined by gel permeation chromatography at 150 °C in 1,2,4-trichlorobenzene versus polyethylene standards. [c]Determined by differential scanning calorimetry, endotherm from 2nd heating cycle. [d]Determined by ^{13}C NMR spectroscopy. No detectable T_m. [e]1.5 ± 0.2 g 1-butene (26.8 mmol). [f]6.0 ± 0.2 g 1-butene (107.0 mmol). [g]Not determined.

Table 4.6. Effect of Solvent on the Polymerization of 1-Butene using Complex **4.5**.[a]

entry	solvent	yield (mg)	M_n[c] (kDa)	$Đ$[c] (M_w/M_n)	T_m[d] (°C)	4,1[e]	4,2[e]	1,2[e]	[*mm*][e]
1	CH_2Cl_2	234	14.7	1.57	85	0.03	0.93	0.03[g]	0.80
2	PhMe	198	12.2	1.96	79	0.02	0.95	0.03	0.79
3	PhCl	338	21.1	1.85	76	0.07	0.90	0.03	0.76
4	$C_6H_4F_2$[f]	223	10.9	2.05	82	0.06	0.86	0.06[g]	0.72

[a]Polymerization conditions: 3.0 ± 0.2 g 1-butene (53.5 mmol), 10 μmol of complex **4.5** in 2 mL solvent, 1.0 mmol MAO; t_{rxn} = 24 h, T_{rxn} = −40 °C. [b]Turnover frequency, TOF = (mol monomer consumed)(mol catalyst)$^{-1}$(time)$^{-1}$. [c]Determined by gel permeation chromatography at 150 °C in 1,2,4-trichlorobenzene versus polyethylene standards. [d]Determined by differential scanning calorimetry, endotherm from 2nd heating cycle. [e]Determined by ^{13}C NMR spectroscopy. [f]1,2-difluorobenzene. [g]Additional signals are present that correspond to long chain branching.

Representative Differential Scanning Calorimetry (DSC) Traces of 4,2-poly(1-butene) Samples.

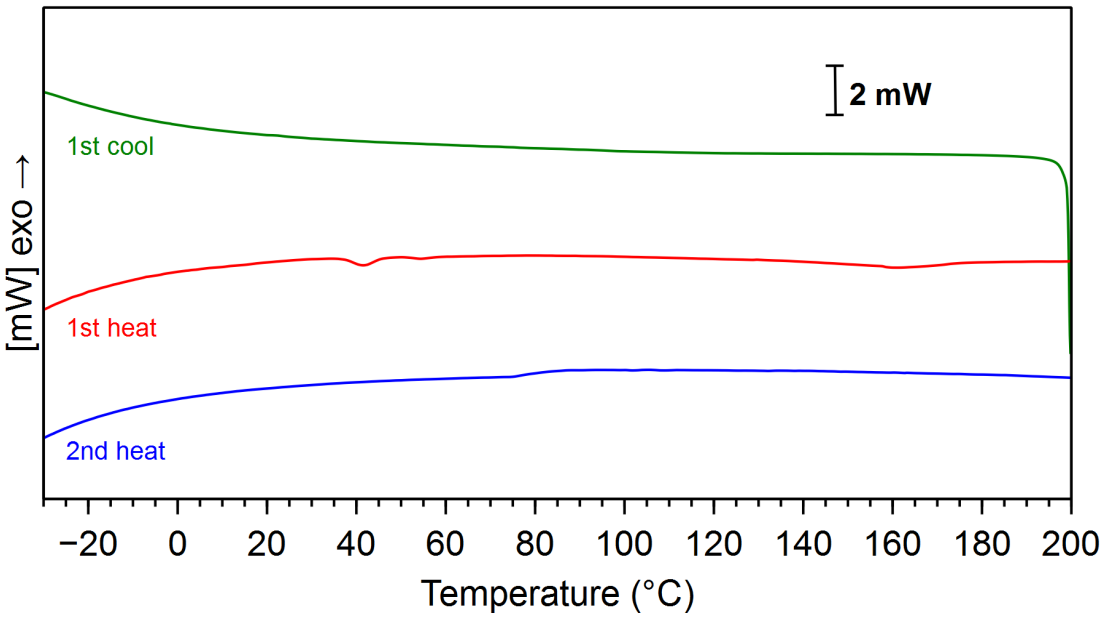

Figure 4.6. 4,2-poly(1-butene) produced by **4.1** (Table 4.1, entry 1).

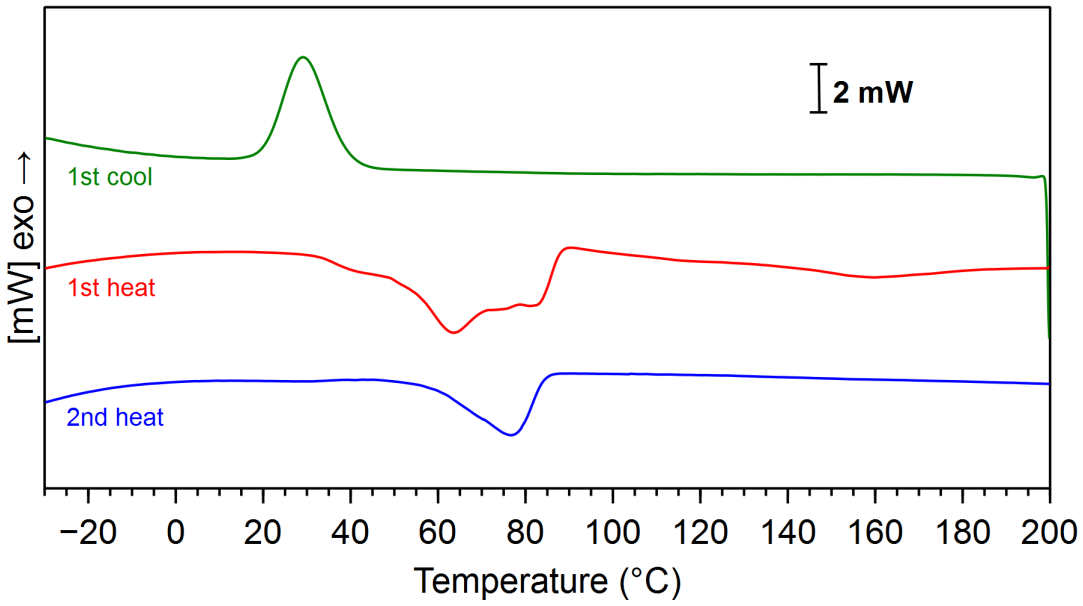

Figure 4.7. 4,2-poly(1-butene) produced by **4.2** (Table 4.1, entry 2).

Crystallographic Data for Complex 4.5

Table 4.7. Crystal data and structure refinement for Rdv1.

Identification code	rdv1_abs2	
Empirical formula	C50 H52 Br2 N2 Ni	
Formula weight	899.46	
Temperature	100.01(10) K	
Wavelength	1.54184 Å	
Crystal system	Monoclinic	
Space group	P 1 21/c 1	
Unit cell dimensions	a = 9.04574(5) Å	α= 90°.
	b = 25.29692(13) Å	β= 103.1909(5)°.
	c = 19.03833(11) Å	γ = 90°.
Volume	4241.58(4) $Å^3$	
Z	4	
Density (calculated)	1.409 Mg/m^3	
Absorption coefficient	3.134 mm^{-1}	
F(000)	1856	
Crystal size	0.198 x 0.08 x 0.019 mm^3	
Theta range for data collection	2.956 to 70.075°.	
Index ranges	-11<=h<=8, -26<=k<=30, -22<=l<=23	
Reflections collected	36578	
Independent reflections	8040 [R(int) = 0.0259]	
Completeness to theta = 67.684°	100.0 %	

Absorption correction	Gaussian
Max. and min. transmission	1.000 and 0.628
Refinement method	Full-matrix least-squares on F^2
Data / restraints / parameters	8040 / 0 / 506
Goodness-of-fit on F^2	1.036
Final R indices [I>2sigma(I)]	R1 = 0.0254, wR2 = 0.0661
R indices (all data)	R1 = 0.0274, wR2 = 0.0671
Extinction coefficient	n/a
Largest diff. peak and hole	0.673 and -0.416 e.$Å^{-3}$

Table 4.8. Atomic coordinates (x 10^4) and equivalent isotropic displacement parameters (Å^{2}x 10^3) for **4.5**. U(eq) is defined as one third of the trace of the orthogonalized U^{ij} tensor.

	x	y	z	U(eq)
Br(1)	4210(1)	2760(1)	7917(1)	24(1)
Br(2)	7352(1)	3023(1)	6740(1)	23(1)
Ni	4806(1)	2930(1)	6803(1)	18(1)
N(1)	4012(1)	2490(1)	5904(1)	14(1)
N(2)	2941(1)	3385(1)	6386(1)	14(1)
C(1)	2067(2)	1746(1)	6909(1)	22(1)
C(2)	585(2)	1925(1)	6848(1)	27(1)
C(3)	-476(2)	1877(1)	6203(1)	26(1)
C(4)	-58(2)	1639(1)	5622(1)	26(1)
C(5)	1415(2)	1460(1)	5683(1)	22(1)
C(6)	2509(2)	1519(1)	6322(1)	18(1)
C(7)	4137(2)	1330(1)	6358(1)	18(1)
C(8)	4721(2)	1548(1)	5716(1)	16(1)
C(9)	5310(2)	1212(1)	5267(1)	18(1)
C(10)	5984(2)	1385(1)	4715(1)	16(1)
C(11)	6134(2)	1926(1)	4635(1)	16(1)
C(12)	5513(2)	2275(1)	5053(1)	16(1)

C(13)	4761(2)	2092(1)	5564(1)	14(1)
C(14)	5274(2)	1502(1)	7050(1)	23(1)
C(15)	4098(2)	721(1)	6358(1)	26(1)
C(16)	6451(2)	978(1)	4208(1)	20(1)
C(17)	4992(2)	736(1)	3742(1)	26(1)
C(18)	7419(2)	537(1)	4643(1)	24(1)
C(19)	7356(2)	1227(1)	3704(1)	24(1)
C(20)	2776(2)	2691(1)	5527(1)	14(1)
C(21)	1765(2)	2572(1)	4826(1)	16(1)
C(22)	1805(2)	2231(1)	4267(1)	19(1)
C(23)	544(2)	2223(1)	3670(1)	24(1)
C(24)	-705(2)	2539(1)	3628(1)	24(1)
C(25)	-773(2)	2898(1)	4191(1)	21(1)
C(26)	-1973(2)	3254(1)	4221(1)	25(1)
C(27)	-1870(2)	3584(1)	4806(1)	26(1)
C(28)	-588(2)	3591(1)	5394(1)	21(1)
C(29)	592(2)	3251(1)	5376(1)	17(1)
C(30)	484(2)	2906(1)	4778(1)	17(1)
C(31)	2095(2)	3152(1)	5842(1)	14(1)
C(32)	2327(2)	3823(1)	6715(1)	16(1)
C(33)	1291(2)	3693(1)	7126(1)	19(1)
C(34)	680(2)	4079(1)	7489(1)	21(1)

C(35)	1106(2)	4606(1)	7455(1)	20(1)
C(36)	2112(2)	4727(1)	7023(1)	20(1)
C(37)	2745(2)	4350(1)	6638(1)	17(1)
C(38)	3863(2)	4517(1)	6176(1)	22(1)
C(39)	3339(2)	4292(1)	5409(1)	22(1)
C(40)	1959(2)	4458(1)	4979(1)	31(1)
C(41)	1447(2)	4274(1)	4280(1)	39(1)
C(42)	2311(3)	3914(1)	3995(1)	38(1)
C(43)	3676(2)	3742(1)	4414(1)	32(1)
C(44)	4194(2)	3930(1)	5115(1)	25(1)
C(45)	453(2)	5029(1)	7876(1)	26(1)
C(46)	1143(2)	5576(1)	7822(2)	44(1)
C(47)	755(2)	4867(1)	8675(1)	40(1)
C(48)	-1262(2)	5066(1)	7575(1)	29(1)
C(49)	5454(2)	4334(1)	6562(1)	28(1)
C(50)	3957(2)	5124(1)	6104(1)	35(1)

Table 4.9. Bond lengths [Å] and angles [°] for **4.5**.

Br(1)-Ni	2.3446(3)
Br(2)-Ni	2.3449(3)
Ni-N(1)	2.0310(13)
Ni-N(2)	2.0473(13)
N(1)-C(13)	1.4460(19)
N(1)-C(20)	1.288(2)
N(2)-C(31)	1.282(2)
N(2)-C(32)	1.4442(19)
C(1)-H(1)	0.9300
C(1)-C(2)	1.395(2)
C(1)-C(6)	1.393(2)
C(2)-H(2)	0.9300
C(2)-C(3)	1.381(3)
C(3)-H(3)	0.9300
C(3)-C(4)	1.385(3)
C(4)-H(4)	0.9300
C(4)-C(5)	1.387(2)
C(5)-H(5)	0.9300
C(5)-C(6)	1.390(2)
C(6)-C(7)	1.535(2)
C(7)-C(8)	1.540(2)
C(7)-C(14)	1.538(2)
C(7)-C(15)	1.540(2)
C(8)-C(9)	1.396(2)
C(8)-C(13)	1.408(2)
C(9)-H(9)	0.9300
C(9)-C(10)	1.400(2)
C(10)-C(11)	1.386(2)
C(10)-C(16)	1.536(2)
C(11)-H(11)	0.9300
C(11)-C(12)	1.391(2)
C(12)-H(12)	0.9300
C(12)-C(13)	1.387(2)
C(14)-H(14A)	0.9600
C(14)-H(14B)	0.9600
C(14)-H(14C)	0.9600
C(15)-H(15A)	0.9600
C(15)-H(15B)	0.9600
C(15)-H(15C)	0.9600
C(16)-C(17)	1.539(2)
C(16)-C(18)	1.538(2)
C(16)-C(19)	1.533(2)

C(17)-H(17A)	0.9600	C(26)-C(27)	1.380(3)
C(17)-H(17B)	0.9600	C(27)-H(27)	0.9300
C(17)-H(17C)	0.9600	C(27)-C(28)	1.415(2)
C(18)-H(18A)	0.9600	C(28)-H(28)	0.9300
C(18)-H(18B)	0.9600	C(28)-C(29)	1.378(2)
C(18)-H(18C)	0.9600	C(29)-C(30)	1.419(2)
C(19)-H(19A)	0.9600	C(29)-C(31)	1.466(2)
C(19)-H(19B)	0.9600	C(32)-C(33)	1.392(2)
C(19)-H(19C)	0.9600	C(32)-C(37)	1.403(2)
C(20)-C(21)	1.467(2)	C(33)-H(33)	0.9300
C(20)-C(31)	1.506(2)	C(33)-C(34)	1.383(2)
C(21)-C(22)	1.377(2)	C(34)-H(34)	0.9300
C(21)-C(30)	1.421(2)	C(34)-C(35)	1.393(2)
C(22)-H(22)	0.9300	C(35)-C(36)	1.393(2)
C(22)-C(23)	1.414(2)	C(35)-C(45)	1.533(2)
C(23)-H(23)	0.9300	C(36)-H(36)	0.9300
C(23)-C(24)	1.371(3)	C(36)-C(37)	1.401(2)
C(24)-H(24)	0.9300	C(37)-C(38)	1.543(2)
C(24)-C(25)	1.417(2)	C(38)-C(39)	1.537(2)
C(25)-C(26)	1.420(2)	C(38)-C(49)	1.531(2)
C(25)-C(30)	1.402(2)	C(38)-C(50)	1.545(2)
C(26)-H(26)	0.9300	C(39)-C(40)	1.391(3)

C(39)-C(44)	1.397(2)	C(49)-H(49A)	0.9600
C(40)-H(40)	0.9300	C(49)-H(49B)	0.9600
C(40)-C(41)	1.385(3)	C(49)-H(49C)	0.9600
C(41)-H(41)	0.9300	C(50)-H(50A)	0.9600
C(41)-C(42)	1.389(3)	C(50)-H(50B)	0.9600
C(42)-H(42)	0.9300	C(50)-H(50C)	0.9600
C(42)-C(43)	1.378(3)	Br(1)-Ni-Br(2)	119.735(13)
C(43)-H(43)	0.9300	N(1)-Ni-Br(1)	123.48(4)
C(43)-C(44)	1.394(3)	N(1)-Ni-Br(2)	100.04(4)
C(44)-H(44)	0.9300	N(1)-Ni-N(2)	83.07(5)
C(45)-C(46)	1.530(3)	N(2)-Ni-Br(1)	96.59(4)
C(45)-C(47)	1.540(3)	N(2)-Ni-Br(2)	131.01(4)
C(45)-C(48)	1.529(2)	C(13)-N(1)-Ni	130.34(10)
C(46)-H(46A)	0.9600	C(20)-N(1)-Ni	110.41(10)
C(46)-H(46B)	0.9600	C(20)-N(1)-C(13)	117.45(13)
C(46)-H(46C)	0.9600	C(31)-N(2)-Ni	109.97(10)
C(47)-H(47A)	0.9600	C(31)-N(2)-C(32)	119.06(13)
C(47)-H(47B)	0.9600	C(32)-N(2)-Ni	128.84(10)
C(47)-H(47C)	0.9600	C(2)-C(1)-H(1)	119.6
C(48)-H(48A)	0.9600	C(6)-C(1)-H(1)	119.6
C(48)-H(48B)	0.9600	C(6)-C(1)-C(2)	120.87(16)
C(48)-H(48C)	0.9600	C(1)-C(2)-H(2)	119.8

C(3)-C(2)-C(1)	120.34(16)	C(13)-C(8)-C(7)	122.91(13)
C(3)-C(2)-H(2)	119.8	C(8)-C(9)-H(9)	117.9
C(2)-C(3)-H(3)	120.4	C(8)-C(9)-C(10)	124.19(14)
C(2)-C(3)-C(4)	119.21(16)	C(10)-C(9)-H(9)	117.9
C(4)-C(3)-H(3)	120.4	C(9)-C(10)-C(16)	119.36(14)
C(3)-C(4)-H(4)	119.8	C(11)-C(10)-C(9)	117.45(14)
C(3)-C(4)-C(5)	120.39(17)	C(11)-C(10)-C(16)	123.12(14)
C(5)-C(4)-H(4)	119.8	C(10)-C(11)-H(11)	119.9
C(4)-C(5)-H(5)	119.4	C(10)-C(11)-C(12)	120.17(14)
C(4)-C(5)-C(6)	121.16(16)	C(12)-C(11)-H(11)	119.9
C(6)-C(5)-H(5)	119.4	C(11)-C(12)-H(12)	119.5
C(1)-C(6)-C(7)	122.75(15)	C(13)-C(12)-C(11)	121.01(14)
C(5)-C(6)-C(1)	117.96(15)	C(13)-C(12)-H(12)	119.5
C(5)-C(6)-C(7)	119.29(14)	C(8)-C(13)-N(1)	123.45(13)
C(6)-C(7)-C(8)	110.61(13)	C(12)-C(13)-N(1)	115.84(13)
C(6)-C(7)-C(14)	113.39(13)	C(12)-C(13)-C(8)	120.69(14)
C(6)-C(7)-C(15)	106.85(13)	C(7)-C(14)-H(14A)	109.5
C(14)-C(7)-C(8)	107.19(13)	C(7)-C(14)-H(14B)	109.5
C(14)-C(7)-C(15)	107.03(14)	C(7)-C(14)-H(14C)	109.5
C(15)-C(7)-C(8)	111.77(13)	H(14A)-C(14)-H(14B)	109.5
C(9)-C(8)-C(7)	121.05(13)	H(14A)-C(14)-H(14C)	109.5
C(9)-C(8)-C(13)	115.98(14)	H(14B)-C(14)-H(14C)	109.5

C(7)-C(15)-H(15A)	109.5	H(18A)-C(18)-H(18C)	109.5
C(7)-C(15)-H(15B)	109.5	H(18B)-C(18)-H(18C)	109.5
C(7)-C(15)-H(15C)	109.5	C(16)-C(19)-H(19A)	109.5
H(15A)-C(15)-H(15B)	109.5	C(16)-C(19)-H(19B)	109.5
H(15A)-C(15)-H(15C)	109.5	C(16)-C(19)-H(19C)	109.5
H(15B)-C(15)-H(15C)	109.5	H(19A)-C(19)-H(19B)	109.5
C(10)-C(16)-C(17)	107.91(13)	H(19A)-C(19)-H(19C)	109.5
C(10)-C(16)-C(18)	110.71(13)	H(19B)-C(19)-H(19C)	109.5
C(18)-C(16)-C(17)	109.27(14)	N(1)-C(20)-C(21)	135.07(14)
C(19)-C(16)-C(10)	112.30(13)	N(1)-C(20)-C(31)	117.73(13)
C(19)-C(16)-C(17)	108.18(14)	C(21)-C(20)-C(31)	107.18(12)
C(19)-C(16)-C(18)	108.40(13)	C(22)-C(21)-C(20)	135.36(15)
C(16)-C(17)-H(17A)	109.5	C(22)-C(21)-C(30)	119.26(15)
C(16)-C(17)-H(17B)	109.5	C(30)-C(21)-C(20)	105.38(13)
C(16)-C(17)-H(17C)	109.5	C(21)-C(22)-H(22)	120.9
H(17A)-C(17)-H(17B)	109.5	C(21)-C(22)-C(23)	118.12(15)
H(17A)-C(17)-H(17C)	109.5	C(23)-C(22)-H(22)	120.9
H(17B)-C(17)-H(17C)	109.5	C(22)-C(23)-H(23)	118.6
C(16)-C(18)-H(18A)	109.5	C(24)-C(23)-C(22)	122.77(15)
C(16)-C(18)-H(18B)	109.5	C(24)-C(23)-H(23)	118.6
C(16)-C(18)-H(18C)	109.5	C(23)-C(24)-H(24)	119.8
H(18A)-C(18)-H(18B)	109.5	C(23)-C(24)-C(25)	120.50(16)

C(25)-C(24)-H(24)	119.8	C(33)-C(32)-N(2)	115.94(13)
C(24)-C(25)-C(26)	127.02(16)	C(33)-C(32)-C(37)	121.03(14)
C(30)-C(25)-C(24)	116.42(15)	C(37)-C(32)-N(2)	123.02(13)
C(30)-C(25)-C(26)	116.56(15)	C(32)-C(33)-H(33)	119.6
C(25)-C(26)-H(26)	119.9	C(34)-C(33)-C(32)	120.71(15)
C(27)-C(26)-C(25)	120.30(16)	C(34)-C(33)-H(33)	119.6
C(27)-C(26)-H(26)	119.9	C(33)-C(34)-H(34)	119.8
C(26)-C(27)-H(27)	118.7	C(33)-C(34)-C(35)	120.48(15)
C(26)-C(27)-C(28)	122.58(16)	C(35)-C(34)-H(34)	119.8
C(28)-C(27)-H(27)	118.7	C(34)-C(35)-C(45)	119.97(15)
C(27)-C(28)-H(28)	120.9	C(36)-C(35)-C(34)	117.51(14)
C(29)-C(28)-C(27)	118.17(16)	C(36)-C(35)-C(45)	122.52(15)
C(29)-C(28)-H(28)	120.9	C(35)-C(36)-H(36)	118.0
C(28)-C(29)-C(30)	119.48(15)	C(35)-C(36)-C(37)	124.06(15)
C(28)-C(29)-C(31)	135.14(15)	C(37)-C(36)-H(36)	118.0
C(30)-C(29)-C(31)	105.34(13)	C(32)-C(37)-C(38)	123.09(13)
C(25)-C(30)-C(21)	122.92(15)	C(36)-C(37)-C(32)	116.11(14)
C(25)-C(30)-C(29)	122.91(15)	C(36)-C(37)-C(38)	120.78(14)
C(29)-C(30)-C(21)	114.17(14)	C(37)-C(38)-C(50)	112.24(13)
N(2)-C(31)-C(20)	117.10(13)	C(39)-C(38)-C(37)	109.89(13)
N(2)-C(31)-C(29)	135.23(14)	C(39)-C(38)-C(50)	107.09(15)
C(29)-C(31)-C(20)	107.36(13)	C(49)-C(38)-C(37)	108.09(14)

C(49)-C(38)-C(39)	113.36(14)	C(46)-C(45)-C(47)	108.89(17)
C(49)-C(38)-C(50)	106.17(15)	C(48)-C(45)-C(35)	109.04(14)
C(40)-C(39)-C(38)	119.27(15)	C(48)-C(45)-C(46)	108.31(16)
C(40)-C(39)-C(44)	117.76(17)	C(48)-C(45)-C(47)	108.79(15)
C(44)-C(39)-C(38)	122.96(16)	C(45)-C(46)-H(46A)	109.5
C(39)-C(40)-H(40)	119.2	C(45)-C(46)-H(46B)	109.5
C(41)-C(40)-C(39)	121.55(18)	C(45)-C(46)-H(46C)	109.5
C(41)-C(40)-H(40)	119.2	H(46A)-C(46)-H(46B)	109.5
C(40)-C(41)-H(41)	120.0	H(46A)-C(46)-H(46C)	109.5
C(40)-C(41)-C(42)	120.0(2)	H(46B)-C(46)-H(46C)	109.5
C(42)-C(41)-H(41)	120.0	C(45)-C(47)-H(47A)	109.5
C(41)-C(42)-H(42)	120.3	C(45)-C(47)-H(47B)	109.5
C(43)-C(42)-C(41)	119.43(19)	C(45)-C(47)-H(47C)	109.5
C(43)-C(42)-H(42)	120.3	H(47A)-C(47)-H(47B)	109.5
C(42)-C(43)-H(43)	119.8	H(47A)-C(47)-H(47C)	109.5
C(42)-C(43)-C(44)	120.48(18)	H(47B)-C(47)-H(47C)	109.5
C(44)-C(43)-H(43)	119.8	C(45)-C(48)-H(48A)	109.5
C(39)-C(44)-H(44)	119.6	C(45)-C(48)-H(48B)	109.5
C(43)-C(44)-C(39)	120.78(18)	C(45)-C(48)-H(48C)	109.5
C(43)-C(44)-H(44)	119.6	H(48A)-C(48)-H(48B)	109.5
C(35)-C(45)-C(47)	109.15(15)	H(48A)-C(48)-H(48C)	109.5
C(46)-C(45)-C(35)	112.58(15)	H(48B)-C(48)-H(48C)	109.5

C(38)-C(49)-H(49A)	109.5	C(38)-C(50)-H(50A)	109.5
C(38)-C(49)-H(49B)	109.5	C(38)-C(50)-H(50B)	109.5
C(38)-C(49)-H(49C)	109.5	C(38)-C(50)-H(50C)	109.5
H(49A)-C(49)-H(49B)	109.5	H(50A)-C(50)-H(50B)	109.5
H(49A)-C(49)-H(49C)	109.5	H(50A)-C(50)-H(50C)	109.5
H(49B)-C(49)-H(49C)	109.5	H(50B)-C(50)-H(50C)	109.5

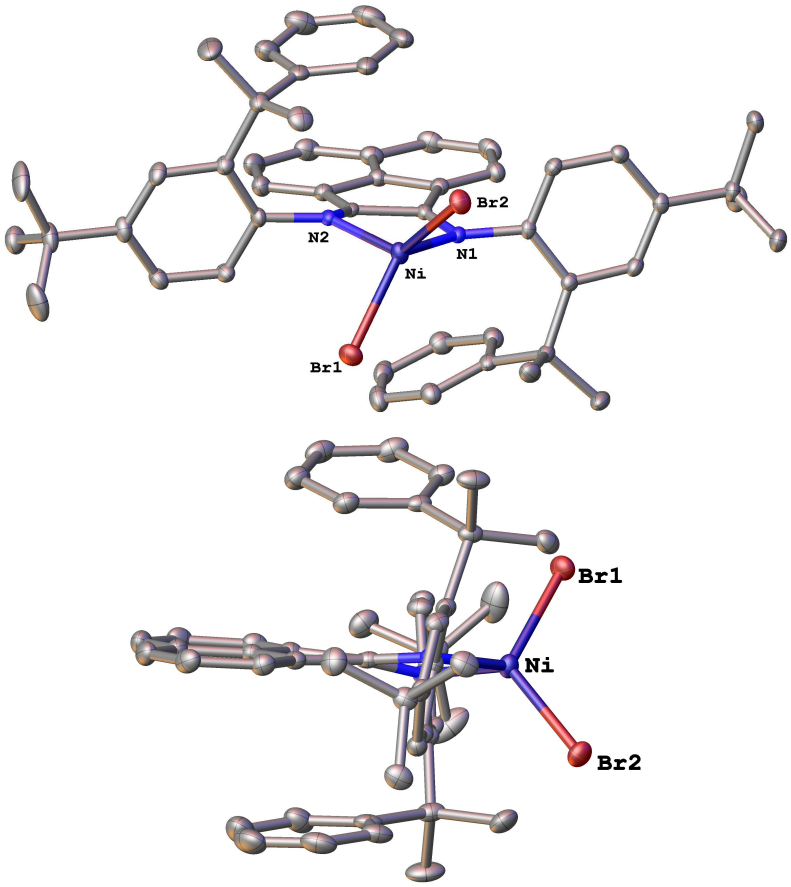

Figure 4.8. X-ray crystal structure of **4.5.**

References and Notes

(1) Takai, T.; Mochizuki, D.; Umeno, M. Method of Producing Propylene Containing Biomass-Origin Carbon. Patent WO2007/55361, 2008.

(2) (a) Dürre, P. *Biotechnol. J.* **2007**, 2, 1525–1534. (b) Kohse-Höinghaus, K.; Oßwald, P.; Cool, T. A.; Kasper, T.; Hansen, N.; Qi, F.; Westbrook, C. K.; Westmoreland, P. R. *Angew. Chem., Int. Ed.* **2010**, 49, 3572–3597.

(3) Komon, Z. J. A.; Bu, X.; Bazan, G. C. *J. Am. Chem. Soc.* **2000**, 122, 1830–1831.

(4) Freeman, A.; Mantell, S. C.; Davidson, J. H., *Solar Energy* **2005**, 79, 624–637.

(5) (a) De Rosa, C.; Auriemma, F.; Resconi, L. *Angew. Chem. Int. Ed*. **2009**, 48, 9871–9874. (b) De Rosa, C.; Auriemma, F.; Ruiz de Ballesteros, O.; Esposito, F.; Laguzza, D.; Di Girolamo, R.; Resconi, L. *Macromolecules* **2009**, 42, 8286–8297.

(6) (a) Johnson, L. K.; Killian, C. M.; Brookhart, M. *J. Am. Chem. Soc.* **1995**, 117, 6414–6415. (c) Gates, D. P.; Svejda, S. A.; Oñate, E.; Killian, C. M.; Johnson, L. K.; White, P. S.; Brookhart, M. *Macromolecules* **2000**, 33, 2320–2334. (d) Ittel, S. D.; Johnson, L. K. *Chem. Rev.* **2000**, 100, 1169–1203. (e) Subramanyam, U.; Rajamohanan, P. R.; Sivaram, S. *Polymer* **2004**, 45, 4063–4076. (f) Bomfim, J. A. S.; Dias, M. L.; Filgueiras, C. A. L.; Peruch, F.; Deffieux, A. *Catal. Today* **2008**, 133–135, 879–885. (g) Camacho, D. H.; Guan, Z. *Chem. Commun.* **2010**, 46, 7879–7893. (h) Liu, J.; Chen, D.; Wu, H.; Xiao, Z.; Gao, H.; Zhu, F.; Wu, Q.

Macromolecules **2014**, 47, 3325–3331. (i) Vaidya, T.; Klimovica, K.; LaPointe, A. M.; Keresztes, I.; Lobkovsky, E. B.; Daugulis, O.; Coates, G. W. *J. Am. Chem. Soc.* **2014**, *136*, 7213–7216. (j) Wang, F.; Tanaka, R.; Cai, Z.; Nakayama, Y.; Shiono, T. *Macromol. Rapid Commun.* **2016**, 37 (16), 1375–1381. (k) Dai, S.; Sui, X.; Chen, C. *Chem. Commun.* **2016**, 52, 9113–9116.

(7) (a) Tempel, D. J.; Johnson, L. K.; Huff, R. L.; White, P. S.; Brookhart, M. *J. Am. Chem. Soc.* **2000**, *122*, 6686–6700. (b) Leatherman, M. D.; Svejda, S. A.; Johnson, L. K.; Brookhart, M. *J. Am. Chem. Soc.* **2003**, 125, 3068–3081.

(8) (a) Wang, J.; Ye, Z.; Joly, H. *Macromolecules* **2007**, 40, 6150–6163. (b) Sun, G.; Guan, Z. *Macromolecules* **2010**, 43, 4829–4832. (c) Xu, Y.; Xiang, P.; Ye, Z.; Wang, W.-J. *Macromolecules* **2010**, 43, 8026–8038.

(9) McLain, S. J.; Feldman, J.; McCord, E. F.; Gardner, K. H.; Teasley, M. F.; Coughlin, E. B.; Sweetman, K. J.; Johnson, L. K.; Brookhart, M. *Macromolecules* **1998**, 31, 6705–6707.

(10) (a) Okada, T.; Park, S.; Takeuchi, D.; Osakada, K. *Angew. Chem., Int. Ed.* **2007**, 46, 6141–6143. (b) Okada, T.; Takeuchi, D.; Shishido, A.; Ikeda, T.; Osakada, K. *J. Am. Chem. Soc*. **2009**, 131, 10852–10853. (c) Okada, T.; Takeuchi, D.; Osakada, K. *Macromolecules* **2010**, 43, 7998–8006. (d) Park, S.; Okada, T.; Takeuchi, D.; Osakada, K., *Chem. Eur. J.* **2010**, 16, 8662–8678. (e) Takeuchi, D.; Osakada, K., *Polymer* **2016**, 82, 392–405.

(11) (a) Mei, T.-S.; Werner, E. W.; Burckle, A. J.; Sigman, M.S. *J. Am. Chem. Soc.*

2013, 135, 6830–6833. (b) Mei. T.-S.; Patel, H. H.; Sigman, M. S. *Nature* **2014**, 508, 340–344.

(12) Cherian, A. E.; Lobkovsky, E. B.; Coates, G. W. *Chem. Commun*. **2003**, 2566–2567.

(13) Rose, J. M.; Deplace, F.; A. Lynd, N.; Wang, Z.; Hotta, A.; Lobkovsky, E. B.; Kramer, E. J.; Coates, G. W. *Macromolecules* **2008**, 41, 9548–9555.

(14) Rose, J. M.; Cherian, A. E.; Coates, G. W. *J. Am. Chem. Soc.* **2006**, 128, 4186–4187.

(15) Cherian, A. E.; Rose, J. M.; Lobkovsky, E. B.; Coates, G. W. *J. Am. Chem. Soc.* **2005**, 127, 13770–13771.

(16) Detailed studies on ion paring in late transition metal complexes are limited, but ion pairing in early transition metal complexes are well documented. Please refer to: Macchioni, A. *Chem. Rev*. **2005**, 105, 2039–2074.

(17) (a) Starck, P.; Rajanen, K.; Löfgren, B. *Thermochim. Acta* **2003**, *395*, 169–181. (b) Isasi, J. R.; Haigh, J. A.; Graham, J. T.; Mandelkern, L.; Alamo, R. G. *Polymer* **2000**, 41*,* 8813–8823.

(18) Analogously, it has been shown that a small percentage (<5%) of branches (C_1 to C_4 in length) can be masked in the highly crystalline portion of high-density polyethylene. Cutler, D. J.; Hendra, P. J.; Cudby, M. E. A.; Willis, H. A. *Polymer* **1977**, 18, 1005–1008.

(19) Ruiz-Orta, C.; Fernandez-Blazquez, J. P.; Anderson-Wile, A. M.; Coates, G. W.; Alamo, R. G. *Macromolecules* **2011**, 44, 3436–3451.

(20) (a) Leatherman, M. D.; Brookhart, M. Macromolecules **2001**, 34, 2748–2750. (b) Endo, K.; Kondo, Y. *J. Polym. Sci. A Polym. Chem.* **2008**, 46, 2858–2846. (c) Azoulay, J. D.; Bazan, G. C.; Galland, G. B. *Macromolecules* **2010**, 43, 2794–2800. (d) McCord, E. F.; McLain, S. J.; Nelson, L. T. J.; Ittel, S. D.; Tempel, D.; Killian, C. M.; Johnson, L. K.; Brookhart, M. *Macromolecules* **2007**, 40, 410–420.

(21) Usami, T.; Takayama, S. *Macromolecules* **1984**, 17, 1756–1761.

APPENDIX

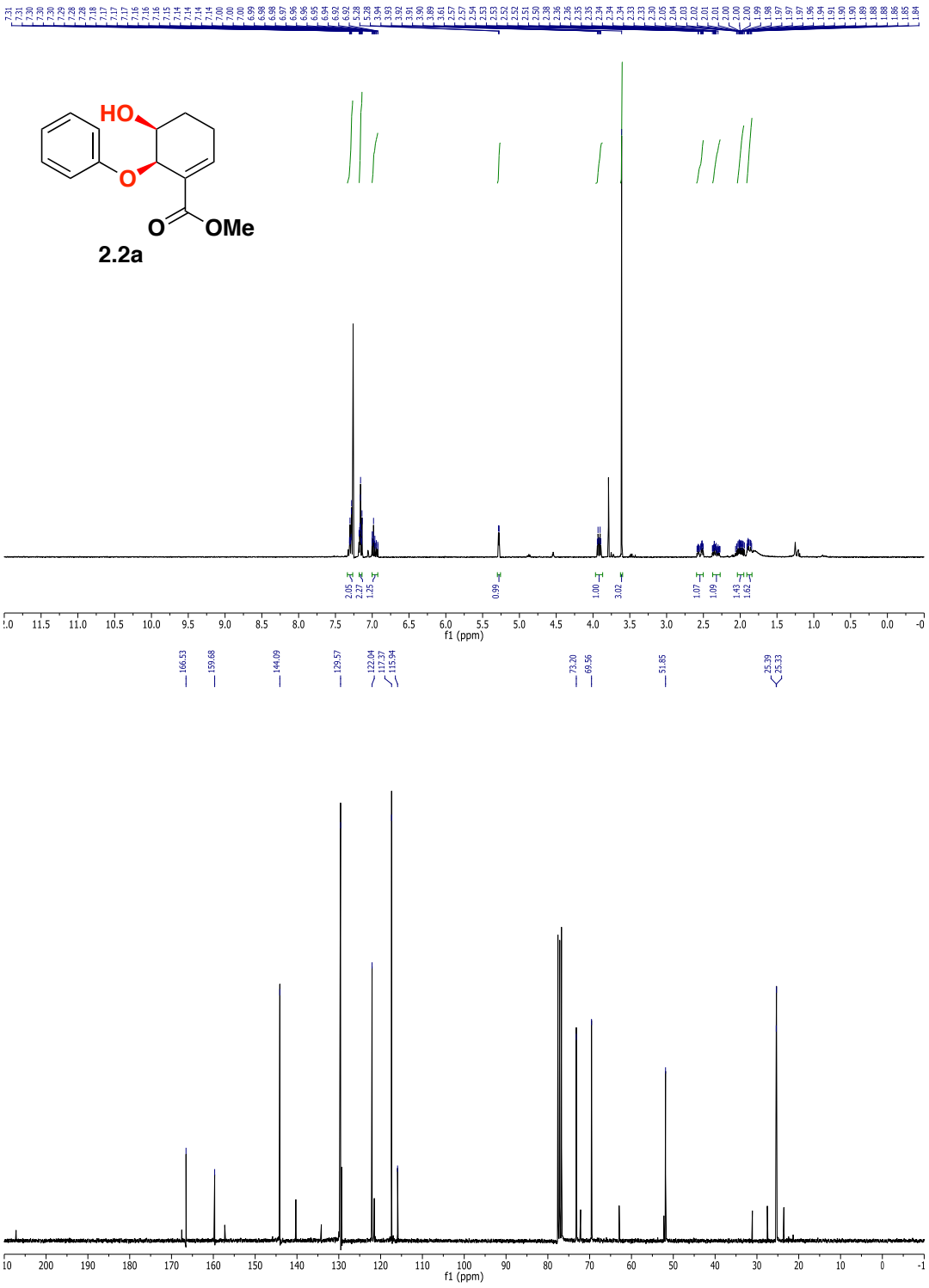
HO
O
O
OMe
2.2a
f1 (ppm)
f1 (ppm)

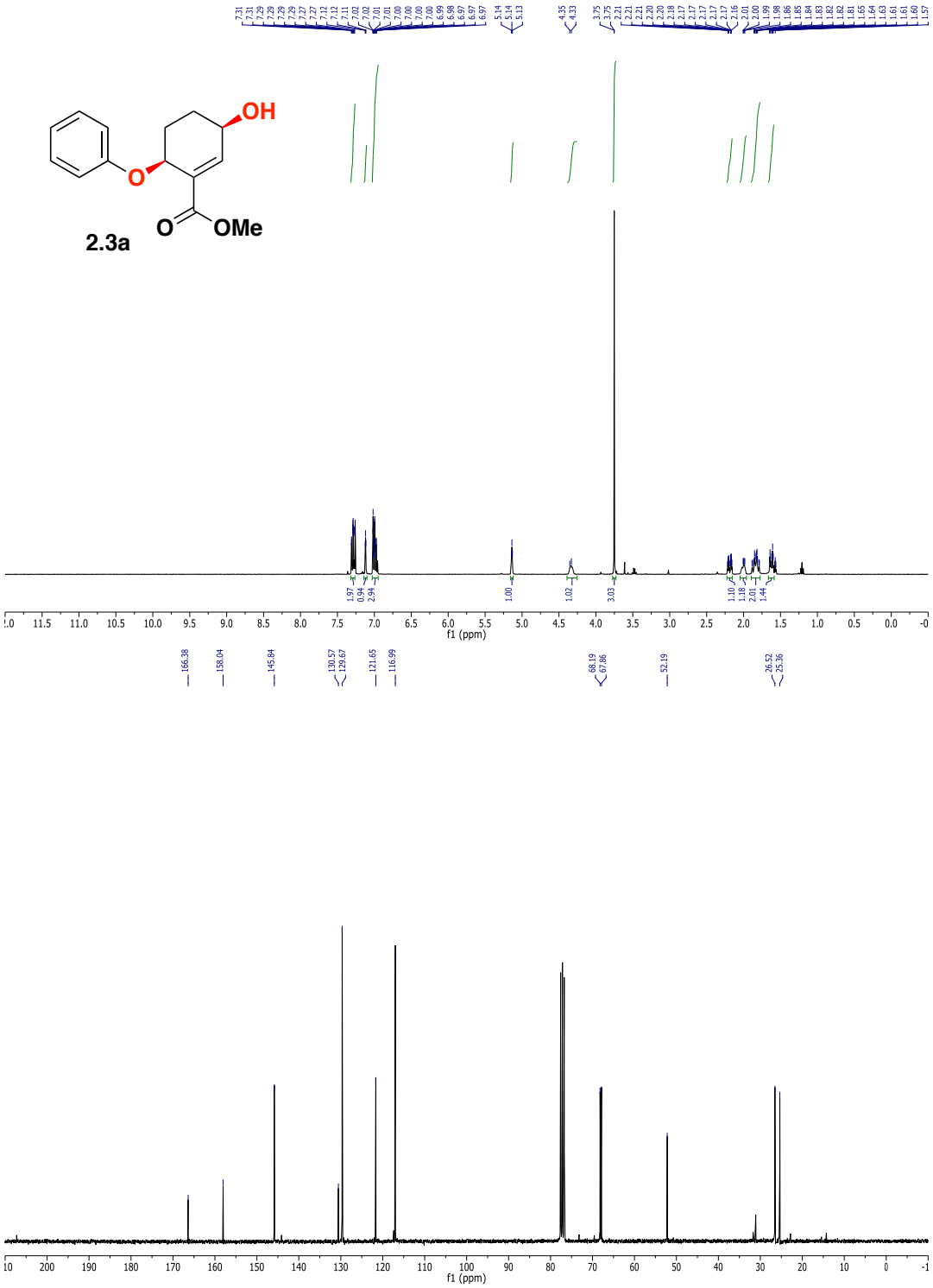
OH
O
O
OMe
2.3a
f1 (ppm)
f1 (ppm)

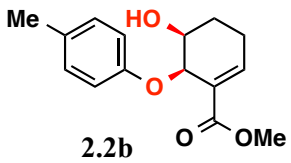

2.2b

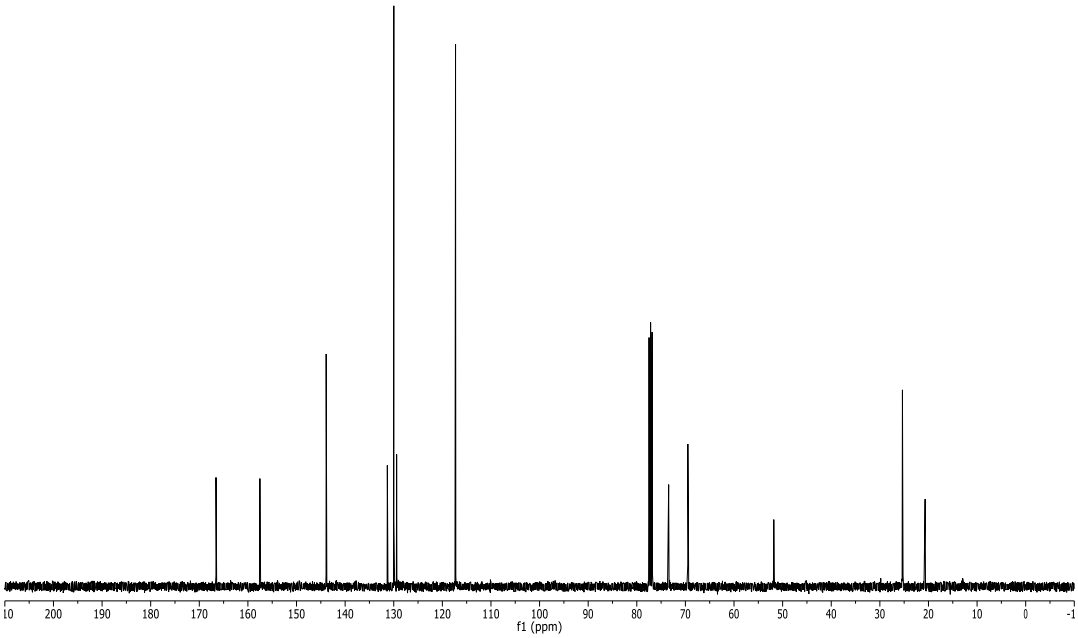

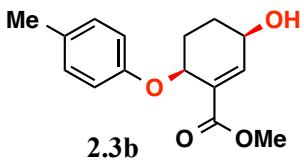

2.3b

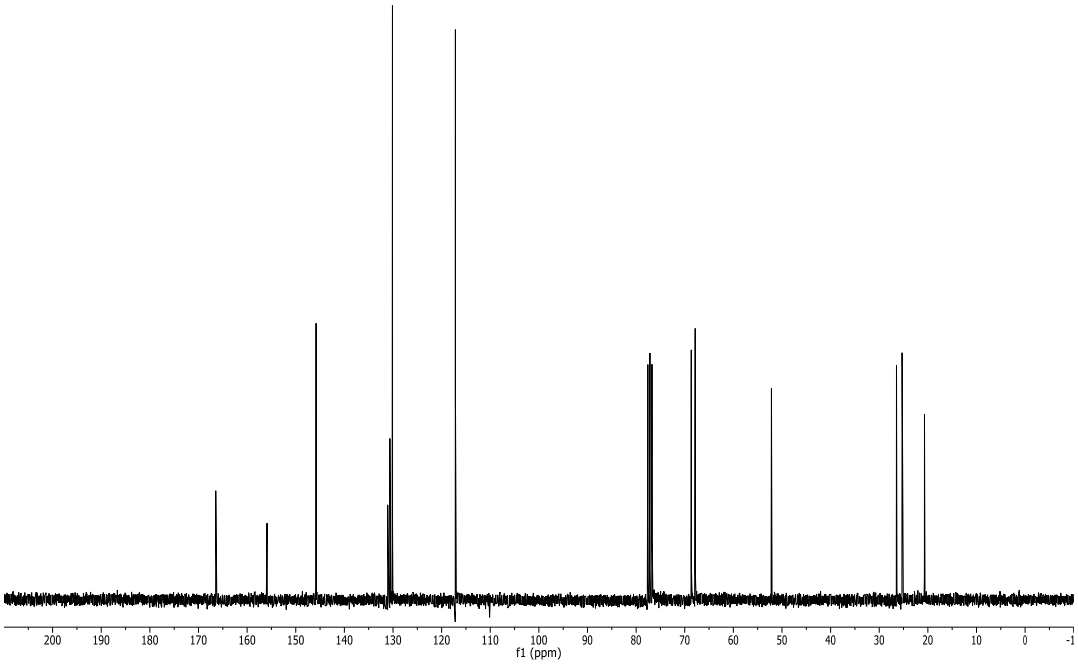

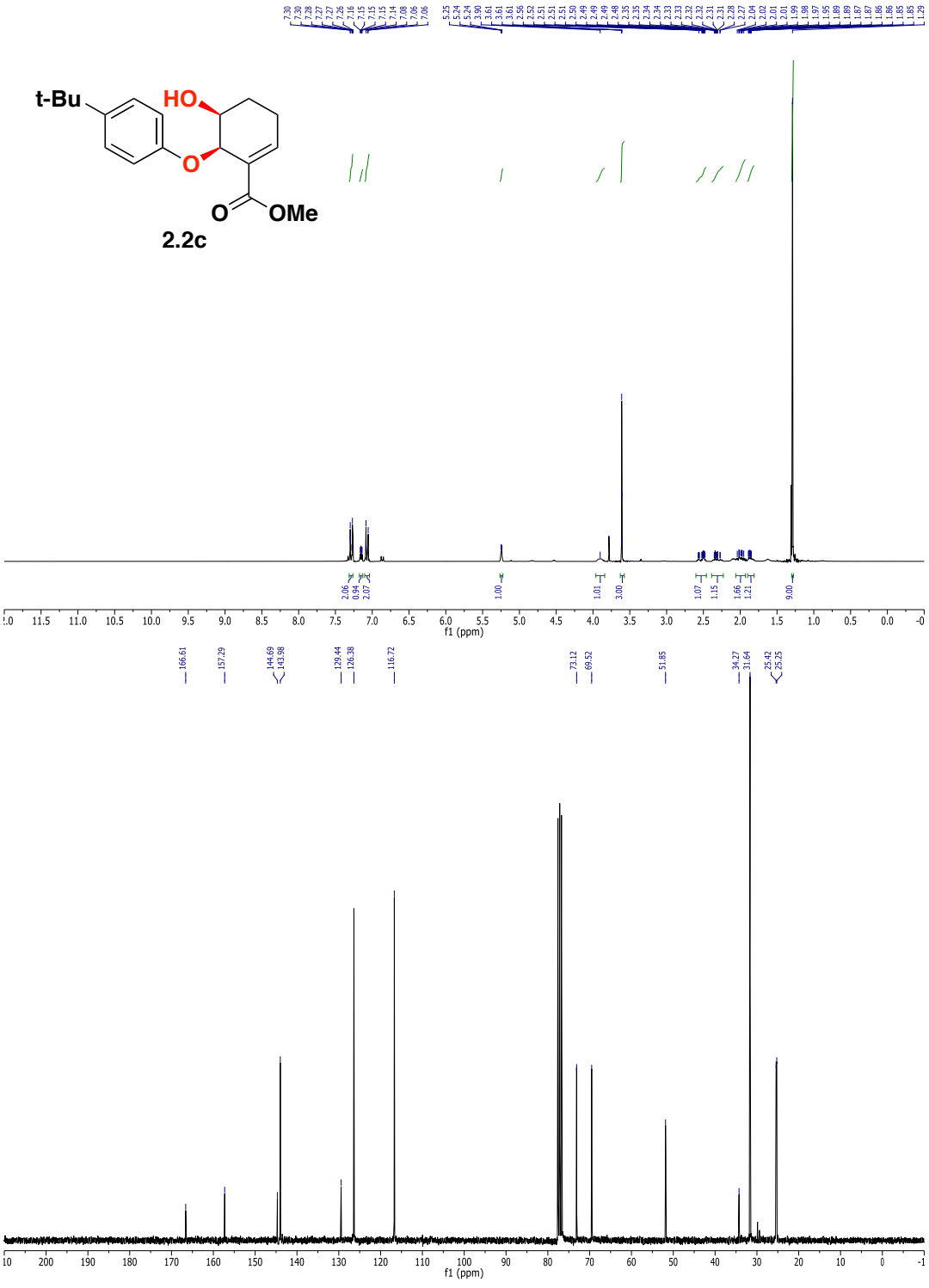
t-Bu
HO
O
O
OMe
2.2c
f1 (ppm)
f1 (ppm)

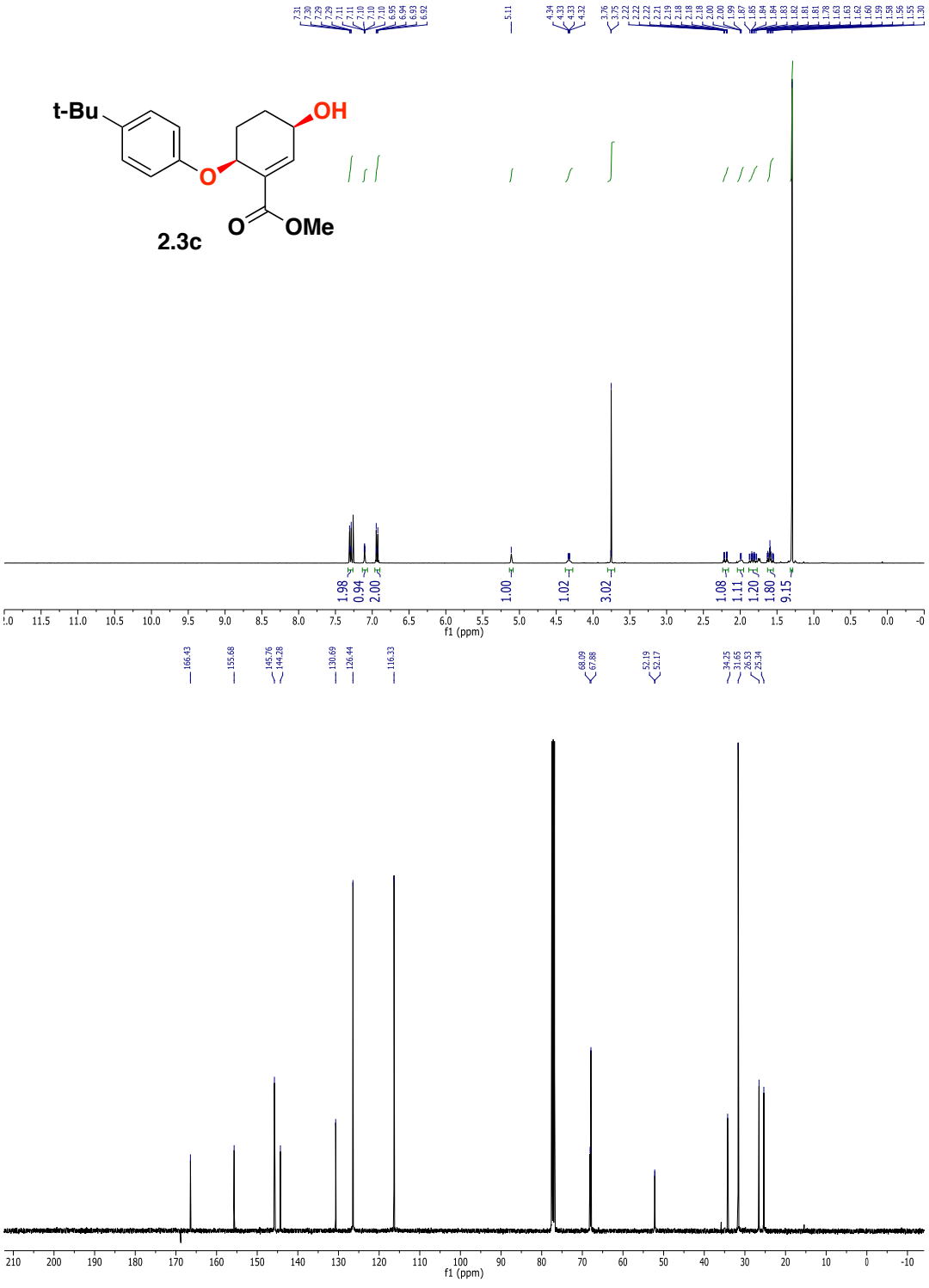
t-Bu
OH
O
O
OMe
2.3c
f1 (ppm)
f1 (ppm)

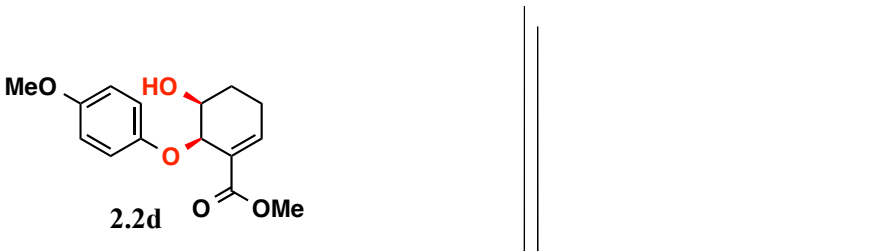

2.2d

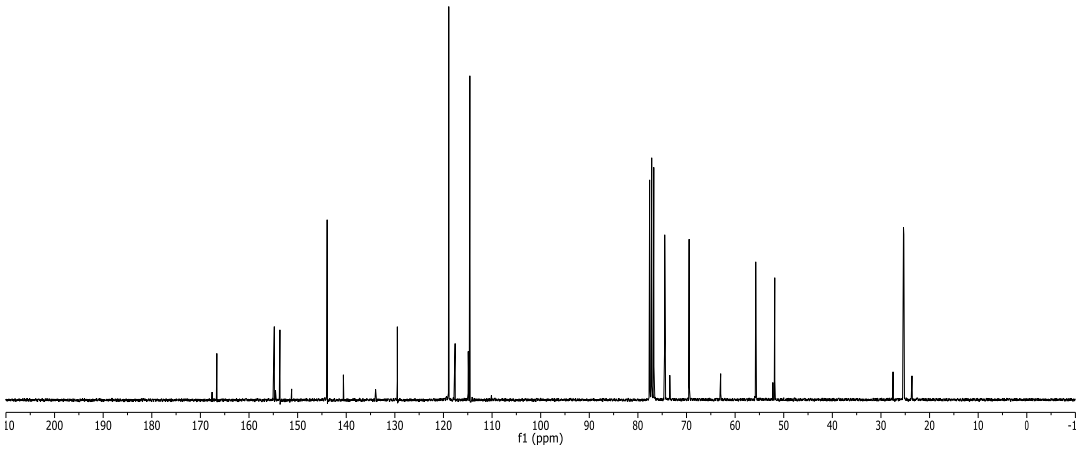

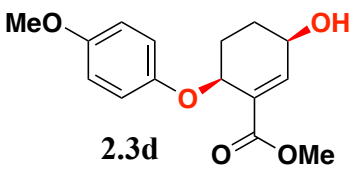

2.3d

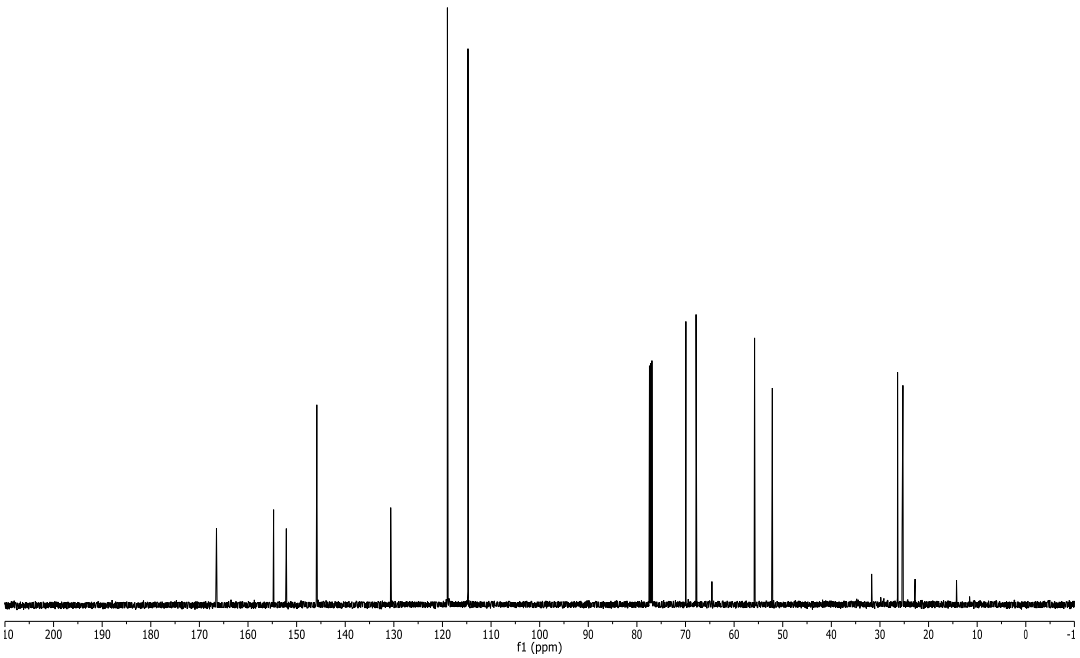

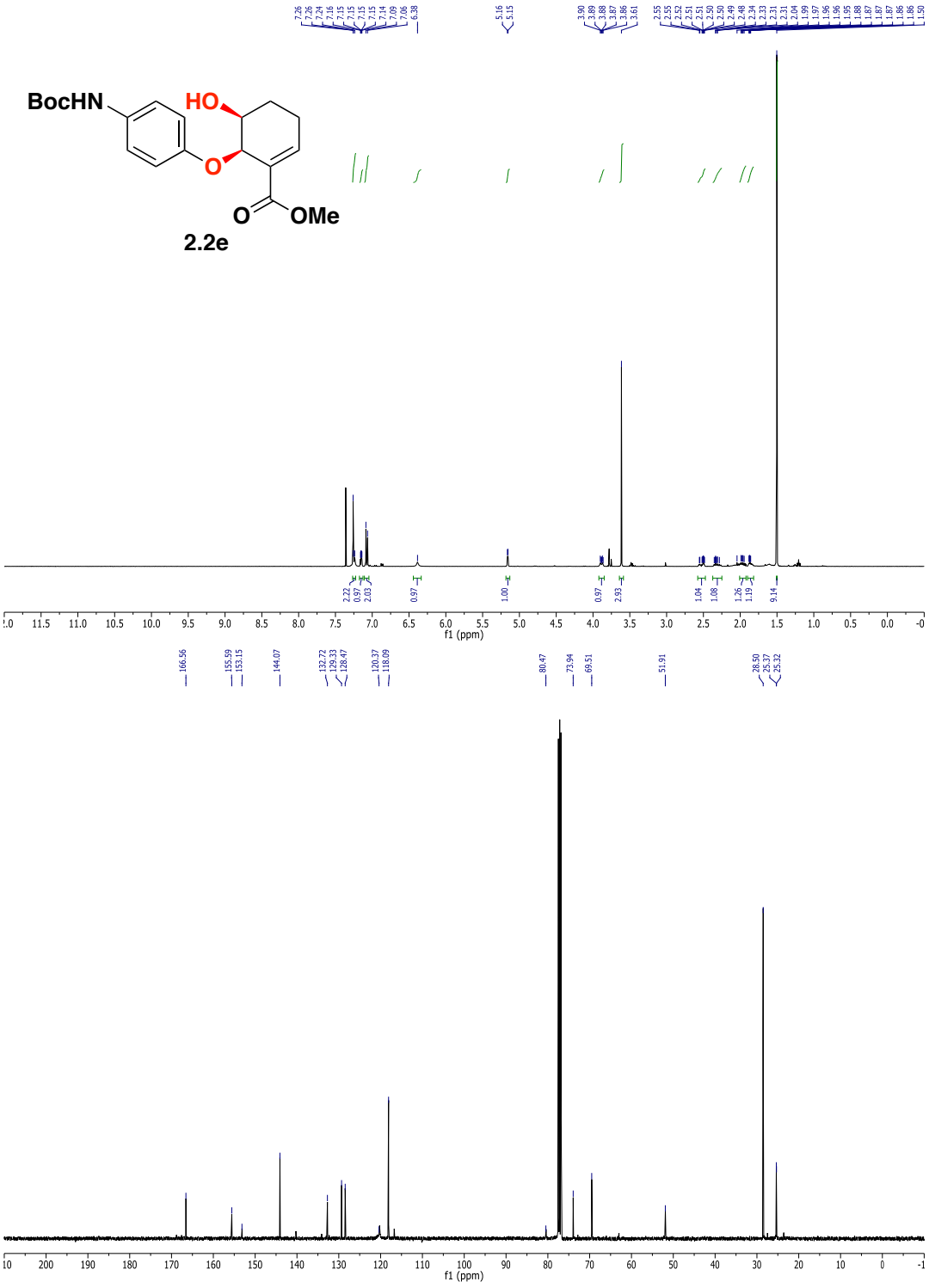
BocHN
HO
O
O
OMe
2.2e
f1 (ppm)
f1 (ppm)

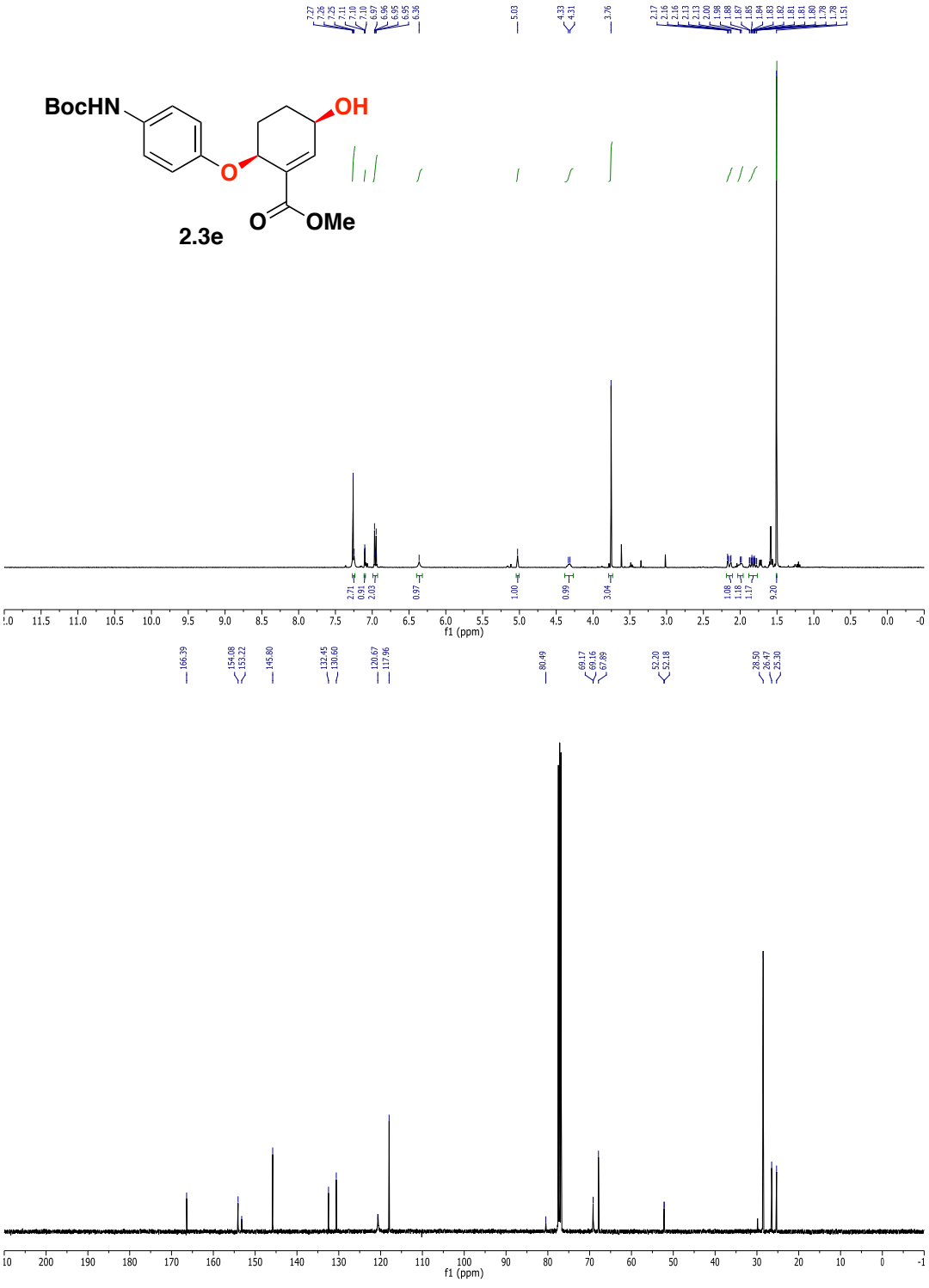
BocHN
OH
O
O
OMe
2.3e
f1 (ppm)
f1 (ppm)

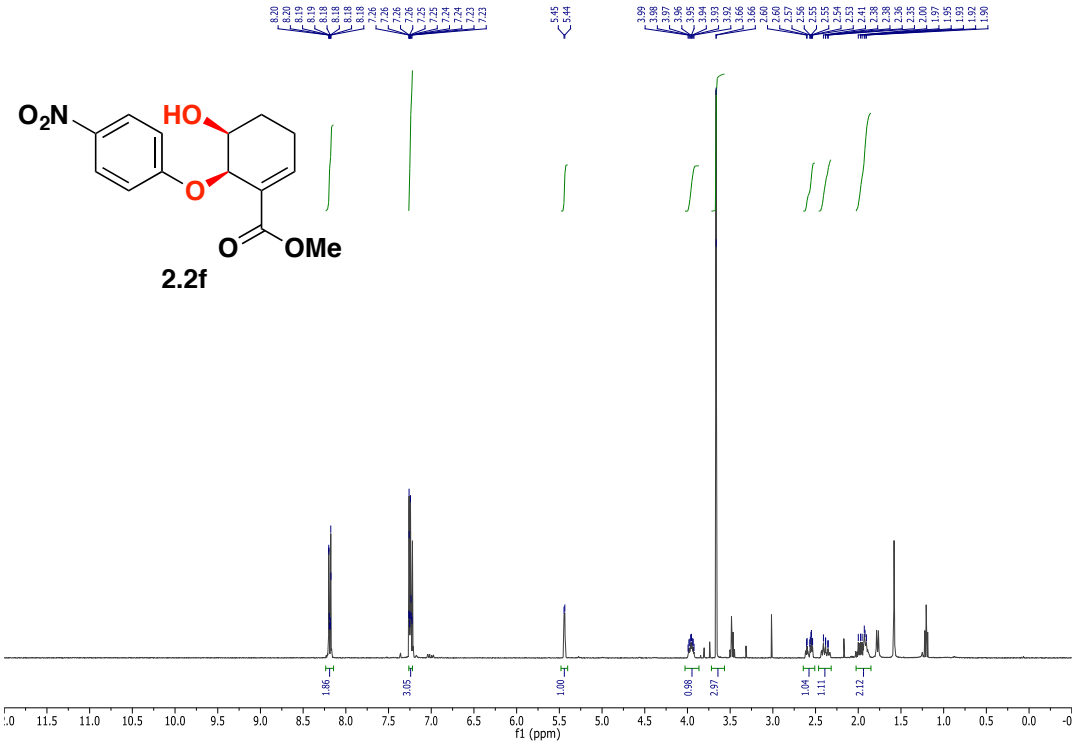
O2N
HO
O
O
OMe
2.2f
f1 (ppm)

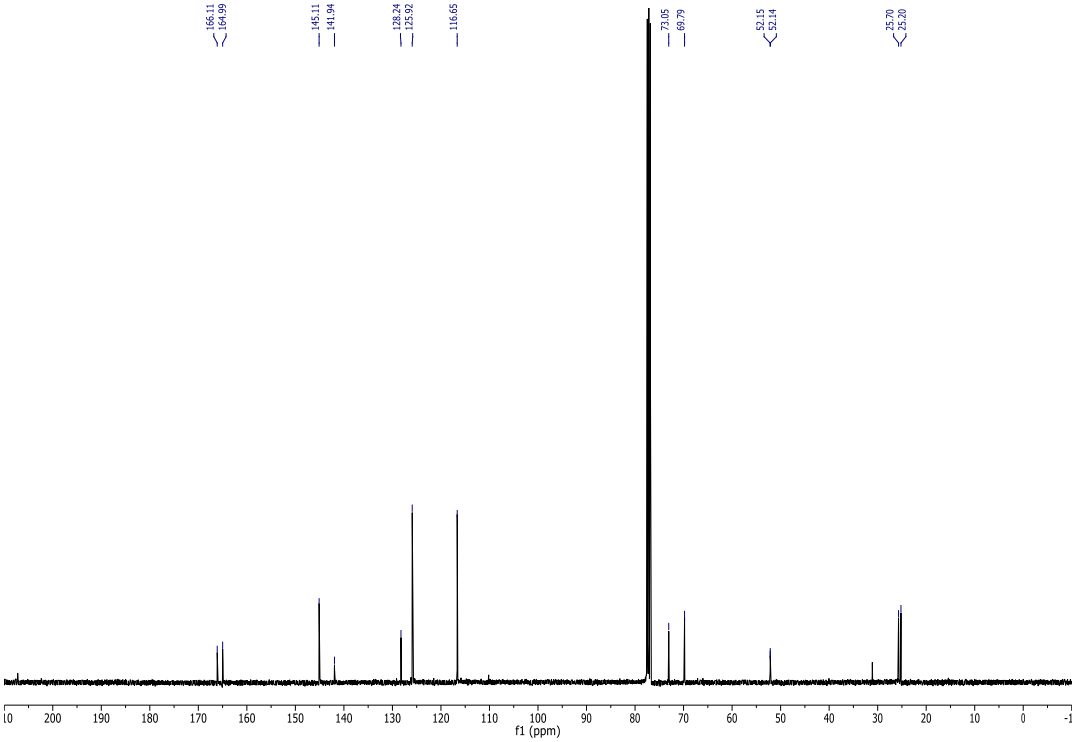
f1 (ppm)

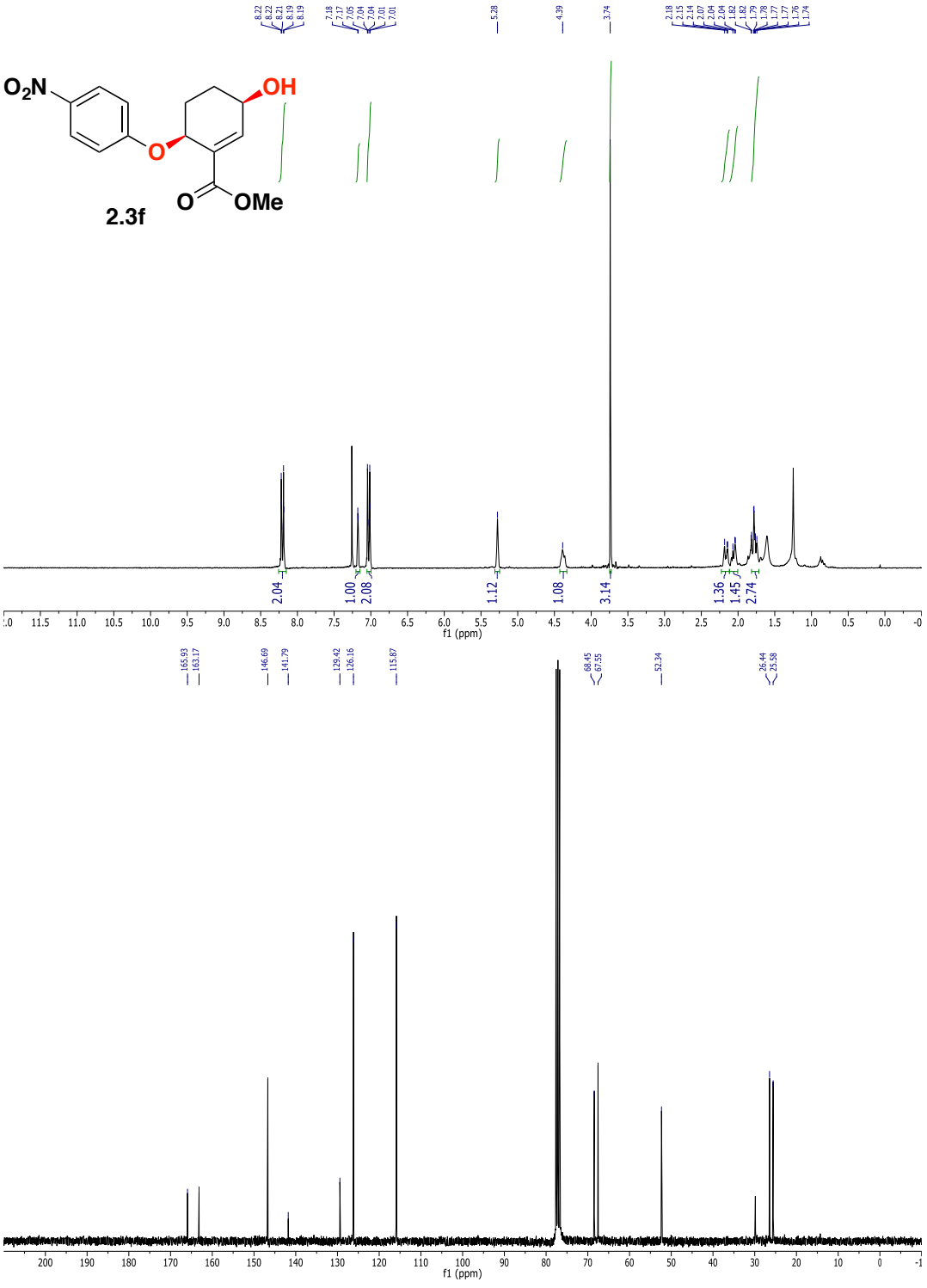
O2N
OH
O
O
OMe
2.3f
f1 (ppm)
f1 (ppm)

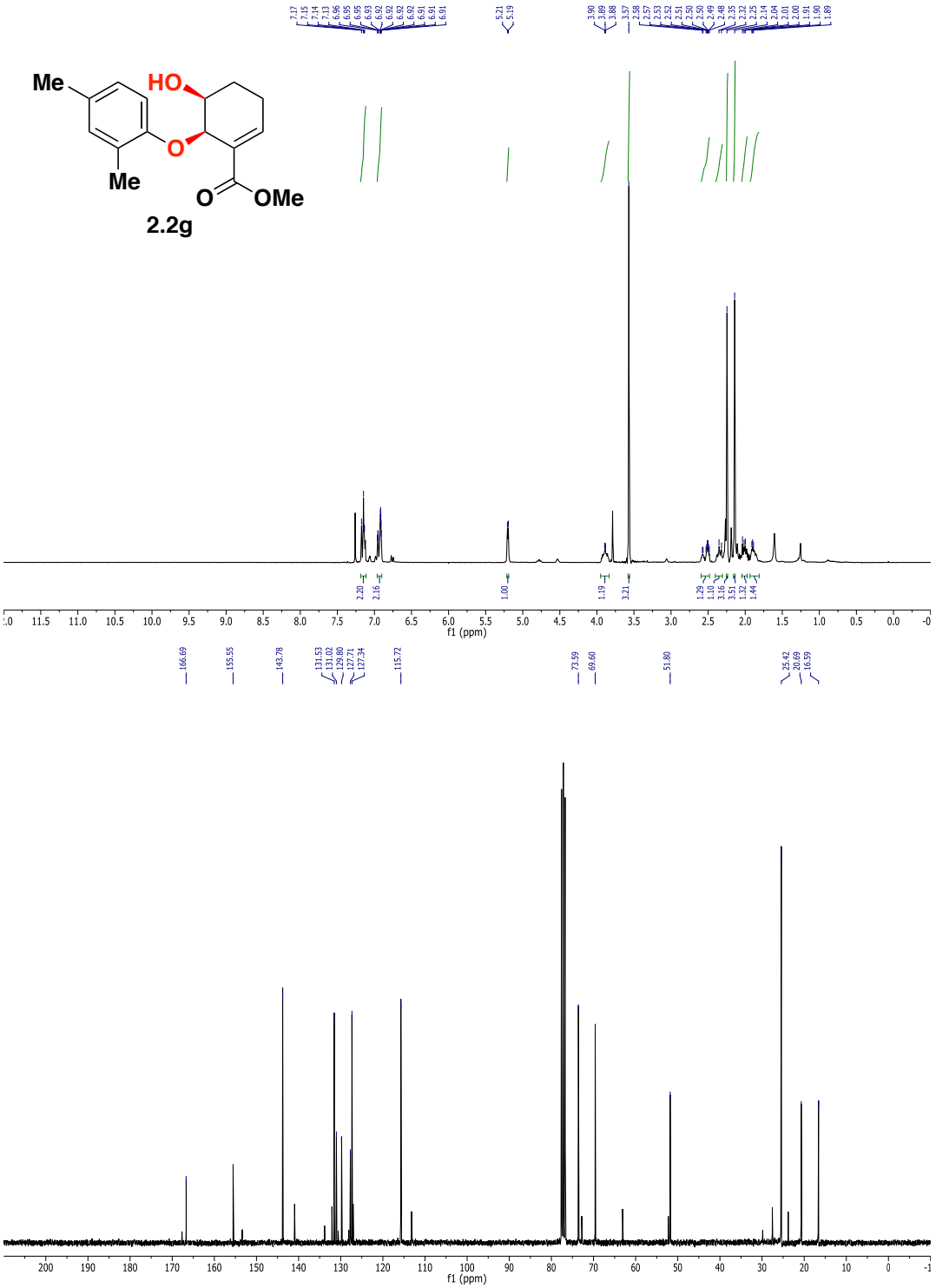
Me
HO
O
Me
O
OMe
2.2g
f1 (ppm)
f1 (ppm)

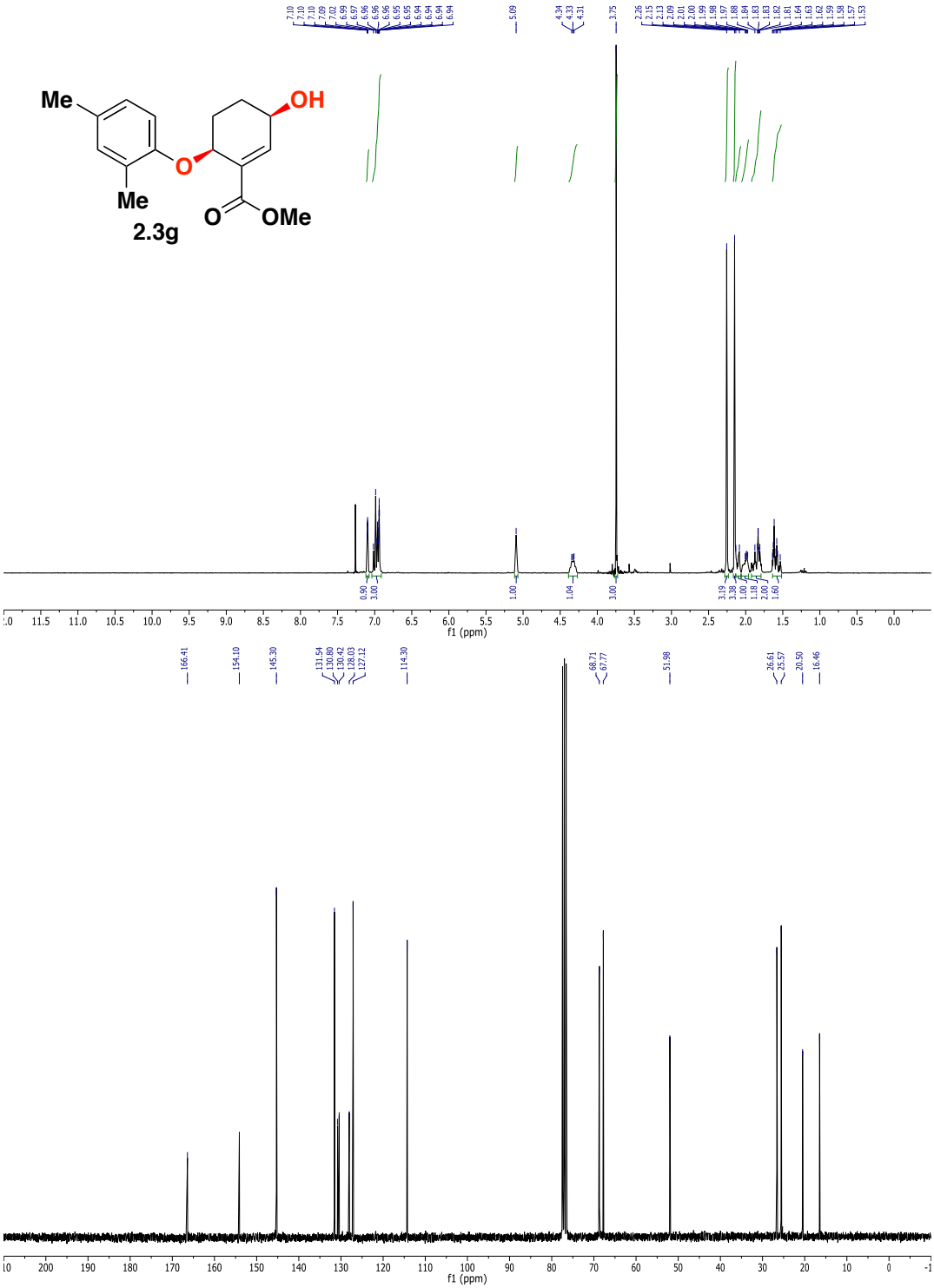
Me
OH
O
Me
O
OMe
2.3g
f1 (ppm)
f1 (ppm)

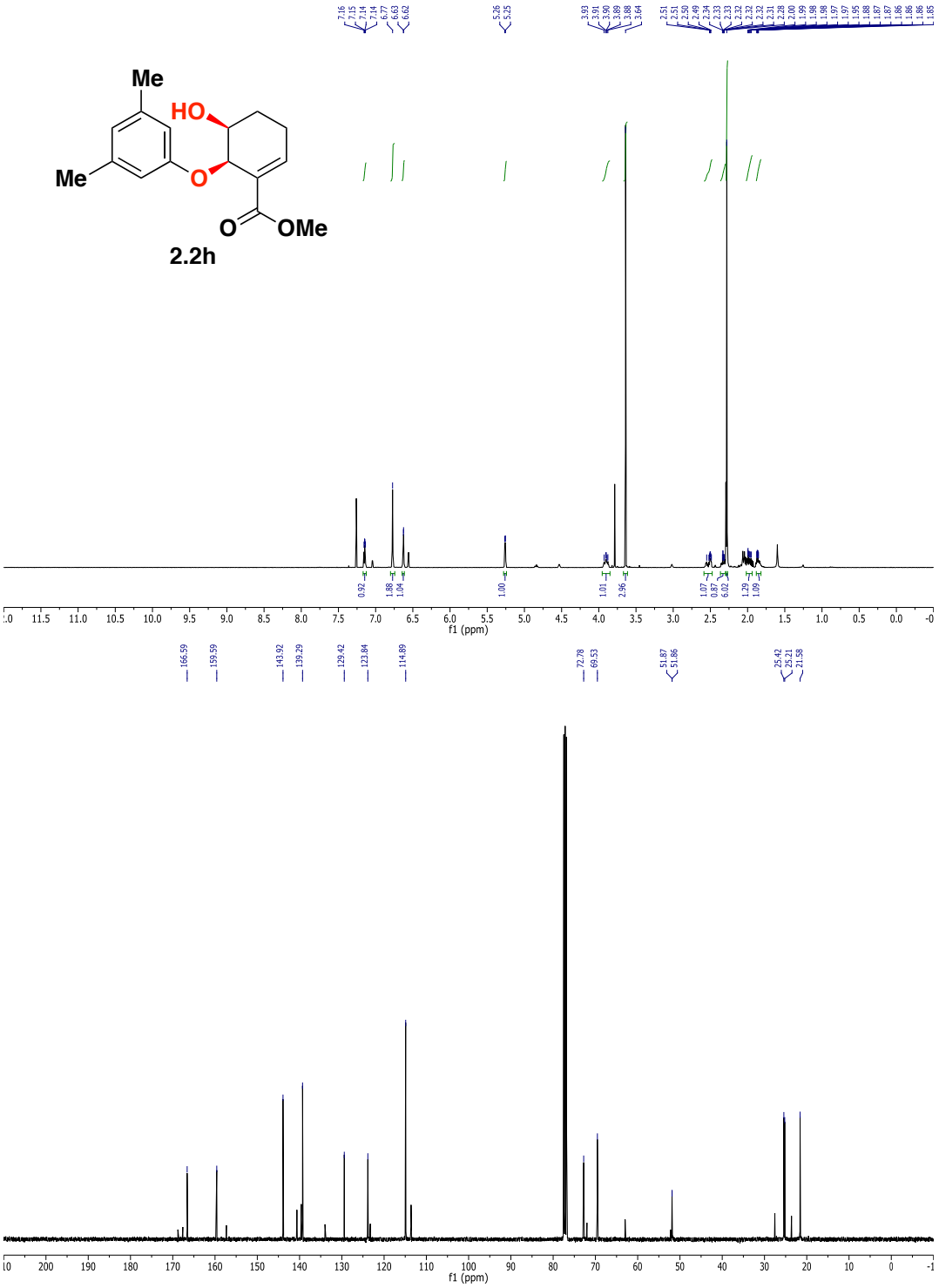
Me
HO
Me
O
O
OMe
2.2h
f1 (ppm)
f1 (ppm)

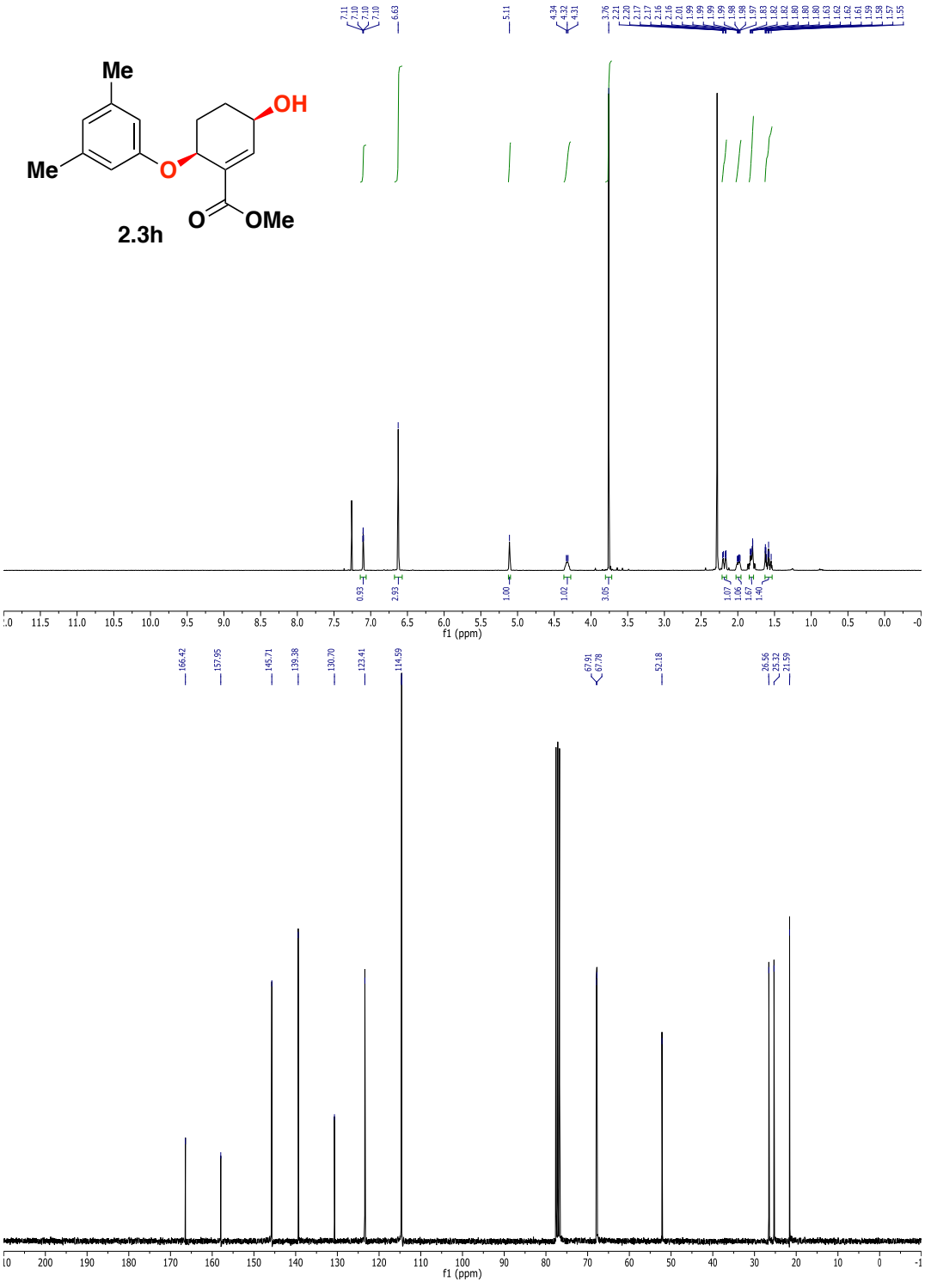
Me
OH
Me
O
O
OMe
2.3h
f1 (ppm)
f1 (ppm)

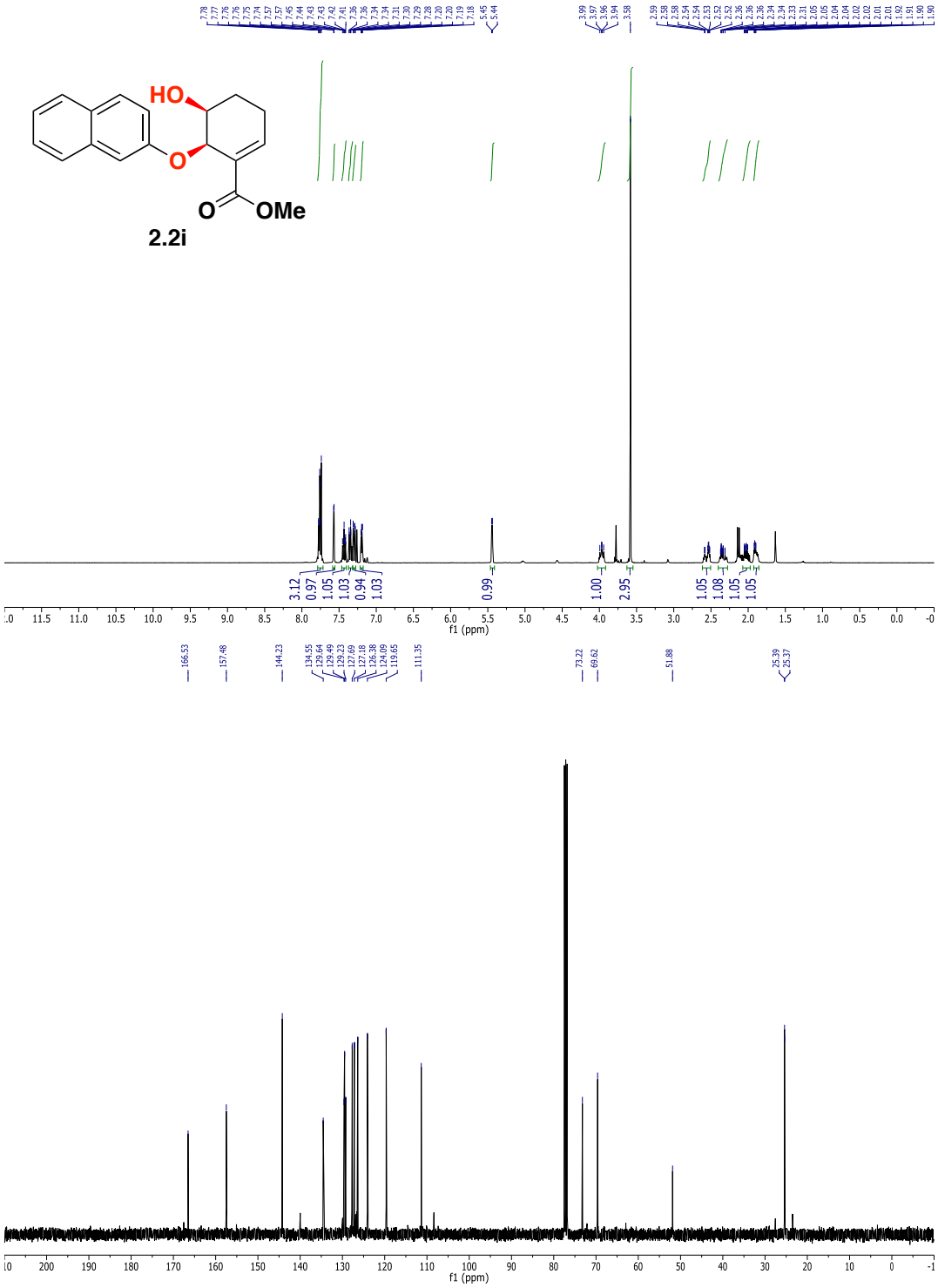
HO
O
O
OMe
2.2i
f1 (ppm)
f1 (ppm)

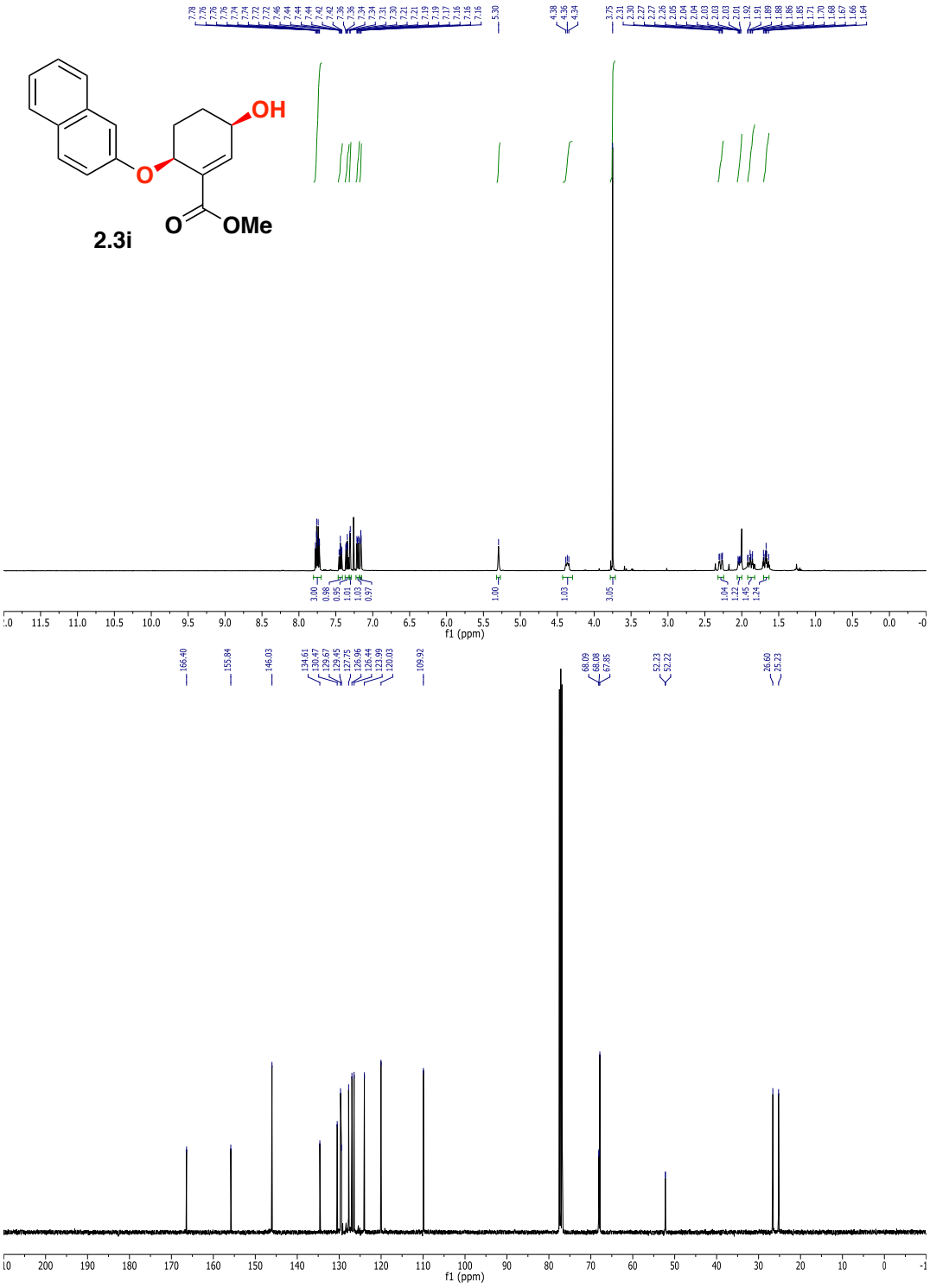
OH
O
O
OMe
2.3i
f1 (ppm)
f1 (ppm)

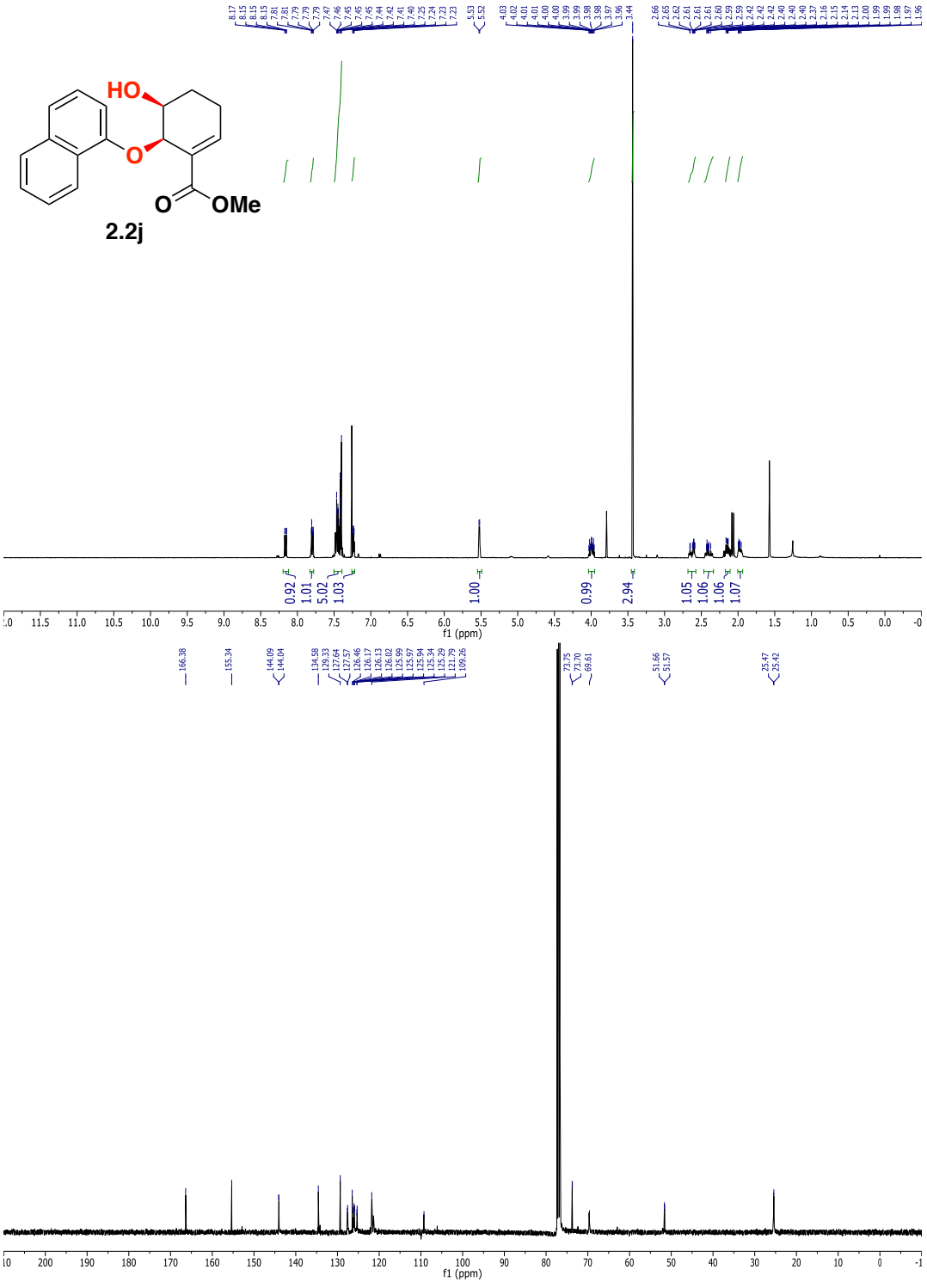
HO
O
O
OMe
2.2j
f1 (ppm)
f1 (ppm)

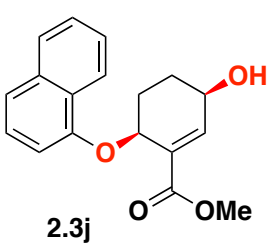
OH
O
O
OMe

2.3j

0.97
1.00
4.17
0.97
1.06
1.04
1.04
3.06
1.09
3.24
1.37
f1 (ppm)

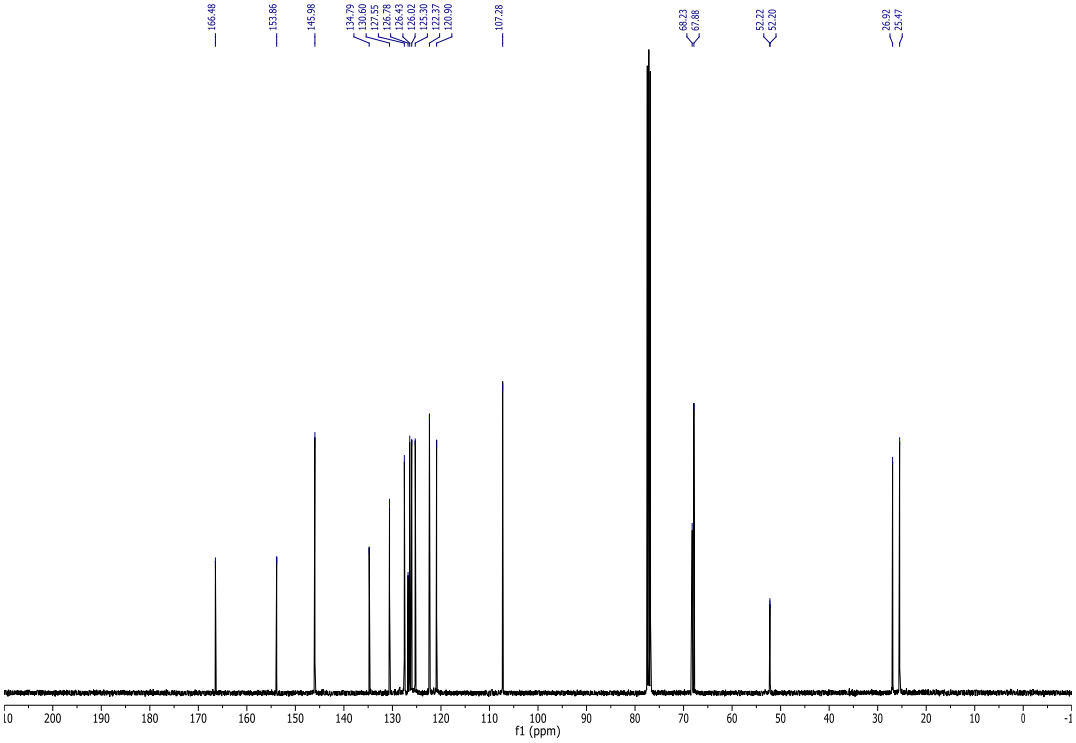
166.48
153.86
145.98
134.79
130.60
127.55
126.78
126.43
126.02
125.30
122.37
120.90
107.28
68.23
67.88
52.22
52.20
26.92
25.47
f1 (ppm)

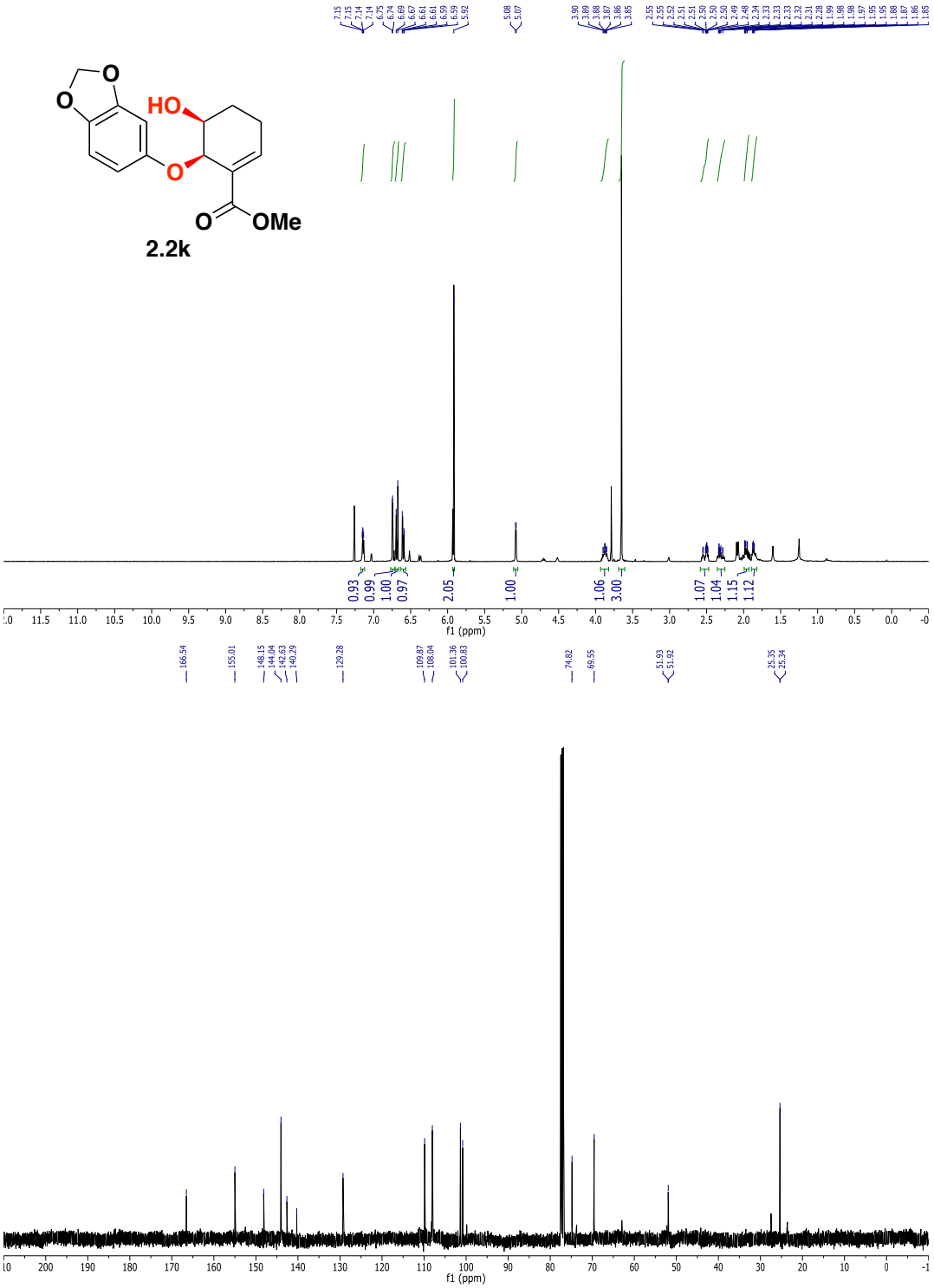
HO
O
O
O
O
OMe
2.2k
f1 (ppm)
f1 (ppm)

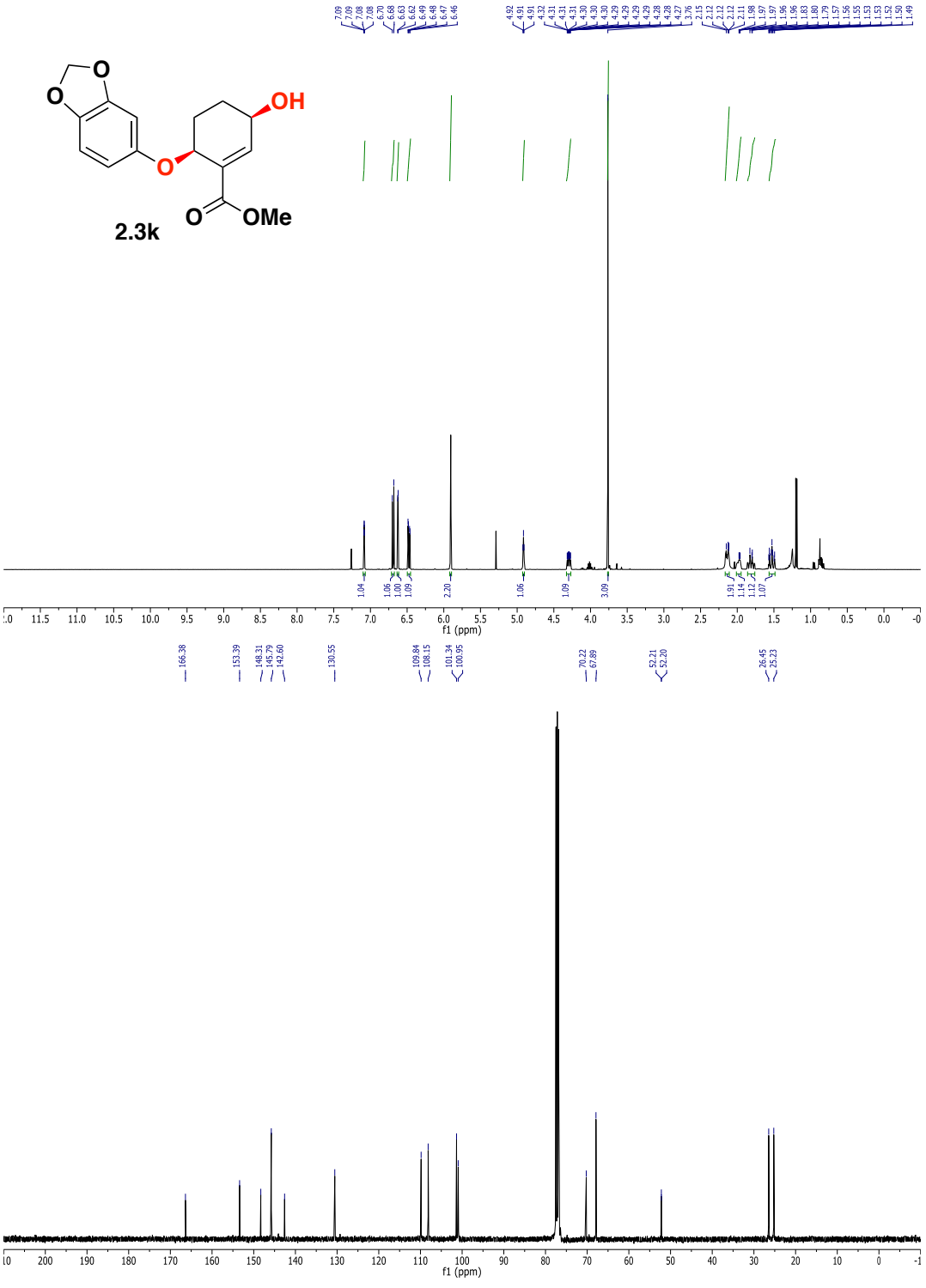
O
O
O
OH
O
O
OMe
2.3k
f1 (ppm)
f1 (ppm)

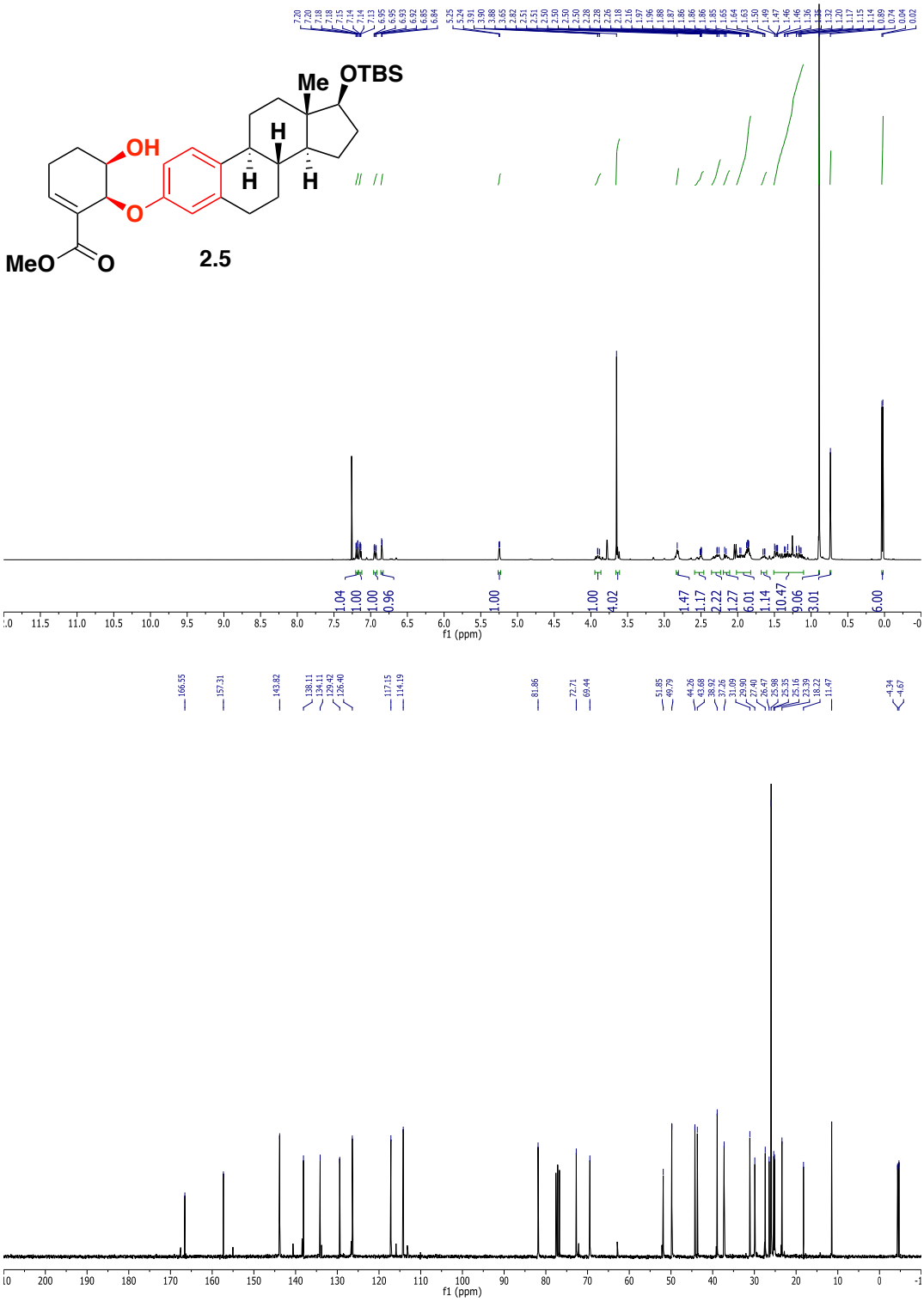
Me
OTBS
OH
H
H
H
O
MeO
O
2.5
f1 (ppm)
f1 (ppm)

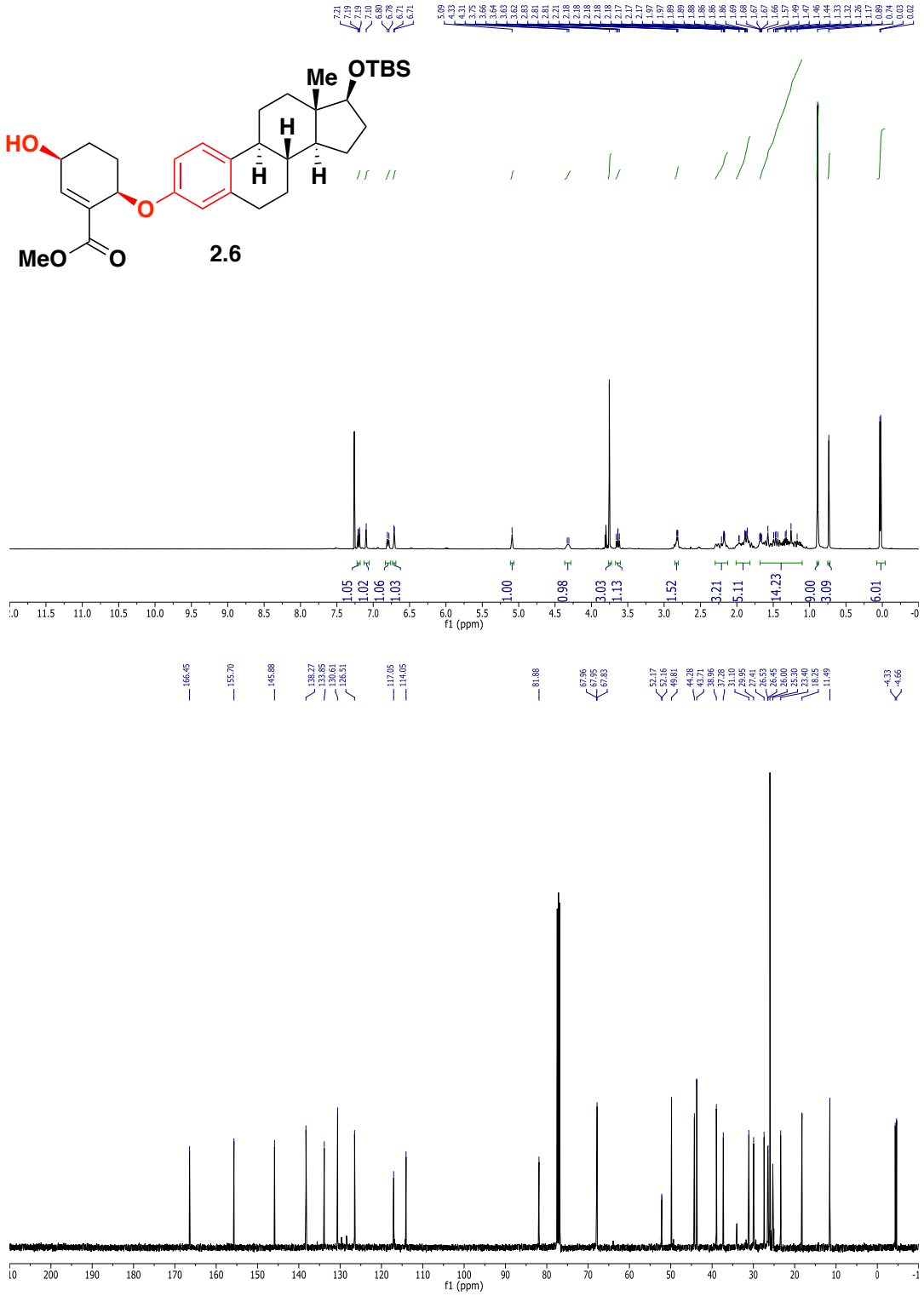
HO
Me
OTBS
H
H
H
O
MeO
O
2.6
f1 (ppm)
f1 (ppm)

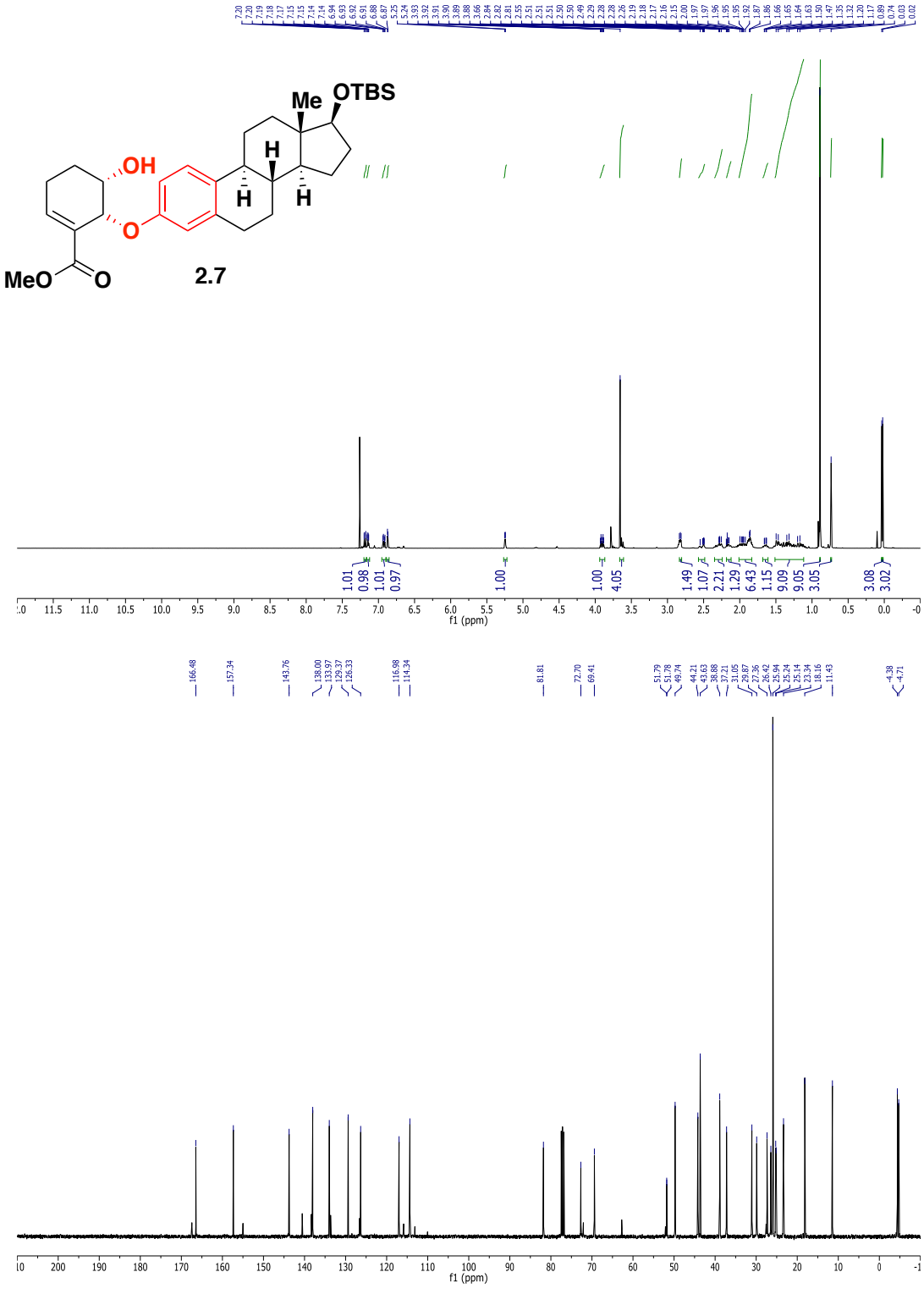
Me
OTBS
OH
H
H
H
O
MeO
O
2.7
f1 (ppm)
f1 (ppm)

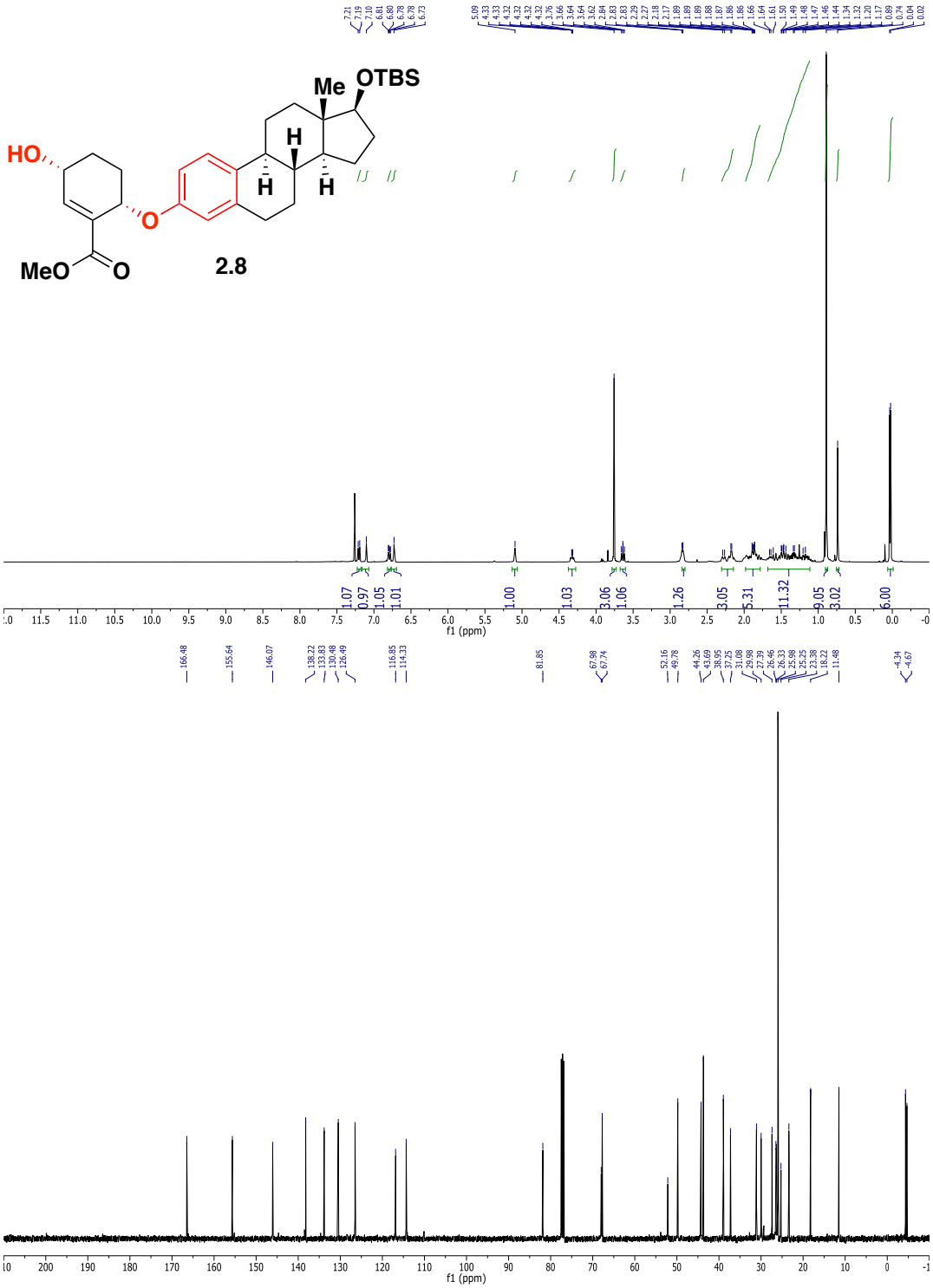
HO
Me
OTBS
H
H
H
O
MeO
O
2.8
f1 (ppm)
f1 (ppm)

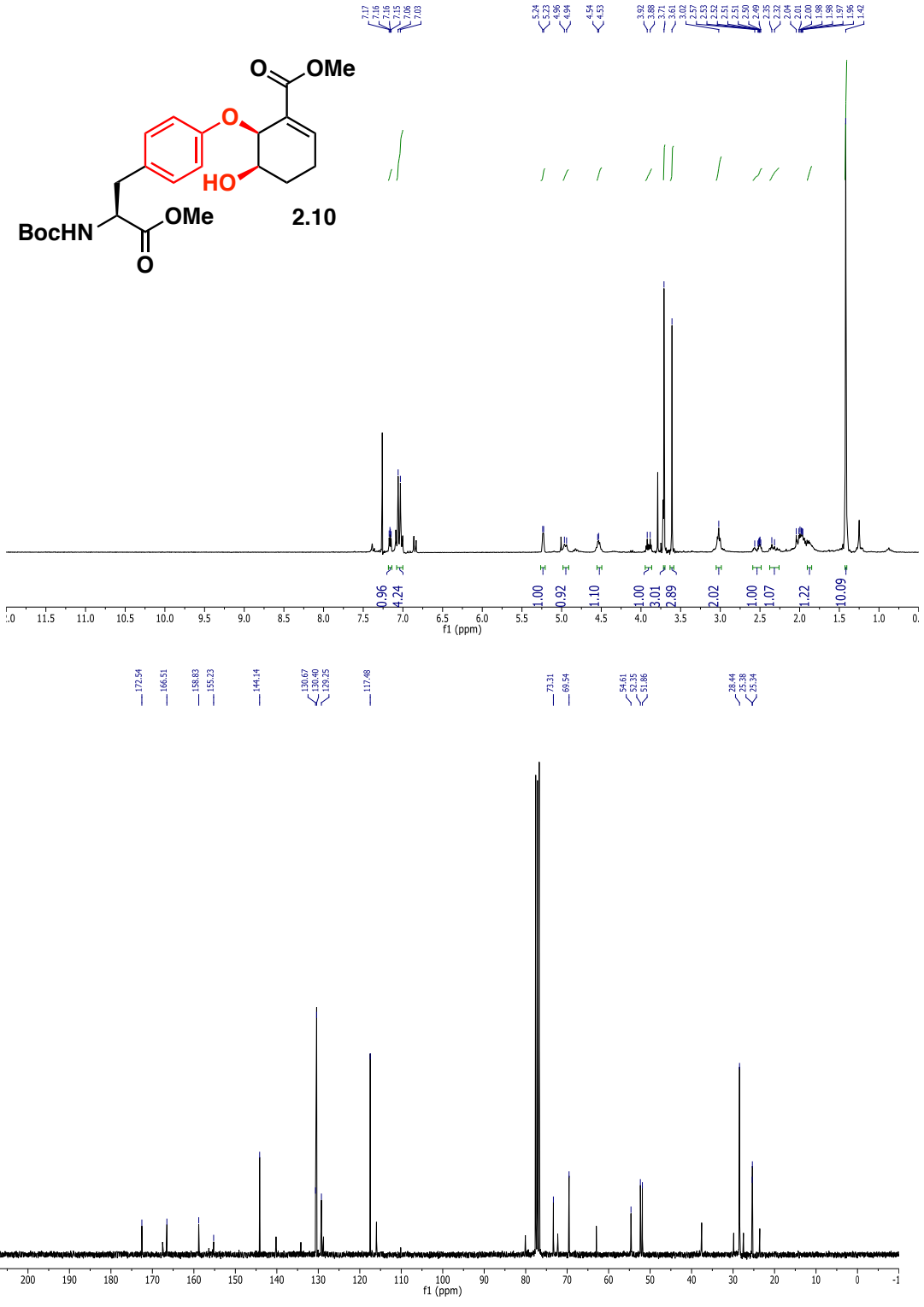
O
OMe
O
HO
BocHN
OMe
O
2.10
f1 (ppm)
f1 (ppm)

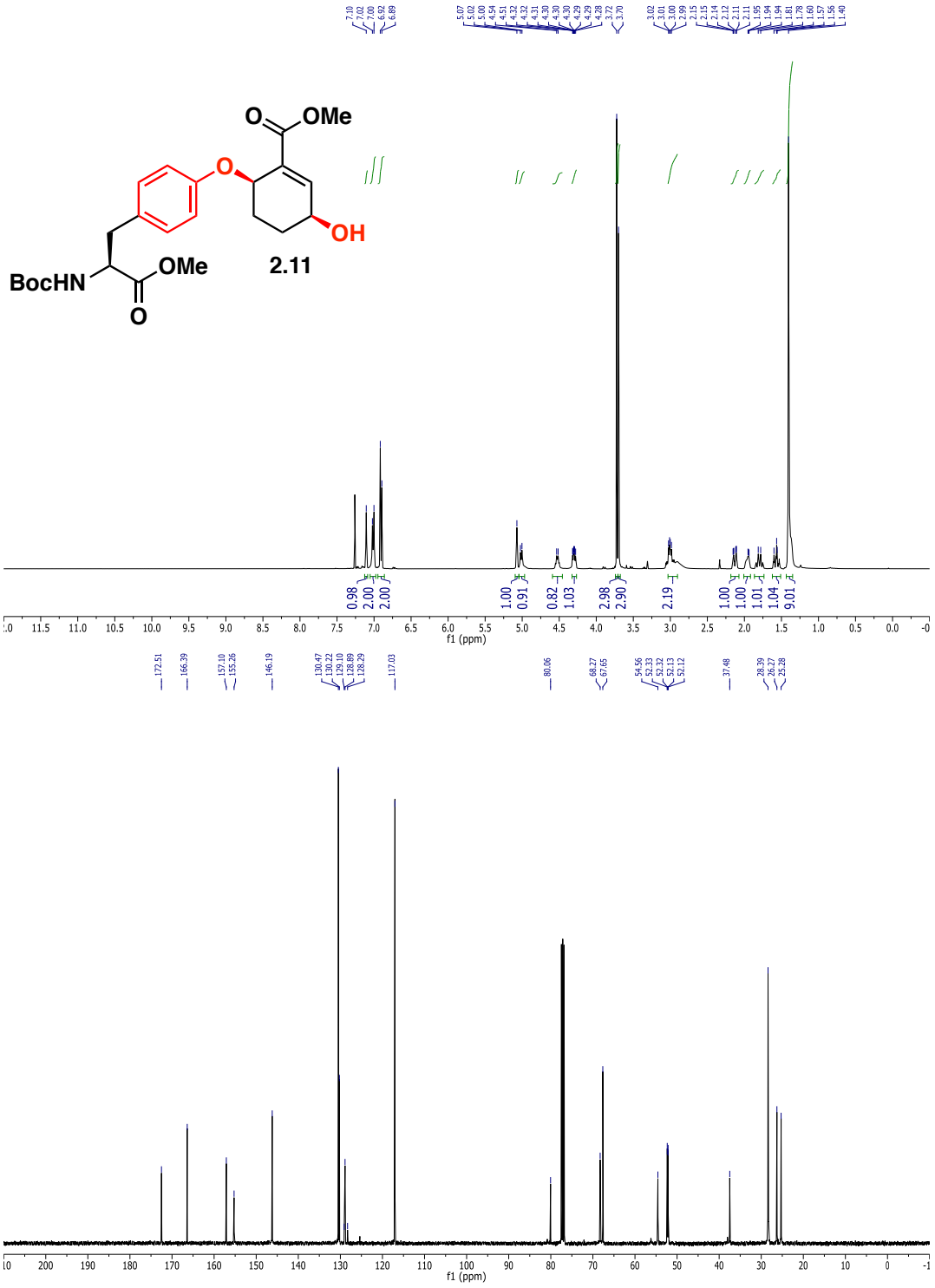
O
OMe
O
OH
BocHN
OMe
O
2.11
f1 (ppm)
f1 (ppm)

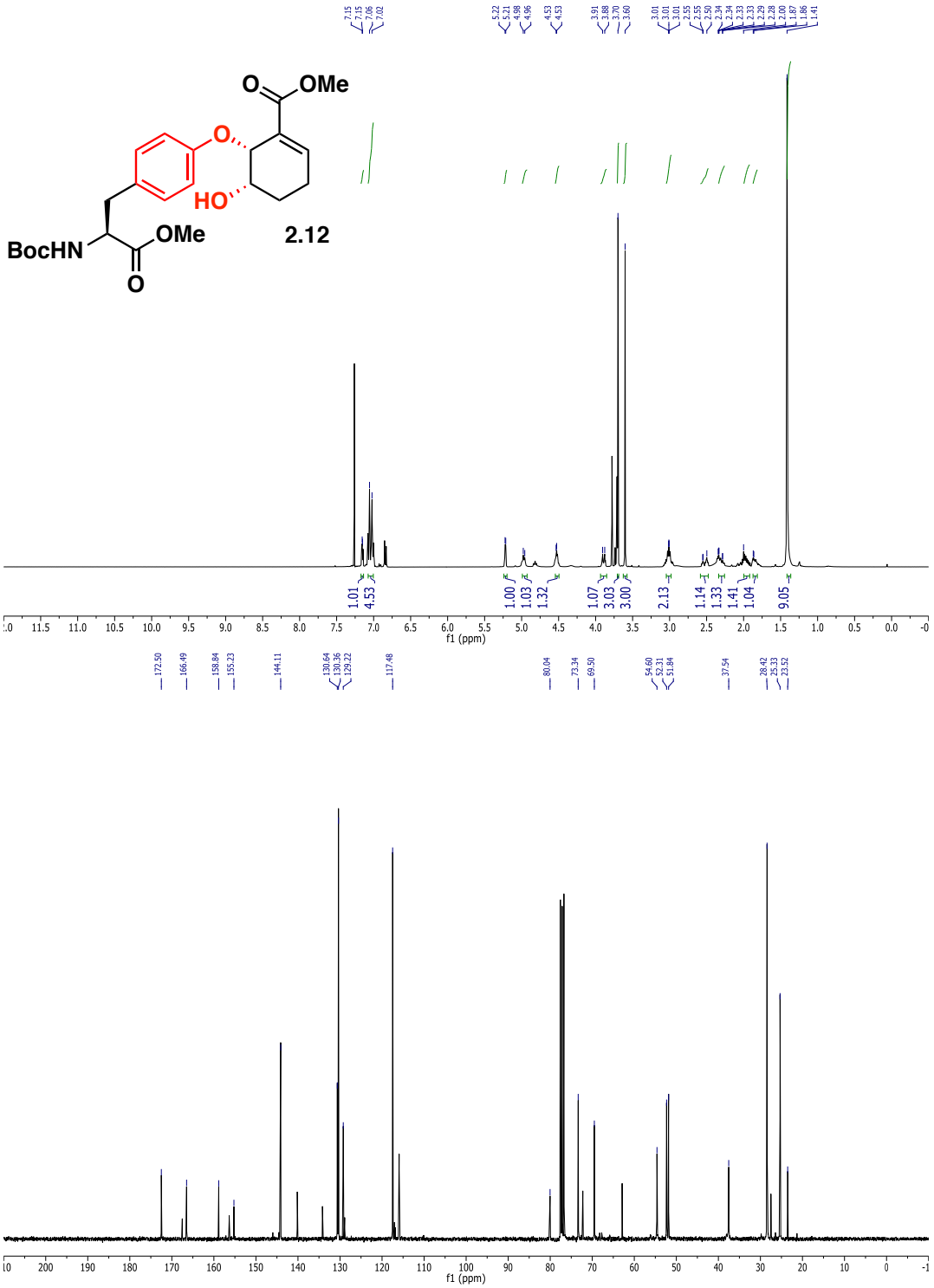
O
OMe
O
HO
BocHN
OMe
O
2.12
f1 (ppm)
f1 (ppm)

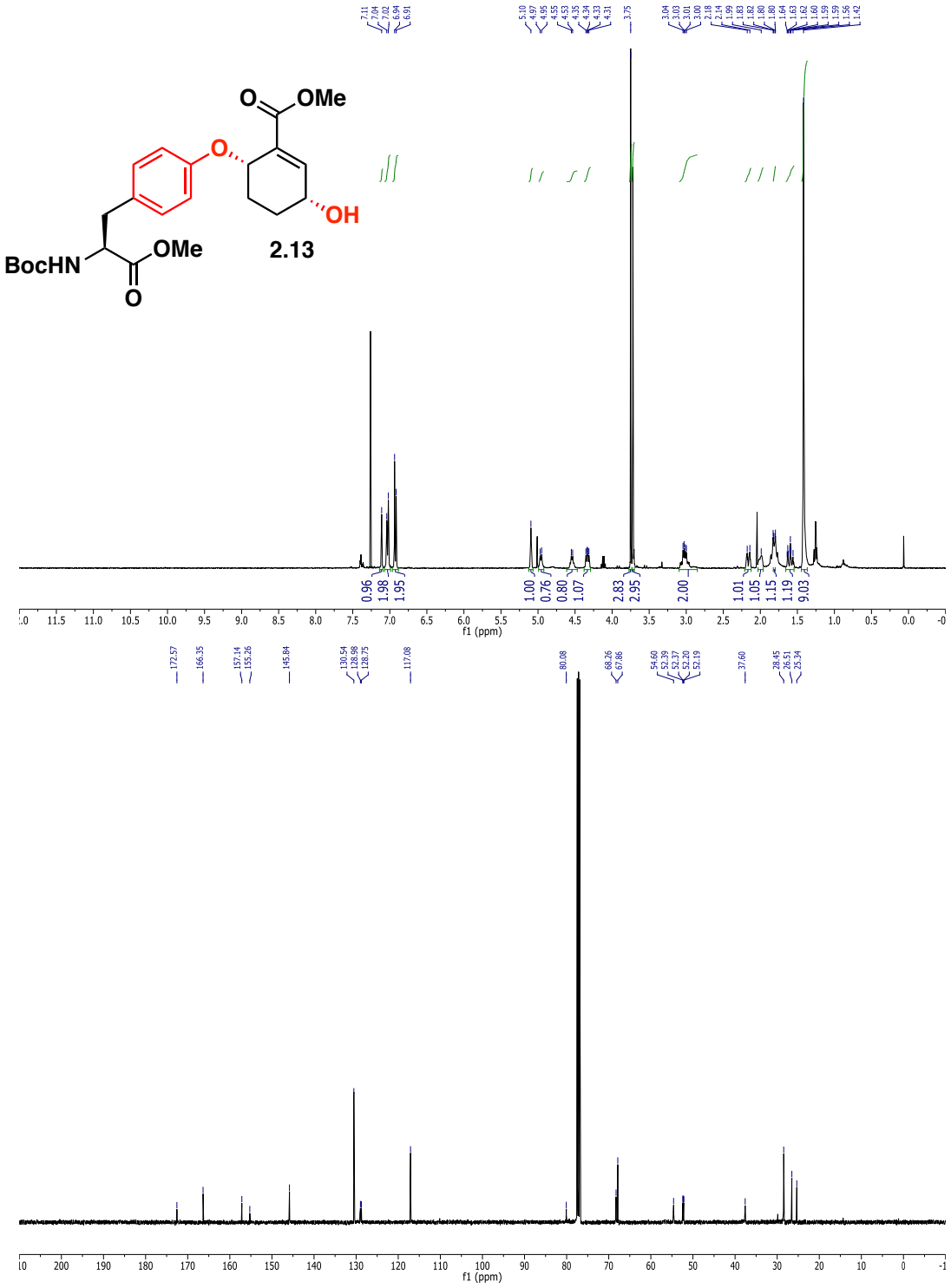
O
OMe
O
OH
BocHN
OMe
O
2.13
f1 (ppm)
f1 (ppm)

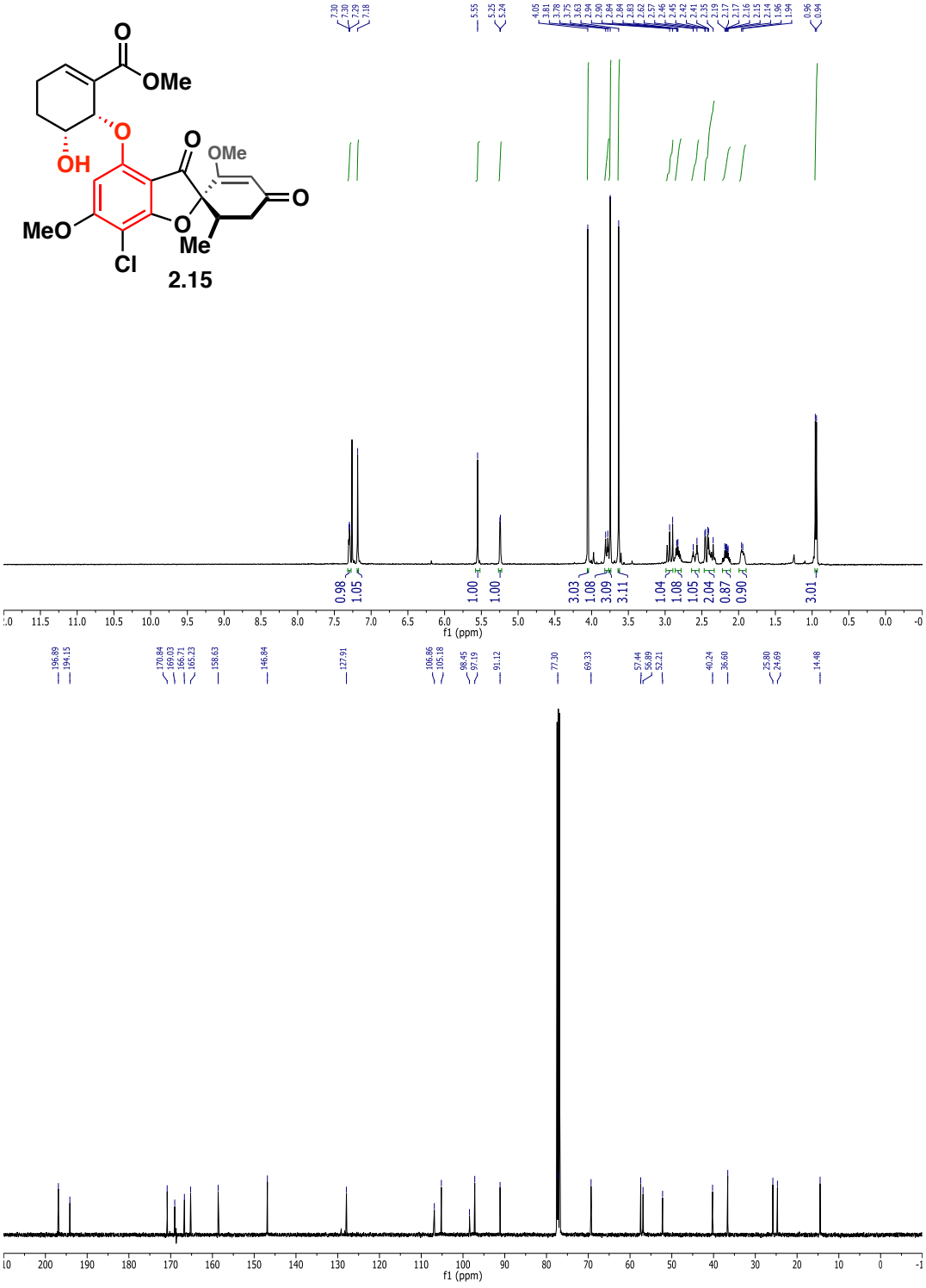
OMe
O
OH
O
OMe
O
MeO
O
Me
Cl
2.15
f1 (ppm)
f1 (ppm)

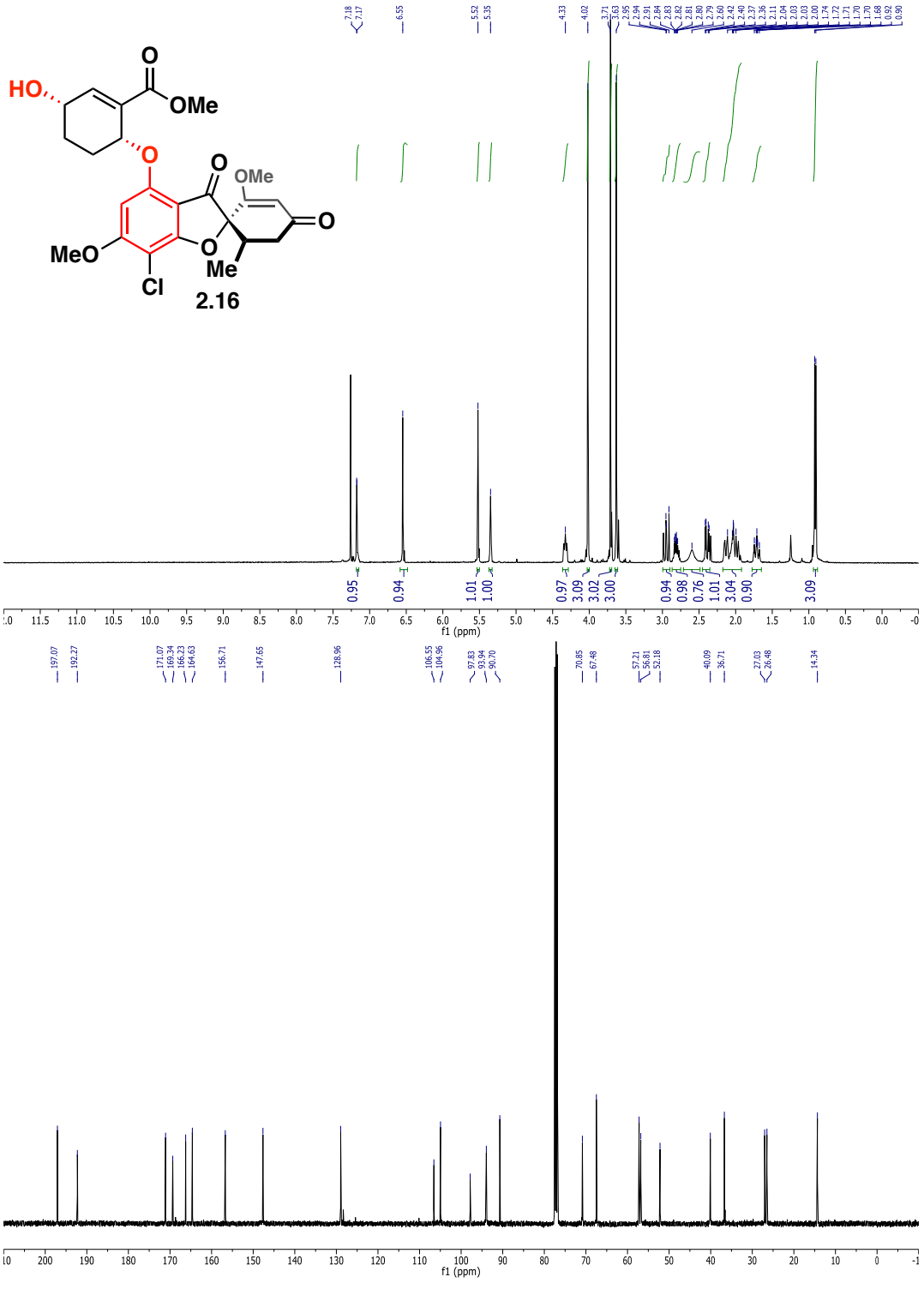
HO
O
OMe
O
O
OMe
O
MeO
O
Me
Cl
2.16
f1 (ppm)
f1 (ppm)

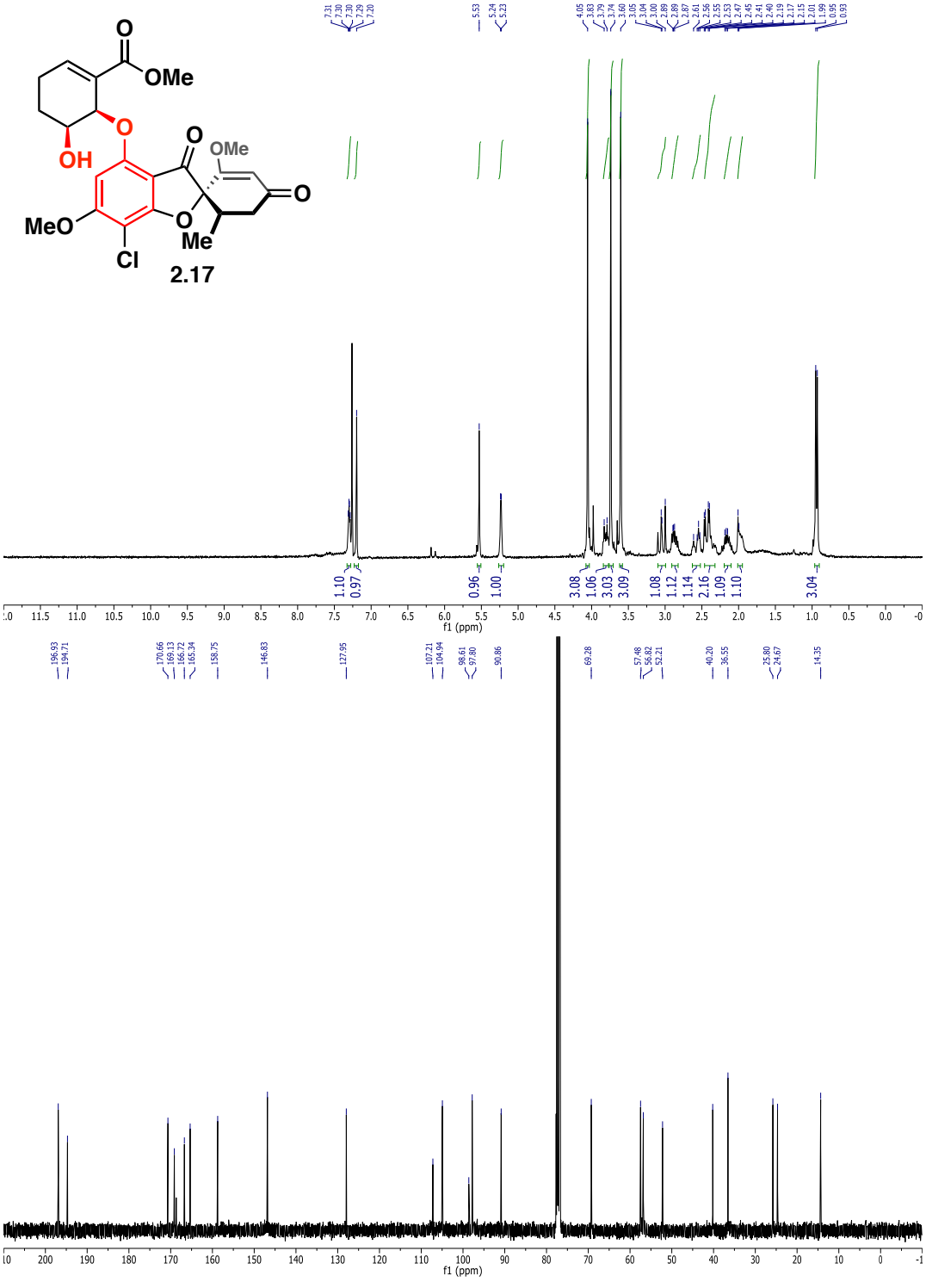
O
OMe
O
OH
O
OMe
O
MeO
O
Me
Cl
2.17
f1 (ppm)
f1 (ppm)

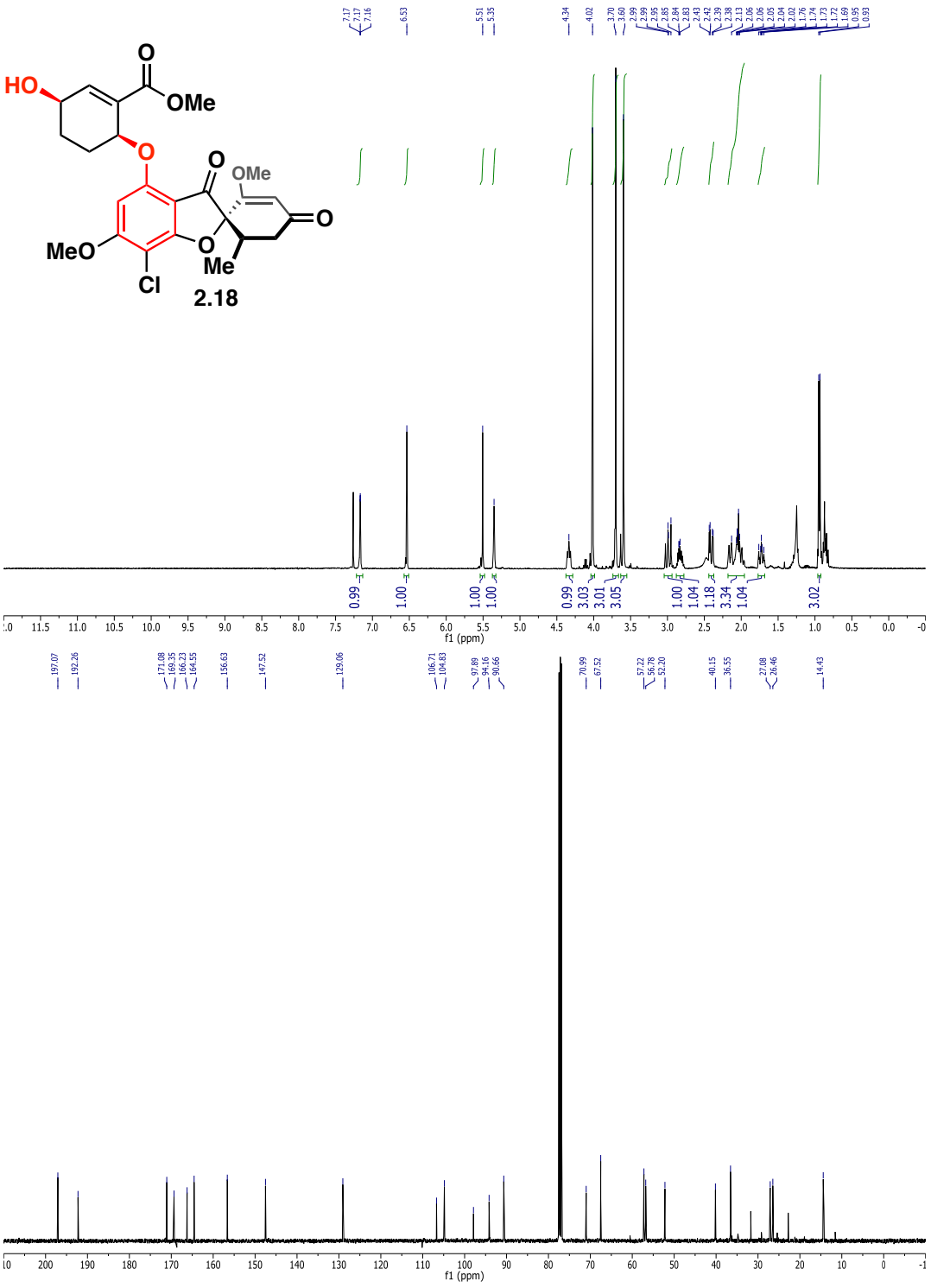
HO
O
OMe
O
O
OMe
MeO
O
Me
Cl
2.18
f1 (ppm)
f1 (ppm)

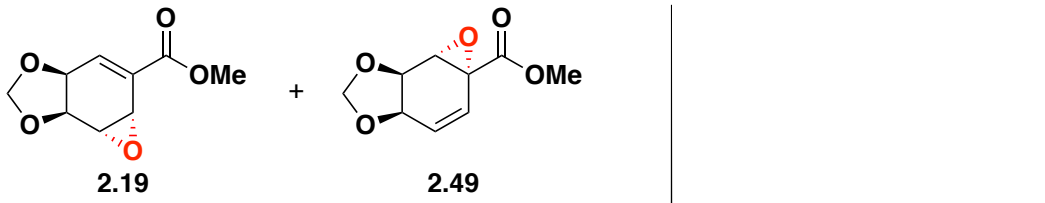
O
OMe
O
O
O
+
O
O
OMe
O
O

2.19 2.49

11.5 11.0 10.5 10.0 9.5 9.0 8.5 8.0 7.5 7.0 6.5 6.0 5.5 5.0 4.5 4.0 3.5 3.0 2.5 2.0 1.5 1.0 0.5 0.0

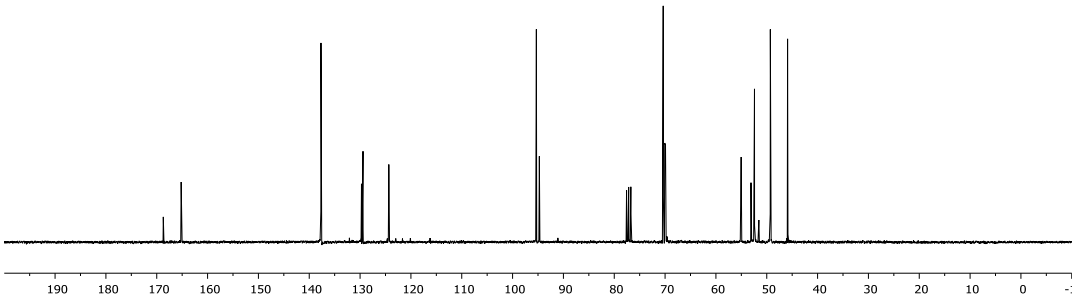
190 180 170 160 150 140 130 120 110 100 90 80 70 60 50 40 30 20 10 0

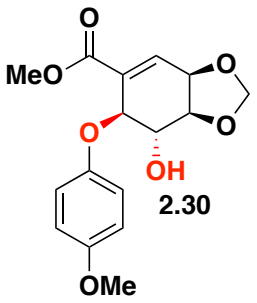

2.30

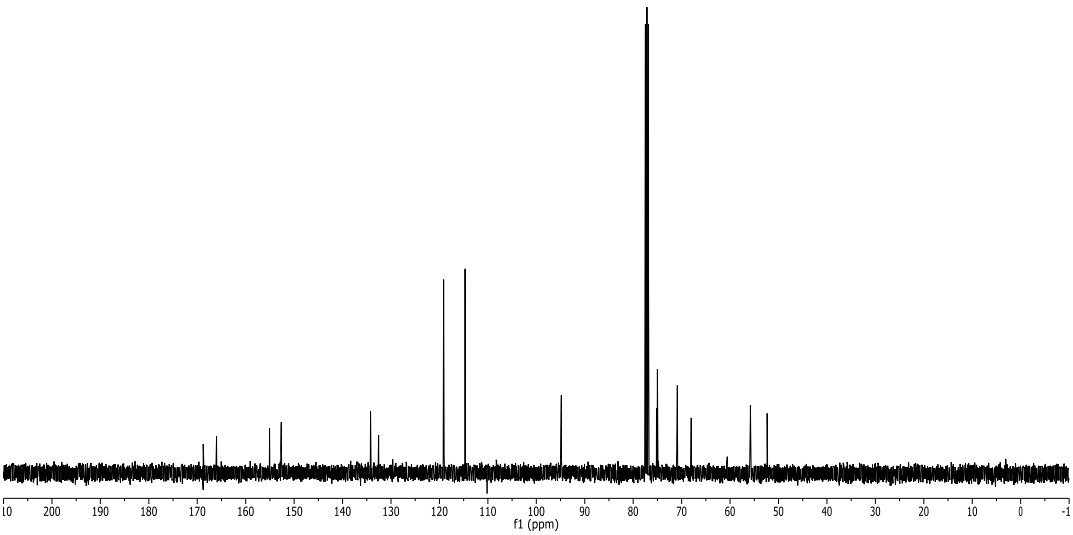

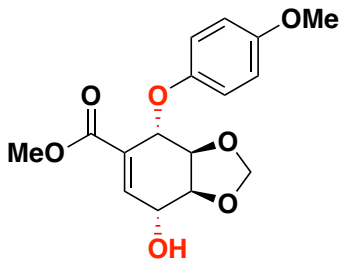

2.31

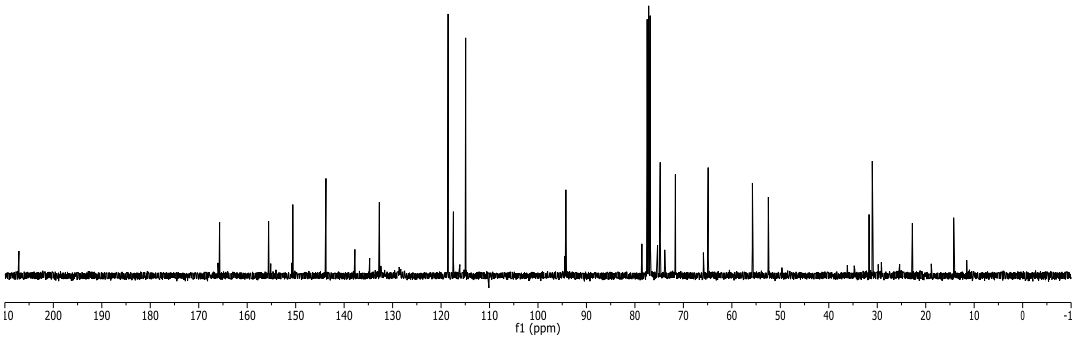

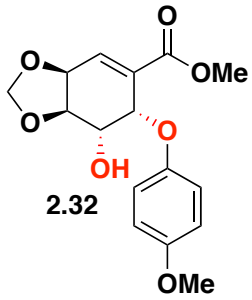

2.32

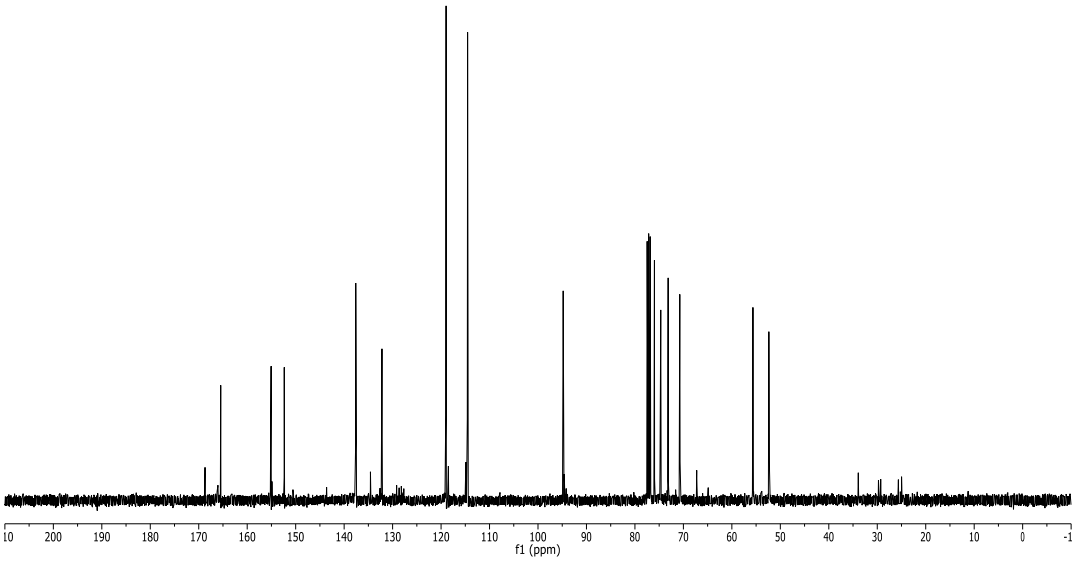

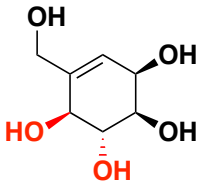

2.34
streptol

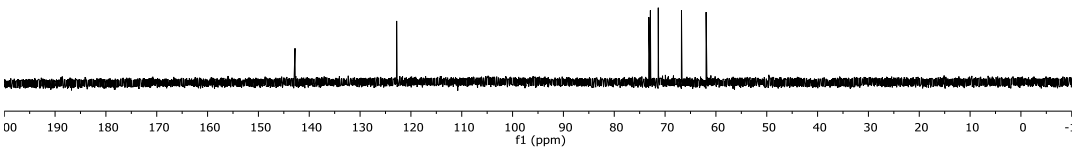

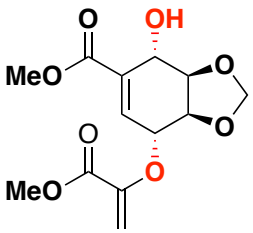

2.35

cyathiformine B type

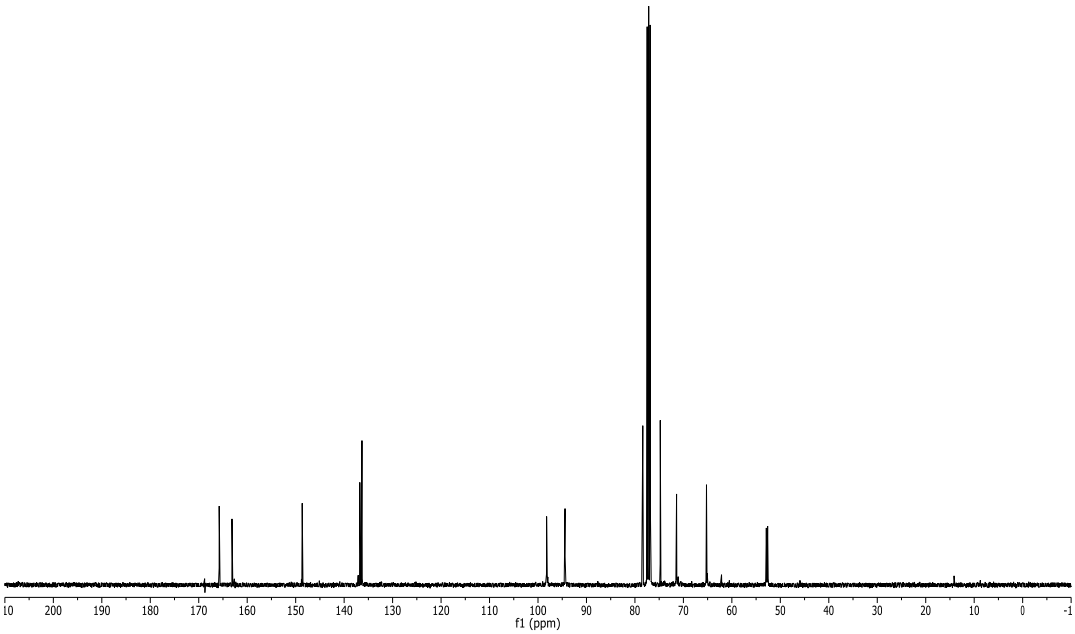

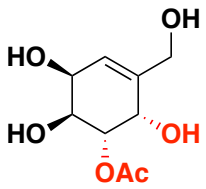

2.36
MK7607

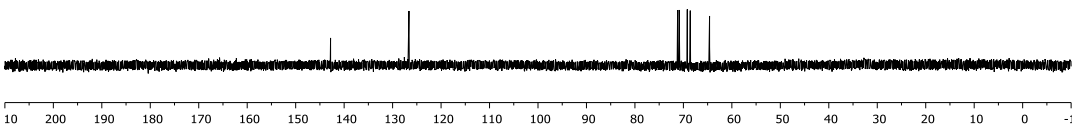

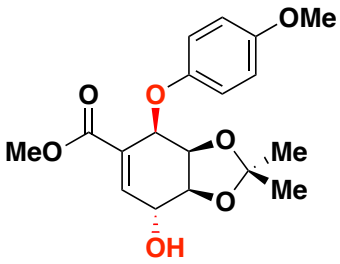

2.41

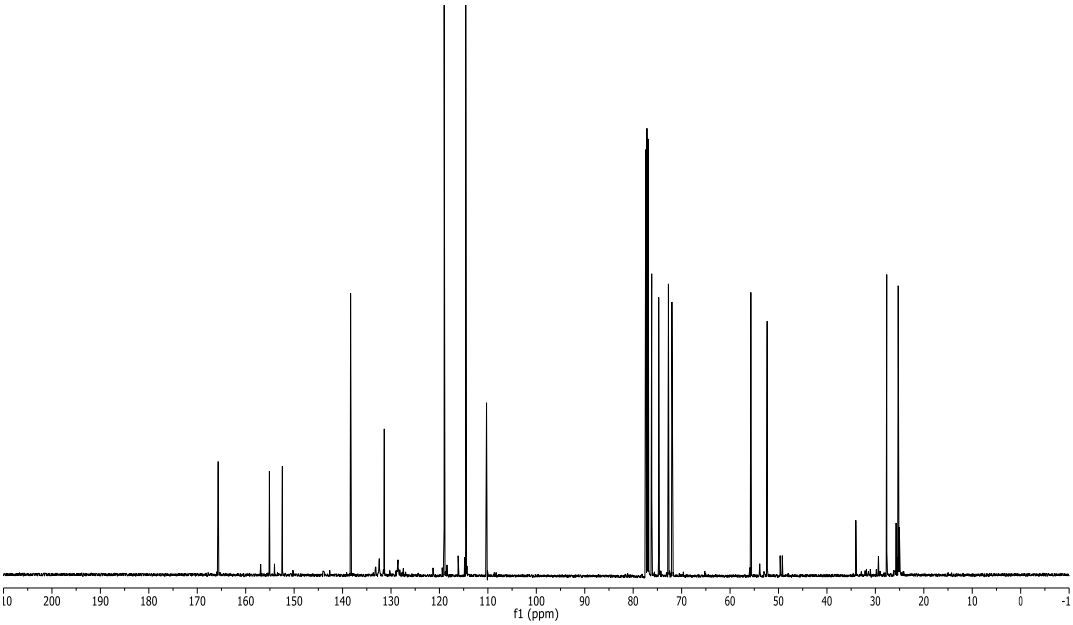

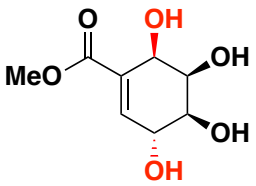

2.42

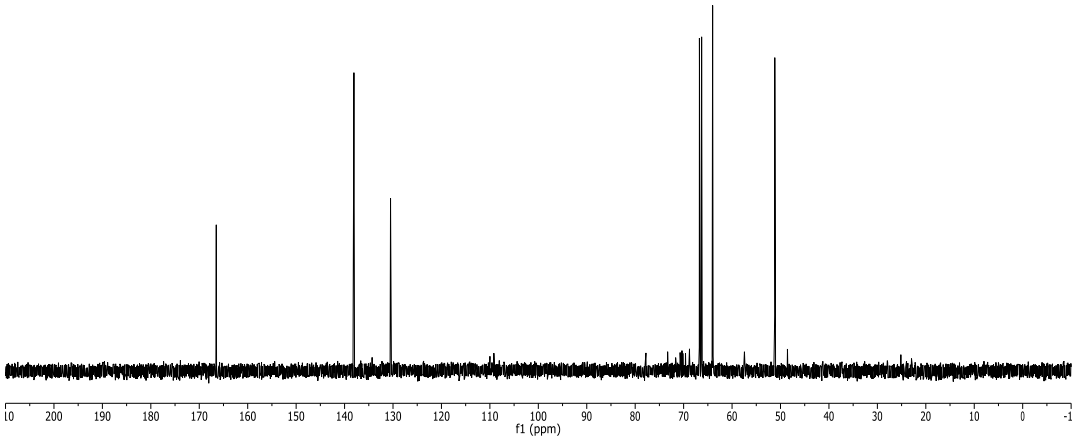

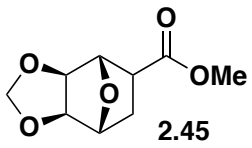
O
O
OMe
O
O

2.45

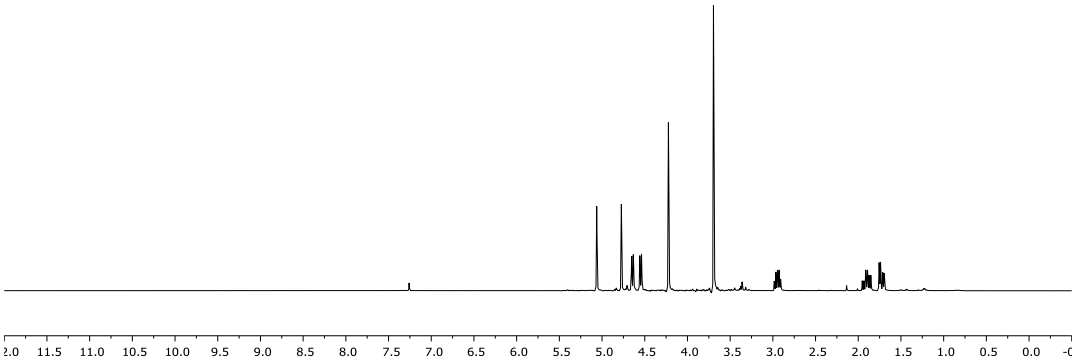
2.0 11.5 11.0 10.5 10.0 9.5 9.0 8.5 8.0 7.5 7.0 6.5 6.0 5.5 5.0 4.5 4.0 3.5 3.0 2.5 2.0 1.5 1.0 0.5 0.0

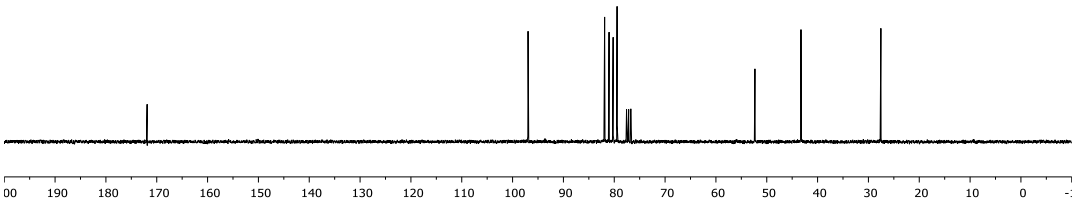
00 190 180 170 160 150 140 130 120 110 100 90 80 70 60 50 40 30 20 10 0

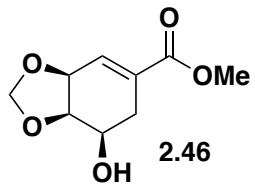
O
O
OMe
O
OH

2.46

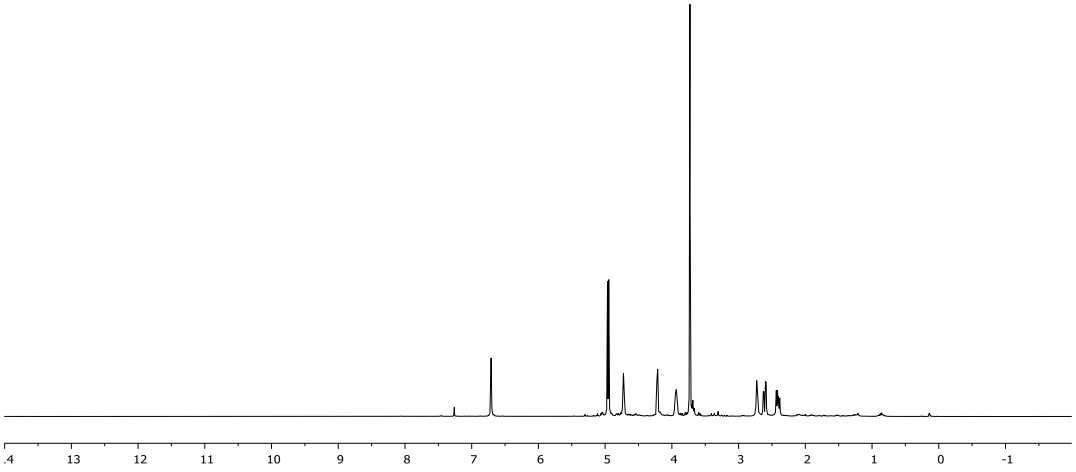
13
12
11
10
9
8
7
6
5
4
3
2
1
0
-1

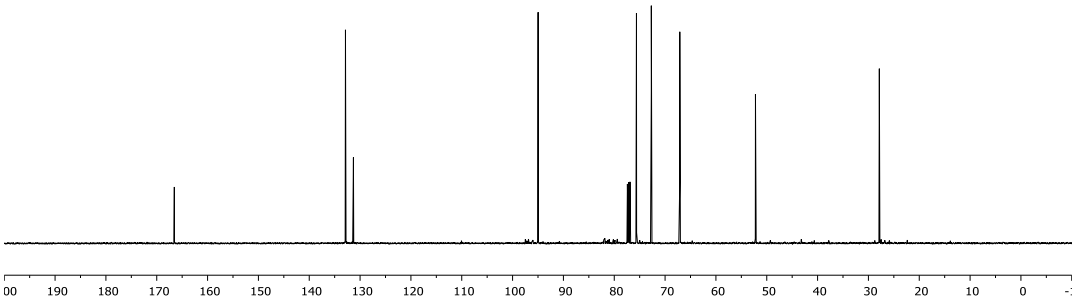
190
180
170
160
150
140
130
120
110
100
90
80
70
60
50
40
30
20
10
0

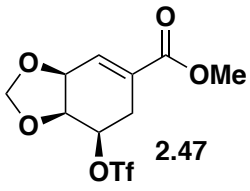

2.47

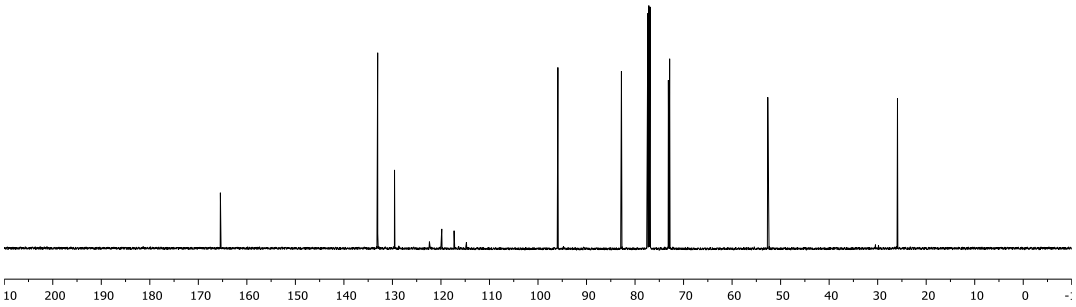

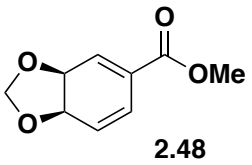
O
O
OMe
O

2.48

2.0 11.5 11.0 10.5 10.0 9.5 9.0 8.5 8.0 7.5 7.0 6.5 6.0 5.5 5.0 4.5 4.0 3.5 3.0 2.5 2.0 1.5 1.0 0

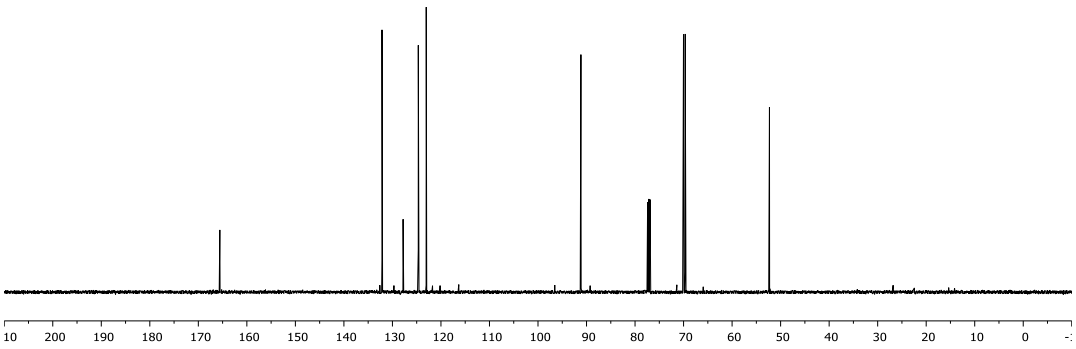
10 200 190 180 170 160 150 140 130 120 110 100 90 80 70 60 50 40 30 20 10 0

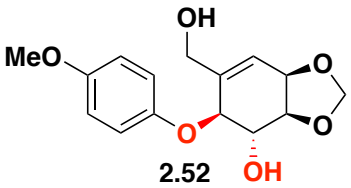
OH
MeO
O
O
O
OH

2.52

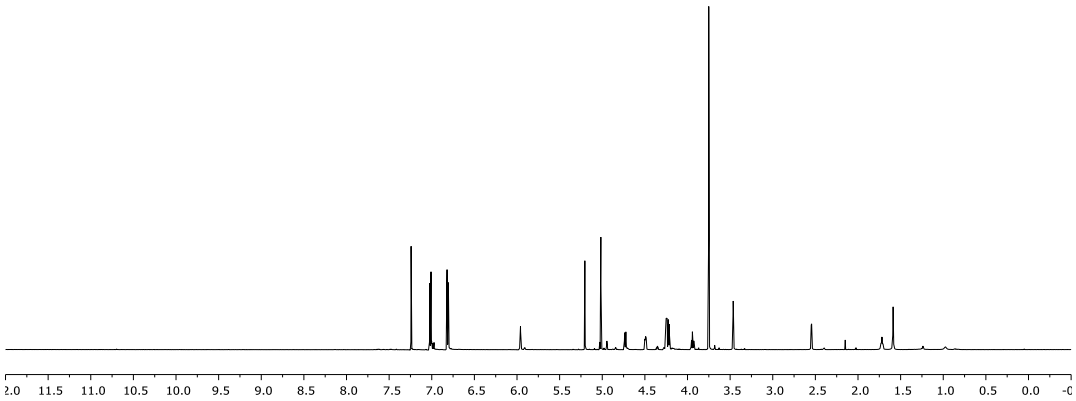
2.0 11.5 11.0 10.5 10.0 9.5 9.0 8.5 8.0 7.5 7.0 6.5 6.0 5.5 5.0 4.5 4.0 3.5 3.0 2.5 2.0 1.5 1.0 0.5 0.0

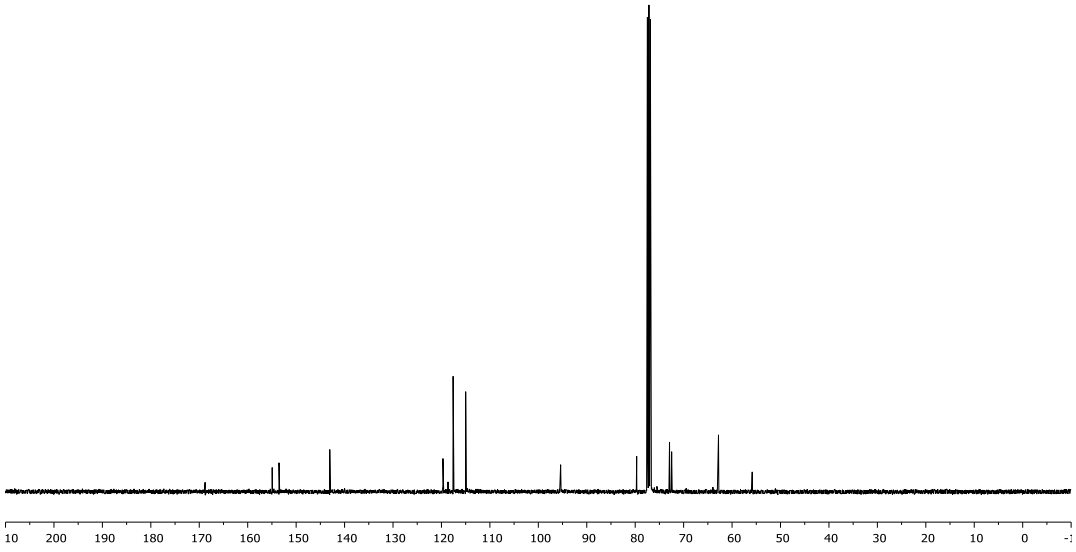
10 200 190 180 170 160 150 140 130 120 110 100 90 80 70 60 50 40 30 20 10 0

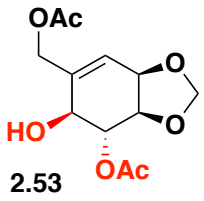

2.53

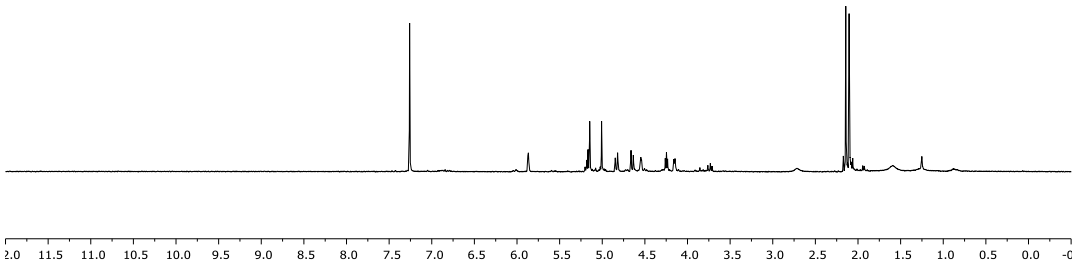

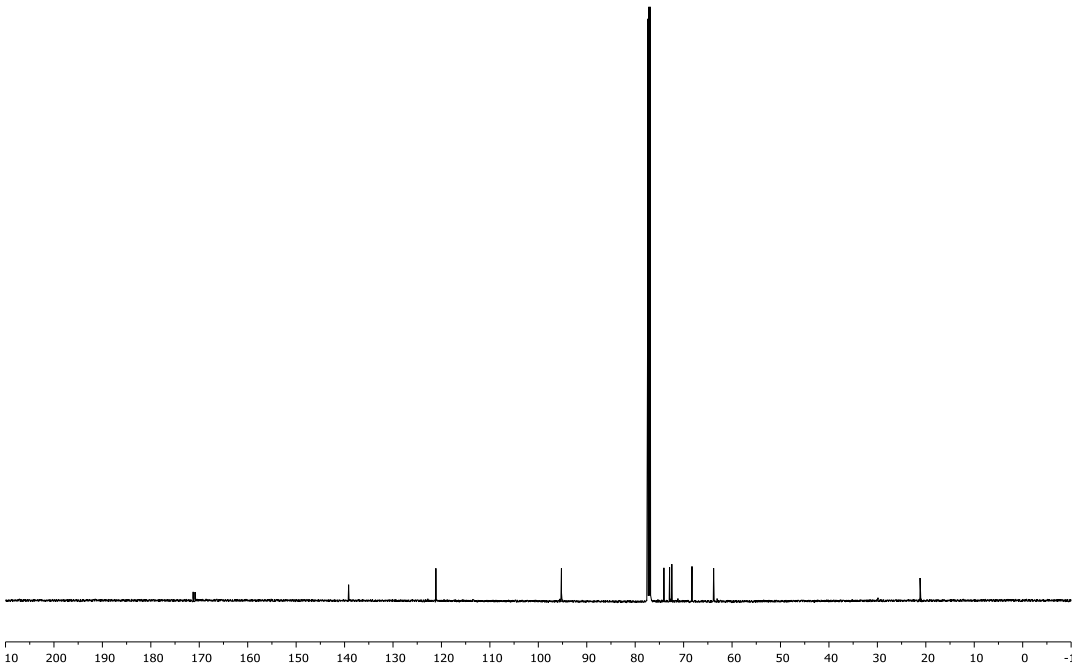

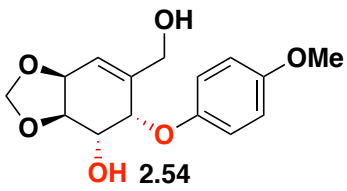
OH
O
O
OMe
O
OH

2.54

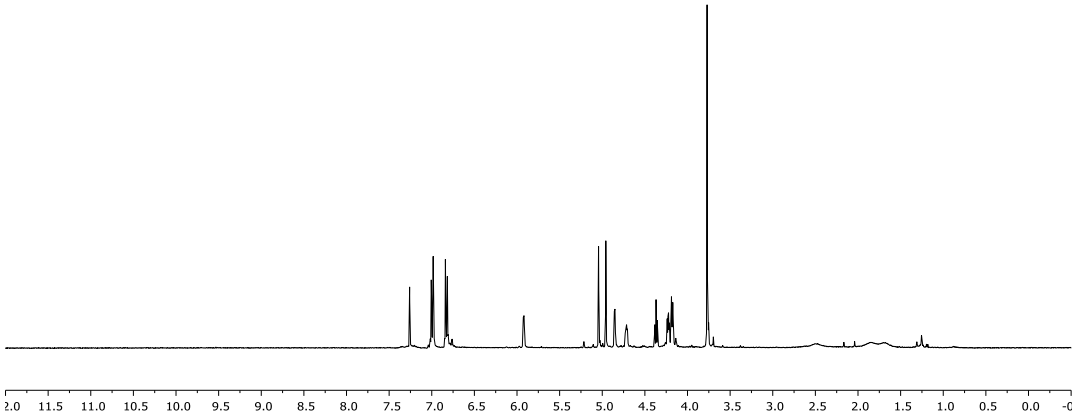
2.0 11.5 11.0 10.5 10.0 9.5 9.0 8.5 8.0 7.5 7.0 6.5 6.0 5.5 5.0 4.5 4.0 3.5 3.0 2.5 2.0 1.5 1.0 0.5 0.0

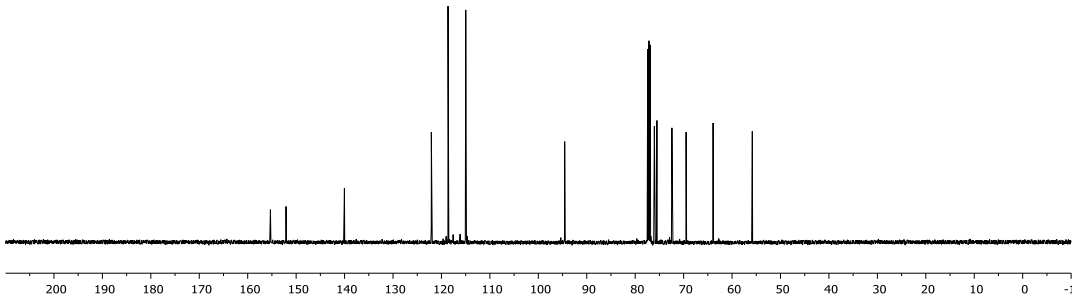
200 190 180 170 160 150 140 130 120 110 100 90 80 70 60 50 40 30 20 10 0

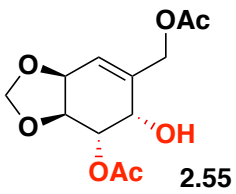
OAc
O
O
OH
OAc

2.55

2.0 11.5 11.0 10.5 10.0 9.5 9.0 8.5 8.0 7.5 7.0 6.5 6.0 5.5 5.0 4.5 4.0 3.5 3.0 2.5 2.0 1.5 1.0 0.5 0.0

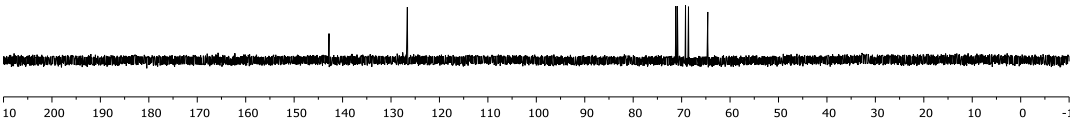
10 200 190 180 170 160 150 140 130 120 110 100 90 80 70 60 50 40 30 20 10 0

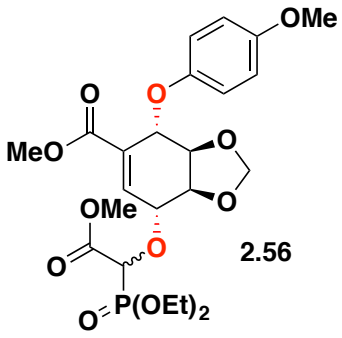

2.56

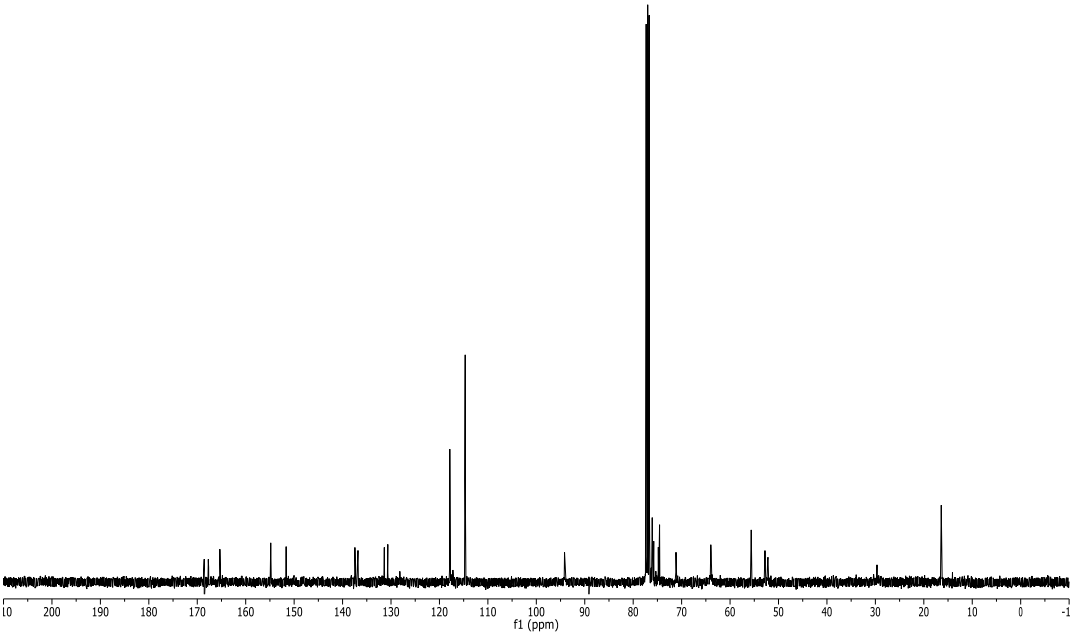

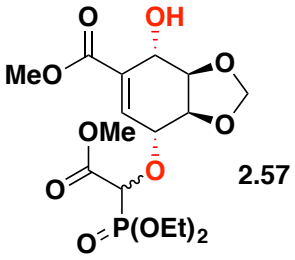

2.57

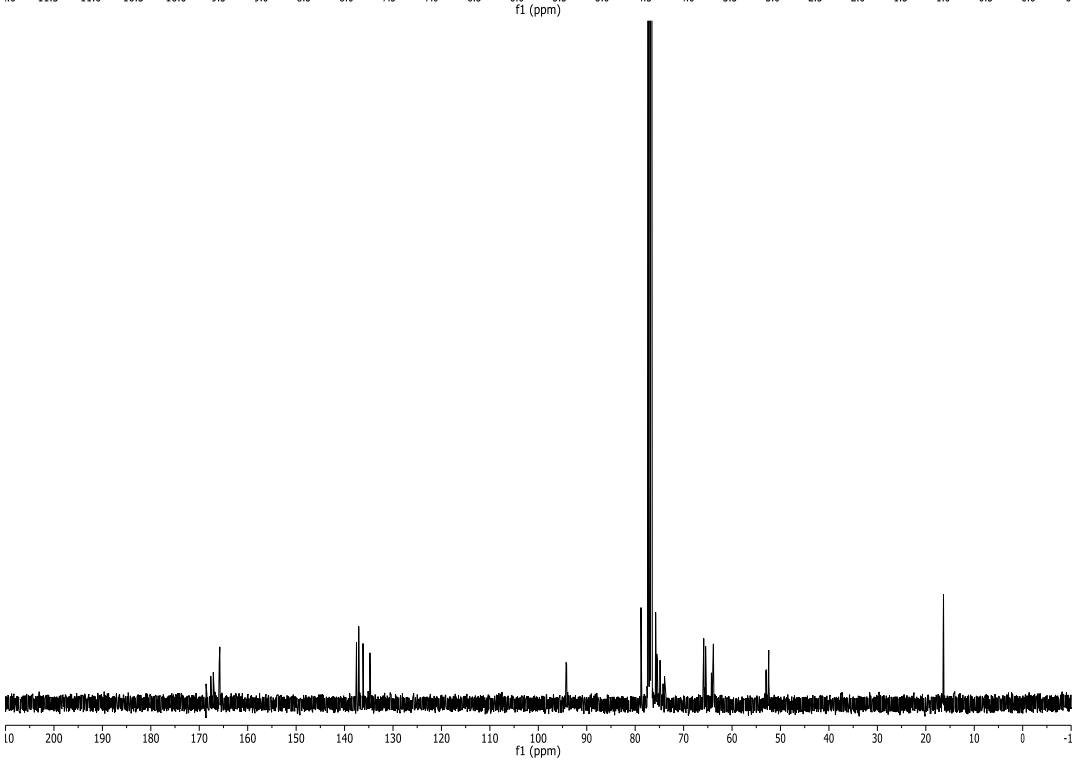

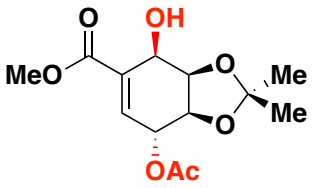

2.58

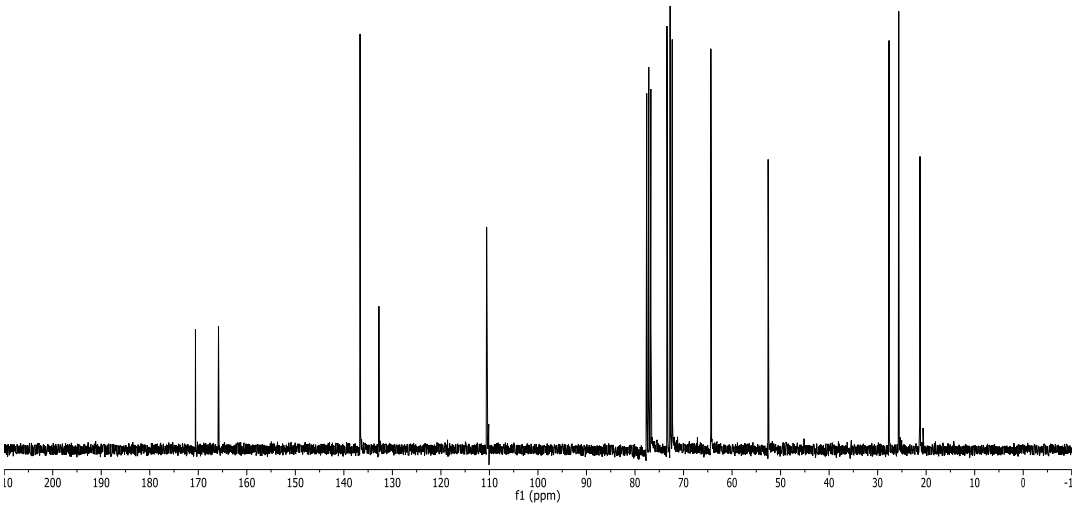

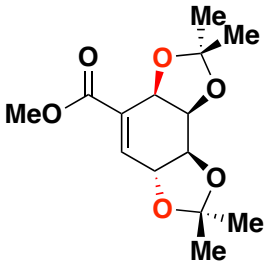

2.60

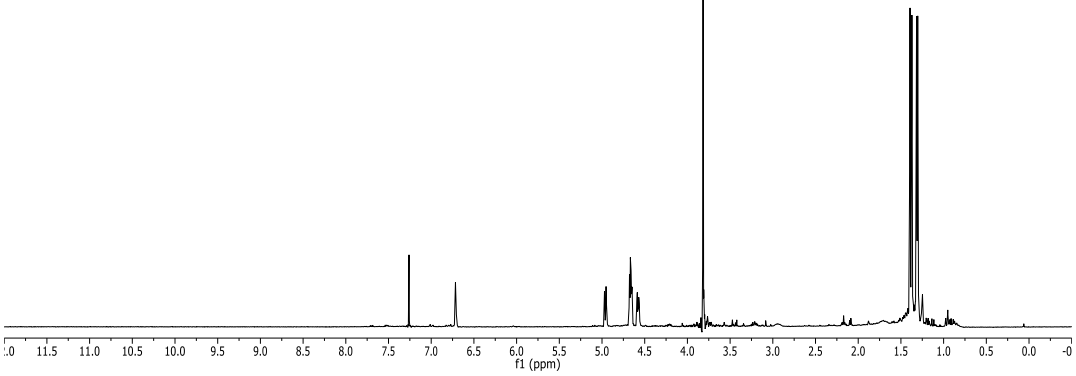

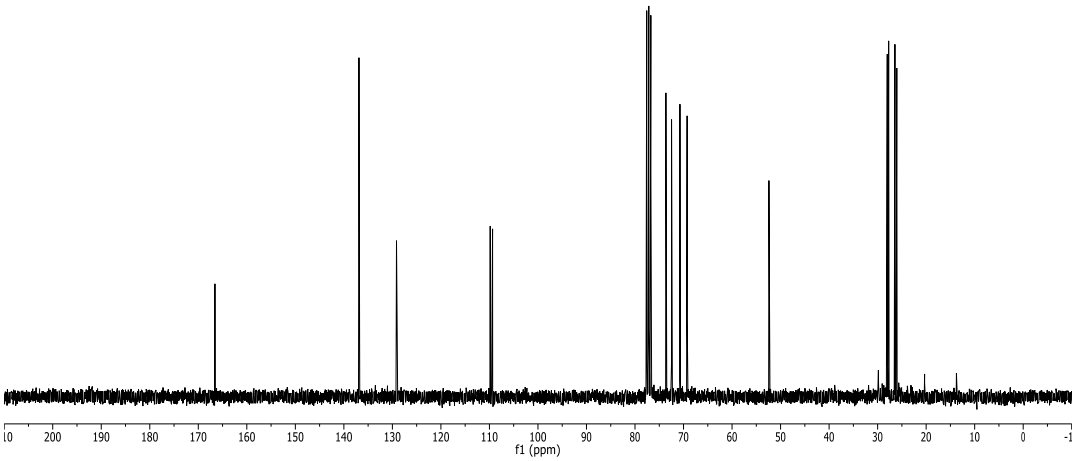

NOESY of compound **2.60**

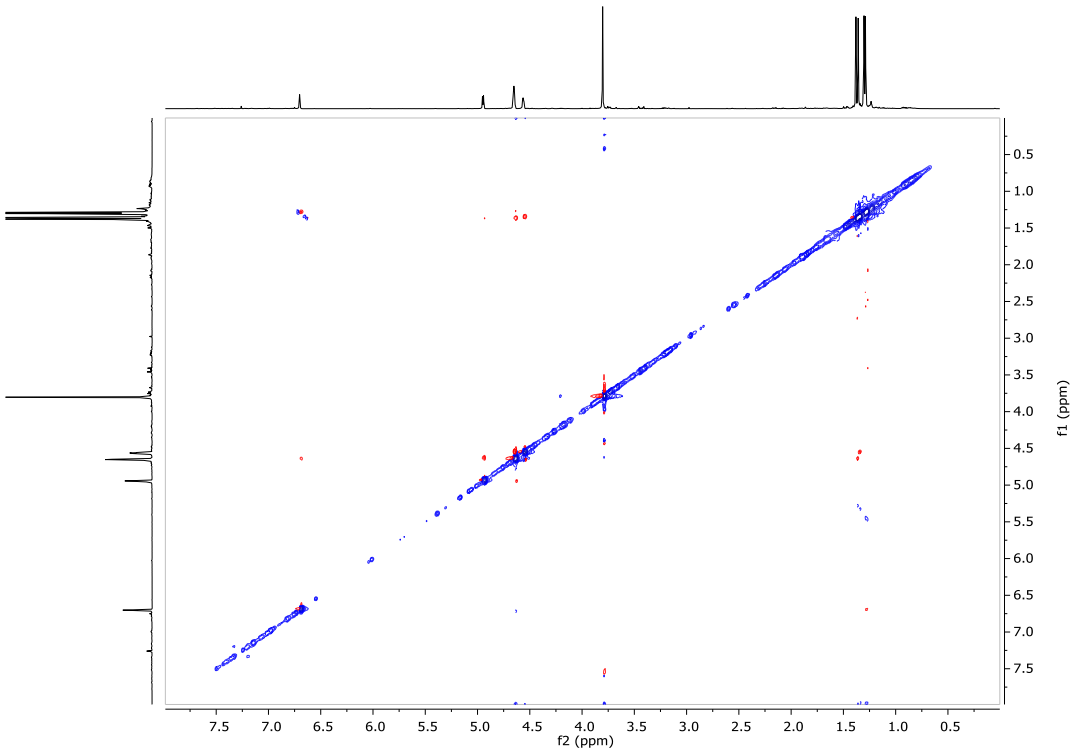

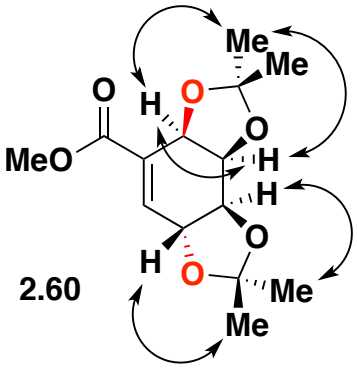

COSY of compound **2.60**

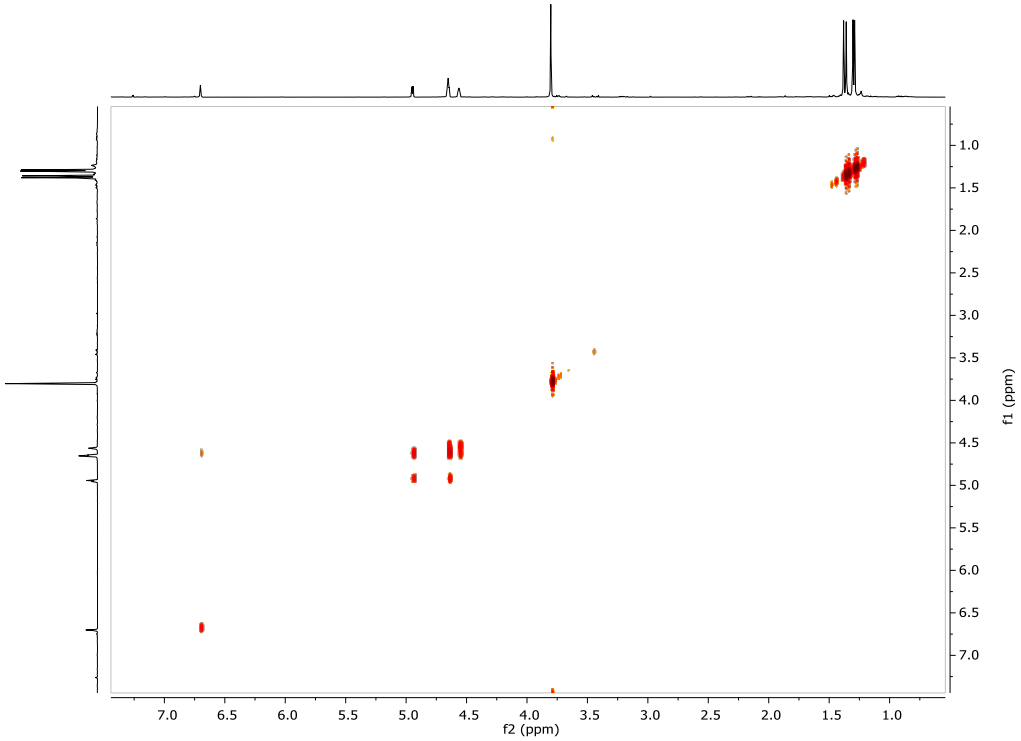

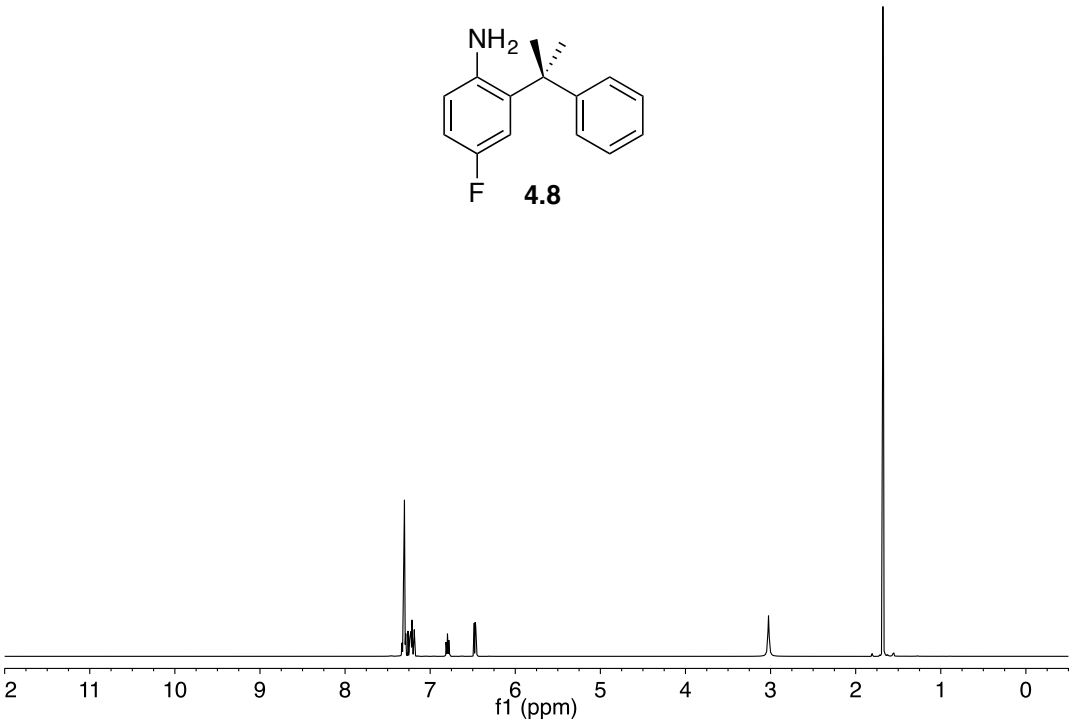
NH2
F
4.8
2 11 10 9 8 7 6 5 4 3 2 1 0
f1 (ppm)

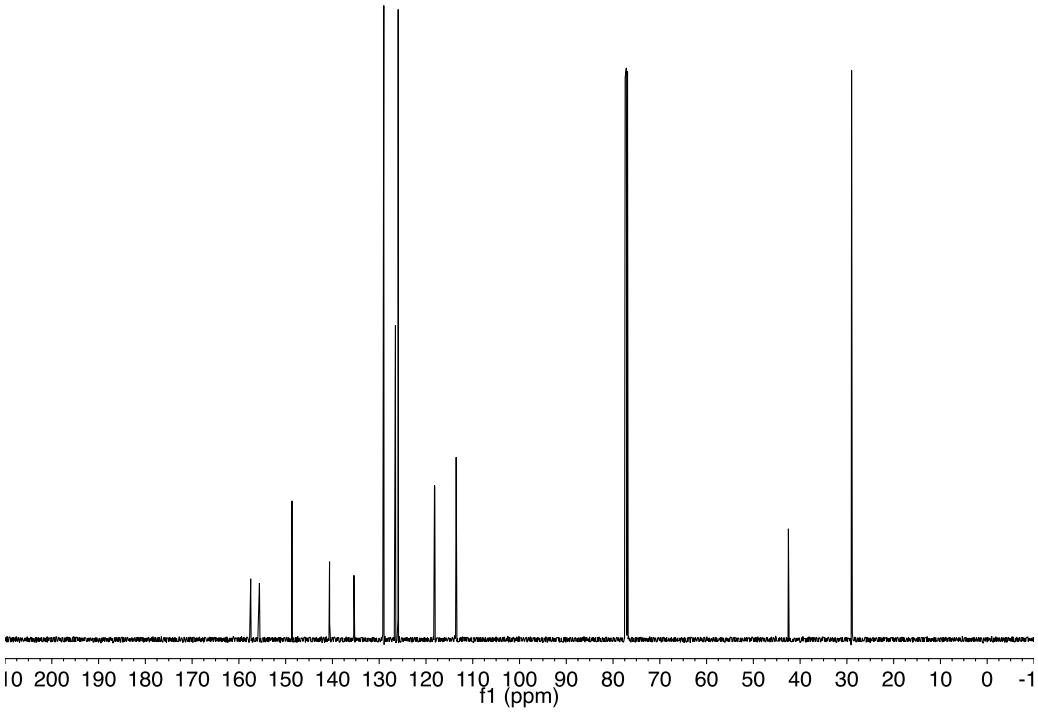
10 200 190 180 170 160 150 140 130 120 110 100 90 80 70 60 50 40 30 20 10 0 -1
f1 (ppm)

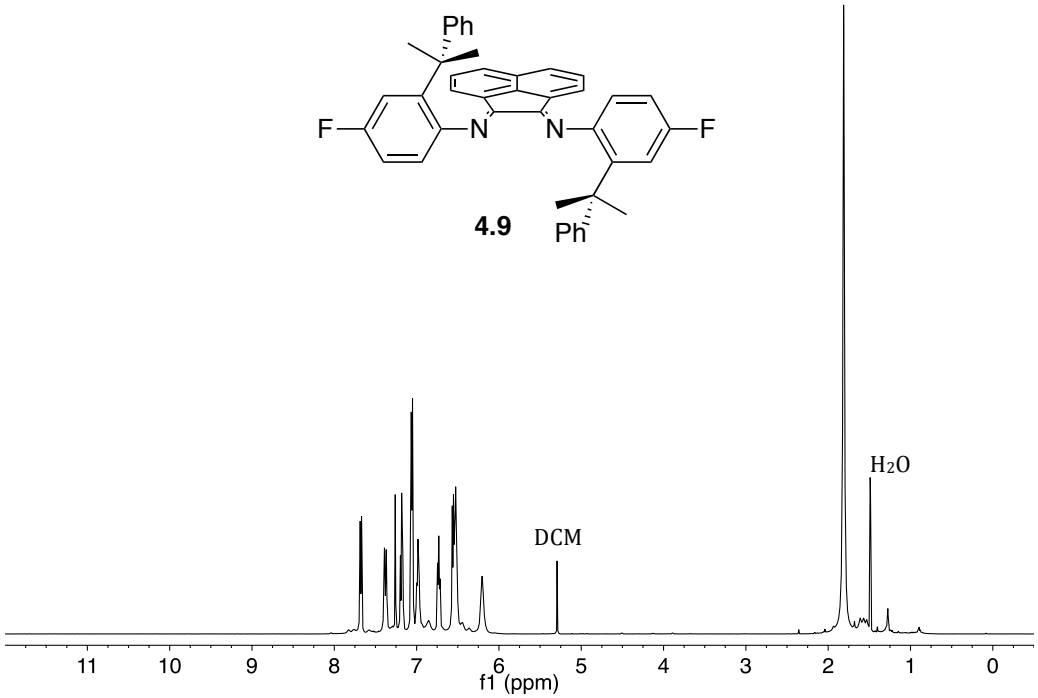
Ph
F
N
N
F
Ph
H2O
DCM
11 10 9 8 7 6 5 4 3 2 1 0
f1 (ppm)

4.9

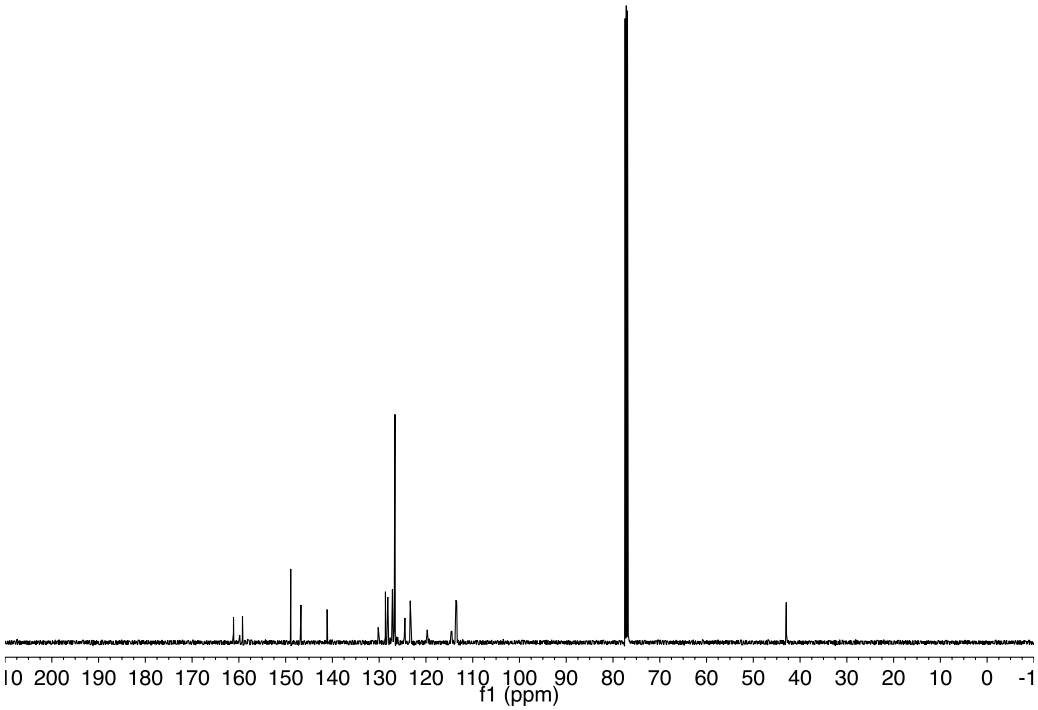
10 200 190 180 170 160 150 140 130 120 110 100 90 80 70 60 50 40 30 20 10 0 -1
f1 (ppm)

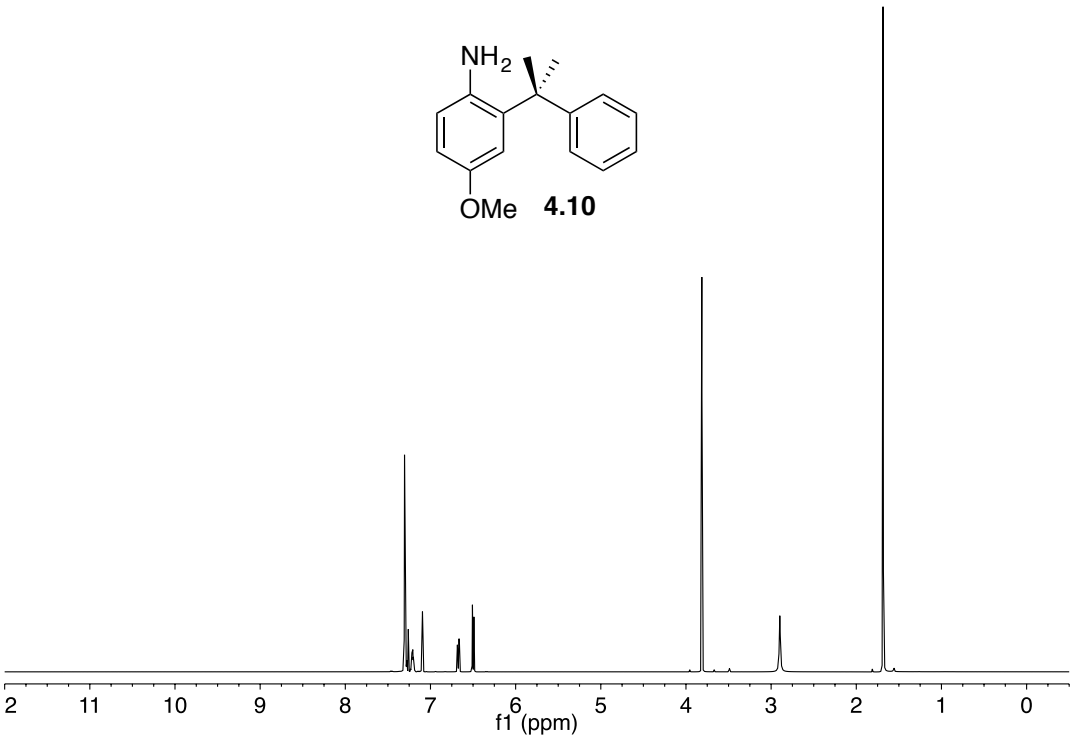
NH2
OMe
4.10
2 11 10 9 8 7 6 5 4 3 2 1 0
f1 (ppm)

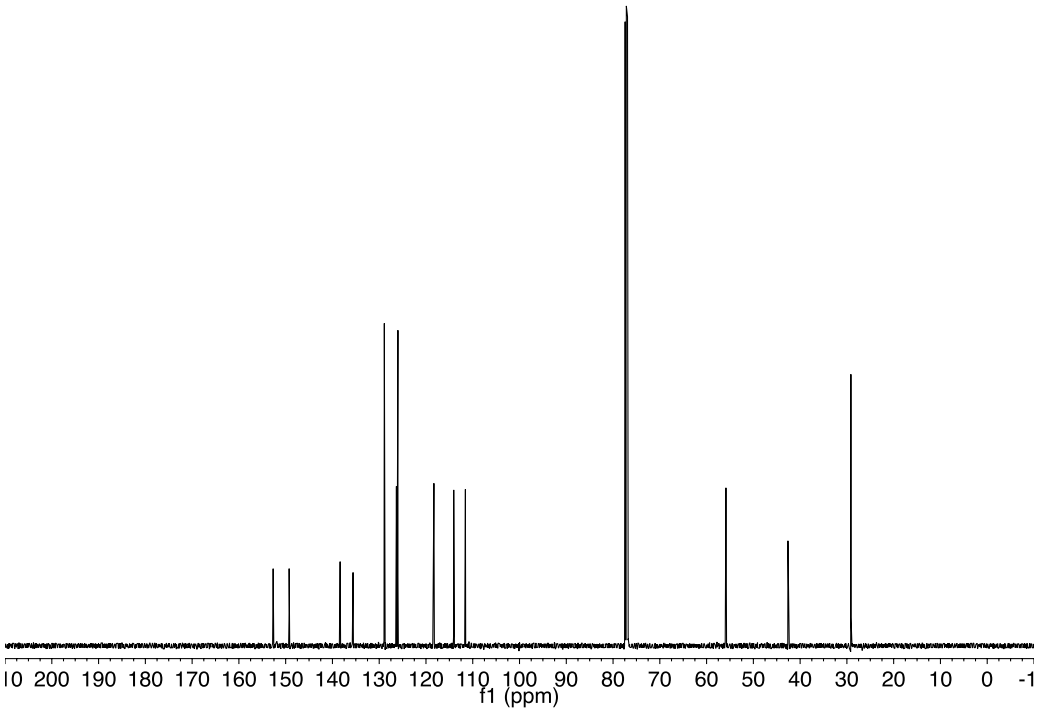
10 200 190 180 170 160 150 140 130 120 110 100 90 80 70 60 50 40 30 20 10 0 -1
f1 (ppm)

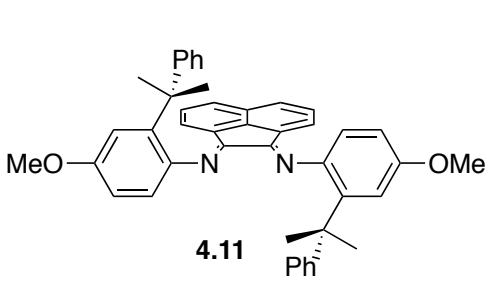
Ph
MeO
N
N
OMe
Ph

4.11

2
11
10
9
8
7
6
5
4
3
2
1
0
f1 (ppm)

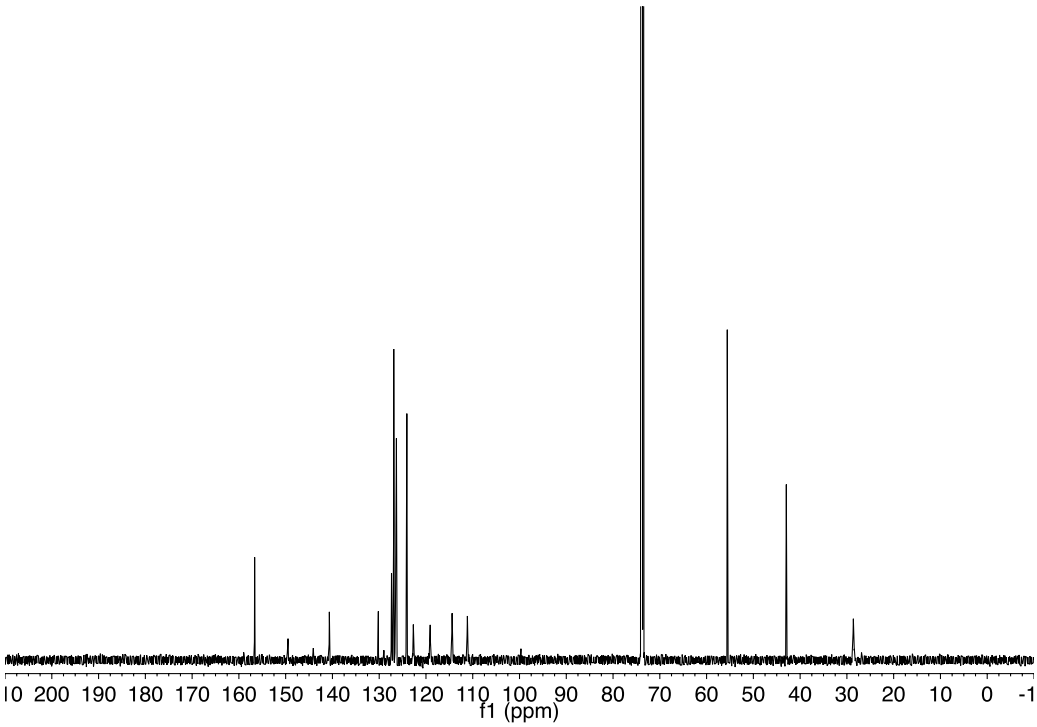
10 200 190 180 170 160 150 140 130 120 110 100 90 80 70 60 50 40 30 20 10 0 -1
f1 (ppm)

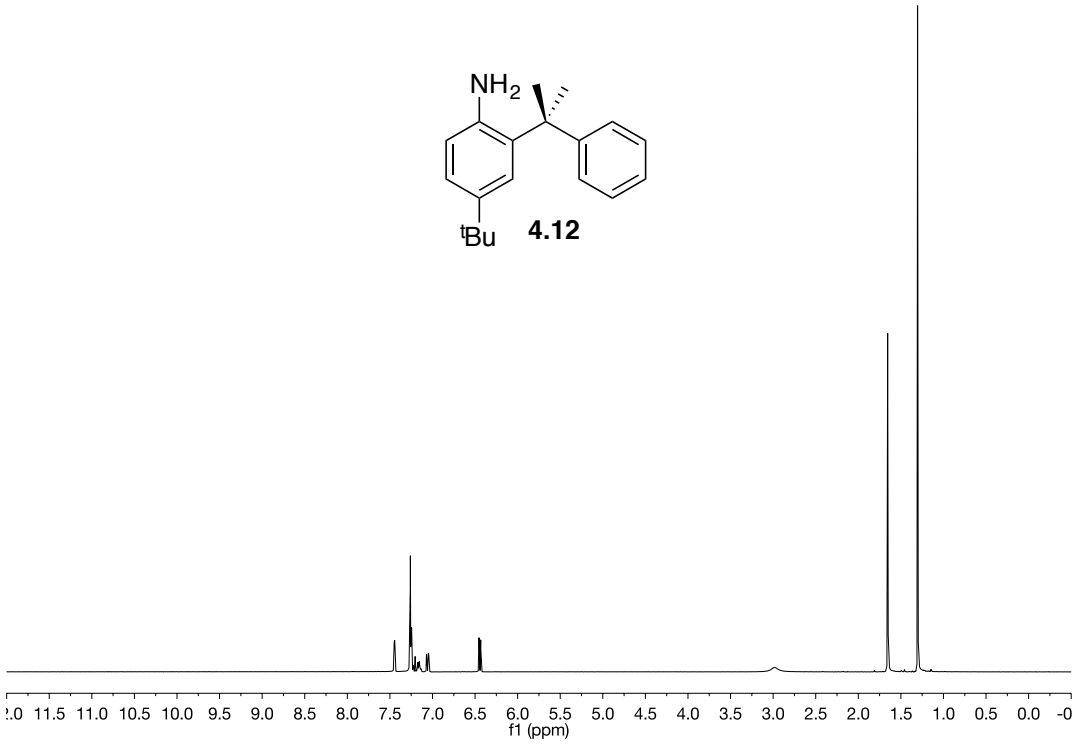
NH2
tBu
4.12
f1 (ppm)
f1 (ppm)

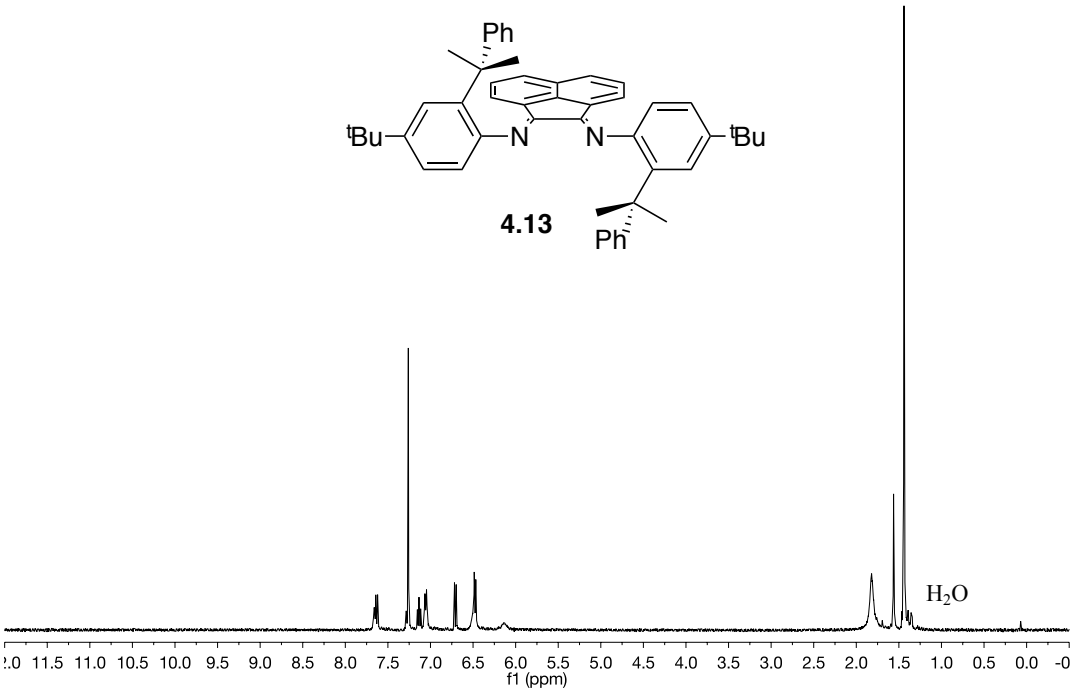

4.13

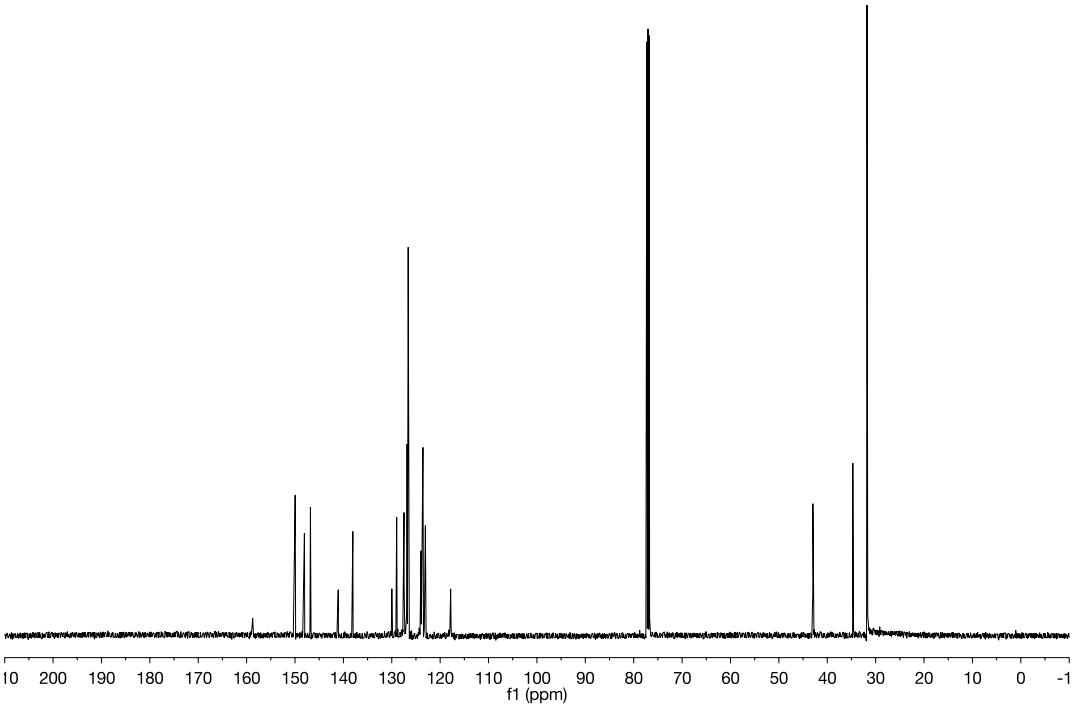

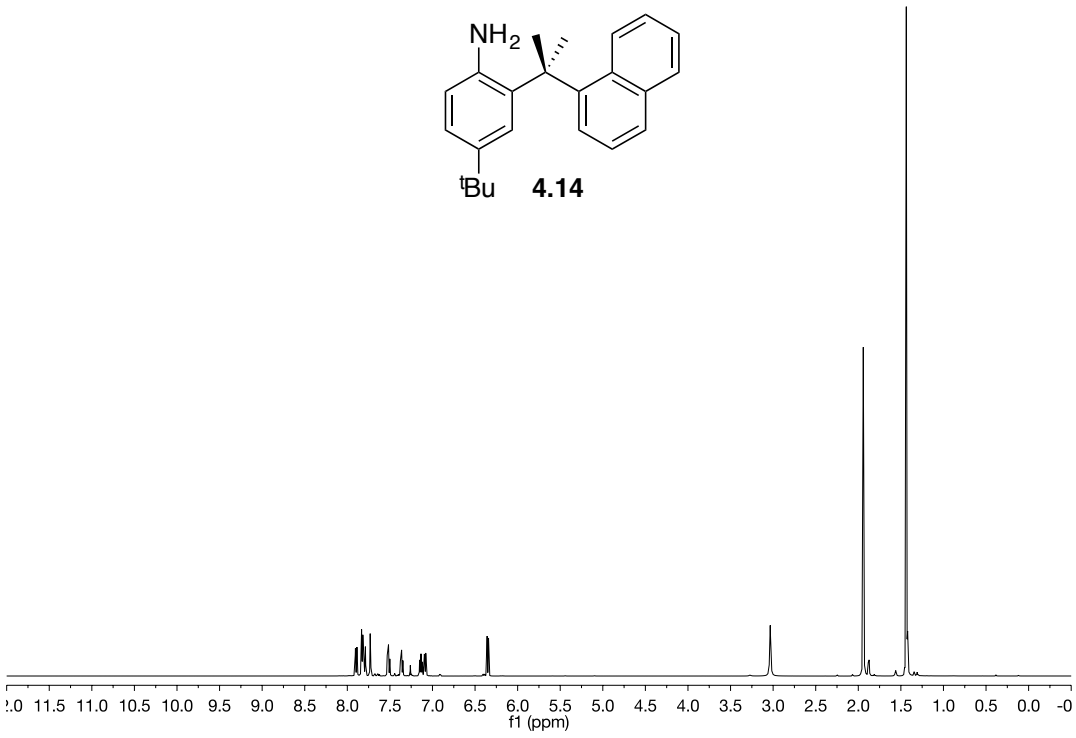
NH2
tBu
4.14
f1 (ppm)

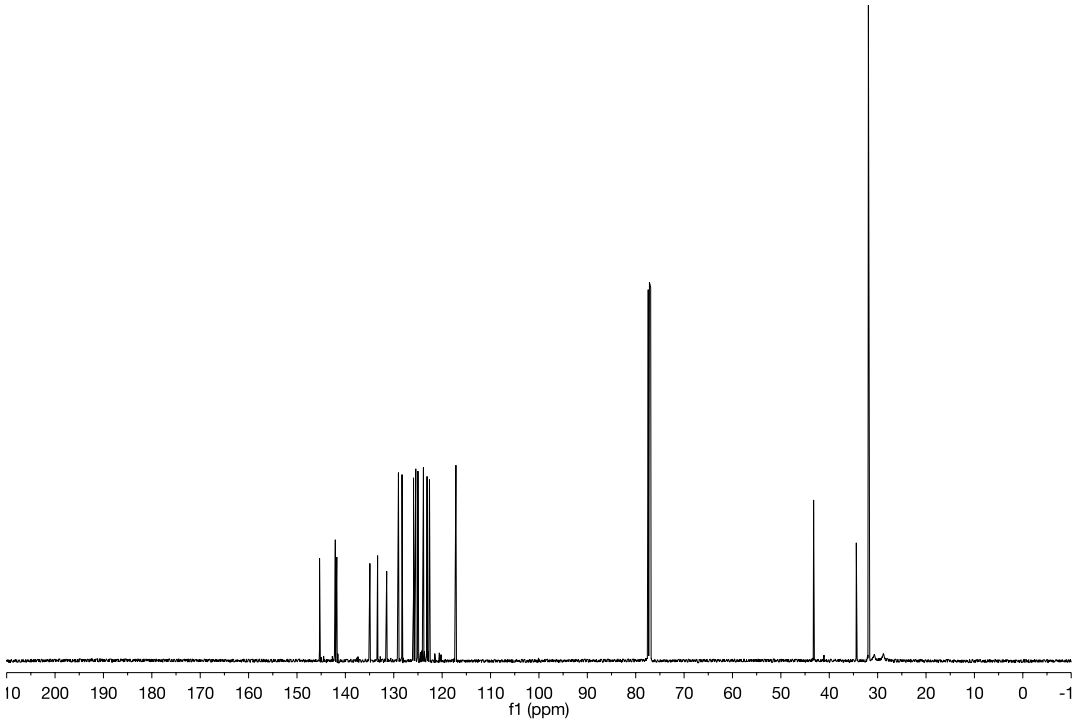
f1 (ppm)

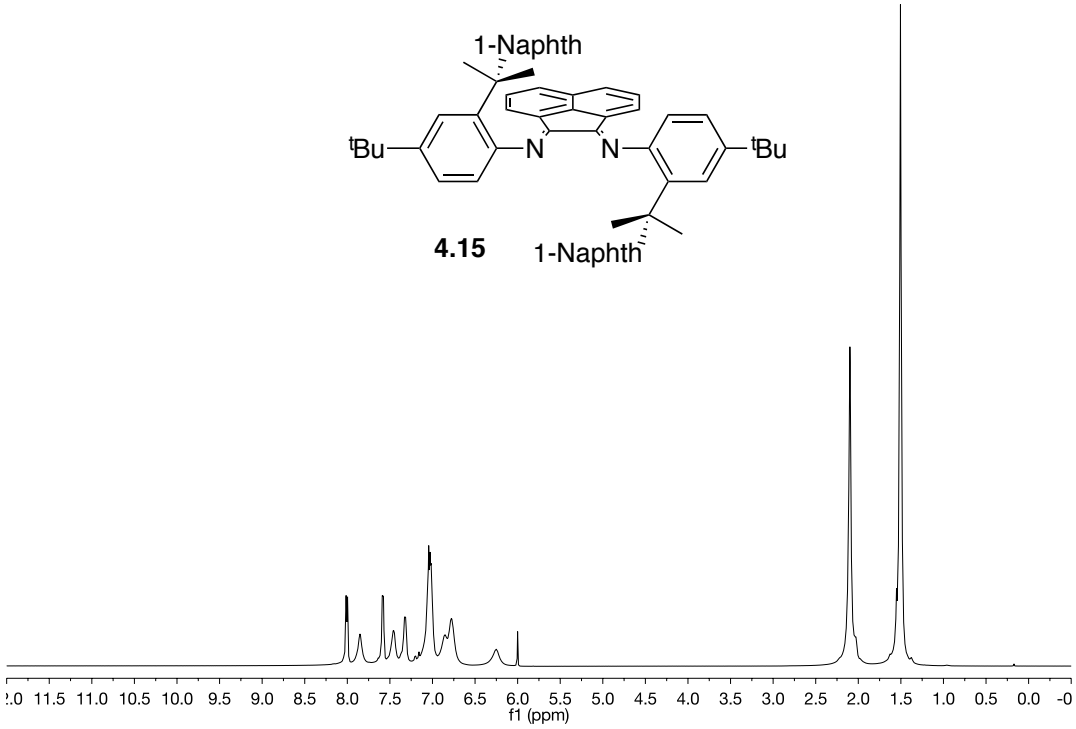

4.15